Utilising Copper for Methodological Advancements in Electro-Organic Synthesis

A dissertation presented by

Peter William Seavill

In partial fulfilment of the requirements for the award of the degree of

DOCTOR OF PHILOSOPHY

at

UNIVERSITY COLLEGE LONDON

Christopher Ingold Building
University College London
20 Gordon Street
WC1H 0AJ

Declaration

I, **Peter William Seavill**, confirm that the work presented in this thesis is my own. Where information has been derived from other sources, I confirm that this has been indicated and acknowledged.

****

Abstract

Electro-Organic Chemistry has great potential to be used extensively in chemical synthesis but remains relatively under-exploited. In an effort to help expand this promising field of research, this PhD project was centred around developing new electrochemical methodology for use in organic reactions, particularly through efficient copper-catalysed processes. Copper(I) acetylides, which are highly useful intermediates found in many organic syntheses, were produced in good to excellent yields and in an energy-efficient manner. This was achieved by using a Cu^0 electrode as the metal source, allowing selective release of Cu^I ions into solution through an applied oxidative potential. This reaction was expanded upon to incorporate quaternary ammonium salt reduction in an undivided cell to generate a base simultaneously with the Cu^I ions. Moreover, it proved possible to regenerate the base electrochemically, making the process catalytic in nature. We then incorporated these methods into the pharmaceutically relevant CuAAC reaction, forming C-N bonds. This Cu^0 oxidation was also used to great effect in a catalytic C-C bond-forming reaction, namely Glaser-Hay dimerization, for which an electrochemistry-led mechanistic investigation was carried out to help shed new light on this long-debated reaction, as well as in the Chan-Lam reaction to form C-O bonds.

In addition, the development of copper-coated graphite electrodes allowed for control over the amount of copper released in these processes (through the application of Faraday's laws of electrolysis) and the determination of the oxidation state of the copper released. This system also offered a promising recovery strategy to extract metal ions electrochemically following the completion of reactions, depositing the metal back onto the graphite surface ready to be used again. This has a clear advantage over existing synthetic processes in terms of sustainability and 'green' credentials and has great potential utility in environmental chemistry for the minimisation of water pollution.

Impact Statement

The impact of this work will most likely be felt within academic spheres, specifically in the fields of organic chemistry and synthetic electrochemistry. We hope that this work may help to encourage more widespread adoption of electrochemistry in synthesis as it is currently an under-exploited area of research. The work presented in this thesis also encompasses organometallic chemistry and catalysis, as well as pharmaceutically relevant reactions like the CuAAC reaction. This means that the highly sustainable processes we have developed may also be of interest to these areas of academia and the chemical industry. Other academic impacts include the possibility of future collaborations on related work as this interdisciplinary project itself was the result of a successful collaboration between Dr Jon Wilden (UCL Organic Chemistry) and Prof. Katherine Holt (UCL Electrochemistry). There is scope for further collaboration with organometallic chemists for mechanistic insights into certain reaction processes and surface scientists for the characterisation of metal coatings. Such collaborations help to bridge the gap between the various disciplines and lead to exciting new results.

Outside of academia the impact of this work will most likely be centred around solving environmental issues as the electrochemical copper recovery methodology we have begun to develop may be used to minimise the heavy metal pollution of water. Indeed, we were fortunate to present some of this work at an international conference (IUPAC 2019, Paris) under the theme of ‘Catalysis, Sorption and Separation for a Cleaner Environment’. Furthermore, there is potential to market this research to industry on the grounds that a reasonable financial saving may be made from the use of the metal-coated graphite electrodes in reactions. The reason for this is that the metal may be released into solution in a specific oxidation state to catalyse a reaction, then recovered simply *via* reduction back onto the graphite rod in an immediately reusable form, saving money on catalyst waste and expensive recovery techniques. Some pre-commercialisation funding was awarded to us during this project to investigate the feasibility of this idea.

The way in which these impacts may be brought about are primarily through the publication of this work in academic journals, as well as in the presentation of results at national and international conferences. We have already made a good start on this as we were fortunate to be able to publish 5 papers from the work in this thesis (P. W. Seavill, K. B. Holt and J. D. Wilden, *Green Chem.*, **2018**, *20*, 5474; P. W. Seavill, K. B. Holt and J. D. Wilden, *Faraday Discuss.*, **2019**, *220*, 269; P. W. Seavill, K. B. Holt and J. D. Wilden, *RSC Adv.*, **2019**, *9*, 29300; D. Li, P. W. Seavill and J. D. Wilden, *ChemElectroChem*, **2019**, *6*, 5829 and Y. Aoki *et al.*, *Faraday Discuss.*, **2019**, *220*, 282) as well as present at several conferences.

Contents

Abbreviations

CE	Counter Electrode
CI	Chemical Ionisation
CV (plot)	Cyclic Voltammetry plot
DABCO	1,4-Diazabicyclo[2.2.2]octane
DBU	1,8-Diazabicyclo[5.4.0]undec-7-ene
DCM	Dichloromethane
DFT	Density Functional Theory
DMEDA	1,2-Dimethylethylenediamine
DMF	Dimethylformamide
DMSO	Dimethyl sulfoxide
EI	Electron Ionisation
EOS	Electro-Organic Synthesis
ESI	Electrospray Ionisation
eq	(Number of) Equivalents
et al.	*Et alia*
Fc or Fc$^+$	Ferrocene or ferrocenium ion
HFIP	Hexafluoroisopropanol
HIV	Human Immunodeficiency Virus
HMPA	Hexamethylphosphoramide
HOMO	Highest Occupied Molecular Orbital
HRMS	High Resolution Mass Spectrometry
IR	Infrared
LED	Light-Emitting Diode
LRMS	Low Resolution Mass Spectrometry
LUMO	Lowest Unoccupied Molecular Orbital
m	*meta*
m.p.	Melting Point
MRSA	Methicillin-Resistant Staphylococcus Aureus
NBS	*N*-Bromosuccinimide
NCS	*N*-Chlorosuccinimide
NHC	*N*-Heterocyclic carbene
NIS	*N*-Iodosuccinimide
NMP	*N*-Methyl-2-pyrrolidone
NMR	Nuclear Magnetic Resonance

p	*para*
PMDTA	*N*,*N*,*N'*,*N''*,*N''*-Pentamethyldiethylenetriamine
QAS	Quaternary Ammonium Salt
QRE	Quasi Reference Electrode
RBF	Round-Bottomed Flask
RE	Reference Electrode
REDOX	**Red**uction/**Ox**idation
RT	Room Temperature
SCE	Saturated Calomel Electrode
SET	Single Electron Transfer
TBA	Tetrabutylammonium
TBAB	Tetrabutylammonium bromide
TBAC	Tetrabutylammonium chloride
TBAF	Tetrabutylammonium fluoride
TBAI	Tetrabutylammonium iodide
TBTA	Tris((1-benzyl-1*H*-1,2,3-triazolyl)methyl)amine
TEA	Tetraethylammonium
TEMPO	(2,2,6,6-Tetramethylpiperidin-1-yl)oxyl
THF	Tetrahydrofuran
TLC	Thin-Layer Chromatography
TMEDA	Tetramethylethylenediamine
TMS	Trimethylsilyl (group)
TTTA	Tris((1-*tert*-butyl-1*H*-1,2,3-triazolyl)methyl)amine
UV	Ultraviolet
WE	Working Electrode

Acknowledgements

Firstly, I'd like to thank my supervisors Dr Jon Wilden and Prof. Katherine Holt for their support and guidance over the last 3 years (4 in the case of Jon) and for being all-around excellent people to work for. It's been a joy to work on a project which none of us had any real experience of beforehand as there was a real sense of exploration in the lab. We had to build our understanding from the ground up and I wouldn't have made it this far without their encouraging and stress-free attitudes to research, which allowed me the freedom to come up with my own ideas and, importantly, not feel bad when a lot of them fell flat. It's been a pleasure. Over these past few years I've shared the lab with many good people: Marc, Vince, Zena, Mira, Theo, Thibault, Diyuan, Raul, Chris, Roomi, Anthusha, Kate, Joana, Joanna, Reuben, Xuanxiao and Theo. I thank you all. In particular, I'd like to thank Vince for being my first mentor and inspiring me to do a PhD in the first place; Marc and Thibault for being excellent influences in the lab and good friends; Mira for being a most excellent student, and Zena, my girlfriend, for lending her name to **Eq. 1** and, more importantly, being my rock for the last 3 years. I love you. I'd like to thank Andre, who has been one of my best friends since we were put together as lab partners in our first organic chemistry lab sessions almost 8 years ago. We've come a long way since then with both of us staying on to do PhD's at UCL. Your immense work ethic really helped me to push myself and I'm grateful for the 3 years we lived together. I'd also like to thank my good friend Lisa, who co-founded 'Tuesday Drinks' with me in the first year of our PhD's. They were a great source of catharsis, complaining about reactions that didn't work, and really good times. Tuesdays were more boring after you left. My good friends Alice, Hassan and Juno also deserve my thanks for many great times over the years, as well as my school friends, Matt and Josh, for years of basketball fun and keeping in touch after we went our separate ways. To my family: Mum, Dad and Julia, I am greatly indebted for all the years of love and support you've given me. A special thanks must go to my Dad for the unenviable task of looking through this thesis for grammatical mistakes despite not knowing an electron from a proton, or an oxidation from a reduction. Your command of the English language and eagle-eyed attention to detail were too valuable not to ask you to look through it. I love you all very much. Finally, about halfway through this project, I was unlucky enough to develop ulcerative colitis, which caused me to spend several months in and out of hospitals. It was the darkest time of my life, but I made it back to where I was supposed to be, largely thanks to the excellent nurses and doctors of the NHS, as well as the support and understanding of Zena, Jon, my family and friends. It all worked out in the end!

“O xein angellein Lakedaimoniois hoti tede
keimetha tois keinon rhemasi peithomenoi”
Translation: “Go tell the Spartans, stranger passing by,
that here, obedient to their laws, we lie”

The epitaph on the monument of the battle of Thermopylae,
Simonides of Ceos

Chapter 1. Introduction to Electro-Organic Synthesis

Electrochemistry is one of the most direct ways in which chemists can interact with molecules.[1] Through the understanding and control of fundamental electron and nucleus relationships it is possible to add or remove electrons to evoke desired reactions. As such, there is a strong literature precedent for the generation of reactive species that can be used in organic synthesis.[2] Many examples exist including, but certainly not limited to: the generation of selenides,[3–5] nitrenes,[6] isocyanides,[7] superoxide,[8] as well as species for aromatic C-H bond functionalisation.[9,10] Indeed, highly useful reactions like environmentally benign oxidations,[11] fluorinations,[12] functionalisations of arenes,[13] decarboxylations,[14] coupling reactions,[15] heterocycle formations[16] and natural product syntheses[17] have all been performed using electrochemistry.[18] The main benefits of using electrochemistry for organic transformations are that potentially hazardous species can be produced and then consumed *in situ* (eliminating the need to handle them directly), species can be produced in a very controlled manner over time and electrochemical reactions can be scaled up with ease.[1]

1.1 A Brief History

The history of Electro-Organic Synthesis (EOS) begins in the year 1800 with the invention of the first electric battery, the Volta Pile, which allowed a continual movement of electrons through a circuit for the first time.[1,19] Around 30 years later Michael Faraday made ground-breaking strides in understanding the nature of electricity. The popularisation of terms like anode, cathode and electrolysis, the observation of ions moving through electrolyte solutions and the development of Faraday's Laws of Electrolysis (which can be summarised in **Eq. 1** and which proved to be very important for work carried out in this project)[20] can all be attributed to Faraday's extensive studies.[21] Faraday also became a pioneer of electro-organic chemistry when he described the electrolysis of sodium acetate which would later form the basis of the well-known Kolbe electrolysis of carboxylic acids to produce alkyl radicals.[1,22]

Faraday's Laws of Electrolysis

$$n_\mathrm{M} = \frac{Q}{zeN_\mathrm{A}} \qquad \text{(Eq. 1)}$$

n_M = Number of moles of metal species
Q = Charge passed
z = Valency number of ions of the substrate
e = Elementary charge
N_A = Avogadro's number

Following this, important advancements in the apparatus used to conduct reactions began to be developed such as divided cells to keep anodic and cathodic reactions from interfering with each other (1889),[23] and the potentiostat, developed in 1942,[24] which allowed reactions to be carried out under constant potential conditions. This was significant because up until this point all reactions were exclusively carried out using constant current conditions. This new dimension of electrochemistry was further bolstered by the first demonstration of cyclic voltammetry (CV) in 1948 which remains to this day an essential technique in an electrochemist's repertoire.[1,25] However, perhaps the greatest drawback of EOS remains the lack of standardised equipment, forcing research groups all over the world to develop and use their own setups. This introduces a lot of variability between groups and leads to a lack of reproducibility of results. This problem is slowly beginning to be addressed with the development of purpose-built electrochemistry kits that can be used in synthetic laboratories,[26] but it will take some time before such equipment becomes standard issue. This is a significant problem in EOS and thus warrants expression, however the focus of this PhD project was on synthetic methodology rather than mechanical concerns and so that is where the discussion will continue.

Many major synthetic developments using electrochemistry were made within the last 60 years[1,26] and some notable examples include Lund's electrogeneration of bases in 1969,[27] the development of Shono oxidation in 1975 (the α-functionalisation of alkyl amides)[28] and the formalisation of the principles of indirect electrolysis, i.e. utilising mediators to promote other REDOX reactions.[29] Furthermore, within the last 35 years a slew of excellent examples of EOS have been reported by names such as Little (electroreductive cyclisation),[30] Moeller (anodic olefin coupling),[31] Yoshida (the use of S and Si electroauxiliaries),[32] Baran (the total synthesis of dixiamycin)[33] and Waldvogel (biaryl coupling),[34] as well as many others. Such work has helped to flesh out the field of EOS and popularise electrochemistry as a strong force in modern-day synthesis. **Figure 1** shows a simplified timeline of these advancements adapted from the work of the Baran group[1,26] with general reaction schemes where necessary. The electrogeneration of bases is particularly important to highlight as it will feature later in this thesis.

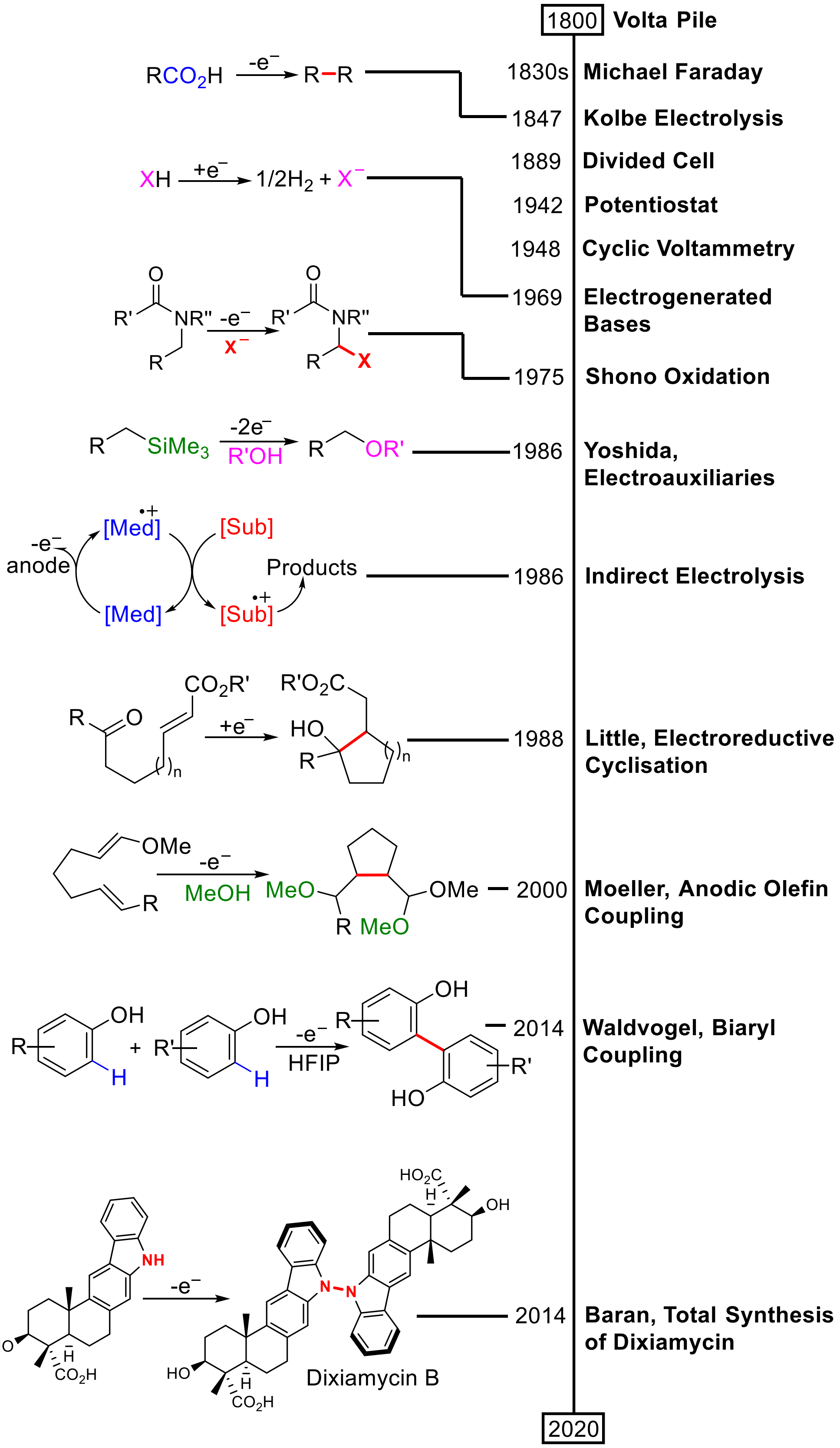

Figure 1: *Timeline showing some of the history of Electro-Organic Chemistry from 1800-2020.*[1,19,29–34,21–28]

Generally, electrochemical reactions proceed by way of either oxidations or reductions to generate the desired product. In these processes a stoichiometric amount of electric charge is needed to achieve full conversion. However, in certain processes sub-stoichiometric charge is adequate and these processes are described as being 'electrocatalysed'.[35] An example of an electrocatalysed synthetic process from the Chiba group shows that a Diels-Alder [4+2] cycloaddition could be promoted by single-electron-transfers (**Scheme 1**).[36]

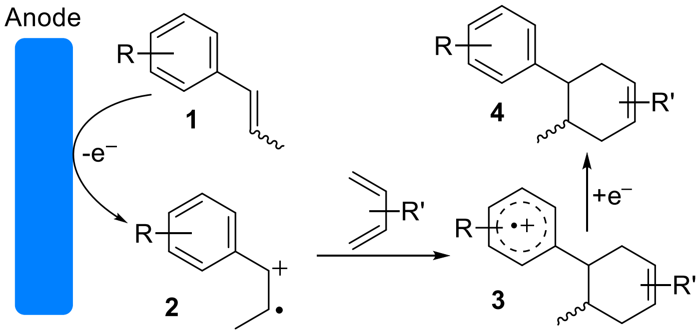

***Scheme 1**: Electrocatalysed Diels-Alder reaction.*[35,36]

It is thought that because **3** is a stronger oxidant than **2** it is reduced to the final product at the potential of the **1** / **2** REDOX couple by a chain process (rather than at the cathode). Due to the observed stereoselectivity of products the authors believe that this electrochemical reaction proceeded stepwise, rather than in the concerted manner usually associated with Diels-Alder reactions.[35] Other examples of electrocatalysed processes in the literature include the Newman-Kwart rearrangement[37] and *E*-*Z* isomerisation of olefins.[35,38]

1.2 Methodology

The experimental work carried out in this project is very often electrochemical in nature, despite the reactions themselves being firmly rooted in organic chemistry. As such, the equipment and methods used to perform such reactions requires some explanation and discussion.

In general, the work-up and purification parts of reactions described in this report remain 'organic' in nature, in that they do not differ from standard organic chemistry practices and so require no further discussion here. The major difference from a standard organic reaction lies in the use of electrodes and electrolyte solutions. This allows electrons to be given to, or taken away from compounds in solution, thus allowing reactions to take place. In other words, this facilitates REDOX chemistry.

Figure 2 shows the apparatus and example electrodes used to carry out reactions in either an undivided cell or a divided cell. The major components in all setups are: i. an electrolyte solution which, in a broad sense, is a charged species dissolved in a solvent that can carry charge from one electrode to the other (e.g. NaBr dissolved in MeOH), ii. electrodes that rest in the electrolyte solution and conduct electrons to or from the potentiostat, iii. a potentiostat, iv. a reaction vessel or cell (divided or undivided).

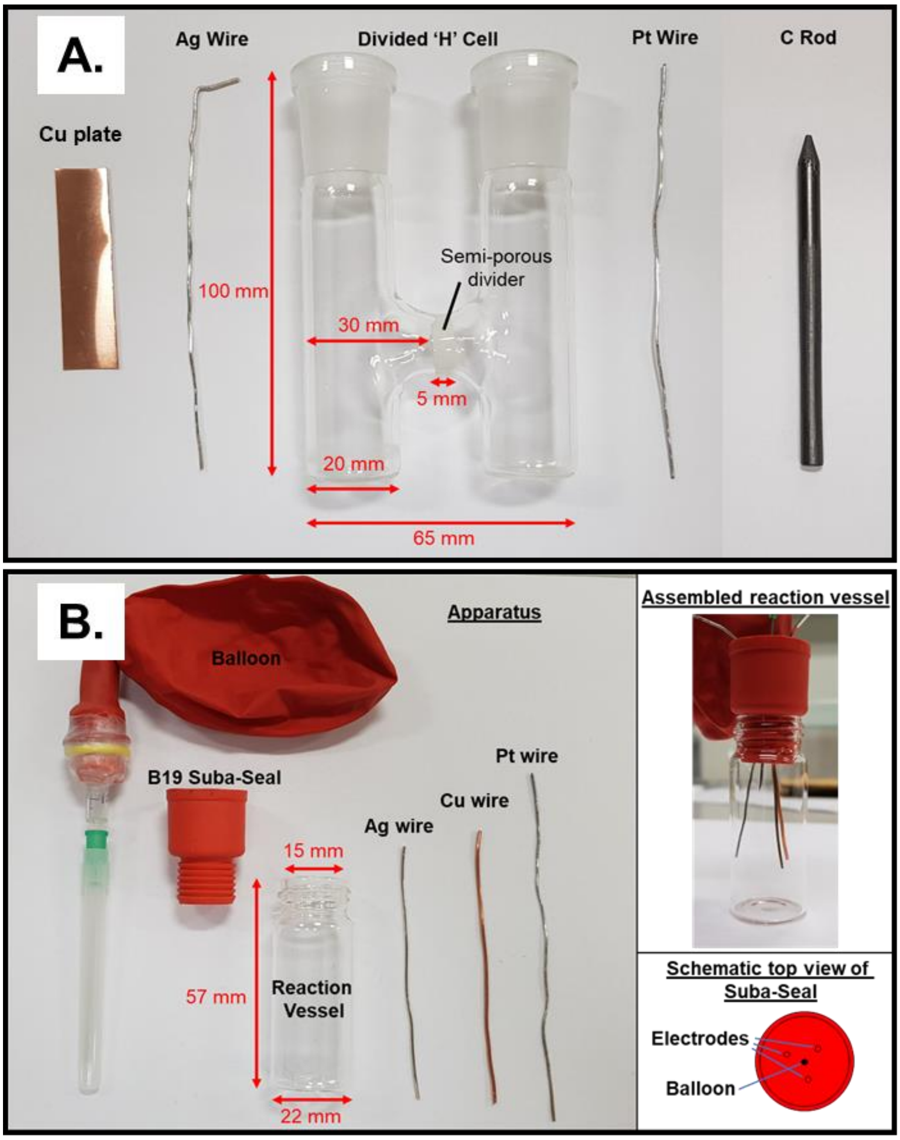

***Figure 2**: A. Example of a divided 'H' cell. B. Example of an undivided cell.*[20,39,40]

Figure 2, A shows a divided (also known as an 'H') cell. **Figure 2, B** shows an undivided cell which in this case is a simple plastic vial, but can also be a round-bottomed flask, or anything that does not separate the working electrode and counter electrode. In the example image a balloon can easily be incorporated into the setup to allow reactions to be carried out under an atmosphere of whatever gas may be required. The same can be done with the divided cell following some modifications to mitigate pressure differences caused by introducing gas to one chamber and not the other (i.e. adding a connective glass tube above the solvent layer to link the two chambers). The difference between the two types of cell is simply whether the working electrode and the counter electrode are separated or not. This separation is easily achieved using an H cell, because it has a chamber either side of a sintered glass semi-porous divider. The divider is designed to prevent the mixing of the solutions that are in each chamber, but still allow small ions through to carry charge and complete the circuit.

Typically, for electrochemical experiments, a three electrode system is used (a working electrode (WE), a reference electrode (RE) and a counter electrode (CE)) to ensure that current only flows between the working electrode and the counter electrode and that the potential of the working electrode is measured relative to that of the reference electrode. Usually the RE is comprised of species in equilibrium which have a well-defined electrode potential, such as Ag metal and AgCl in an aqueous solution (the AgCl reference electrode). The RE draws negligible current and hence its composition is unchanged during the measurement. This means that the equilibrium and resulting potential at the interface remain constant.

The reference electrode is used as a means of replication of experimentation across different setups and equipment, because any applied potential is compared against this reference. In other words, if the potential is set to +1.30 V on the potentiostat, there will be a potential difference of +1.30 V between the WE and the RE. In a divided cell the working electrode and the reference are kept in the same chamber to limit the potential drop caused by resistance from keeping the electrodes far apart. During this project we elected to use a Ag wire on its own as a Quasi Reference Electrode (QRE) instead of using a full reference electrode. This was partly for convenience, but also because there are few universal reference electrodes that are suitable for non-aqueous solvents. Ag had the benefit of being a very malleable electrode which did not interfere with other components of our experimental apparatus (such as stirrer bars and argon balloons) but had the drawback of not being a rigorously accurate reference, as a well-defined equilibrium may not have existed at its interface during reactions. This meant that the potential of the QRE was sensitive to changes in solution composition and could drift over time. Generally, such QREs maintain a constant potential during a measurement if the solution composition or the area in contact with solution does not change too much. However, their potential can vary between different experiments (e.g. if carried out on different days). To overcome this, we employed ferrocene as an internal reference to measure potentials in Cyclic Voltammetry (CV) plots as discussed later in this chapter. This is a standard calibration procedure that is commonly carried out for electrochemical measurements in non-aqueous electrolytes.

The working electrode is used to deliver the potential or current the potentiostat is set to. This can be a constant potential, chronoamperometry (also known as bulk electrolysis), or a constant current, chronopotentiometry.[41] In this project, chronoamperometry was exclusively used because we believe it allowed for more precise selectivity over which reagents were oxidised and reduced than chronopotentiometry. A constant current experiment will move through a range of potentials, which can allow a range of reactions to take place. The current essentially controls the rate of reaction. Potential is more akin to how much energy is needed to move the electrons. Another method that can be used to perform electrochemical reactions is switching current electrolysis in which pulses of differing currents are applied. This can be useful for switching the polarity of the WE to remove precipitates that may foul the surface of the electrode throughout a reaction. Compared to chronoamperometry and chronopotentiometry this technique is quite rarely used in the literature and applications in organic synthesis are limited.[42]

The counter electrode opposes the working electrode by maintaining an equal but opposite current to keep charge flowing around the circuit.

A potentiostat is capable of delivering oxidative and reductive potentials to reaction mixtures, which promotes REDOX chemistry. An applied oxidative potential, with enough energy, will remove electrons from the HOMO of certain chemical species, i.e. oxidation, and an applied reductive potential with enough energy will donate electrons into the LUMO, i.e. reduction. Electrons are drawn into the anode and given out from the cathode. A key thing of note is that anode/anodic oxidation and cathode/cathodic reduction are often used as nomenclature in the literature. An electrode with an oxidising potential is the anode and an electrode with a reductive potential is the cathode.[43–47]

When deciding what potential to apply in reactions, a crucial technique that is often employed is to record a CV plot of the reagents in question. This technique involves using a potentiostat to measure changes in current as the potential is altered incrementally. This creates certain peaks when a species is oxidised or reduced as an increase in current accompanies these REDOX processes, and these peaks indicate what potential is best to use in a reaction to achieve REDOX of the reactive species in question. **Figure 3** shows a CV plot of ferrocene recorded in the Wilden group.

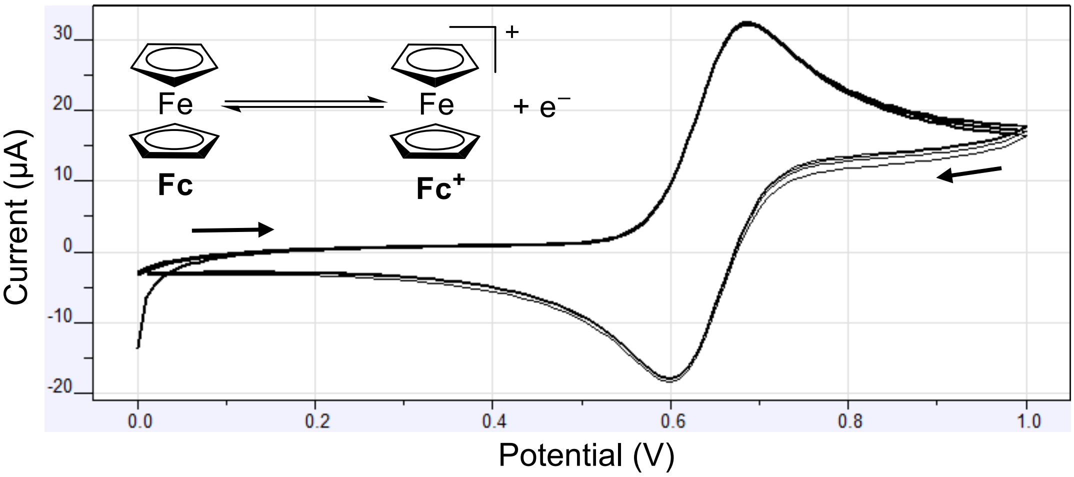

Figure 3: *Showing a CV plot of ferrocene recorded in 0.1 M* Bu_4NPF_6 */ MeCN using a glassy carbon WE, Ag QRE and Pt CE.*

It is clear from the CV plot of ferrocene that as the potential is increased in a more positive direction from 0 V, a peak forms, denoting the oxidation of ferrocene (Fc) to the ferrocenium ion (Fc^+), Fe^{2+} to Fe^{3+}. On the reverse scan, a negative peak appears where this is reversed: reduction of the ferrocenium ion back to ferrocene. The oxidation and reduction peaks appear very similar in magnitude, which indicates a highly reversible process. If only an oxidation or a reduction peak were present, with no REDOX couple, then this would indicate an irreversible process has taken place. It is important to mention that after this PhD project was completed, we received guidance on ways to improve how we carry out CV plots for future reference. The use of multiple cycles layered over each other as seen in the CV plots in this thesis is unnecessary and only the first cycle should be used. This is because after the first cycle the environment within the solution is no longer the same and so multiple cycles are not comparable. Also, the presence of the erroneous starting line (at 0 V in **Figure 3** which rises sharply from -15 µA on the first cycle) can be avoided by simply holding the potential at 0 V for 1-2 seconds before proceeding with the CV scan. However, these errors did not invalidate the information gleaned from our CV plot analysis in this thesis and values for potential were taken from the first cycle to ensure accuracy.

Using CV plots to measure the potential at which oxidation and reduction occurs is very useful and indeed, due to the very characteristic, clear and well-defined nature of the ferrocene REDOX couple, ferrocene is actually used as an internal reference, against which other potentials are measured (as shown in this report and quoted as ‘vs Fc/Fc^+’).[48–50] Furthermore, because ferrocene has a stable and highly reversible REDOX couple it is often employed as a mediator in electrochemical reactions (see ‘Indirect Electrolysis’ in **Figure 1** and **Scheme 2**). Occasionally, direct electrolysis of a substrate proves difficult due to the heterogeneous electron transfer process to/from an electrode having slow kinetics. Conductivity to the bulk solution can be hindered by organic species adsorbing to the surface of electrodes and forming layers. In these cases, a mediator which is stable in both oxidation states may be used which undergoes more efficient electron transfer processes with an electrode than the direct electrolysis of the substrate. The mediator can then efficiently, homogeneously transfer electrons to/from the substrate, facilitating the reaction at lower REDOX potentials than would be required for direct electrolysis. A fast, irreversible follow-up reaction for the electrolysed substrate to the desired product is usually necessary to achieve this effect.[42]

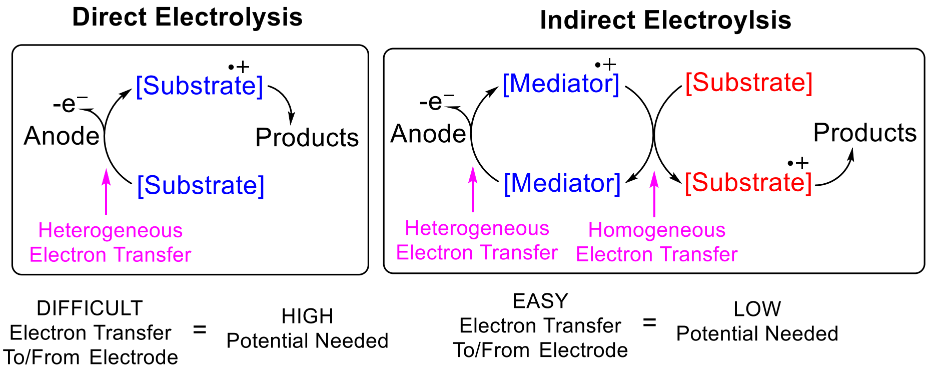

***Scheme 2**: A situation in which indirect electrolysis facilitated by a mediator may be preferred over direct electrolysis.*[42]

When carrying out reactions, and producing CV plots, an electrolyte solution must be used. This is very often ‘inert’ in the sense that the salts used require high applied potentials to enable any sort of REDOX to take place on them. This allows the electrolytes to simply carry charge in solution without interfering with experiments. Often Bu_4NPF_6 or $LiClO_4$ are used as electrolytes, which are dissolved in standard organic solvents. However, other (non-inert) electrolyte salts can purposefully be used to enable reactions to take place.

The next chapter in this thesis outlines our work in halogenation chemistry, which was the first area we worked on in this PhD project to help build our understanding of electro-organic synthesis. **Chapter 3** then explains why we chose to investigate copper chemistry for the remainder of the project. **Chapter 4** details our work on the synthesis of copper acetylides, which leads into reactions that rely on copper acetylides as intermediates: **Chapter 5**, the CuAAC reaction and **Chapter 6**, the Glaser-Hay reaction. **Chapter 7** then looks at the generation of copper ions to promote a non-copper acetylide-based reaction, the Chan-Lam reaction. Finally, **Chapter 8** shows our investigation into the sustainable recovery of Cu after reactions have been completed and **Chapter 9** gives overall conclusions and details of proposed future work.

Chapter 2. A Foray into Halogenation

The first work carried out in this project was centred around halogenation chemistry, as we wanted to develop our understanding of how electrochemical reactions are performed. This work gave vital understanding of processes which would later be applied to the main topic of this thesis, copper chemistry, and thus warrants discussion in this chapter.

2.1 Introduction

Halogen-containing compounds make for attractive substrates in electro-organic chemistry because they can be both oxidised and reduced relatively easily, as well as being quite useful as a means to oxidise other species. In electrochemical setups, REDOX reactions usually take place directly at electrode surfaces and either involve a substrate (e.g. a halogen-containing compound that is added to the solution as a starting material) or the electrolyte salt itself (which is often a halide salt such as Bu_4NI due to its solubility in organic solvents) adsorbing onto the electrode. The first few literature examples in this section demonstrate substrate-based chemistry and are all reductions, whereas the later examples all stem from oxidation of the electrolyte salt.

In terms of reduction, 1,3-dihalogenated species have been shown to undergo reductive ring closure reactions when subjected to a reductive potential with enough energy. In work carried out by Hoffman and Voß[51] 1,3-dibromocyclopentane and 1,3-dibromocyclohexane were shown to form their respective ring-closed products as depicted in **Scheme 3**.

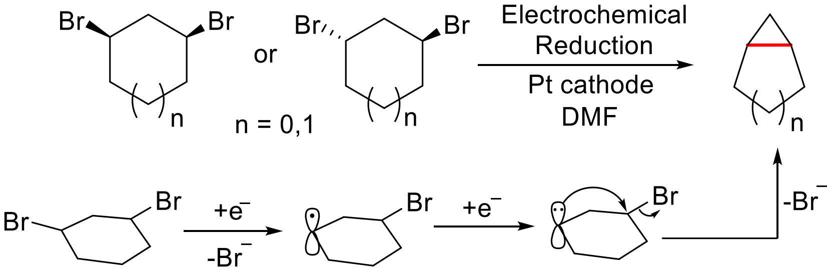

***Scheme 3**: Reductive ring-closure of 1,3-dibromocyclic compounds.*[51]

A similar process was reported by Leonel *et al.*[52] who showed that the 1,2-dibrominated compound **5** formed stilbene upon electrochemical reduction as shown in **Scheme 4**, presumably *via* a very similar process as seen in **Scheme 3**.

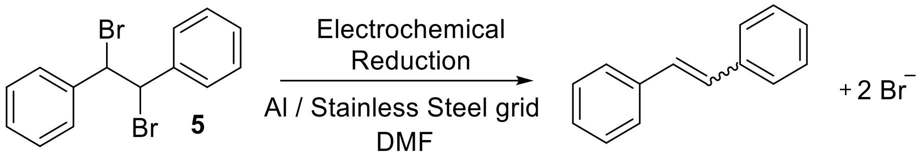

***Scheme 4**: Reduction of a 1,2-dibromo compound to yield the complementary alkene.*[52]

Reduction of alkyne-based systems has also been demonstrated with an interesting example coming from D. G. Peters *et al.*,[53] who showed that the electrochemical reduction of C-I bonds in substrates could be achieved to promote intramolecular cyclisation using a mercury pool cathode. The use of a mercury electrode is important as it was thought to drastically increase the lifetime of the carbon-centred radical (see **Scheme 5**).

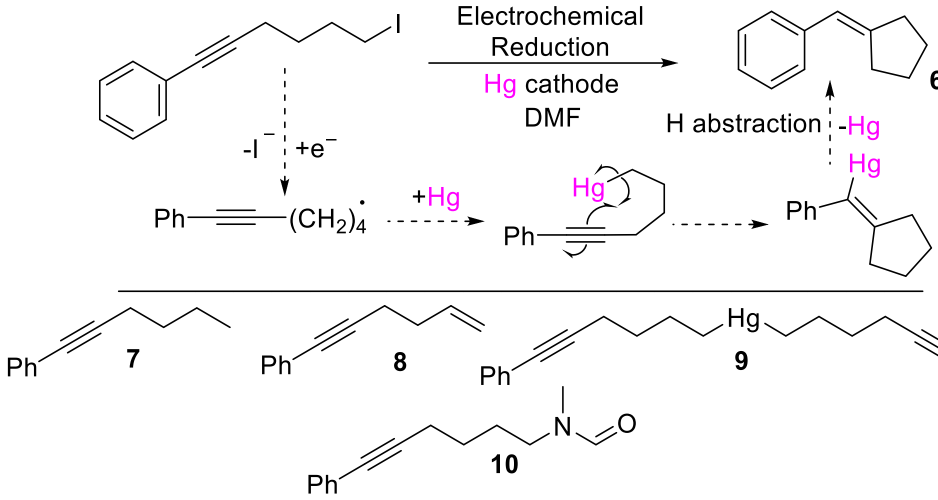

***Scheme 5**: Reduction of a C-I bond in the presence of mercury to promote cyclisation.*[53]

It is worth noting that the cyclised product **6** was only isolated in a fairly low yield, the best being around 25%, as many side reactions also took place, producing de-halogenated species such as **7** and **8**, as well as the acyclic dialkyl mercury species **9**. Reaction with the DMF solvent was also observed, producing **10**.[53]

There has been quite a lot of research showing how transition metal complexes can effectively be utilised as meditators in this sort of reduction.[54] This approach appears to require a lower applied potential to proceed than the examples already seen, as the previous examples work *via* direct reduction of the carbon-halogen bond. An example of a mechanistic pathway using 1-bromobutane and a cobalt tetraphenylporphyrin complex (Co(II)TPP) is shown in **Scheme 6**. Nickel and samarium examples are also known.[54–56]

A. $Co(II)TPP + e^- \xrightarrow[\text{Reduction}]{\text{Electrochemcial}} [Co(I)TPP]^-$

B. $[Co(I)TPP]^- + C_4H_9Br \longrightarrow H_9C_4Co(III)TPP + Br^-$

C. $H_9C_4Co(III)TPP + e^- \xrightarrow[\text{Reduction}]{\text{Electrochemcial}} [H_9C_4Co(II)TPP]^-$

D. $[H_9C_4Co(II)TPP]^- \xrightarrow[\text{Decomposition}]{\text{Two types of}} \begin{matrix} [Co(I)TPP]^- + {}^{\bullet}C_4H_9 \\ Co(II)TPP + {}^{-}C_4H_9 \end{matrix}$

***Scheme 6**: Mechanistic pathway for Co(II)TPP-mediated 1-bromobutane reduction.*[54,55]

It is noteworthy that the two types of decomposition seen in step **D** produce more reduced Co(I) species (which can go straight back into the pathway at step **B**) and the regenerated Co(II) complex (which can start a new cycle as in step **A**), as well as the alkyl radicals and carbanions which go on to form the products.[54,55]

Oxidising halide anions is often easier than oxidising other molecules in solution. This means that it is possible to carry out a range of reactions[2] without also oxidising the substrate of interest, as demonstrated in a series of papers published by Sigeru Torii between 1979 and 1981.[2,5,43,57–59] The core idea in all of these papers was the use of constant current to oxidise an X^- species from the electrolyte solution to X^+, by removing a pair of electrons. This allowed the halonium ion to react directly with an olefin substrate or to react with another X^- molecule in solution, forming X_2, before reacting with the substrate. As this same approach is used in work carried out in this project, it is worth discussing these examples in more detail.

Torii found that different products were isolated when the reaction conditions were altered even slightly (see **Scheme 7**).[43,57] This approach is elegant because the reactive species is generated from the electrolyte itself, which is needed in all electrochemical reactions to carry charge between electrodes. Also, the use of cheap and non-hazardous salts to effectively produce X_2 species in solution, in a controlled manner, is a very attractive alternative to adding the potentially harmful halogen species directly (especially on larger scales).

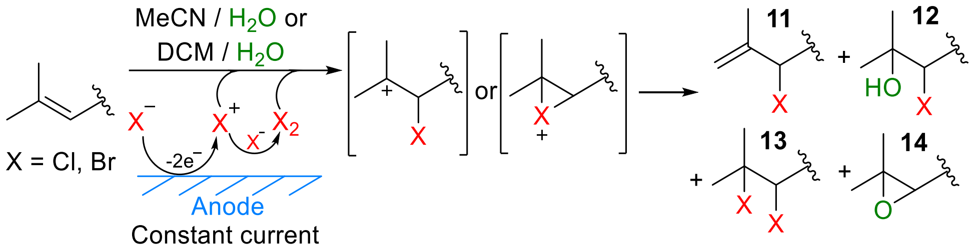

***Scheme 7**: Showing oxidation of a halide salt producing the halonium ion, which has been shown to form a range of products depending on the reaction conditions used.*[5,43,57–59]

In **Scheme 7** the halide salts used were either NaCl or NaBr in MeCN/H_2O or DCM/H_2O mixed solvent systems. The amount of halide salt used was altered to produce varying amounts of the allylic halide **11**, the halohydrin **12**, the dihalide **13** and the epoxide **14**. It appeared that when 1-2 eq of NaBr was used in MeCN/H_2O (7:2 mL) the epoxide product was formed almost exclusively, but as the amount of NaBr was increased up to 4 eq, the product selectivity decreased, yielding a mixture of **12**, **13**, and **14**. When NaCl was used, it was in great excess (12 eq) to try and force the dichloride product to form, however, this proved unsuccessful and another range of products (**11**, **12** and **14**, but not **13**) were observed. Switching to a two-phase DCM/H_2O (6:3 mL) solvent system yielded a mixture of **11**, **12** and **13** when NaBr (19 eq) was used. However, and quite interestingly, when NaCl (12 eq) was used, only the allylic chloride product **11** was observed and isolated in 91% yield. This, coupled with the fact that no dichloride product was observed in either solvent system, led Torii to hypothesise that the reaction of the chloronium ion with the alkene, and the deprotonation of the adjacent methyl group, to yield **11**, was a concerted process.[43,57]

Another use of this approach was the production of alkoxyselenide compounds[5] directly from a diselenide starting material, as shown in **Scheme 8**. This conversion required a sub-stoichiometric amount of the halide salt, most likely because larger amounts would produce some of the products seen previously in **Scheme 7**. In this example, a haloselenide compound is formed first, which reacts with the alkene substrate. This then allows the alkoxyselenide product to form.

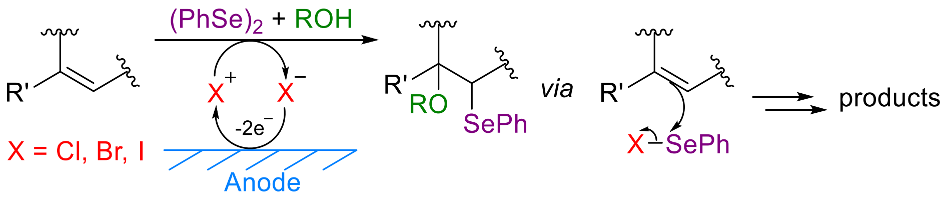

***Scheme 8**: Showing the formation of alkoxyselenides using electrochemically oxidised halide salts.*[5]

2.2 Results

The first part of this project was centred on electrolyte halide salts, and how they could be used to generate halogen species in solution, through oxidation. The literature shows that it is certainly possible to produce X^+/X_2 using a constant current *via* anodic oxidation, but we wanted to use a constant potential approach.

Initially, iodide salts were used on the basis that they should be relatively easy to oxidise, and as a simple substrate, we decided to try iodinating *trans*-stilbene. For the first few tests we used 0.1 M Bu_4NI dissolved in DMF at +0.50 V vs Ag Quasi Reference Electrode (QRE). Under these conditions, the solution turned yellow, which suggested that I_2 and, by extension, I_3^- ions, were being generated, but there did not appear to be any new products formed (from TLC). A review of the literature showed that the iodinated product of stilbene has not actually been isolated from any reaction before, probably due to the large size of iodine atoms which would make the diiodinated stilbene product quite sterically-hindered, as well as the fact that carbon-iodine bonds are relatively weak, possibly meaning the reaction with stilbene is reversible. Also, given that any iodine generated in this reaction would probably form I_3^- ions, this approach seemed unlikely to be successful. We decided, therefore, to use bromide salts instead. This time, when 0.1 M Bu_4NBr was dissolved in MeCN and the potential was set to +1.00 V, a new product did start to form. However, after approximately 7 h TLC showed that the reaction had still not reached completion. It was hypothesised that under the current conditions, very little bromine was being produced. As a result, the reaction was attempted again, but with the amount of TBAB in solution increased to 1 M dissolved in MeCN. This had an immediate effect as now the solution turned a dark brown colour upon application of the potential, instead of the pale yellow colour seen in the previous reactions. In addition, after 7 h, some white precipitate had formed. But again, TLC showed that the reaction had not reached completion. Upon collection by filtration and characterisation, this white solid turned out to be the desired dibrominated stilbene product **5** in 45% yield. The most obvious next step was to leave the potentiostat running overnight (~16 h total) to see if, given more time, the reaction could be pushed to completion. When this was attempted, product **5** was isolated in 68% (see **Scheme 9**). When no electricity was used in a control test, the reaction did not proceed.

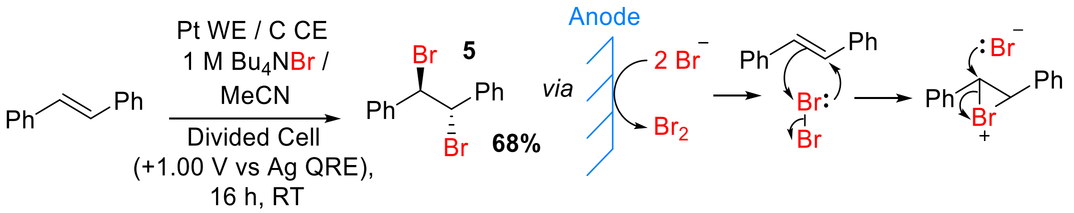

Scheme 9: Electrochemical bromination of stilbene.

Up to this point, the potential selected for reactions was quite trial-and-error, i.e. +1.00 V (vs Ag QRE) because at lower applied potentials of around +0.50 V, no reaction occurred. It was at this juncture that we decided a more accurate approach should be adopted to find the optimal potentials to use. To this end, we decided to investigate the bromide salt Bu_4NBr (TBAB) further and record various CV plots. Our results are outlined in **Figure 4**.

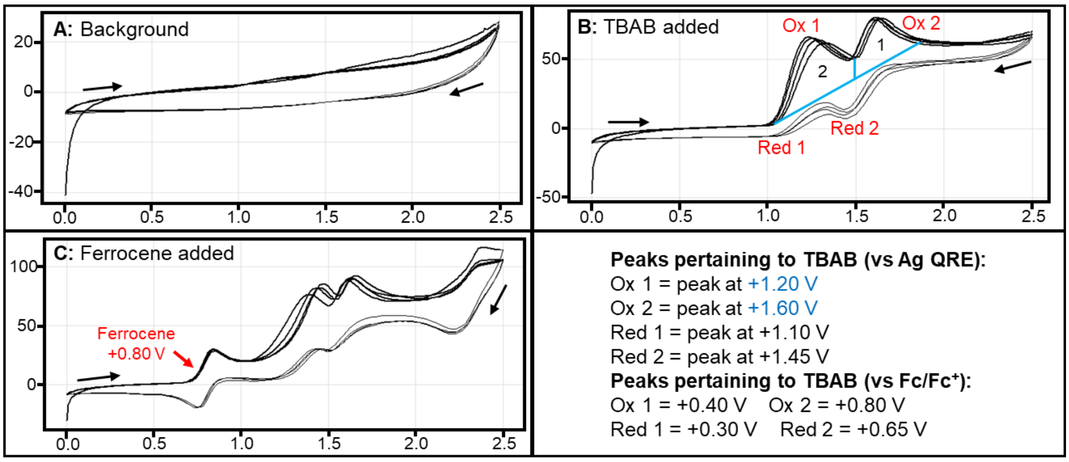

Peaks pertaining to TBAB (vs Ag QRE):
Ox 1 = peak at +1.20 V
Ox 2 = peak at +1.60 V
Red 1 = peak at +1.10 V
Red 2 = peak at +1.45 V
Peaks pertaining to TBAB (vs Fc/Fc$^+$):
Ox 1 = +0.40 V Ox 2 = +0.80 V
Red 1 = +0.30 V Red 2 = +0.65 V

***Figure 4**: Showing the CV plot of TBAB recorded in 0.1 M Bu_4NPF_6 / MeCN using a glassy carbon WE, Ag QRE and a Pt CE. Y axes = Current (µA), X axes = Potential (V). Axes redrawn for clarity.*

When recording CV plots, it was important to thoroughly degas the electrolyte solution before any electricity was passed to remove oxygen from the solution, which would otherwise give rise to unwanted peaks. Plot **A** is a background CV plot, showing a smooth line with no peaks until around +2.50 V, where the electrolyte solution starts to oxidise. Plot **B** was obtained after TBAB was added, clearly showing two oxidation peaks (Ox 1 and Ox 2) and two smaller reduction peaks (Red 1 and Red 2). Note that Ox 1 and Red 1 are a REDOX couple, as are Ox 2 and Red 2. Essentially, the oxidation seen at Ox 2 is reversed at Red 2 and the same for the other REDOX couple. Plot **C** was obtained after ferrocene was added to the solution and shows the characteristic reversible REDOX couple at approximately +0.80 V. This was undertaken to calibrate the potentials recorded on our setup and make them relatable to other potentiostats and systems. The box in the bottom right summarises the potentials of the observed peaks, and the relative potentials when compared to the ferrocene/ferrocenium ion REDOX couple (Fc/Fc$^+$). Plots carried out using NaBr gave identical results. The most important thing to take away from **Figure 4** is that there are two discrete oxidation peaks for TBAB, the first at +1.20 V and the second at +1.60 V (both vs Ag QRE). After reviewing the literature, it appears that these two peaks relate to the formation of Br_3^- ions, and Br_2 molecules respectively.[60,61] The full equation for this being shown in **Eq. 2**:

$$6Br^- \xrightleftharpoons{-4e^-} 2Br_3^- \xrightleftharpoons{-2e^-} 3Br_2 \qquad \textbf{(Eq. 2)}$$

This is supported by the fact that the relative area under each peak appears to be in a 2:1 ratio, which is indicative of there being twice as many electrons being removed in the first oxidation compared to the second. It also suggests that we had generated a weak bromine source in the form of Br_3^- in solution with the +1.00 V vs Ag QRE we had been using so far for the bromination reactions. This is in contrast to the constant current approach used by Torii that appeared to give only the halonium ion as seen in **Scheme 7**.[43,57]

Following on from the results seen in **Figure 4**, we decided to record CV plots of TBAC (**Figure 5**) and TBAI (**Figure 6**).

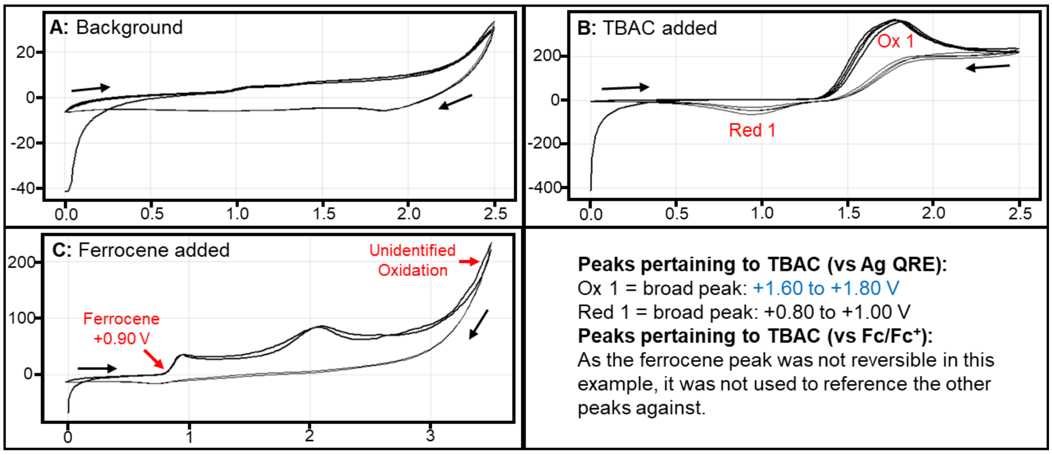

Peaks pertaining to TBAC (vs Ag QRE):
Ox 1 = broad peak: +1.60 to +1.80 V
Red 1 = broad peak: +0.80 to +1.00 V
Peaks pertaining to TBAC (vs Fc/Fc⁺):
As the ferrocene peak was not reversible in this example, it was not used to reference the other peaks against.

***Figure 5**: Showing the CV plot of TBAC recorded in 0.1 M Bu_4NPF_6 / MeCN using a glassy carbon WE, Ag QRE and a Pt CE. Y axes = Current (μA), X axes = Potential (V). Axes redrawn for clarity.*

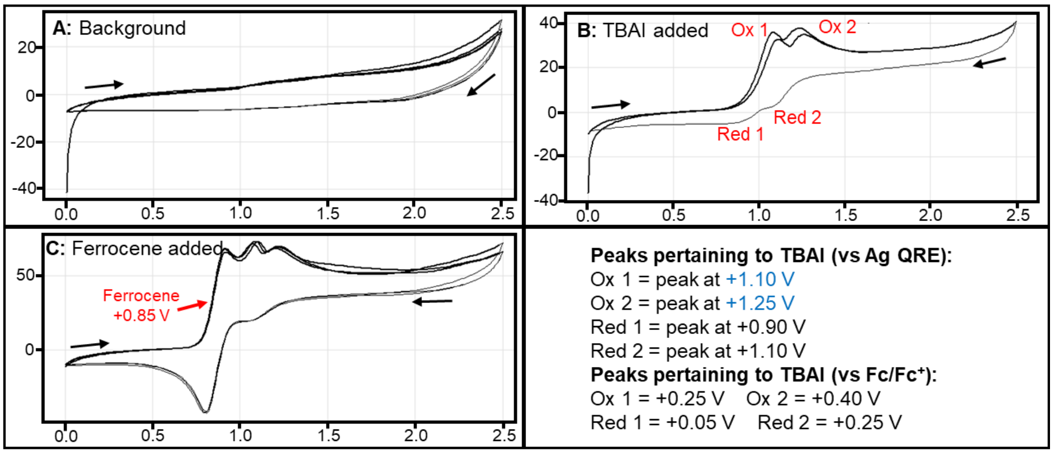

Peaks pertaining to TBAI (vs Ag QRE):
Ox 1 = peak at +1.10 V
Ox 2 = peak at +1.25 V
Red 1 = peak at +0.90 V
Red 2 = peak at +1.10 V
Peaks pertaining to TBAI (vs Fc/Fc⁺):
Ox 1 = +0.25 V Ox 2 = +0.40 V
Red 1 = +0.05 V Red 2 = +0.25 V

***Figure 6**: Showing the CV plot of TBAI recorded in 0.1 M Bu_4NPF_6 / MeCN using a glassy carbon WE, Ag QRE and a Pt CE. Y axes = Current (μA), X axes = Potential (V). Axes redrawn for clarity.*

Figure 5 shows that only one oxidation peak was observed for the chloride ions in the range we were investigating, because above +3.00 V a large peak that overshadows everything else, which we tentatively ascribe to electrolyte solution oxidation, appears. This peak is listed as the ‘unidentified oxidation’ peak in **Figure 5** as we did not further investigate this assignment. Notably, the oxidation of the chloride ions takes place at a higher potential than the bromide ions, as expected due to the greater electronegativity and smaller atomic radius of chlorine atoms. Note that in this example the ferrocene peak was not reversible, meaning that it was not used to reference the other peaks against. **Figure 6** shows a very similar CV plot to that produced from TBAB, but with two major differences: the oxidation takes place at a lower potential, which is what we expect given iodine's larger atomic radius, and the oxidation peaks are closer together.

With the numbers gleaned from these CV plots, a few attempts were made to form the chlorinated stilbene product **15**. In many ways, the ability to produce chlorine in solution is a lot more useful synthetically than the other halogens, given that bromine and iodine are reasonably simple to handle, whereas chlorine usually has to be bubbled through solutions from gas cylinders. Unfortunately, when an analogous reaction to that seen in **Scheme 9** was attempted with TBAC, a mixture of products was observed, which proved extremely difficult to separate and isolate. This is likely because a much higher potential had to be used in order to get any reaction to occur, compared to the TBAB example, which may have caused side reactions to take place. The crude ^{1}H NMR spectrum seemed to show a lot of activity in the aromatic region, suggesting that perhaps the chlorine species may have reacted with the phenyl groups, or that the stilbene substrate itself was oxidised and went on to form unanticipated products (see **Scheme 10**).

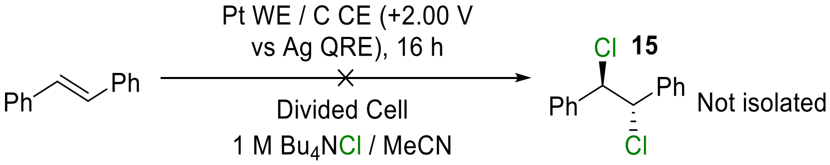

***Scheme 10**: Attempted electrochemical chlorination of stilbene.*

A few attempts were made to produce mixed halide products using mixtures of TBAB and TBAF. Usually, mixed bromo-fluoro compounds are produced using highly dangerous Br-F produced *in situ*.[62] We believed that with the +1.00 V potential already established for the TBAB, only the bromide ions would be oxidised, hopefully allowing fluoride ions to attack the halonium ion formed, as in **Scheme 11**. Unfortunately, this approach proved unsuccessful, with not even the dibrominated product being observed.

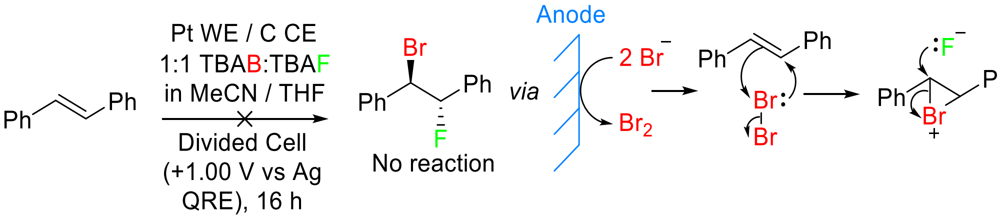

***Scheme 11**: Attempted mixed bromo-fluorination of stilbene.*

In an effort to prove that the use of electrochemistry to perform reactions can be accessible and does not require an expensive potentiostat to work, the use of batteries as a source of electrons was investigated. Using, again, the same reaction seen in **Scheme 9**, a pair of household AAA batteries, with a voltage reading of +1.50 V each (reading around +3.00 V in total*) were connected in series, and the exact same electrodes and reaction conditions were used. Interestingly, the dibrominated stilbene product **5** was formed, but only in around 1% yield in the same amount of time that the reaction connected to the potentiostat yielded 68%. This highlights a very significant point, in that the potentiostat delivers a higher current (i.e. more electrons per unit time) than a standard household battery, making the reaction proceed faster, despite the potential likely being sufficient to oxidise bromide ions to bromine in both cases. Over time, full conversion to **5** could be achieved, but it would take a very long time.

The bromination of stilbene using NaBr in MeOH was attempted to compare against the established TBAB in MeCN reaction. Interestingly, this reaction produced quite a different result. Firstly, the solution never appeared to go as dark orange/brown as the TBAB reaction, which suggests less bromine was being produced. This could be due to the fact that at the potential used in this reaction (+1.30 V vs Ag QRE) the MeOH was also susceptible to oxidation, meaning the bromide ions had to compete with the vast excess of solvent molecules in order to be oxidised. Secondly, both the expected product **5** and a new product, methoxy-brominated stilbene **16**, were formed in a 1:3 ratio respectively (conversion = 9% **5** and 33% **16**) by ^{1}H NMR). See **Scheme 12**. Due to solubility issues, complete separation of these products proved difficult, however, an isolated yield of 14% was obtained for **16**. The dibrominated product **5** unfortunately coeluted with **16**.

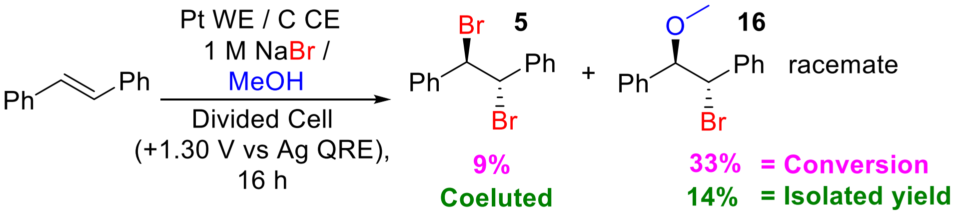

***Scheme 12**: Formation of bromo-methoxy stilbene.*

---

* There was an important difference between the potential measured for the household batteries and that measured on the potentiostat. The potential measured on the batteries comes from the potential difference between the 'positive end' and the 'negative end', whilst the potential on a potentiostat is measured between the reference electrode and the working electrode. This means that the batteries would have experienced much more resistance between the points of measurement and thus a larger potential drop. This is precisely why two batteries were used, at around +3.00 V total, rather than only one.

Although the formation of bromo-methoxy stilbene in this way was successful, the reaction and mechanism had already been comprehensively studied previously by J.-E. Dubois *et al.*[63] and J. R. Chretien *et al.*[64] Our initial investigations replicated the work of those researches and as such served as valuable proof-of-concept studies that gave us confidence in our approach and the equipment. This allowed us to move forward to novel and more speculative work.

Chapter 3. Why Use Copper?

We became inspired by the generation of catalytic species from electrode materials as a means to promote synthetic reactions. This approach, with examples, is described in the following chapter, as is the reason why we believed copper would be a perfect element to use in this capacity, i.e. because it is immensely versatile in synthesis.

3.1 Generating Catalytic Species from Electrodes

The electrochemically promoted reactions seen so far have centred on direct REDOX reactions of reagents at electrodes, or on the generation of reactive species from electrolytic salts. Another method is the generation of reactive species from the electrode material itself. In some ways, this method may appear unusual because electrodes are often expensive metals such as platinum and are important for the movement of current around the circuit. Breaking them down may seem counterintuitive. However, only very small quantities of metal need be extracted from the electrodes to catalyse reactions. There also exists the possibility that if the electrodes can be dismantled electrochemically, producing reactive metal species, they could also theoretically be recovered using electrochemistry.

In 2013, an interesting paper published by M. Mellah *et al*.[65] showed how a samarium anode in an electrolyte solution containing Bu_4NI could produce Sm^{2+} from the bulk Sm^0 electrode as shown in **Scheme 13** (stage 1). The current was allowed to flow until around 10 mol% Sm^{2+} was formed, at which point, aldehydes or ketones were added and the polarity of the electrodes was switched to make the samarium anode now the cathode. The carbonyl compounds underwent a pinacol-type coupling reaction, catalysed by the Sm^{2+} (stage 2) forming Sm^{3+}. The switch from anode to cathode was a very elegant touch which allowed the Sm^{2+} to be regenerated after catalysing the reaction (Sm^{3+} back to Sm^{2+}, stage 3), thus keeping the overall amount of Sm^{2+} needed (and the amount taken from the expensive samarium electrode) to a minimum. This is summarised in **Scheme 13**.[65]

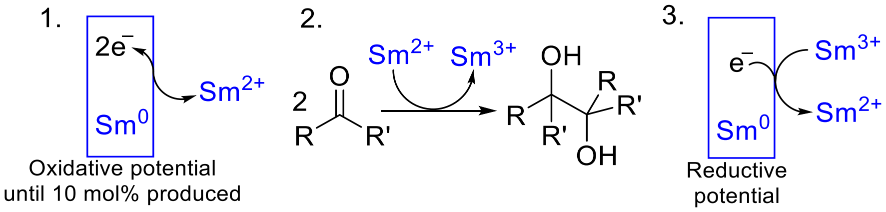

Scheme 13*: Showing the use of a samarium electrode as an effective means to produce reactive* Sm^{2+} *in solution for homocoupling reactions.*[65]

Another example of this sort of approach comes from H. Tanaka *et al.*[44] in 2010 who showed that a silver electrode could be used effectively to produce Ag^+ ions in solution, which were used to form silver acetylides from terminal aryl alkynes, in an acetonitrile/water solvent system (7:1 mL). These silver acetylides were then also generated in the presence of arylboronic acids and 5 mol% $Pd(OAc)_2$, which allowed for the immediate reaction of the acetylides in a Sonogashira-type process to produce homo- and hetero-coupled alkynes. See **Scheme 14** for the catalytic cycle involved (starting materials in blue, product in red). 15 mol% 4-BzO-TEMPO was used as the oxidant to convert the Pd(0) back into Pd(II), however, it was noted that when no oxidant was used, the reaction still proceeded as the silver ions could act as the oxidant instead.[44]

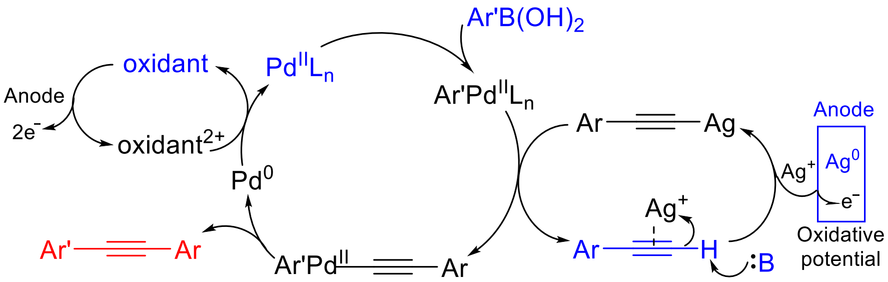

Scheme 14: *Showing the catalytic cycle involved in the production of coupled products from electrochemically-produced silver acetylides and boronic acids.*[44]

A number of bases were screened in this work to best determine the optimal conditions needed to produce the silver acetylides. It was found that 2 equivalents of DBU proved most effective, however, DABCO and triethylamine also worked reasonably well.[44]

While this work shows an effective method for producing biaryl alkynes electrochemically, it also has a few drawbacks, notably, the breakdown of reasonably expensive silver electrodes and the requirement of a palladium catalyst. A cheaper and arguably more versatile alternative would be to use copper instead of silver. Whilst still being a group 11 transition metal, copper is much more abundant, and cheaper, than silver, making it a more attractive electrode material given the inherent loss incurred by using it to produce catalytic species in solution. To the best of our knowledge, however, the electrochemical generation of copper ions from an electrode has only ever been used to produce various copper cyanate[66] or copper alkoxide[67,68] species rather than to help facilitate organic synthetic reactions. On top of this, copper has been employed in a vast number of coupling reactions[69] and has potential to replace some existing expensive palladium-catalysed processes in industry.[70] Furthermore, copper has been party to a rapid ascent in visible light-mediated photoredox chemistry,[71] showing that across multiple fields of chemistry scientists are very interested in looking into alternative, cheaper, Cu-based means of catalysing reactions than the current Pd (or Ir/Ru for photoredox)-dominated processes. This means there is great potential scope for new electrochemical approaches as, theoretically at least, copper produced electrochemically in the right oxidation state could be used in any copper-catalysed reaction. A brief overview of some of the types of Cu-coupling reactions that exist is given in the next section.

3.2 Copper Coupling Reactions Used to Form C-C, C-N, C-O, C-S and C-P Bonds

One of the earliest discovered and most important types of copper coupling reaction is the Ullmann reaction,[72] which was discovered in 1901 by Fritz Ullmann.[73] Ullmann reported that when bromonitrobenzene was heated in the presence of a stoichiometric amount of copper powder, the pure biaryl product was formed, along with some copper bromide. Furthermore, this process not only worked with a bromo-substituted aromatic system but also with iodo- and even chloro-substituted systems, making it a very versatile reaction indeed.[72] See **Scheme 15**.

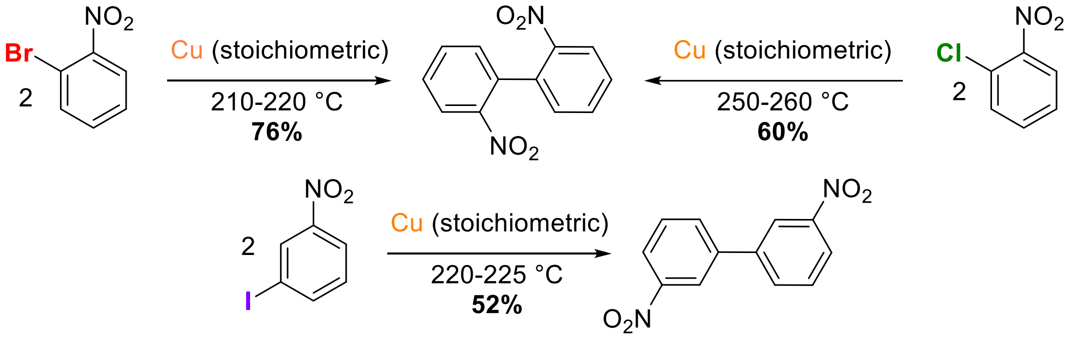

***Scheme 15**: The earliest described examples of the Ullmann reaction.*[72,73]

Two years after this initial discovery, Ullmann published another paper, this time detailing the arylation of aniline with chlorobenzoic acid in the presence of Cu powder (**Scheme 16**),[74] thus reinforcing in people's minds that copper could be an extremely useful way to promote cross-coupling reactions.[72] A colleague of Ullmann would later go on to show that this same conversion could be carried out using sub-stoichiometric quantities of copper (**Scheme 16**).[75] This colleague was Irma Goldberg, for whom the Goldberg reaction is named, and who proved to be another pioneer of this developing field. Goldberg built on her earlier work with anilines by showing that arylations could also be performed on amide systems.[72]

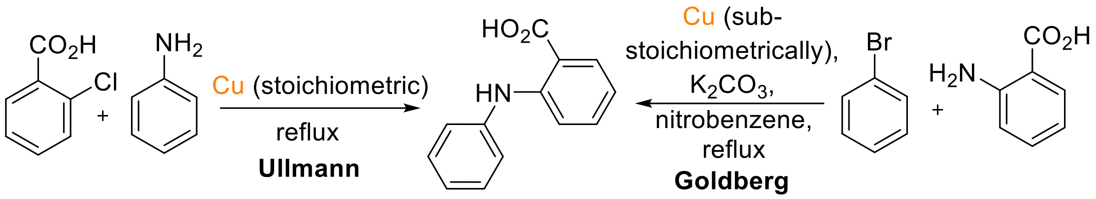

***Scheme 16**: Early Ullmann and Goldberg reactions showing the arylation of anilines.*[72,74,75]

Ullmann would later go on to show that arylation could successfully be carried out on alcohols,[72] which would most elegantly be demonstrated almost 100 years later (in 1999) when Ullmann-type reactions were utilised to great effect in Nicolaou's outstanding total synthesis of vancomycin, as shown in **Scheme 17**.[76] Nicolaou designed a substrate that had a triazene motif *ortho* to the aryl bromines that were to be used in the Cu-coupling steps, and this proved very important for two reasons. Firstly, the triazene acted as an electron sink, drawing charge away from the aromatic ring thus making it easier to perform the planned Ullmann reactions. Secondly, the lone pairs present in such close proximity to the bromine atoms aided the coordination of the introduced copper species, again, improving the efficiency of the coupling reactions. This all meant that the couplings could be carried out with remarkably mild conditions, i.e. simply refluxing in acetonitrile.[72,76]

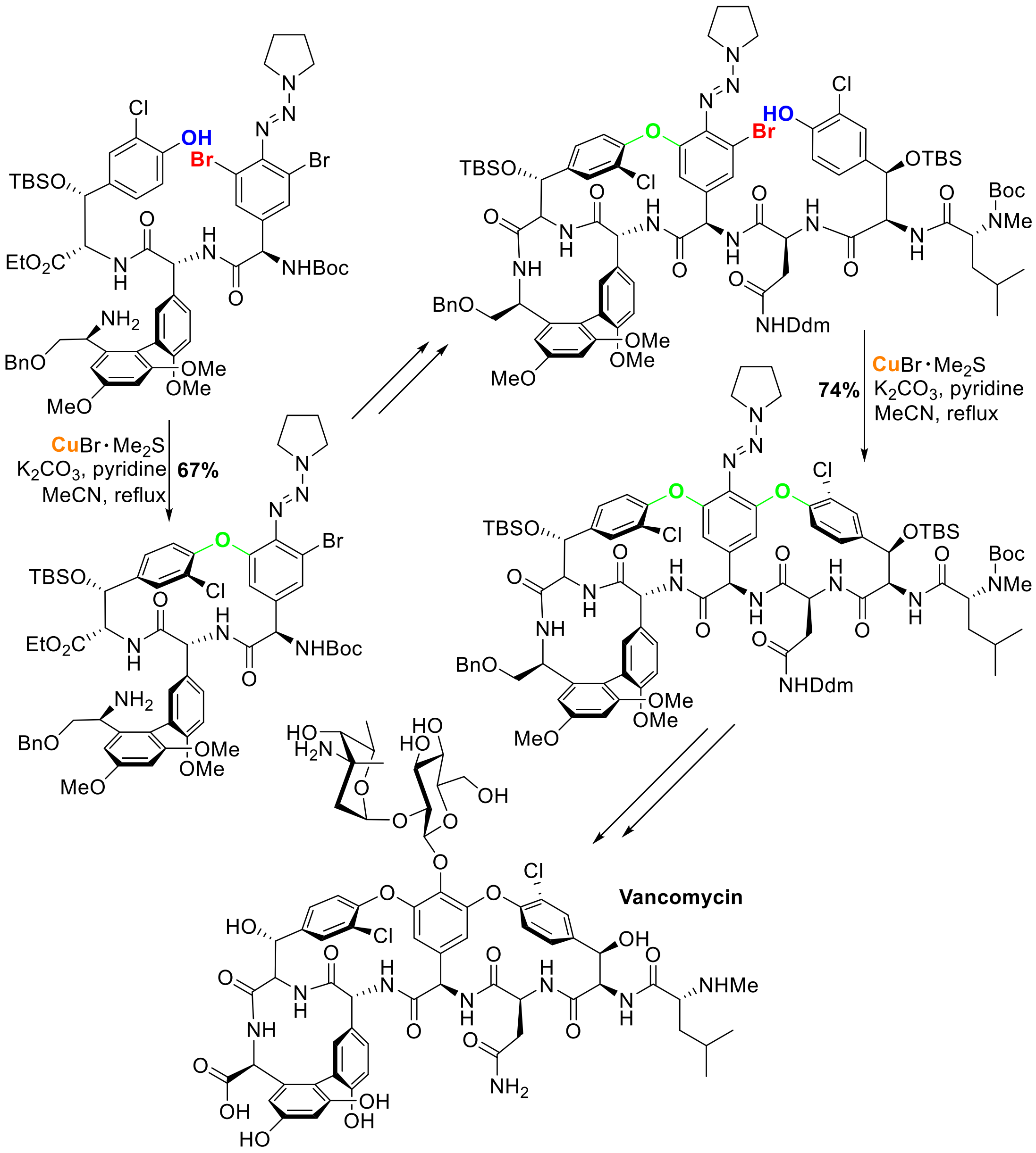

***Scheme 17**: The elegant use of Ullmann reactions in Nicolaou's total synthesis of vancomycin.*[72,76]

Having already seen how Cu has been used to form C-C, C-N and C-O bonds, we will now look briefly at the formation of C-S and C-P bonds. Considering the amount of literature centred around forming new C-O and C-N bonds using Cu, there has been significantly less dedicated to sulfur and phosphorus analogues.[77] However, there have still been some interesting examples, such as a study by Xu *et al.*[78] which explored the arylation of various thiols using a copper oxide and 1,10-phenanthroline system. This work showed the viability of producing thioethers using copper from both aryl and alkyl thiols. Some examples of which are shown in **Scheme 18**.[77,78]

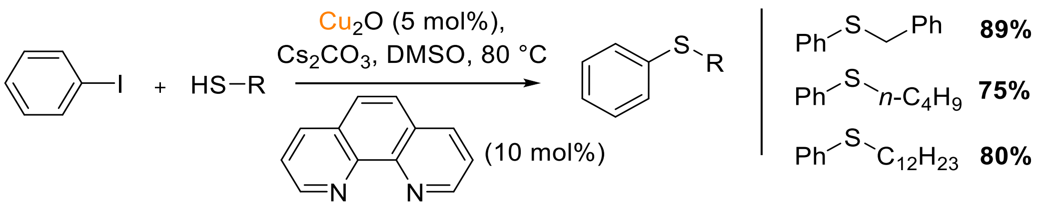

Scheme 18: The Cu-mediated formation of C-S bonds to form thioethers.[77,78]

The field of Cu-catalysed phosphorus-arylation is a relatively new and developing field,[79] however, even early examples in this area, such as the work of Osuka *et al.* in 1983,[80] showed great scope and functional group tolerance as seen in **Scheme 19**. The use of stoichiometric amounts of copper and toxic HMPA is undesirable, but since then, improvements in the conditions used in these types of reactions mean that Cu has emerged as a cheaper and less toxic way to carry out some of these reactions than some analogous Pd-catalysed examples.[79]

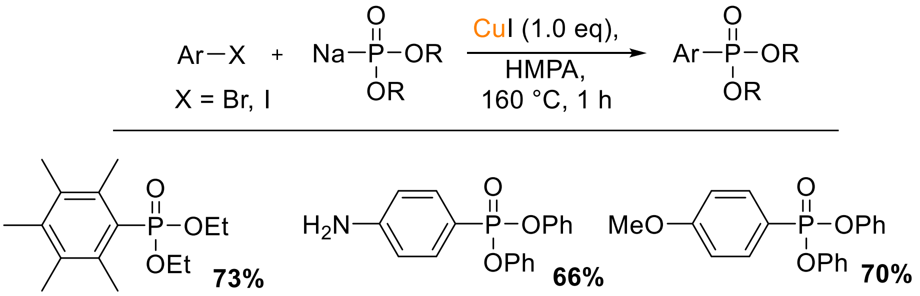

Scheme 19: The Cu-mediated formation of C-P bonds to form aryl phosphonates.[79,80]

Whilst copper has most commonly been used to facilitate arylation reactions, it has also been used for some other very useful purposes. One of these is to aid the exchange of chlorides and bromides with iodides in the aromatic Finkelstein reaction.[81] This conversion is important because many coupling reactions rely upon the use of weak C-I bonds in coupling partners. Often the analogous C-Cl and C-Br bonds are too strong for efficient coupling to take place. Finkelstein reactions require alkali iodide salts which are important for two reasons: they provide the necessary iodine atoms, and they create a significant driving force for these reactions when the often insoluble chloride and bromide alkali salts that are formed, precipitate out of solution.[81] One of the most significant contributions to the methodology of the Finkelstein reaction was made in 2002 when Buchwald and Klapars[82] developed conditions capable of forming aryl iodides quantitatively as shown in **Scheme 20**. The key to this efficiency was the use of the diamine ligand shown, which appeared to be much more active than other ligands assessed. These conditions proved very tolerant of a variety of functional groups, though in the case of carboxylic acids, hexamethyldisilazane had to be included in the reaction mixture to first form the trimethylsilyl ester, as it made the substrate more soluble. The carboxylic acid was reformed by cleavage of the TMS group in the work up. It appears that vinyl iodides could also be synthesised using similar conditions, but only one example was reported.[81,82]

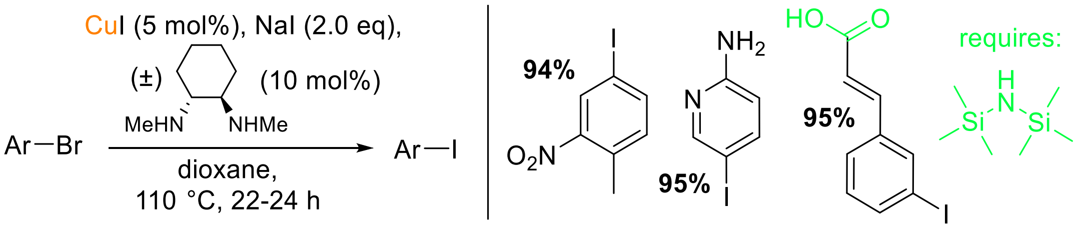

***Scheme 20**: An example of the Finkelstein reaction used to produce a range of synthetically-useful aryl iodides.*[81,82]

Another important type of reaction that copper has been used for is the cyanation of aryl species. As benzonitriles are important building blocks for dyes, agrochemicals and natural products,[83] methods to produce them have been of interest to many synthetic chemists. Not only that, but the nitrile group can serve as an intermediate for other functional groups such as: aldehydes and primary amines through reduction, heterocycles through cycloaddition, and amides through hydration.[83] Two major types of Cu-catalysed routes have traditionally been used for cyanations, known as the Rosenmund-von Braun reaction and the Sandmeyer reaction. Examples of these are shown in **Scheme 21**.[83]

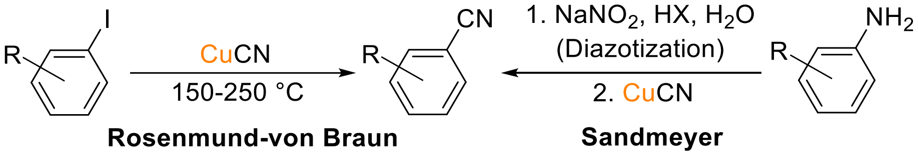

***Scheme 21**: Examples of the traditional Cu-based methods used to produce benzonitriles: the Rosenmund-von Braun and the Sandmeyer reactions.*[83]

Both methods rely upon using quite toxic CuCN as the source of both the catalyst and cyanide group, but where the Rosenmund-von Braun reaction can proceed directly from an aryl halide, the Sandmeyer reaction first requires diazotization of an aniline. An interesting literature example of the Rosenmund-von Braun reaction developed in the Buchwald group is shown in **Scheme 22**,[84] coming just a year after Klapars and Buchwald first demonstrated very efficient conditions for the Finkelstein reaction in aryl systems.[82] This reaction in fact proceeds *via* conversion of the starting aryl bromides to the respective aryl iodides *in situ*, followed by cyanation.[83,84]

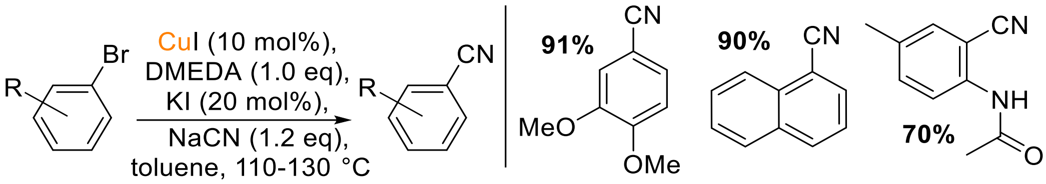

Scheme 22*: The Rosenmund-von Braun-type cyanation of aryl bromides.*[83,84]

It is worth noting that today the most common method for producing benzonitriles in industry is the ammoxidation (heating with ammonia and oxygen) of toluene derivatives, as the previously very popular Cu-based reactions often produced stoichiometric quantities of copper waste.[83]

There are many more types of reactions, and reports in the literature, where copper has been employed as a catalyst which have not been mentioned, such as in numerous natural product total syntheses[85] and in the formation of many heterocycles.[86] There are far too many interesting examples to go into in this report. But there is one important class of copper compounds yet to discuss which will be the subject of the next chapter: copper acetylides.

Chapter 4. Copper Acetylides: Versatile Intermediates

4.1 Introduction

Copper acetylides are crucial intermediates for many reactions investigated in this PhD project, and hence require discussion in greater detail. There is strong literature precedent for utilising these compounds in a large array of reactions as intermediates, the reason for this being that they are extremely versatile when exposed to the correct conditions, possessing the capability to undergo several key modes of reactivity. Copper acetylides in the '+ 1' oxidation state may react with electrophiles, oxidatively insert into carbon-halogen bonds, undergo transmetallation as part of coupling reactions, and react very efficiently with azides (as in the CuAAC reaction – a detailed description of which is given in **Chapter 5**). Following oxidation they can also react with nucleophiles in an umpolung fashion as popularised by the work of Evano.[87,88] These general modes of reactivity are summarised in **Scheme 23**.

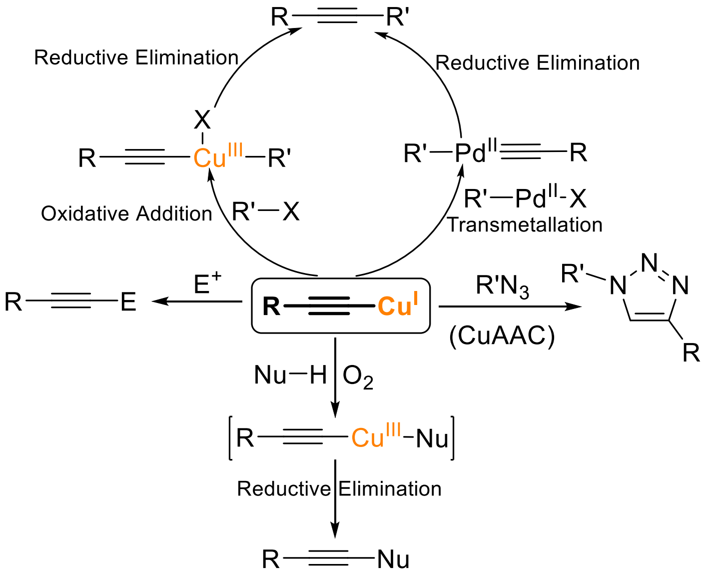

***Scheme 23**: General modes of reactivity for copper acetylides.*

Some specific examples of these types of reactions are shown in **Scheme 24**. The Castro-Stephens reaction is an example of the oxidative addition reactivity where the copper acetylide inserts into a C-X (halide) bond to produce di-substituted alkynes and heterocycles.[89] The Sonogashira reaction shows the transmetallation capability of copper acetylides where the alkyne unit is given to a Pd^{II} centre.[90] Ynamide formation and phosphorus-substitution reactions are shown and are examples of umpolung reactivity with nucleophiles, however examples of reactions with imines, boronic acids and TMS-CF_3 in this way are also known.[87]

Examples of a CuAAC reaction[91] and a halogenation reaction (reaction with an electrophile)[92] are also shown.

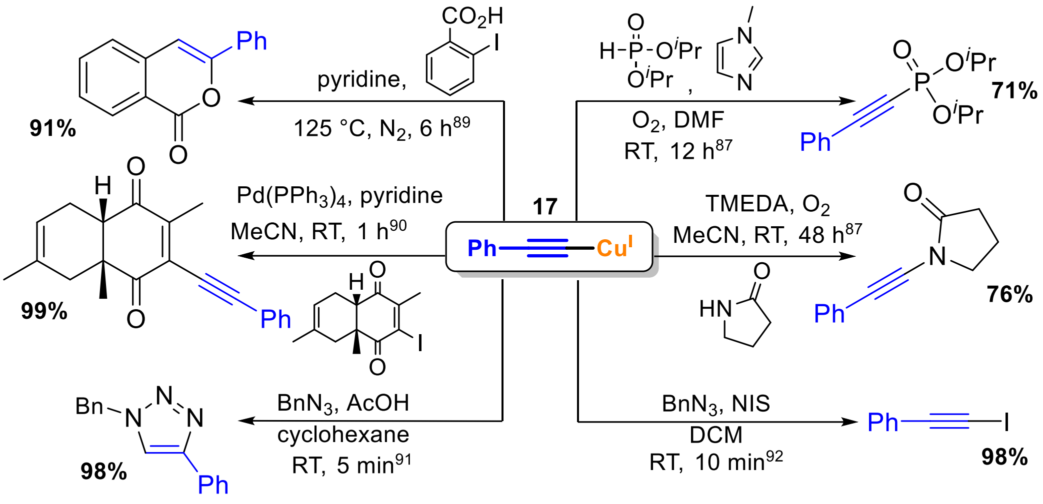

Scheme 24: Showing some specific examples of the reactivity of copper acetylides.[87,89–92]

In addition, work carried out recently by K. C. Hwang's group has utilised copper acetylides in photoredox reactions to produce important compounds like indoles,[48] functionalised ketones[93] and α-keto esters[94] *via* some interesting reaction mechanisms as shown in **Scheme 25**. The mechanisms all start with the production of copper acetylides *in situ* through the reaction of terminal alkynes with a base and a Cu(I) salt. Copper halides are very commonly used. The copper(I) acetylides are then excited by a blue LED to allow oxidation to take place easily, often delivering electrons to aerial oxygen. The proposed mechanisms for their indole (**A**), functionalised ketone (**B**) and α-keto ester (**C**) syntheses are shown, often highlighting O_2 playing a very active role.

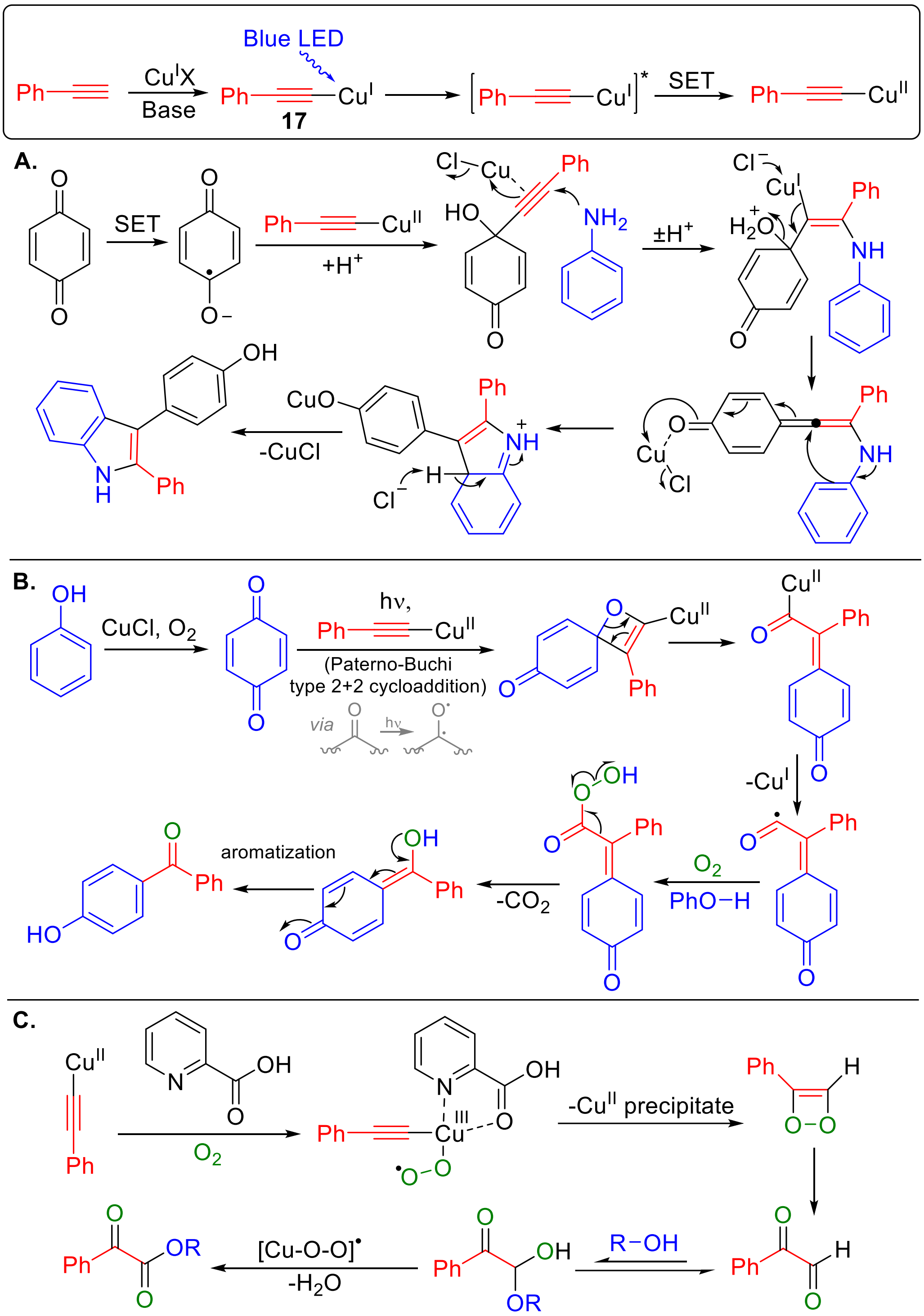

Scheme 25: The use of copper acetylides in photoredox reactions to produce A. indoles, B. functionalised ketones and C. α-keto esters.[48,93,94]

Clearly then, copper acetylides are versatile intermediates, however, what makes this large range of reactivity quite surprising is the fact that copper(I) acetylides are very stable, isolable species. With this thought in mind along with their obvious utility, we wondered if these polymeric yellow solids could potentially be produced electrochemically, in a similar fashion to the silver acetylides seen in **Scheme 14**. The classical method for their production is well established (and possible on a multi-gram scale) by simply adding a terminal alkyne to an aqueous ammoniacal solution with ethanol and copper iodide. Under these conditions, the solution turns bright blue upon addition of copper, and once the terminal alkyne is added the copper acetylide product immediately precipitates out of solution, allowing collection *via* filtration.[88,95] (**Scheme 26**). This method works well for a range of R groups, including alkyl and aryl substituents.

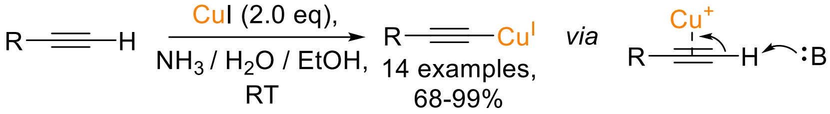

***Scheme 26**: Showing the well-established method for producing copper acetylides.*[87,88,95]

Another common method of production is the use of CuI in DMF with K_2CO_3 present as base.[20] Note that both of these methods produce halide waste that must be disposed of afterwards. Furthermore, DMF has been identified as problematic for industrial-scale synthesis and so MeCN has been suggested as a more favourable alternative solvent, not least because new 'green' processes for producing MeCN have been developed from benign feedstocks.[20,96,97]

Whilst effective methods for copper(I) acetylide synthesis and isolation exist, it is important to mention that copper acetylides are very often prepared *in situ* (to easily allow further reactions to take place) rather than prepared separately and used in the desired reaction. In general, as long as a terminal alkyne, a base and a Cu(I) source are present, the desired copper(I) acetylide should begin to form, allowing isolation of this species or further reactions to take place.

4.2 Electrochemical Synthesis of Copper Acetylides

4.2.1 A Divided Cell Approach

The classical method of preparing copper acetylides has already been seen in **Scheme 26**,[87,88,95] which involves stirring copper iodide in a mixture of $NH_4OH_{(aq.)}$ solution (~30%) and ethanol, in a ratio of 5:3 NH_4OH solution : EtOH. This creates a strongly blue-coloured solution (likely due to copper(II)tetraaminodiaqua complexes forming). A terminal alkyne is then added to this solution, immediately precipitating out the copper acetylide product as a polymeric yellow solid. The insolubility of copper acetylides is well known[95] (in most organic solvents), which is quite useful when synthesising them, but can create difficulties when trying to use them as reagents.

We decided to synthesise copper acetylides from terminal alkynes using electrochemical methods, in much the same way that silver acetylides have been.[44] There is a strong literature precedent for the use of alkynes in EOS, generally in highly selective hydrogenation reactions[98] and various heterocycle-forming reactions,[99–102] however we do not believe that copper acetylides have been prepared electrochemically before. To begin our investigation, a series of qualitative tests was carried out to assess the feasibility of this approach: leaving metallic copper sheets in 5:3 NH_4OH solution : EtOH gave colourless solutions (i.e. no Cu(I)/Cu(II) released from the Cu(0) sheets), adding phenylacetylene did not produce any copper acetylide precipitate. However, when this same experiment was attempted in a divided cell, with the copper sheets connected up to the potentiostat and an oxidative potential of +2.00 V was applied, the solution began to turn a pale blue colour.

Pleasingly, upon addition of phenylacetylene, a yellow precipitate (the copper acetylide **17**) formed. This reaction was repeated immediately to see what sort of yield could be obtained for the copper acetylide, as shown in **Scheme 27**. 0.05 M $LiClO_4$ was used as an inert electrolyte to carry charge in this reaction.

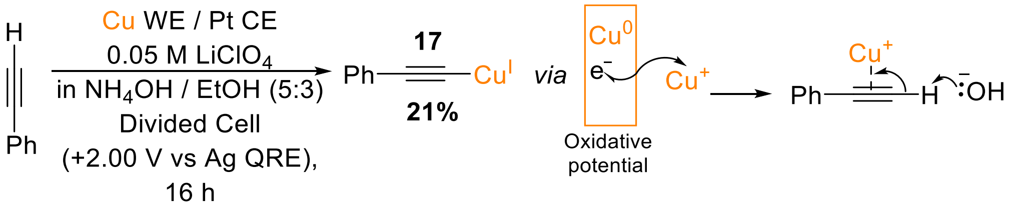

***Scheme 27**: Electrochemical generation of copper acetylides using an aqueous ammoniacal solution.*[20,95]

Unfortunately, even after 16 h of applied potential, only 21% of the yellow solid **17** was isolated (Entry 1 of **Table 1**). The insolubility of copper acetylides and their polymeric nature makes accurate characterisation difficult to achieve. We opted to use melting/decomposition points and IR in this project (as others in the literature have), however in future work it is possible that elemental analysis could be adopted as an additional characterisation technique. It became clear that the $LiClO_4$ we used as an electrolyte was unnecessary in this highly polar solution (Entry 2 of **Table 1**). It was reasoned that the low yields observed were likely due to an overall low concentration of copper ions being generated, coupled with the tendency of Cu(I) ions to disproportionate in aqueous solutions to Cu(0) and Cu(II). This is somewhat supported by the fact that 2 equivalents of CuI are used in the established method,[95] thereby providing an excess of Cu(I) ions to react, whereas we were generating it on demand from the beginning of the reaction.[20]

We therefore decided to attempt the synthesis of **17** in MeCN instead of a water-based solvent, in the hopes that the Cu(I) ions produced would be stabilised by the weakly coordinating MeCN solvent acting as a ligand, thereby preventing overoxidation to Cu(II). **Figure 7** shows the CV plot obtained for a Cu^0-coated glassy carbon electrode in an MeCN solution, indicating the ease with which Cu^0 can be oxidised in this solvent, as it was oxidised as soon as an oxidative potential was applied. This CV plot was achieved by coating a glassy carbon rod with a fine layer of Cu(0) by passing a reductive potential through a 0.5 M $CuSO_4$ / H_2O solution (reducing the Cu(II) to Cu(0) thereby forming a metallic coating). This was then placed into the Bu_4NPF_6 / MeCN electrolyte solution.[20,40]

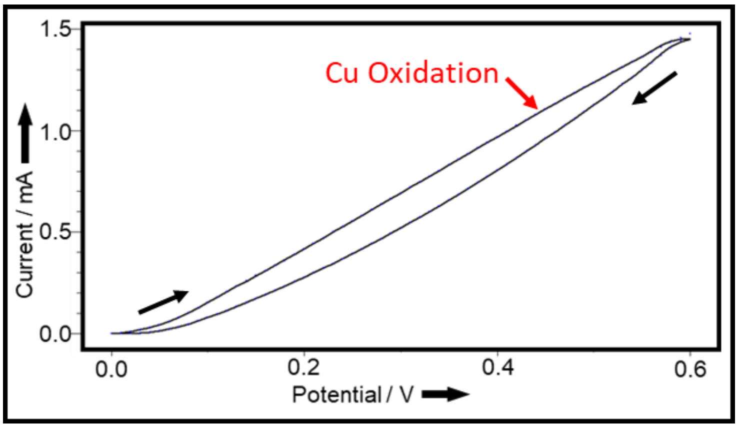

***Figure 7**: CV plot using a Cu^0-coated glassy carbon WE, Pt CE, and Ag QRE. Recorded in 0.1 M Bu_4NPF_6 / MeCN. Axes redrawn for clarity.*[20,40]

Encouraged by this we used Bu_4NPF_6 as an electrolyte in a divided cell and applied a potential of +0.5 V for 4 h to the solution (whilst exposed to air). We then transferred this solution to a sealed flask and degassed it thoroughly with argon before adding phenylacetylene and DABCO (2 equivalents). To our delight, this resulted in an excellent yield of 92% for **17** as shown in **Table 1** (Entry 3).[20]

Table 1: *Optimisation and control reactions carried out for the electrochemical synthesis of copper acetylides in a divided cell.* [a] [20]

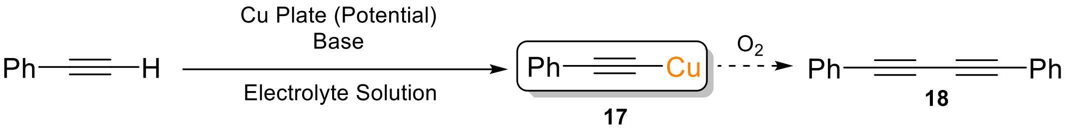

Entry	Electrolyte Solution	Potential (vs Ag QRE)	Base	Yield/ %[b]
1[c]	0.05 M $LiClO_4/NH_4OH$: EtOH (5:3)	+2.00 V for 16 h	None[d]	21
2[c]	NH_4OH : EtOH (5:3)[e]	+0.50 V for 4 h	None[d]	9
3	0.10 M Bu_4NPF_6/MeCN	+0.50 V for 4 h	DABCO (2.0 eq)	92
4	0.10 M Bu_4NPF_6/MeCN	+0.50 V for 4 h	None	3
5	0.10 M Bu_4NPF_6/MeCN	+0.50 V for 2 h	DABCO (2.0 eq)	68
6	0.10 M Bu_4NPF_6/MeCN	+0.50 V for 4 h	DABCO (1.0 eq)	69
7	0.10 M Bu_4NPF_6/MeCN	No potential applied	DABCO (2.0 eq)	0
8[f]	0.10 M Bu_4NPF_6/MeCN	+0.50 V for 4 h	DABCO (2.0 eq)	0[f]

[a] *In all cases 0.50 mmol phenylacetylene was used, except in Entry 1 where 2.00 mmol was used. All reactions were carried out using a Cu plate (5.30 cm^2 surface area) working electrode, a Pt wire (1.26 cm^2) counter electrode and a Ag wire (0.79 cm^2) quasi reference electrode.* [b] *Isolated yield of copper acetylide* ***17****.* [c] *Based on conditions reported by C. Theunissen* et al.[95] [d] *No base added as the electrolyte solution functioned as the base.* [e] *Ammonium hydroxide solution acted as the electrolyte.* [f] *Reaction mixture exposed to O_2 causing copper acetylide* ***17*** *to oxidise and form diyne* ***18*** *in 63% isolated yield.*

Various control reactions were carried out as shown in **Table 1**. The requirement of an added base such as DABCO was confirmed (Entry 4), the length of time for the applied potential was investigated and we found that 2 h of applied potential was insufficient to obtain complete conversion (Entry 5). We found that 2 equivalents of DABCO were required (Entry 6). The vital control reaction showing that an applied electrical potential is required to carry out this reaction is shown in Entry 7, and the need to exclude O_2 from the reaction vessel (to remove the possibility of oxidation and further reaction of the copper acetylide product - Entry 8) was also examined. In this last instance the copper acetylide was found to readily undergo Glaser-Hay coupling to produce **18** unless the flask was kept under argon. It is important to note that the amount of charge passed in these electrochemical tests should be included as another means of comparing the tests to one another, but we did not learn the importance of this until later in the PhD project. Therefore, the charge was not measured during these experiments and is not presented in this table. **Scheme 28** shows the optimised conditions for this new electrochemical method for preparing copper acetylides.[20]

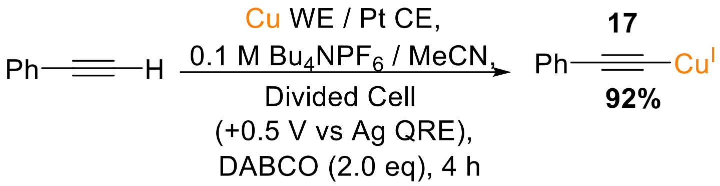

Scheme 28: Electrochemical generation of copper acetylides using an MeCN-based system.[20]

This method was far superior to the water-based classical method we attempted originally due to the shorter reaction time and much higher yield. We believe the key to this improvement lay in the type of copper complex formed in both cases. In the water-based method we believe the Cu(II)-centred cation **19** (**Figure 8**) was produced due to the strongly-coordinating species present and the characteristic deep blue colour of the solution, whilst in the MeCN-based method, we hypothesised that the Cu(I)-centred cation **20** was the active copper species produced.

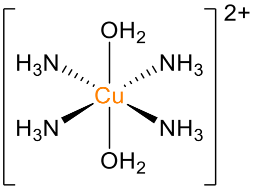

19

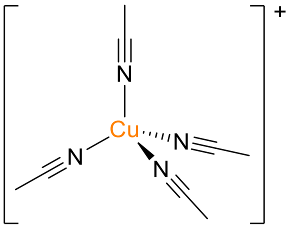

20

Figure 8: Proposed cationic copper-centred cations generated electrochemically.

To test this hypothesis, we designed a control experiment using commercially-obtained $Cu(MeCN)_4PF_6$ (**20**). Two equivalents were dissolved in MeCN degassed with argon. The solution was then further degassed with argon, before DABCO (2 eq) and phenylacetylene (1 eq) were added, which immediately caused the bright yellow precipitate **17** to form in 79% yield. This shows that **20** is indeed likely to be the copper complex that is generated electrochemically.[20]

With the conditions for producing **17** in hand, we next wanted to produce a range of different copper acetylides to assess the scope and capabilities of this method. The results are shown in **Scheme 29**.[20]

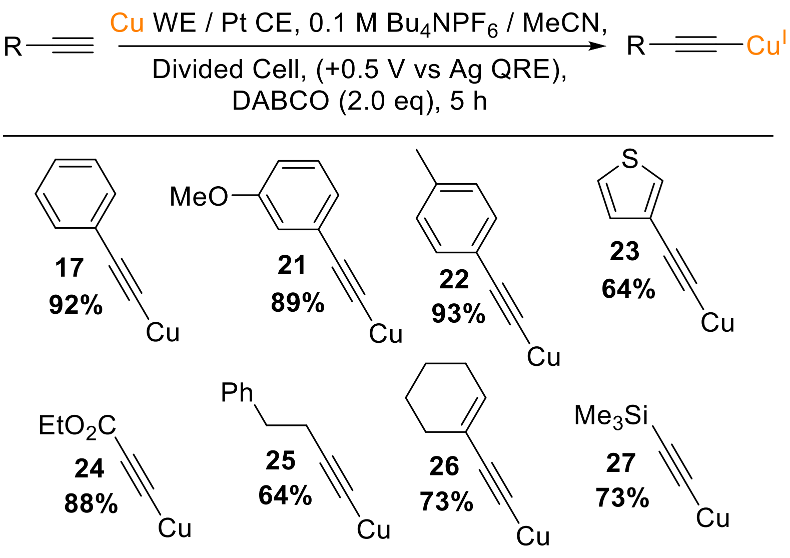

***Scheme 29**: Scope of divided cell method for electrochemical copper acetylide production.*[20]

An array of substituents and functional groups was tolerated using these conditions and the yields ranged from good to excellent. It is worth noting that in general aryl groups appeared to give better yields than their alkyl counterparts. We were pleased to obtain the trimethylsilyl copper acetylide in good yield as this has particular synthetic utility owing to the ease with which the TMS group may be cleaved for later-stage functionalisation.

In order to confirm that the oxidation state of the copper we were releasing from the sacrificial WE was '+1', we devised an experiment in which a graphite rod was coated with Cu^0 from $CuSO_{4(aq.)}$ by using a reductive potential of -0.5 V vs Ag QRE (13.40 C passed during coating = a maximum of 6.94×10^{-5} moles of Cu^0. This was calculated by using Faraday's Laws of Electrolysis, **Eq. 1, page 1**). This Cu^0-coated C electrode (pictured in **Figure 9**) was then used to produce copper acetylide **17** from 0.5 mmol phenylacetylene with the conditions seen in **Scheme 29**, with the exception that all of the Cu present on the graphite rod was released in around 10 min and in this experiment the alkyne was in excess. The theoretical yield for this experiment was 11.43 mg of **17** if all available oxidised Cu reacted and we isolated 8.10 mg (4.92×10^{-5} moles) of **17**. This gave us an excellent 71% efficiency of Cu atom integration into the product, however the most interesting result from this experiment was that the charge passed during the oxidation of Cu was measured to be 6.17 C. Substituting this value into **Eq. 1** (**page 1**), along with the number of moles of isolated **17** gives a good approximation of the oxidation state of the copper released into solution, 'z', as being 1.30. In other words, it is more probable that we are releasing Cu^I ions rather than Cu^{II}. **Figure 10** shows the charge passed as a function of time for coating of the graphite rod (**A**) and the release of the Cu^I ions (**B**). It is noteworthy that even at a glance, these graphs show that there was twice as much charge passed when reducing Cu^{II} onto the graphite rod than there was charge passed in the oxidative release (indicating Cu^{I} release).[20]

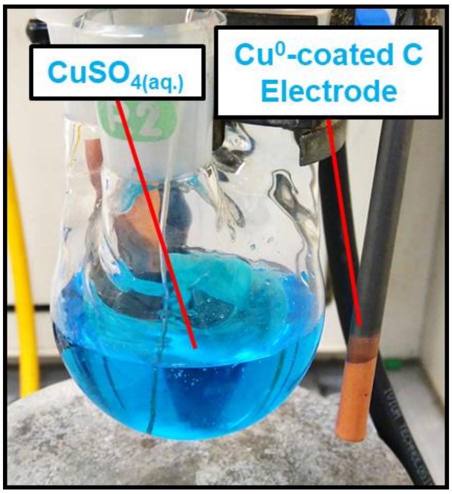

***Figure 9**: The coating of a graphite rod with a layer of Cu^0.*

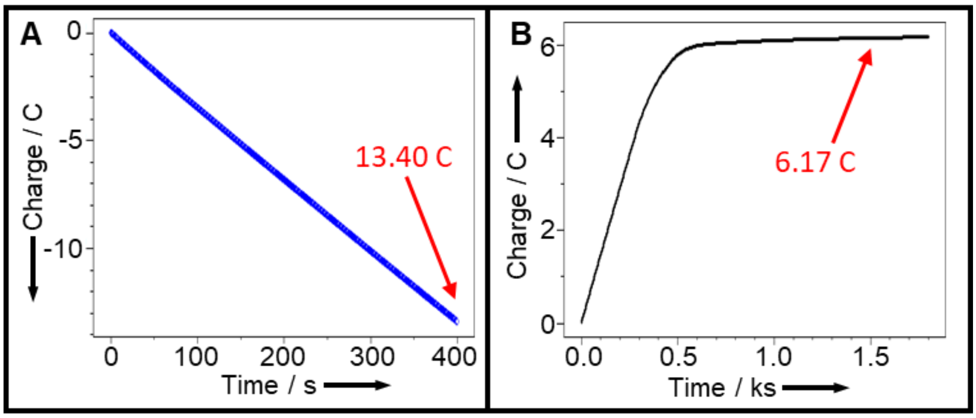

***Figure 10**: Charge passed when: A. reductively coating a graphite rod from a $CuSO_{4(aq.)}$ solution and B. oxidatively releasing Cu^{I} ions. Axes redrawn for clarity.*[20]

Furthermore, when we repeated this experiment, to be certain of the validity of this method, we used a graphite rod CE (instead of a Pt wire) of identical dimensions to the WE. When this experiment was carried out, we found that -12.51 C charge was passed in the coating, 77% efficiency of Cu atom integration was achieved and 5.37 C charge was passed in the release, which gives a value of the oxidation state of the copper as 1.12.[20]

Whilst this divided cell method for producing copper acetylides is efficient and has a reasonably wide scope, we were curious to see if we could improve this method in terms of sustainability.

4.2.2 An Undivided Cell Approach

We believed that the current flowing at the CE to maintain the charge in the divided cell was causing the electrochemically mediated Hofmann-type elimination of the electrolyte salt, Bu_4NPF_6. This reduction would take place in the cathodic chamber to generate tributylamine. There is a strong literature precedent for this.[20,39,103–106] If this was indeed the case, we wondered if we could exploit this reactivity to perform this same reaction in an undivided cell, combining the oxidative production of copper with the reductive production of an amine base, thereby obviating the requirement for any added base, such as DABCO, from our method entirely. We also anticipated that the base we generated could also perform as a catalyst. Once it reacted with a molecule of terminal alkyne to become protonated it could be electrochemically reduced back to its basic form. This would release H_2 gas, a clean by-product, making this process highly sustainable.[107] Such factors, if enacted successfully, embody several of the key principles of green chemistry.[108] These proposed improvements to the method are summarised in **Figure 11**.[39]

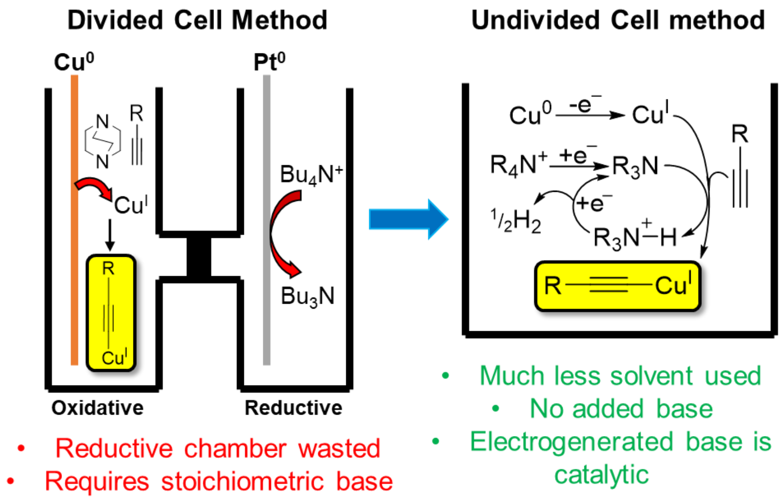

***Figure 11**: Proposed improvements to the divided cell method for preparing copper acetylides.*[39]

This undivided cell method would have several key advantages over the divided cell method. Most notably, the lack of need to add a base to the reaction mixture and the catalytic nature of the electrogenerated base. A decrease in the resistance between the WE and the CE would also be achieved. The use of an electrochemical approach to generate bases *in situ* over simply adding an amine base to solution is appealing because quaternary ammonium salts (QAS) are generally less hazardous than their tertiary amine counterparts (through careful selection of the associated anions) making the overall hazards of the starting materials preferable as there is no direct handling of the base.[39]

These key advancements in the new method would rely upon the single-electron-transfer/Hofmann-type elimination of the QAS electrolyte. Essentially the electrolyte we were using would also behave as a probase. This reactivity has been investigated in detail[39,103–106] and it is believed that the QAS undergoes a single electron reduction to produce a tertiary amine and a radical. This radical is then probably reduced, producing an anion that can initiate Hofmann elimination of another molecule of QAS. Certain R groups of QAS have a proclivity to dimerization where others do not. For instance, $[PhCH_2NMe_3]^+$ often produces dibenzyl upon reduction. However, tetraethylammonium (TEA) salts give only ethane (RH) and ethene (R(-H)).[103,104] The presence of water in the solution offers alternative fates for the resultant R radicals and anions. **Scheme 30** gives an overview of the reactions associated with electrochemical QAS reduction.[39,103–106] In the specific case of using a sacrificial Cu anode in an undivided cell to promote copper acetylide synthesis, we were cognisant of the fact that there also exists the possibility of electro-reduction of the generated Cu(I) ions at the counter electrode, which may negatively affect the synthesis.

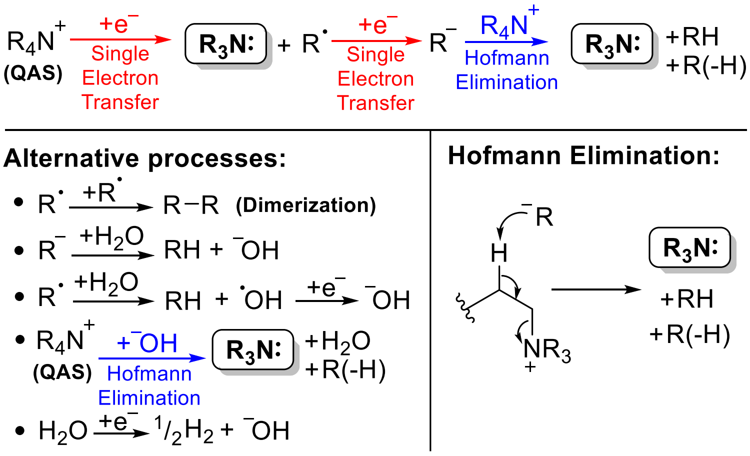

Scheme 30: QAS electro-reduction and associated reactions.[39,103–106]

Quaternary ammonium salts are generally more resistant to electrochemical reduction than most probases. It has been found that factors such as R group chain length, steric hindrance and branching have very little effect on the overall stability towards reduction and to the electronic environment around the cationic nitrogen centres.[39,109] Despite these difficulties, an example of electrochemical QAS reduction for synthetic purposes does exist. In 1995, J. Gal *et al.*[110] used benzylic QAS as a means to produce benzylic radicals that reacted with CO_2 to generate carboxylic acids as in **Scheme 31.**[110] The anion X^- used in these examples were all halides, and switching between different halides did not appear to affect the yield of the products.

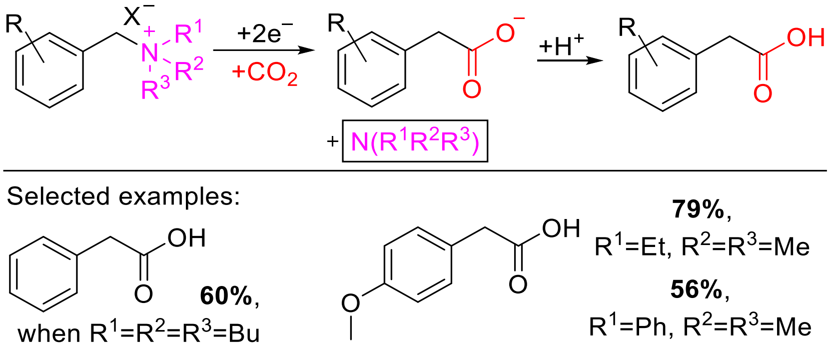

Scheme 31: Example of electro-reduction of QAS.[110]

However, this example does not make use of the electro-generated tertiary amine base that is formed in this reaction. Whilst we were encouraged by the relative ease with which these reductions appeared to have been harnessed, we expected the reduction of purely alkyl QAS to be more difficult than the benzylic ones seen in **Scheme 31**. Despite this, we remained confident that in the absence of other potential probase species we could successfully utilise Hofmann-type elimination to facilitate copper acetylide synthesis in an undivided cell.

We began by using almost identical conditions to our previous method, therefore Bu_4NPF_6/MeCN was used as the electrolyte solution, causing Cu^I ions to be produced from the sacrificial Cu^0 WE and (so we initially believed) Bu_3N to be formed directly at the Pt CE.[39] Over the course of 2 h of an applied potential of +0.50 V vs Ag QRE, a modest yield of 54% for **17** was achieved (**Table 2**). This yield falls well below the 92% achieved with the optimised divided cell conditions however, so further optimisation reactions were carried out as shown in **Table 2**. The reaction vessel was kept under argon to prevent any diyne forming. To demonstrate the proposed catalytic regenerative nature of the base, 0.1 mmol electrolyte was used with respect to 0.3 mmol phenylacetylene. Hence, if all present QAS was converted into the amine bases **28** and **29**, (and neither of these bases was regenerated), we would expect a maximum theoretical yield for **17** of 33%. Yields greater than this would demonstrate that the base must be electrochemically regenerated after initial deprotonation of a molecule of alkyne as shown in **Figure 11**.[39]

Table 2: *Optimisation and control reactions carried out for the electrochemical synthesis of copper acetylides in an undivided cell.* [a] [39]

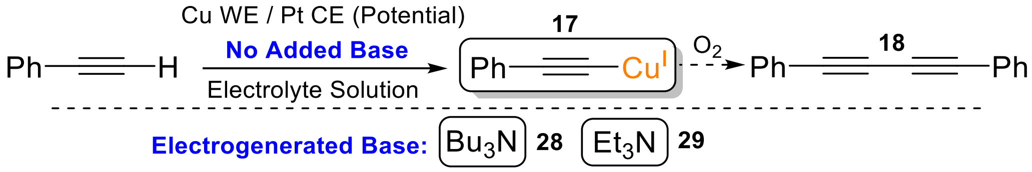

Entry	Electrolyte/ Solvent Used	Potential (vs Ag QRE) and Charge Passed	Additive(s)	Yield/ %[b]
1	Bu_4NPF_6/ MeCN	+0.50 V for 2 h, 19.2 C	—	54
2	Bu_4NPF_6/ MeCN	No potential applied (20 h)	—	0
3	MeCN	No potential applied (2 h)	$Cu(MeCN)_4PF_6$ (1.1 eq), Bu_3N (0.33 eq)	3
4	MeCN	No potential applied (2 h)	$Cu(MeCN)_4PF_6$ (1.1 eq), Bu_3N (1.1 eq)	38
5	$LiClO_4$/ MeCN	+0.50 V for 2 h, 14.8 C	—	0
6	$LiClO_4$/ MeCN	+0.50 V for 2 h, 5.0 C	Bu_3N (0.33 eq)	9
7	$Et_4N(CH_3C_6H_4SO_3)$/ MeCN	+0.50 V for 2 h, 19.0 C	—	66
8	$Et_4N(CH_3C_6H_4SO_3)$/ MeCN	No potential applied (2 h)	—	<1
9	MeCN	No potential applied (2 h)	$Cu(MeCN)_4PF_6$ (1.1 eq), Et_3N (0.5 eq)	44
10	MeCN	No potential applied (2 h)	$Cu(MeCN)_4PF_6$ (1.1 eq), Et_3N (1.1 eq)	51
11	$Et_4N(CH_3C_6H_4SO_3)$/ MeCN	+0.50 V for 4 h, 45.7 C	—	**97**

[a] *In all cases 0.3 mmol phenylacetylene and 0.1 mmol electrolyte salt in 10 mL reagent grade MeCN (0.01 M) were used. All reactions carried out under argon with a Cu wire WE, a Pt wire CE and a Ag wire QRE each with an effective surface area of 64 mm^2.* [b] *Isolated yield of copper acetylide* ***17****.*

We believe that the active Cu species in this reaction is $Cu(MeCN)_4X$ (where X = PF_6^- or $CH_3C_6H_4SO_3^-$, which both contain the cationic complex **20**). This is based on our previous method and supported again by control reactions carried out in this current work. Entry 3 shows that when no potential was applied, the reaction proceeded when this Cu species was added along with an amount of **28** that mirrored the total available QAS used in Entry 1 (i.e. 0.33 eq with respect to the alkyne). It is worth noting however that the reaction was much less efficient. We also found that when a stoichiometric/slight excess of **28** was used the yield increased significantly. This further indicated to us that when a potential is applied, the base is regenerated, making this process catalytic in nature.[39]

The absence of an appropriate QAS probase completely shut the reaction down ($LiClO_4$ was used as a substitute), even when a potential was applied as shown in Entry 5. During this test **17** was not produced over the 2 h of applied potential. However, once this test had been completed, Bu_4NPF_6 was added to this same solution and a potential (+0.5 V vs Ag QRE) was applied again. Within 15 min a bright yellow precipitate of **17** was produced. Whilst we initially interpreted this to be evidence for the direct electrochemical reduction of a QAS that we were hoping to observe, as in **Scheme 30**, we decided to run CV plots of the various components of this reaction mixture to obtain more conclusive evidence for this hypothesis (CV plots shown in the **Figure 12**).[39]

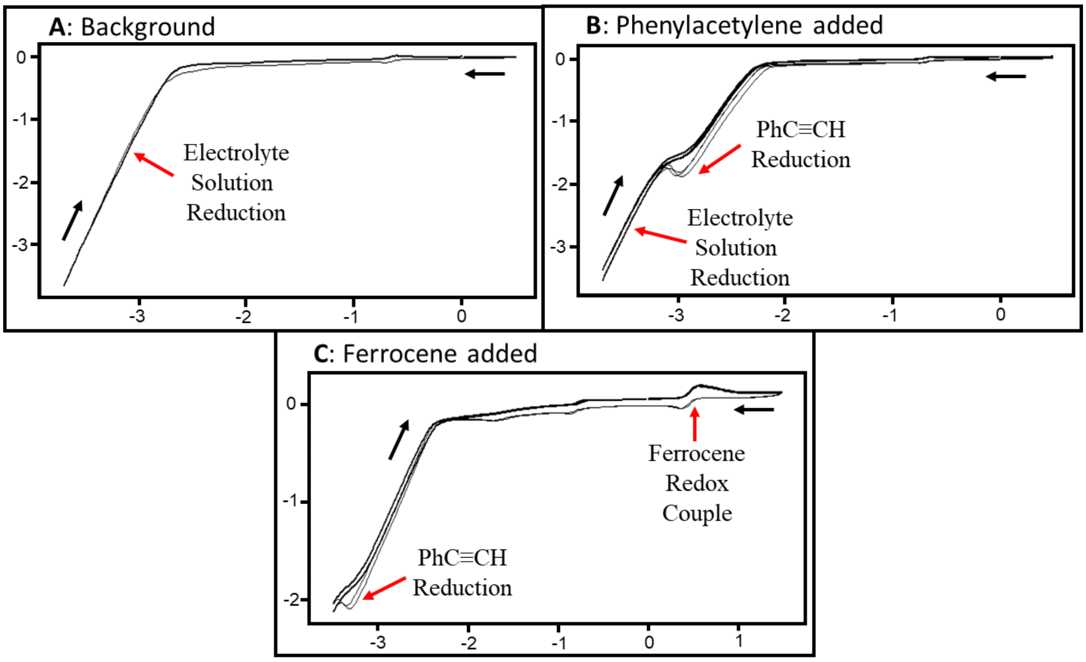

Figure 12*: CV plots of phenylacetylene recorded in 0.1 M $Et_4NO_3SC_6H_4CH_3$ / MeCN using a glassy carbon WE, Ag QRE and a Pt CE. Y axes = Current (mA), X axes = Potential (V). Axes redrawn for clarity.*[39]

Plot **A** appears to show that at around -2.9 V (vs Ag QRE) the background electrolyte solution begins to be reduced. It has been reported that under a reducing potential MeCN itself can form a strong base, $[NCCH_2]^-$,[111–114] which has been shown to be capable of initiating β-lactam synthesis through substrate deprotonation.[112–114] However, this direct reduction of MeCN appears to only take place when no other proton donors are present,[111] suggesting that the reduction peak shown in plot **A** likely pertains to QAS reduction. This distinction is rendered somewhat moot by the fact that in plot **B**, at the lower potential of around -2.2 V vs Ag QRE (-2.7 V vs Fc/Fc^+), phenylacetylene starts to be reduced to either $[PhCC]^-$, through loss of

½H_2, or to the radical anion. This shows that under the conditions used here, the first reductive process to take place is likely to be the reduction of phenylacetylene rather than the reduction of the electrolyte solution, however, given the overlap of the electrolyte and phenylacetylene reduction peaks, both processes are possible. Plot **C** merely shows this same reduction of phenylacetylene but with ferrocene included as an internal reference.[39]

If the $[PhCC]^-$ anion is formed, deprotonation of a QAS *via* Hofmann elimination would then produce a stable tertiary amine base, thereby initiating the copper acetylide-producing reaction. If the radical anion is formed, the single electron transfer from this species to a QAS would reform phenylacetylene and form an amine base *via* the pathway outlined in **Scheme 30**. In either case, the result would ultimately be the same. The ensuing electrochemical reduction of any protonated tertiary amine bases would then almost certainly take over as the dominant reductive process for the duration of the reaction, given the comparative ease with which these species may be reduced. If the anion is formed, it is not immediately apparent as to why this does not directly lead to the formation of **17**. One explanation could be that this reactive anion, formed in low concentration at the very beginning of the electrolysis, is quenched very quickly, thereby stopping it from reacting with the similarly low concentration of Cu^I ions produced at the anode. The stable amine bases **28** and **29**, produced by way of Hofmann elimination, would not suffer from this issue. **Scheme 32** shows these proposed reaction initiations (anion formation = Reaction Initiation 1, radical anion formation = Reaction Initiation 2).[39]

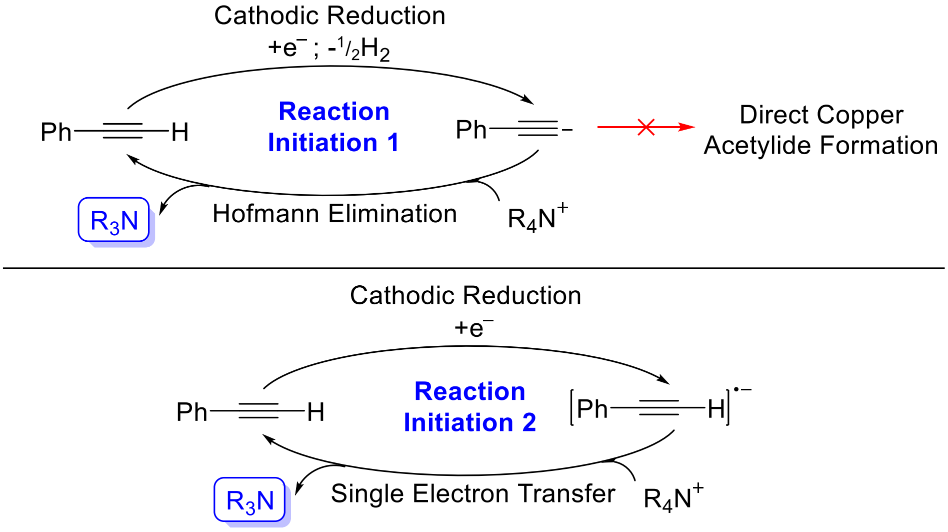

***Scheme 32**: Proposed reaction initiations by way of phenylacetylene reduction.*[39]

Entries 5 and 6 of **Table 2** proved important for ruling out the interference of hydroxide ions. Given that these reactions were carried out in the presence of reagent grade (rather than rigorously anhydrous) MeCN, it was postulated that a build-up of hydroxide ions might occur, as outlined in the 'alternative processes' section of **Scheme 30**. This could facilitate the reaction by providing another base for the deprotonation step of the copper acetylide-forming reaction and also increase the rate at which **28** and **29** were regenerated through the deprotonation of any protonated **28** and **29**. Given that we would expect some product to form in Entry 5 if hydroxide ions were generated, it seems that hydroxide ions were not formed, or were quenched before they could effectively promote this reaction.[39]

At this juncture we decided to test an alternative electrolyte salt which we had in the lab, $Et_4N(O_3SC_6H_4CH_3)$, in the hopes of improving the yield and atom efficiency of the reaction by producing the less sterically hindered base **29**. Tetraethylammonium salts with other anions may also work but were not tested. Work carried out by Dahm and Peters[103] shows that during the formation of **28** from TBA^+, a sterically-demanding gauche interaction is essential for allowing the antiperiplanar geometry that is required in Hofmann elimination processes. However, this same interaction causes much less steric hindrance when TEA^+ is used, promoting the generation of **29** much more readily than **28**. This gauche interaction is why Hofmann elimination generally leads to the least-substituted (non-Zaitsev) alkene product. A summary of these concepts is shown in **Figure 13** where the atoms in blue show the required anti-periplanar geometry of the β-hydrogen with the quaternary ammonium centres, and the disfavoured gauche interactions are shown in red.[39,115]

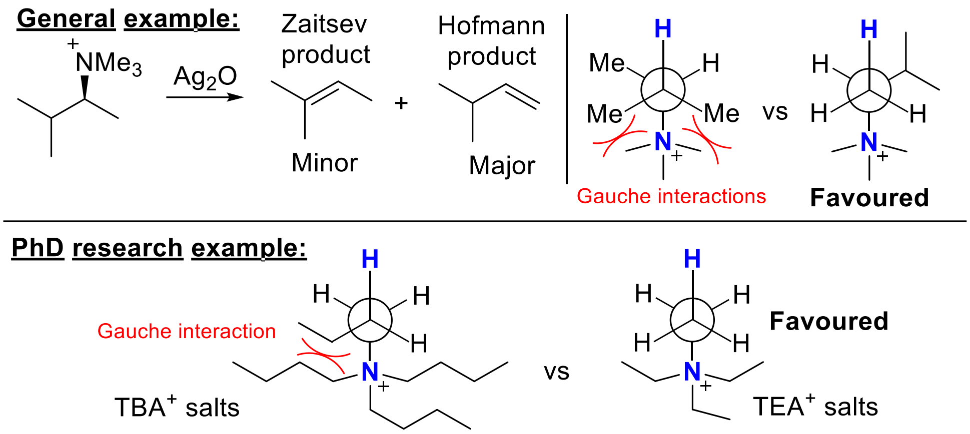

***Figure 13**: Representations of the selectivity of Hofmann elimination reactions in a general sense and in the context of this PhD project using Newman projections.*[115]

When we moved over to the TEA salt ($Et_4NO_3SC_6H_4CH_3$) the yield increased significantly. The catalytic nature of the base was maintained and as this salt was more atom-efficient we continued its use. We also found that the optimal yields of **17** were obtained when the potential was applied for 4 h. This gave us our optimised conditions as shown in Entry 11 of **Table 2**, highlighted in yellow. When we applied these conditions to a range of substrates, as shown in **Scheme 33**, yields compared well with classical literature methods[95] and a variety of substituents and functional groups were tolerated. However, unlike the divided cell method,[20] when trimethylsilyl acetylene was used, the product appeared to decompose *in situ*. Presumably exposure of the TMS group to the reducing potential was the cause of this decomposition, perhaps allowing cleavage to take place. A bulkier silane, **33**, was produced, albeit in low yield. Also, when 3-ethynylanisole was used in an attempt to produce **21**, the product consistently decomposed, which was strange given the high yields obtained in the divided cell method (**Scheme 29**) and given that 4-ethynylanisole worked extremely well to produce **32**. The reason for this remains unknown to us.[39]

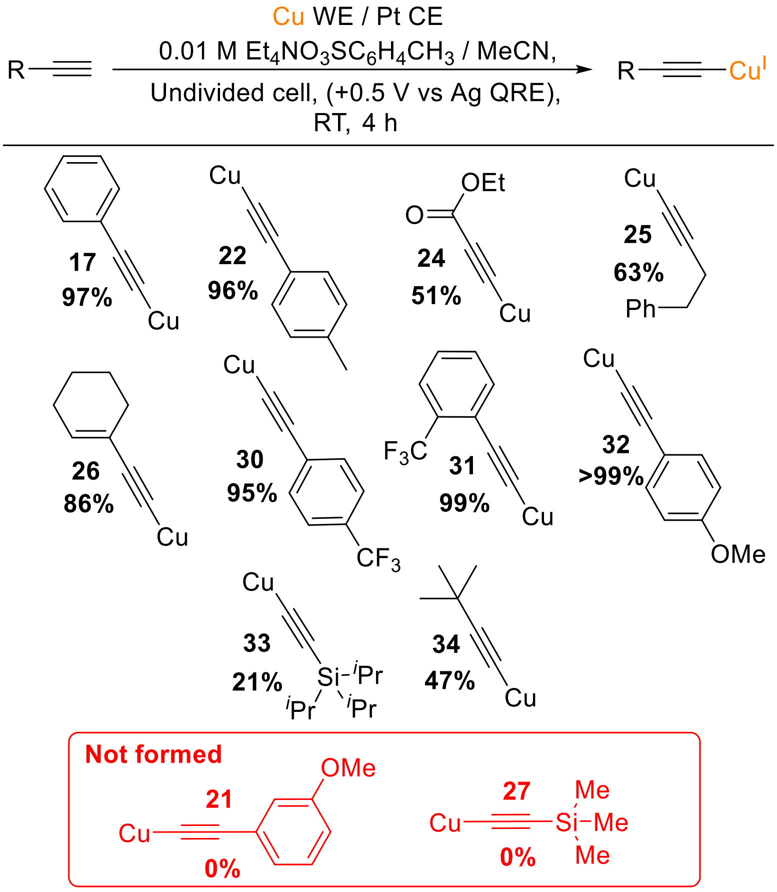

***Scheme 33**: Scope of undivided cell method for electrochemical copper acetylide production.*[39]

It is noteworthy that we initially found certain substrates gave impure products when reagent grade MeCN was employed as the solvent. We believe this may be due to overoxidation of the copper caused by the presence of water as when we switched to anhydrous MeCN, we obtained better results.

A schematic mechanism for this reaction is given in **Figure 14**, highlighting the various single-electron-transfer REDOX reactions taking place at electrode surfaces (red arrows). The possible ‘initiation’ reactions are shown in **Scheme 32**.[39]

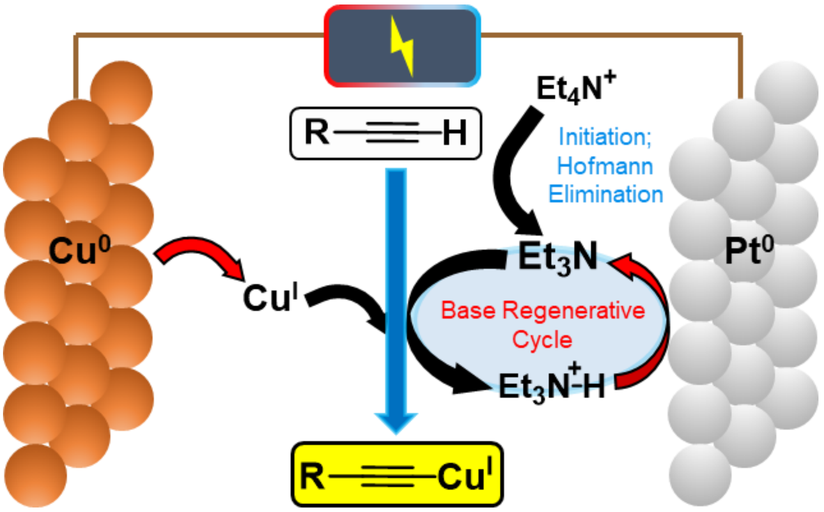

***Figure 14**: Schematic mechanism of electrochemical Cu(I) and base generation/catalytic regeneration.*[39]

Now that methods for preparing copper acetylides electrochemically had been developed (in a divided system and an undivided one) we felt that the next logical step would be to expand into reactions that utilise copper acetylides as intermediates. As such, the CuAAC reaction (the most famous of the 'Click' reactions)[116] became our next reaction of interest.

Chapter 5. CuAAC Click Chemistry

5.1 Introduction

The Cu-mediated Azide-Alkyne Coupling (CuAAC) reaction, as the name suggests, is the coupling of a terminal alkyne with an azide to produce a 1,2,3-triazole product when catalysed by copper. The reaction traces its origin back to the 1960s with the first description of the Huisgen reaction,[117] a dipolar, 1,3-cycloaddition between azides and alkynes. This reaction proceeds under thermal conditions and yields both the 1,4 and 1,5 regioisomers, as shown in **Scheme 34**.[118]

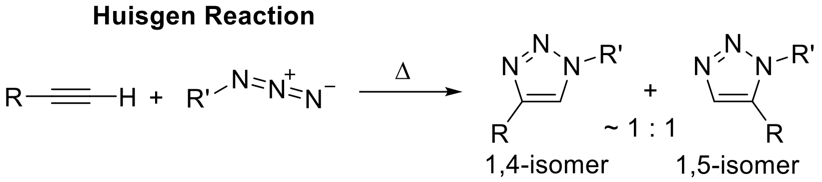

***Scheme 34**: General Huisgen thermally promoted cycloaddition.*[118]

In the early 2000s Meldal[119] and Sharpless[120] found that this reaction could be extremely efficiently catalysed by Cu(I) salts, leading to short reaction times, mild conditions and very high regioselectivity for the 1,4 product only.† This new CuAAC reaction went on to become the epitome of 'Click' chemistry, the joining of smaller molecules in stereospecific, high-yielding and simple reactions.[121,122] Furthermore, the affordability of copper catalysts, ease with which azide and alkyne moieties can be incorporated into a range of compounds to act as coupling partners, and the broad utility of the resulting triazole product have all contributed to this reaction's widespread popularity and success, particularly amongst those in pharmaceutical chemistry.[118]

The mechanism of the CuAAC reaction has been studied extensively over the years. An early proposal of the mechanism by Sharpless (2002)[120] suggested a simple mono-nuclear approach in which a copper(I) acetylide intermediate is formed, followed by ligation to a molecule of azide. This then allowed concomitant formation of a C-N bond and a double bond between the copper ion and a carbon atom of the acetylide, creating a 6-membered Cu(III) species. This then undergoes transannular ring contraction to yield **35**, which can be protonated to yield the 1,2,3-triazole product as shown in **Scheme 35**.[120,123,124]

---

† Subsequently, ruthenium-catalysed protocols (RuAAC) have been developed which select for the 1,5 product from terminal alkynes and which can even produce 1,2,3-triazoles from internal alkynes.[228]

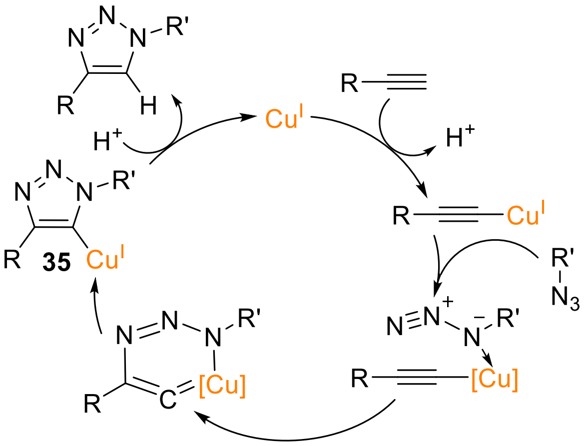

***Scheme 35**: Early proposed mono-nuclear CuAAC mechanism.*[120,123,124]

However, it was later (2004 onwards) repeatedly found from kinetic studies that the rate law of this reaction is second order with respect to the concentration of the Cu^I catalyst, suggesting that two copper centres are required in the mechanism.[123,125] It has also been reported that the rate of reaction increases more slowly than predicted with increasing Cu^I concentration, suggesting the formation of aggregates at higher copper concentrations.[123] Recently, further evidence, such as isolated intermediates, have suggested that both mono-nuclear and di-nuclear copper mechanisms are viable, but that the di-nuclear system is favoured kinetically.[126] The most widely accepted di-nuclear mechanism is shown in **Scheme 36**.[124,126,127] It is worth mentioning that a tri-nuclear copper system has also been proposed, but this did not seem to gain much traction.[127]

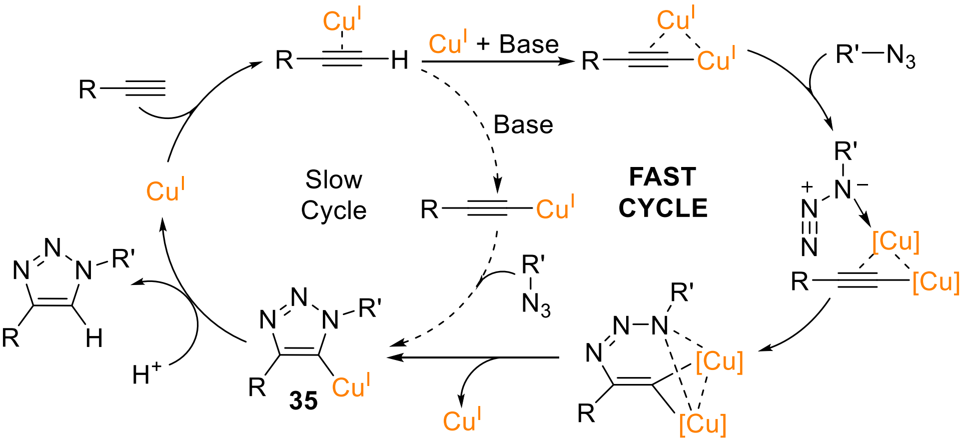

***Scheme 36**: Commonly accepted di-nuclear CuAAC mechanism with proposed slower mono-nuclear cycle incorporated.*[124,126,127]

The CuAAC reaction is very robust in that it is tolerant of a vast host of conditions and reagents whilst still giving very high yields.[127] In terms of ligands, often N-based additives fill the role of both ligand and base, which also helps to solubilise Cu^I species that are used. Many examples exist including triazole-containing amines which have been shown to stabilise Cu^I

in aqueous media for use in cells, such as TBTA.[128] Beyond N-based ligands a number of P, C, O and S-based ligands have also been employed, such as acetate anions (in Cu(I)OAc) and *N*-heterocyclic carbenes (NHC). **Figure 15** shows a very small selection of the array of ligands that have been used.[129]

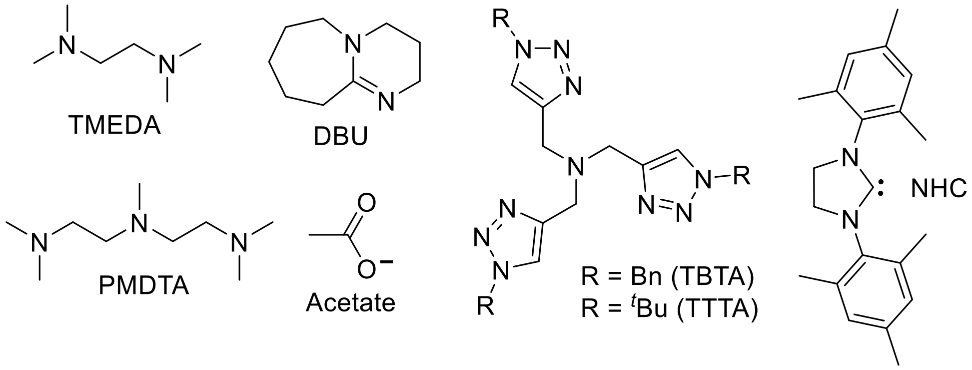

***Figure 15**: A handful of ligands that have been used in the CuAAC reaction.*[129]

In terms of solvents, a review from 2008[127] (a mere 6 years after the reaction was first described) showed that the CuAAC reaction had been carried out in: H_2O, MeOH, toluene, THF, DMF, NMP, pyridine, DCM, $CHCl_3$, DMSO, MeCN, as well as combinations of these and others besides. The main determining factor for which solvent is used appears to be the Cu^I source and its solubility. Often these solvents were used at RT, showing again the broad range of conditions that may be employed with this reaction and ease with which it is carried out.[127]

It has been found that whilst the reaction is dependent upon a Cu(I) catalytic cycle, various oxidation states of the Cu source can be used. Beyond the direct use of Cu(I) salts, mixed Cu(0)/Cu(II) species (such as Cu^0 wire with $CuSO_4$) have been used wherein comproportionation yields the active Cu^I species.[118,127,130] (This gave us inspiration to carry out a CuAAC reaction electrochemically using a Cu wire WE and applying an oxidative potential to it to generate the active Cu^I species.) Cu(II) salts can be employed in this reaction so long as a reductant such as ascorbic acid or sodium ascorbate is also added. This allows Cu(I) to be generated *in situ*, even in the presence of air, as shown in **Scheme 37**.[120,131]

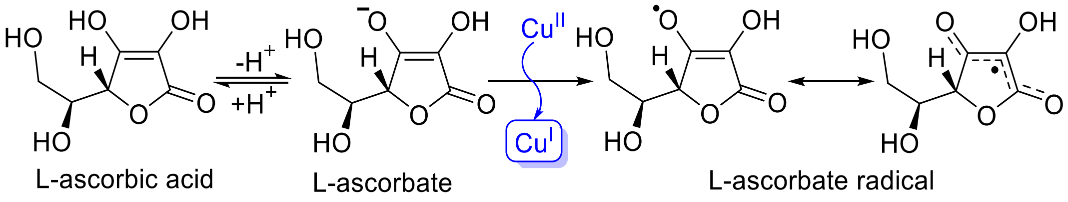

***Scheme 37**: The* in situ *reduction of Cu^{II} by ascorbate.*[120,131]

In terms of practicality this has proved quite beneficial because Cu(II) salts are very stable and easy to handle, and commercial Cu(I) salts are often contaminated with Cu(II), which can lead to a range of unwanted by-products forming such as diynes **36** and bis-triazoles **37**.[120] It has also been reported that the formation of alkynyl-1,2,3-triazoles **38** is also possible and these various by-products and the proposed mechanisms of their synthesis are shown in **Scheme 38**.[132] Note that these by-products all arise from the oxidation of Cu^{I} and that the use of bases (carbonates proving to be the most effective) has been shown to promote their synthesis by removing protons that would otherwise hydrolytically cleave the C-Cu bond in **35** to yield the 1,2,3-triazole product,[127,133] whilst the rigorous exclusion of oxygen has been shown to suppress their production.[120]

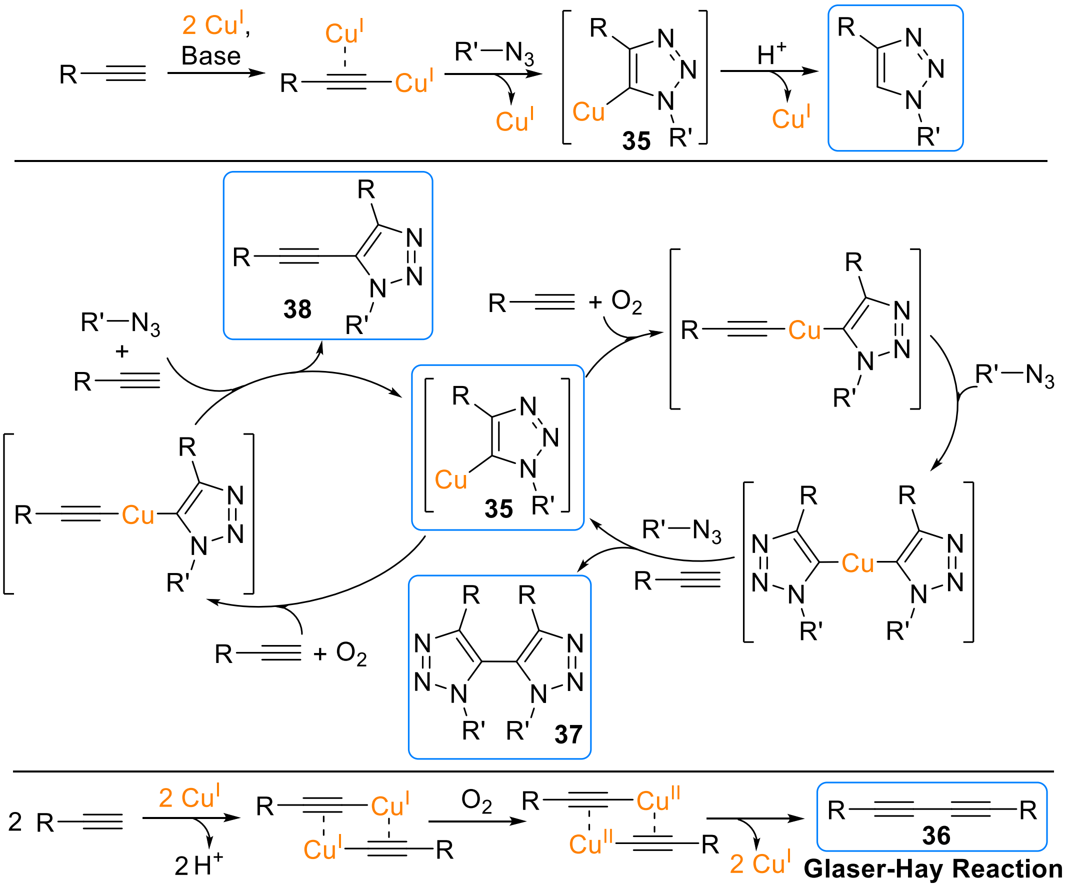

***Scheme 38**: General proposed mechanisms for the formation of various by-products of the CuAAC reaction.*[132]

The CuAAC reaction is not just limited to the production of di-substituted 1,2,3-triazole products as it has been shown that the addition or *in situ* generation of electrophilic halogen species can allow reaction to occur with **35** to yield tri-substituted products. Examples of this include the addition of NCS,[92] NIS or I_2 (**Scheme 39, a)**[134] to the reaction mixture, as well as the simultaneous generation of Cu^{I} and I_3^- from a copper(II) perchlorate/alkali metal iodide mixture (**Scheme 39, b**).[135] There have also been reports of using NBS + CuI to generate I$^+$ *in* *situ* (**Scheme 39, c**).[136] This last method is particularly interesting as it was found that none of the bromo-substituted triazole product was produced at all, suggesting the role of the NBS here is solely as an oxidant for the I^- starting material, as opposed to being an electrophile that reacts with **35** before the bromide is displaced by iodide.

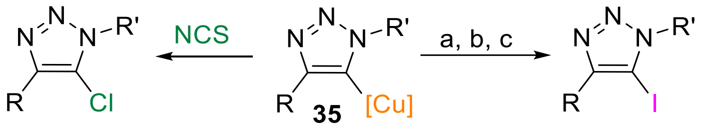

a. NIS or I_2
b. $Cu(ClO_4)_2{\cdot}6H_2O$ + KI or NaI to generate Cu^I + I_3^-
c. NBS + CuI to generate I^+

Scheme 39*: The addition or production of electrophilic halogen species in modified CuAAC reactions.*[92,134–136]

The potential issue with this approach, however, is that often the reaction of **35** with the electrophile gets overshadowed by protonation, leading to large amounts of the standard di-substituted triazole product. Indeed, one of the reasons the standard CuAAC reaction works so well is that the proton source for the reaction can be the terminal alkyne starting material itself, meaning that the protonation pathway is always accessible.[92] To overcome this the approach of using substituted alkynes, such as 1-bromo[137] or 1-iodo[138] alkynes, as starting materials has been developed and is shown in **Scheme 40** (see **Figure 15** for structures of ligands) along with a proposed mechanism for this new mode of reactivity. There has even been an example of using 1-alumino alkynes in this same way,[139] which is potentially very useful as the aluminotriazole that is formed is capable of reacting with a range of electrophiles, including NCS, NBS, NIS and $ClCO_2Me$, to produce stable, substituted products.[139]

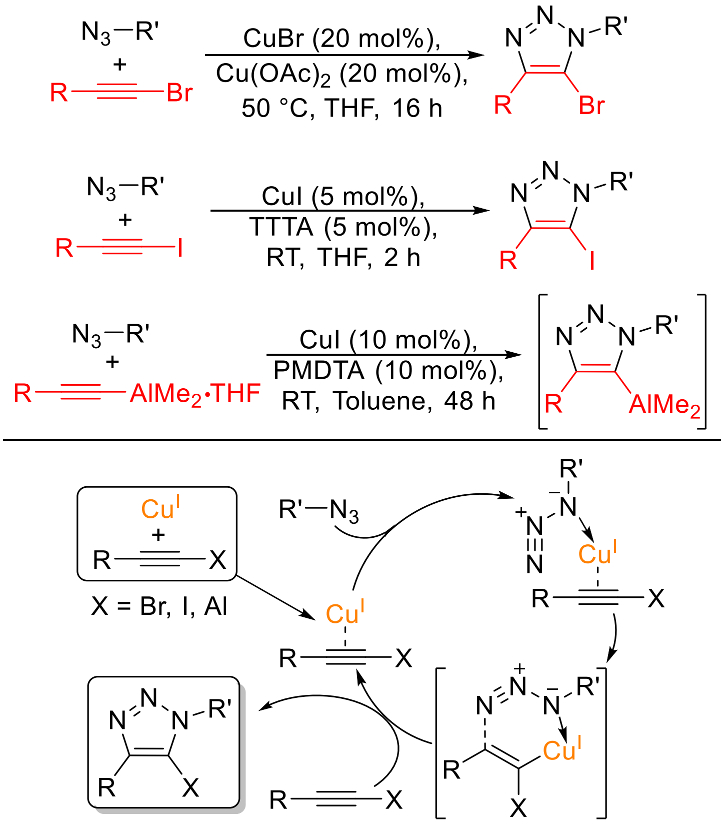

Scheme 40: *The use of substituted alkynes in the CuAAC reaction.*[92,137–139]

The ease with which the CuAAC reaction can be carried out in a wide array of conditions has led to a large number of applications for this reaction in the areas of organic synthesis and pharmaceutical chemistry through bioconjugation.[92,116,118,140] For synthetic purposes, iodo-substituted triazoles (produced by way of methods shown in **Scheme 39** and **Scheme 40**) have been used for halide substitution reactions,[141] and as coupling partners in Suzuki cross-coupling reactions to help make new anti-inflammatory drugs,[142] in Sonogashira cross-coupling reactions to help make carbonic anhydrase inhibitors (as part of new anti-cancer drugs)[143] and in Heck reactions to produce triazole-fused heterocycles.[144]

The standard CuAAC reaction has been used extensively in the realm of bioconjugate chemistry for the production of various drugs and biomolecules (such as chemoenzymatic probes),[145] for polymer synthesis, for surface functionalisation and for the production of biomaterials such as nanoparticles and hydrogels.[140] This is summarised schematically in **Figure 16**.[140]

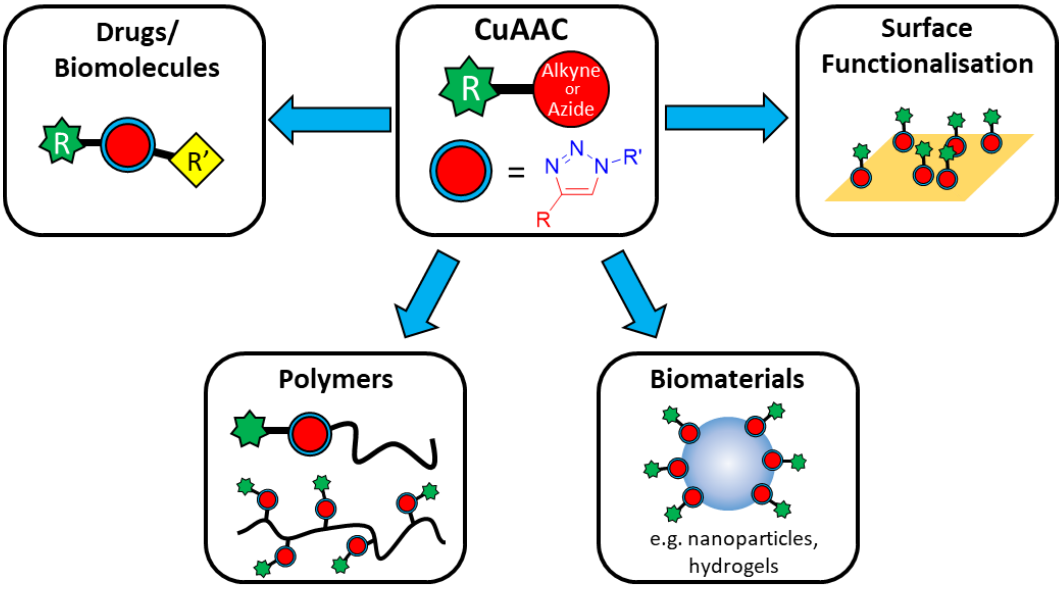

***Figure 16**: Schematic representation of uses of the CuAAC reaction in bioconjugate chemistry.*[140]

Given the obvious importance of this reaction, we wanted to try performing it electrochemically by applying an oxidative potential to a Cu^{0} sacrificial WE to generate the Cu^{I} ions necessary to catalyse the reaction. This approach would be similar to, but the reverse of, Cu^{II} salts being reduced *in situ* by sodium ascorbate. Our proposed electrochemical method would share the same benefits of using Cu^{II} to generate Cu^{I} in that Cu^{0} is extremely easy to handle and much more stable than Cu^{I}. The use of a metal sheet as the source of copper in this reaction would also be the simplest possible source that could be employed.

In the past, people have carried out electro-assisted CuAAC reactions on electrode surfaces coated with either alkyne[146] or azide[147] functionality, where Cu(II) salts that have been added to solution are electrochemically reduced to Cu(I), thereby initiating the CuAAC reaction. This approach is shown in **Scheme 41**.[146,147]

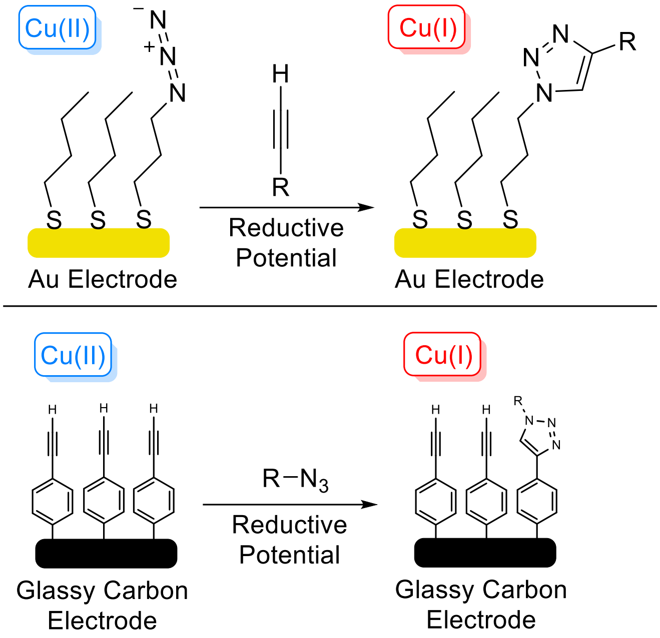

***Scheme 41**: The CuAAC reaction on surface-functionalised electrodes through the reduction of Cu(II) to Cu(I).*[146,147]

Another approach involving the generation of the alkyne moiety on the surface of electrodes through the reduction of $Co_2(CO)_6$ has also been demonstrated.[148] The authors of this work first protected the alkyne by reacting it with $Co_2(CO)_8$, which was reduced electrochemically to reveal the alkyne again when a potential was applied to the electrode that the alkyne was attached to. The alkyne then underwent a CuAAC reaction. The reaction of $Co_2(CO)_8$ with alkynes is most often used in the Pauson-Khand reaction (first described in 1973),[149] which is the [2+2+1] cycloaddition of an alkyne, an alkene and CO to form cyclopentenones. An example mechanism for this reaction is given in **Scheme 42**.[150]

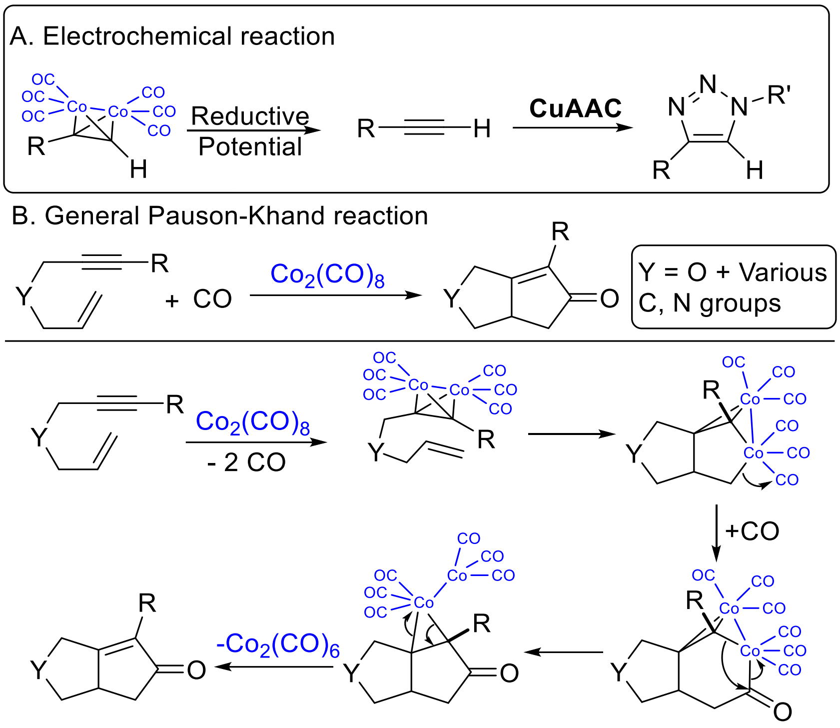

Scheme 42*: A. Example of electrochemical CuAAC reaction using $Co_2(CO)_6$ protection. B. General example of the Pauson-Khand reaction to form cyclopentenones.*[149,150]

5.2 Results of Electrochemical CuAAC Reactions

As we were developing the undivided cell method for preparing copper acetylides, we were mindful of the need to rigorously test the validity of our electrochemical method. The absence of any detectable diyne by-products, generally high yields obtained, and lack of degradation of the materials following completion of the reactions strongly suggested that our products were pure, but we nevertheless decided to carry out a CuAAC reaction using our electrochemically-produced copper acetylides to test their fidelity. The CuAAC reaction is widely-used, especially in pharmaceutical chemistry where many drug molecules, biomaterials and polymers are routinely produced using this chemistry.[118,127,140] It is also a reaction known to be efficient and relies upon a Cu^I-based catalytic cycle, meaning that if our copper acetylides were in a mixed oxidation state this should be highlighted clearly, simply from the isolated yield. This became known to us as the ‘Click test’. We therefore adapted conditions from Shao *et al.*,[91] deliberately selecting a method without a reducing agent such as sodium ascorbate to remove the possibility of Cu^{II} being converted into Cu^I mid-reaction. See **Figure 17**.[39]

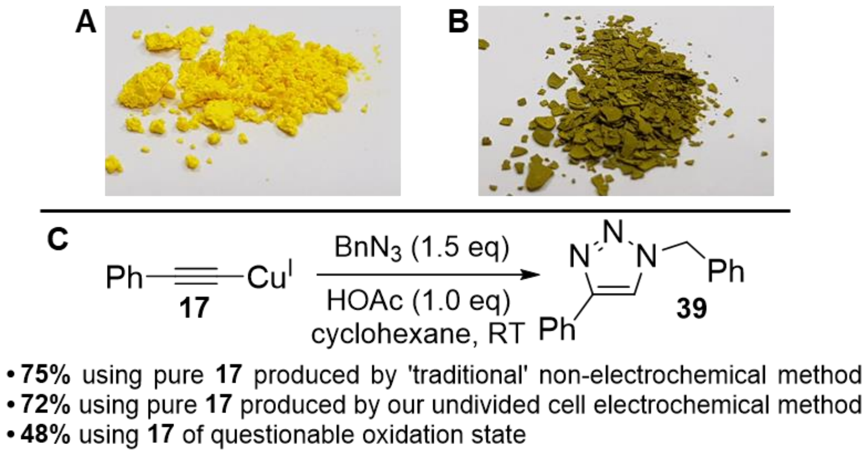

- **75%** using pure **17** produced by 'traditional' non-electrochemical method
- **72%** using pure **17** produced by our undivided cell electrochemical method
- **48%** using **17** of questionable oxidation state

Figure 17*: A. Picture of* ***17*** *that matches literature descriptions. B. Picture of* ***17*** *that is of questionable oxidation state. C. 'Click test' of copper acetylides to assess product purity*.[39,91]

We found that the yields and spectral data for **39** produced using **17** from both the traditional method (synthesised using CuI in $NH_4OH_{(aq.)}$-EtOH[88,95]) and our new electrochemical method compared very well with one another. This reaffirmed in our minds that our electrochemical method for producing copper acetylides is robust. We also discovered that when **17** of questionable oxidation state was used, i.e. samples that were not the characteristic bright yellow colour associated with most copper acetylides, but instead a darker yellow colour as in picture **B** of **Figure 17** (suggesting a possible mixture of Cu^{I} and Cu^{II} acetylides), a significantly lower yield of 48% was obtained for **39**. This result lends support to the use of the CuAAC reaction as a good way to test copper acetylide purity in the future as a so-called 'Click test'.[39]

Emboldened by these results, we next attempted to integrate our electrochemical copper(I) acetylide formation with the CuAAC reaction to produce a sustainable, one-pot electrochemical process, as shown in **Scheme 43** (the potential was applied for 3 h, then the solution was left to stir for a further 13 h). To the best of our knowledge this would be the first example of both an electro-oxidised Cu(0) to Cu(I) approach and of such a reaction on a preparative-scale. When we attempted the reaction, we were pleased to obtain yields of 49% for **39** when $Et_4NO_3SC_6H_4CH_3$ was used as the electrolyte and 79% when $Et_4NOAc\cdot 4H_2O$ was used. The control reactions where no potential was applied yielded 2% and 0% respectively. These results suggest that the presence of acetate anions allows for the generation of a potent copper acetate catalyst. We therefore wondered whether Cu(I)OAc could be the active copper catalyst in this reaction. Attempting to confirm this, we carried out a control reaction using Cu(I)OAc (1 eq – a large excess for this catalytic reaction) and Et_3N (1.1 eq) which were dissolved in anhydrous MeCN. Benzyl azide (1.5 eq) and phenylacetylene were then added, the solution was degassed and then left to stir at RT overnight. This gave **39** in

59% yield which shows a copper acetate species is certainly capable of catalysing this reaction, but the yield falls short of the electrochemical method. Furthermore, trace amounts of diyne **18** were also produced in this control experiment (presumably from Cu(II) contamination of the Cu(I)OAc catalyst) which was not observed in any of the electrochemical tests where Cu(I) is generated *in situ*.[39]

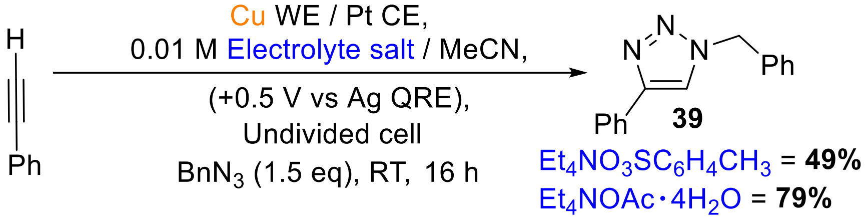

***Scheme 43**: One-pot electrochemical CuAAC reaction.*[39]

Another question we were keen to investigate was, how much copper was being generated in this reaction? To answer this question is not at all simple. In the undivided protocol we were using, copper ions produced at the anode can also be reduced at the cathode, making accurate determination of the amount of copper produced difficult when looking only at the total charge passed during the reaction. Also, carrying out non-electrochemical control reactions with varying loadings of commercially-available copper catalysts would not work well either, as shown with the Cu(I)OAc control reaction, as this can lead to Cu(II) contamination and it does not sufficiently represent the conditions used in the electrochemical one-pot approach. So, a new electrochemical method was devised. We wanted to simulate the electrochemical conditions as closely as possible; to this end we used a divided cell and opted to deposit a layer of copper onto the surface of graphite electrodes through reduction from an aqueous copper sulfate solution. This would allow us to coat only as much copper as we wanted to use in our tests. This same approach is utilised in **Chapter 4**. We controlled the amount of copper by using **Eq. 1** (**page 1**) and calculated how much charge must be passed in order to coat a graphite rod with, for example 5 mol% Cu, if we used 0.2 mmol phenylacetylene starting material. In this way we coated 4 separate graphite rods, one with a 5 mol% Cu loading, another with 10 mol%, then 20 mol% and finally 30 mol%. We then carried out 4 electrochemical reactions, where the Cu loading was first released into the 0.01 M $Et_4NOAc\cdot4H_2O$ / MeCN solution using an oxidative potential of +0.5 V vs Ag QRE. Once all the Cu had been oxidised to Cu(I) ions in solution (as confirmed visually and, more importantly, by the charge that had been passed), the solution was transferred to a sealed flask and degassed thoroughly with argon. In this solution, BnN_3 (1.5 eq), Et_3N (1.5 eq) and phenylacetylene (1.0 eq) were then dissolved, before the solution was left to stir at RT overnight. **Scheme 44** outlines this general approach.

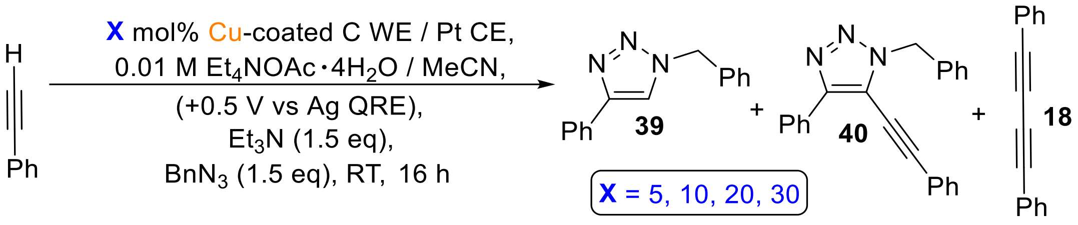

***Scheme 44**: Copper catalytic loading determination using Cu-coated C electrodes.*

Interestingly, in practice this approach generated three products when attempted, in varying ratios depending on the Cu catalytic loading. The desired 1,2,3-triazole product **39** (formed by way of Cu^I catalysis) was indeed produced, however, alkynyl-1,2,3-triazole **40** and diyne **18** (both formed through Cu^{II} catalysis) were also produced. In terms of trying to accurately determine how much Cu^I catalyst is needed to efficiently produce **39** using our electrochemical method, this approach clearly failed, but the trends in the distribution of products **39**, **40** and **18** over the varying Cu catalyst loadings is itself quite interesting and warrants discussion. **Table 3** shows this distribution of products in terms of isolated yields with respect to the phenylacetylene starting material.

***Table 3:** Distribution of products formed at various catalytic loadings of copper.*

Cu loading / mol%[a]	**4.5**	**9.9**	**21.5**	**30.2**
Diyne, **18** yield / %[b]	4	8	14	21
1,2,3-Triazole, **39** yield / %[b]	10	27	23	9
Alkynyl-1,2,3-triazole, **40** yield / %[b]	20	8	45	46
Total conversion of phenylacetylene / %	34	43	82	76
Unreacted phenylacetylene / %	66	57	18	24

[a] Corrected catalytic loading after taking into account exact mass of phenylacetylene used and exact charge passed whilst coating C rods. [b] Isolated yields of obtained products.

Some important details about this table and the associated experiments require a brief explanation. Owing to the way the copper was plated onto the carbon rods to give us our catalytic loadings, the corrected loadings are shown in the table, i.e. a maximum of 4.5 mol% instead of 5 mol%, etc. These values were obtained by first taking into account the exact charges passed when coating the rods: '5 mol% test' = 1.928 C passed, '10 mol% test' = 3.946 C passed, '20 mol% test' = 7.754 C passed, '30 mol% test' = 11.580 C passed. Then dividing these values by 2 for the fact that 2 electrons are given to each Cu(II) sulfate species to plate Cu(0) onto the carbon rod, then divided by the elementary charge constant, 1.602×10^{-19} C and

Avogadro's number, 6.022x10^{23} mol^{-1} to give the amount of copper plated in mol. Finally, the exact masses of phenylacetylene used in each test is taken into account, '5 mol% test' = 0.0225 g, '10 mol% test' = 0.0211 g, '20 mol% test' = 0.0191 g, '30 mol% test' = 0.0203 g, to give the corrected catalytic loading values shown in the table. The yields for the products formed also take the exact mass of phenylacetylene used into account.

Table 3 shows the product distribution from the 4 tests that were carried out, but the best way to represent this data is in the graphs shown in **Figure 18**.

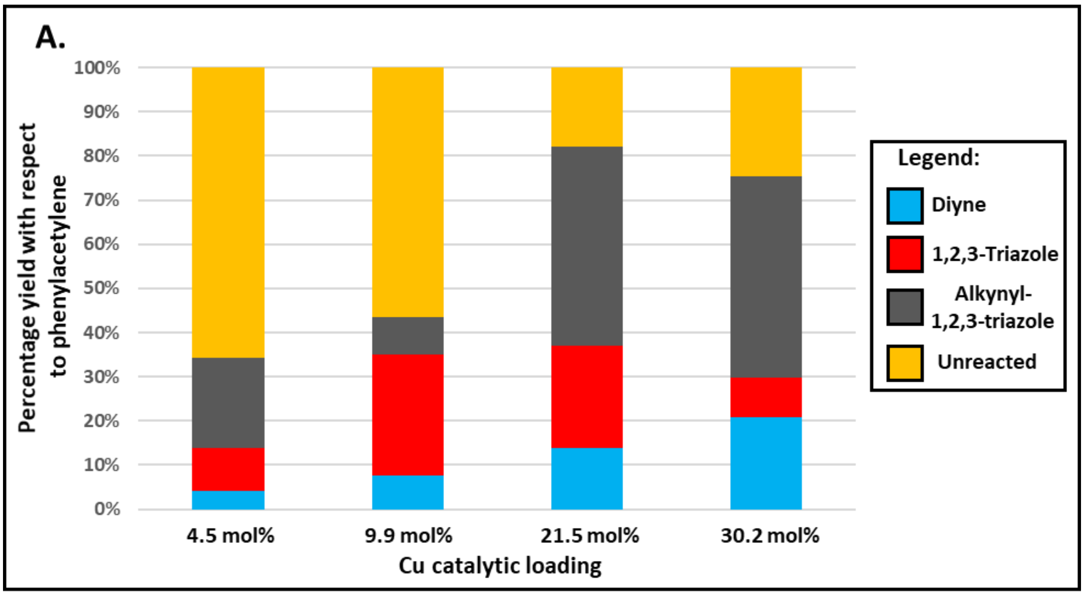

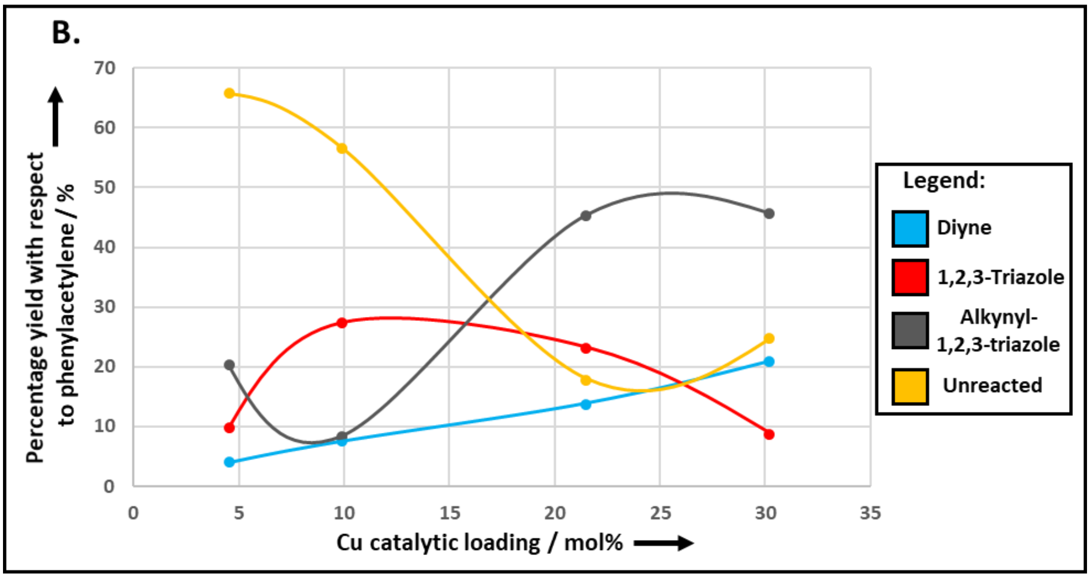

***Figure 18**: A. Bar chart showing the fate of the phenylacetylene starting material in percentage yield. B. Scatter graph showing the trends in product distribution at various catalytic loadings.*

It is important to note that these graphs should be taken as preliminary results and that interpretations of the data should be tentative. This is because only one test was run at each of the catalytic loadings used. Furthermore, the method we used to introduce the copper to solution suffers from a key point of uncertainty in that as we plate the Cu(0) onto the surface of the carbon rod, a small amount of water electrolysis takes place. This side reaction contributes to the total charge passed (which we use to calculate the catalytic loadings) and so gives an overestimate of these values. This overestimate will be proportional to the length of time the reducing potential is passed through the aqueous $CuSO_4$ solution, meaning for example that the overestimate will be greater for the 30 mol% test, which requires longer to coat the carbon rod, than the 10 mol% test. With these inaccuracies in mind, some basic analysis of this data was carried out.

The clearest trend from these graphs is that at higher catalytic loadings there is generally a greater conversion percentage compared to lower loadings, which is intuitive. However, this trend appears to level off and even decrease slightly between 20 mol% and 30 mol%. It could be that a point of diminishing returns is reached at around 20 mol% beyond which adding more catalyst to this reaction does not significantly improve the overall conversion.

Another key trend from this data is the almost linear increase in diyne yield with an increasing catalytic loading. This is in contrast to the much more variable yields observed for **39** and **40**. The most likely explanation for this is simply due to the diyne being formed from a different catalytic pathway than **39** and **40**. Despite all three species deriving from a copper acetylide intermediate, the two triazole-based species of course rely upon interaction with a molecule of azide, which may cause the complex trends observed in their yields. However, the production of **18** in the first place indicates that an oxidation process must be taking place. The solutions were sealed and degassed with argon to prevent O_2 interfering with the reactions. Also, given that the same amount of anhydrous MeCN was used in each test it seems that electrolysis of water molecules in the reaction vessel is unlikely to be the cause. Therefore, it seems most likely that the linear increase in diyne yield is related instead to the coating process of the Cu-coated C electrodes. It is also possible that the linear increase is related to the length of time it takes to oxidise the copper coating at the start of these tests, but given the efficiency with which we produced Cu(I) acetylides in a divided cell with MeCN previously,[20] without forming diyne by-products (**Scheme 29**), this seems less likely. As mentioned previously, the larger the quantity of copper that needs to be plated onto a carbon rod, the longer it takes. This fact may allow more aerial oxidation of the Cu(0) coating to take place with greater catalytic loadings (as the coating process is carried out whilst exposed to air). This would therefore mean that the Cu-coated C electrodes are in fact mostly Cu(0), but with a small amount of

Cu(I) and Cu(II) contamination present (allowing the Cu(II)-catalysed processes to take place in our tests). Thorough characterisation of the Cu-coated C electrodes would be needed to test this hypothesis, but if it proves true in future work it may be possible to use the yield of diyne product from tests such as those discussed here to determine a relationship between the length of time required to coat the carbon rods with copper and the amount of Cu(II) contamination that might be expected.

The final observation to make from **Figure 18** is that the best selectivity for the desired triazole process was obtained when 10 mol% Cu was used, whereas by around 30 mol% the selectivity had shifted much more in favour of Cu(II)-catalysed processes. This likely relates to the possible increasing Cu(II) contamination of the Cu-coated C electrodes theory. It could also be that there is a degree of disproportionation of Cu(I) ions to form Cu(II) taking place. However, the results from the 4.5 mol% run appear to somewhat contradict these ideas. In short, more tests need to be carried out to make confident assertions about the reactivity and nature of this reaction, but the initial results are interesting and promising.

Some other substituents were tested using the conditions shown in **Scheme 45** in an attempt to test the scope of this electrochemical protocol for the CuAAC reaction. As in **Scheme 43**, the potential was applied for 3 h, then the solution was left to stir for a further 13 h.

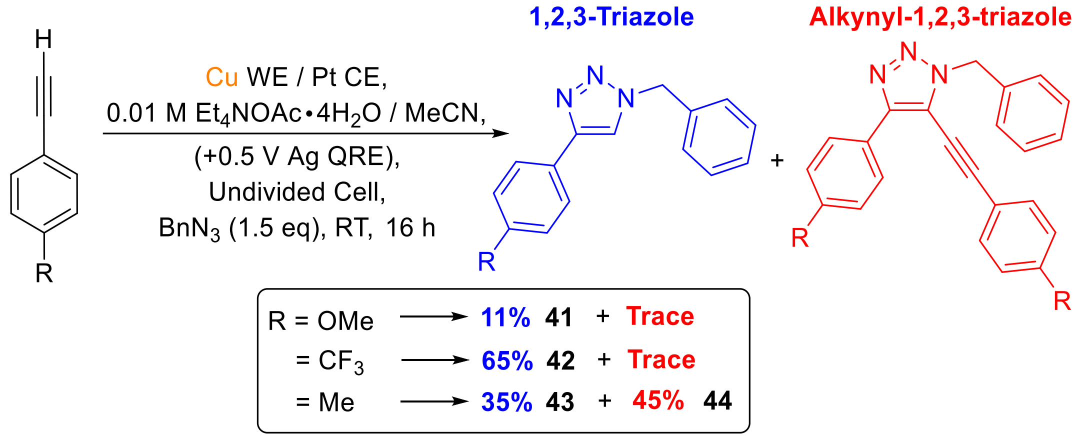

***Scheme 45**: Tests of the scope of the electrochemical CuAAC reaction.*

Unfortunately, the yields across the board for these tests were fairly low, showing that more optimisation work needs to be done for these conditions. In the case of the *p*Me R group reaction, a significant quantity of the alkynyl-1,2,3-triazole product **44** was obtained, suggesting Cu(II) must have been present. For the other two R groups, traces of what is presumably the alkynyl-1,2,3-triazole product were observed by TLC, but in too low a quantity to isolate and characterise properly. In all these tests, O_2 was excluded through degassing the reaction vessel with argon, and no diyne products were observed. The traces of alkynyl-1,2,3-triazole product can perhaps be explained by a small amount of O_2 infiltrating the reaction vessel as it is hard to completely exclude from our setups, but the 45% yield obtained for **44** suggests a large amount of oxygen was present in that test. As no diyne by-product was detected, this may indicate that the vinyl copper species **35** (formed from the initial cycloaddition of copper acetylide and azide) is more reactive than the copper acetylide species, thereby allowing **44** to form in preference of the diyne.

The fact that the yields for the 1,2,3-triazole product appeared to follow a trend whereby the more electron-donating the substituent, the lower the yield stood out to us. The very low yield of 11% for **41** seemed particularly unusual as the copper acetylide we produced from the same alkyne starting material, using an undivided cell, was synthesised almost quantitatively. During this CuAAC reaction however, the current appeared to essentially stop flowing within 40 mins of the electrolysis starting and as a result the overall charge passed was very low. The same result was obtained when the reaction was repeated. It is also important to note that a small amount of bright yellow precipitate (copper acetylide) did form in both tests. We decided to carry out a control reaction using Cu(I)OAc (0.5 eq – a large amount for this type of reaction, to assess whether a lack of copper catalyst being generated was the issue), BnN_3 (1.5 eq) and Et_3N (1.0 eq) dissolved in MeCN. This solution was kept under argon and stirred at RT for 16 h. In this test, lots of bright yellow copper acetylide appeared to have formed, along with a yield for **41** of 25%. Therefore, it appears as if the issue in this case is a mixture of not enough copper catalyst being generated electrochemically (as the yield was improved slightly in this control reaction with abundant catalyst present), and this particular substrate not efficiently reacting with the benzyl azide to yield the triazole product (given the still low yield of 25% for **41** despite the greater amount of copper acetylide produced compared to the electrochemical test).

More experiments need to be carried out on this particular reaction to draw any meaningful trends in reactivity with respect to electron-donating or electron-withdrawing groups impacting the yield, as well as more optimisation work to improve the yields of this reaction as a whole. Given the CuAAC reaction's widespread use in pharmaceutical chemistry, a reliable electrochemical synthetic route, that can compete in terms of yield and scope with non-electrochemical approaches, would be very useful to develop and research further. The potential benefits, such as improved sustainability from such an approach, are an attractive proposition and we hope that these initial results are a good start on the road to achieving this.

Chapter 6. The Glaser-Hay Reaction: An Electrochemical Point of View

6.1 Introduction

Copper acetylides have been used as viable reagents for producing a range of compounds (**Scheme 24**), but an important class of compounds thus far only alluded to, which are also produced from copper acetylides, are 1,3-diynes. These compounds were first described in 1869 when Carl Glaser[151] reported that the homocoupling of two terminal alkynes had been achieved using stoichiometric copper chloride and atmospheric oxygen in aqueous ammonia.[152] In 1960, this same reaction was reported by Hay,[153] but carried out using CuCl and TMEDA in sub-stoichiometric quantities, with TMEDA acting as a convenient ligand for the catalytic copper species. The Glaser and Hay reactions have subsequently been unified and are now thought of as one and the same. More recently, other metals have been employed alongside Cu to further facilitate alkyne homocoupling reactions such as iron,[154] nickel[155] and palladium.[156–158]

1,3-Diynes have important applications in synthesis, having been used for making heterocycles[159] such as, isoxazoles *via* Cope-type hydroamination,[160] and pyrroles and furans *via* gold catalysis.[161] Examples of these reactions are given in **Scheme 46**.[156]

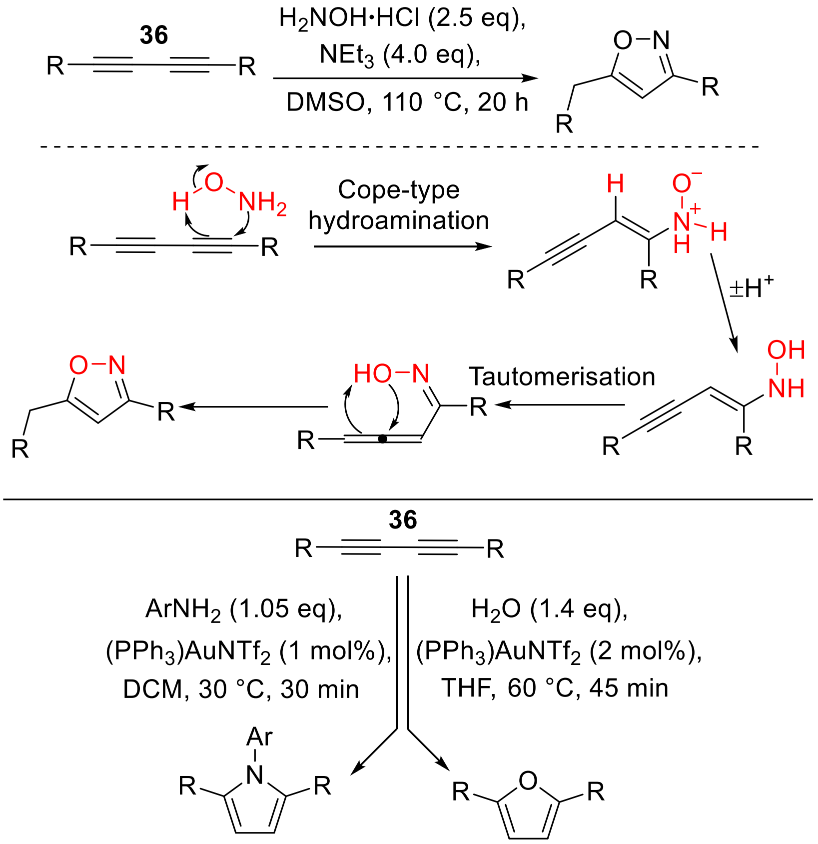

Scheme 46*: Examples of heterocycles formed from 1,3-diynes.*[156,160,161]

Furthermore, the diyne moiety is important because it features in many useful natural products[162] such as: falcarindiol (an anti-MRSA agent),[163] panaxytriol (an anti-tumor agent),[164] repandiol (also an anti-tumor agent),[165] cicutoxin (a plant toxin)[166] and diplyne E (an HIV inhibitor).[167] **Figure 19** shows these structures.[156]

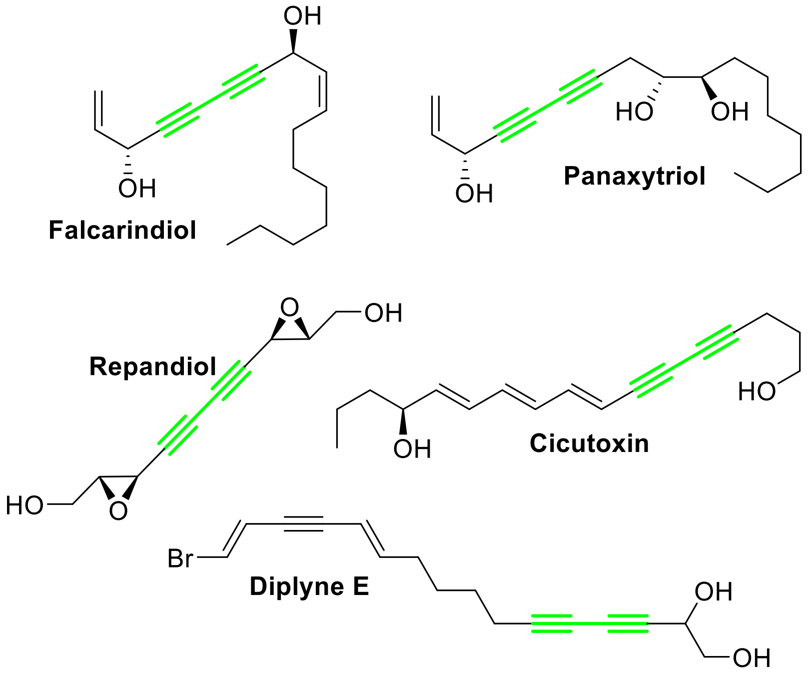

***Figure 19**: Structures of various natural products that contain a diyne unit.*[156,162–167]

Owing to their high level of conjugation, 1,3-diynes have been used to produce π-conjugated linear polymers[168] and as a result they have also found use in the area of molecular electronics.[169] It is thought that molecular wires, switches and circuitry (based on chemical motifs like the diyne) could be used to miniaturise classical silicon-based electronics,[156,170] so clearly these compounds are very useful and merit investigation.[171]

Since its first discovery, a lot of debate has taken place as to what the mechanism for the copper-mediated Glaser-Hay reaction is, but to simplify things the proposals can be grouped into two main schools of thought. Those that follow a Cu^I/Cu^{II}-type mechanism, and those that follow a $Cu^I/Cu^{II}/Cu^{III}$-type mechanism. We will start with the former.

The most commonly accepted mechanism is shown in **Scheme 47** as proposed by F. Bohlmann *et al.* in 1964.[172] This mechanism relies on the interaction of a pair of copper acetylides coming together to form the dimerised product. However, no specific details were given in this original paper as to exactly how the two copper acetylides interact to yield the diyne product, or how Cu(I) is released after coupling, which leaves a lot of room for debate.

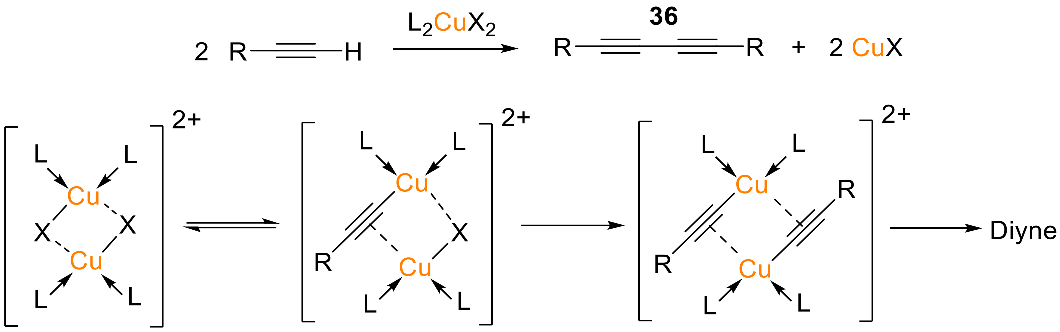

***Scheme 47**: The mechanistic pathway laid out by Bohlmann for the Glaser coupling reaction.*[152,172]

L. G. Fedenok *et al.*[173] represented the diyne-forming step by showing the C-Cu^{II} bonds of the acetylides fragmenting in a homolytic-like fashion to produce the diyne product and Cu(I) in the key coupling step,[173] as shown in **Scheme 48**.

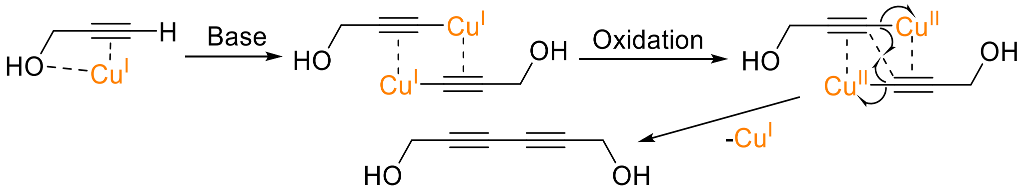

***Scheme 48**: A proposed homolytic fragmentation of copper acetylides to form diynes.*[173]

More recently, a Cu^I/Cu^{II}/Cu^{III}-type mechanism has gained a lot of traction, following certain DFT, kinetic and NMR experiments.[174,175] A proposed catalytic cycle is shown in **Scheme 49** which moves through Cu(I) to Cu(II) to Cu(III) then back to Cu(I).[152] The nature of the ligand and base are important in this type of reaction and it has been reported that the optimal catalytic cycle can be achieved if CuCl (2 mol%) is used with TMEDA (1.5 mol%) as the ligand and DBU or DABCO (1.0 eq) being used as the base.[152] Note that this mechanism differs from the Bohlmann-suggested mechanism as it does not explicitly show the interaction of two copper acetylide molecules.

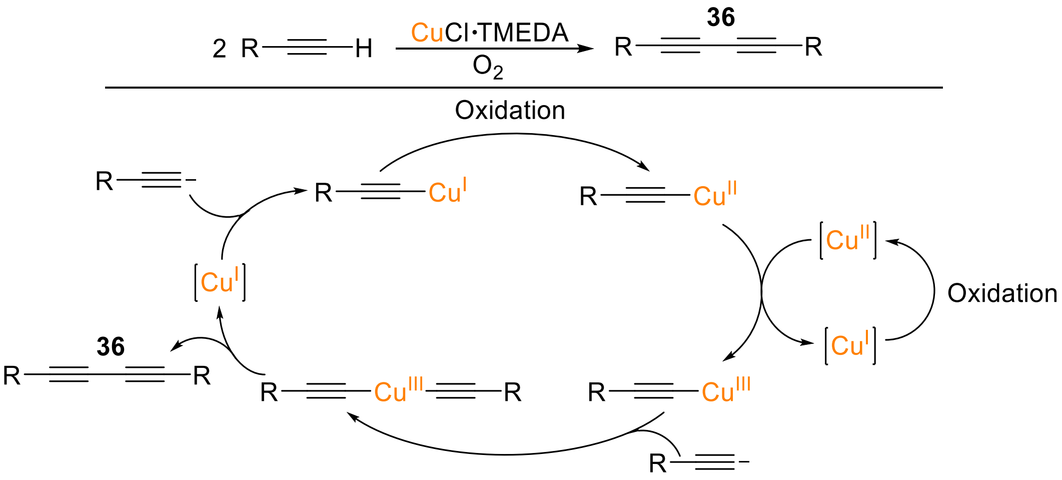

***Scheme 49**: Showing a proposed catalytic cycle based on DFT calculations for the Hay coupling reaction.*[152,153,174]

The mechanism seen in **Scheme 49** was only tentatively suggested by the authors,[174] but it seems to encompass a lot of the modern ideas surrounding this reaction. The authors also report a strong case for Glaser-Hay mechanisms initially requiring Cu(I) catalysts rather than Cu(II), based on their kinetic studies which showed that whilst Cu(I) and Cu(II) could both be used as catalysts in these reactions, an initiation period was observed when Cu(II) was used, which the authors postulate is the time needed for the concentration of Cu(I) in solution to reach a steady state. They suggest that traces of Cu(I) salts in the Cu(II) catalysts used were in fact the reason why Cu(II) catalysts worked at all.[174]

Another important, and rather similar, reaction for the homocoupling of alkynes to form diynes is the Eglinton coupling reaction. First described in 1956,[176] this reaction specifically uses pyridine and an equivalent, or excess, of $Cu(OAc)_2$ as the copper source. This method can be thought of as distinct from the Glaser-Hay reaction as it does not use a copper halide salt and thus likely follows a different mechanistic pathway. While there is no definite, established mechanism for this reaction, a proposed mechanism is shown in **Scheme 50**, though it should be said that radical mechanisms have also been proposed.[152,156,176]

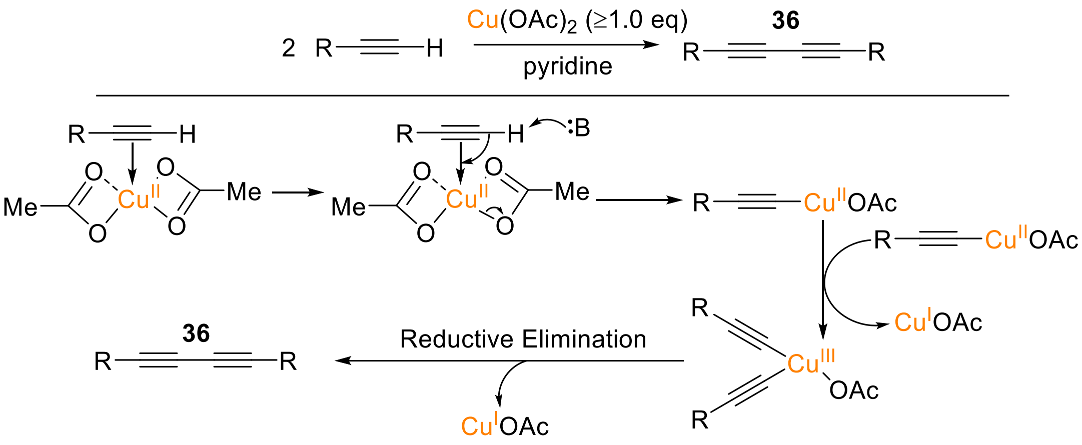

***Scheme 50**: Showing the Eglinton coupling reaction and a proposed mechanism.*[152,156,176]

The Glaser-Hay and Eglinton coupling reactions are useful for the production of symmetrical diynes through homocoupling but are not very selective when attempting hetero-coupling to form unsymmetrical products. For this, the most effective method was first shown in 1955 by Cadiot and Chodkiewicz[177] who showed that reacting a copper acetylide with a halo-substituted (generally bromo) alkyne could effectively produce the cross-coupled product in preference of the homocoupled one (**Scheme 51**). It is also possible to start from a terminal alkyne and produce the copper acetylide as an intermediate in the reaction mixture. Usually an amine base is used in this reaction.[152]

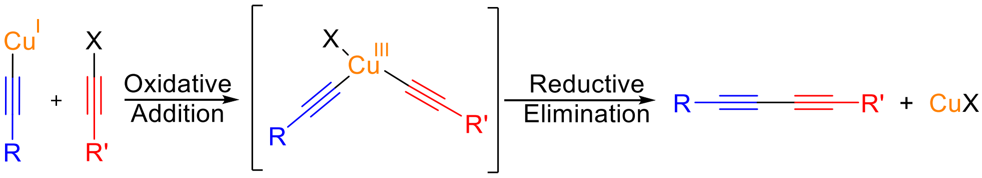

***Scheme 51**: Showing the Cadiot-Chodkiewicz unsymmetrical alkyne coupling reaction.*[152,177]

Interestingly, this method has also proved viable when one of the R groups is Et_3Si. This opens up the possibility of converting the C-Si bond into C-H after coupling, which, in turn, opens up the possibility of synthesising linear polyynes.[152]

6.2 Electrochemical Glaser-Hay Mechanistic Investigation

Whilst developing the electrochemical synthesis of copper acetylides, we tested **17** for solubility in a range of solvents. DCM appeared to be the best solvent in that partial solubility was exhibited, whereas all other solvents tested did not appear to show any solubility at all. This is in line with what others have reported.[95] When we were initially developing our conditions to produce copper acetylides, we noticed that a new product began to form in some cases when O_2 was not completely excluded from the reaction vessel, in addition to the copper acetylide that precipitated out. This product turned out to be the diyne **18**. To the best of our knowledge, the Glaser-Hay reaction to produce diynes has only been facilitated electrochemically once before when electrodes that had been coated with alkyne units were subjected to oxidative potentials to generate Cu(II) ions from Cu(I) species, thereby turning on the Glaser-Hay reaction.[146] This general technique has already been shown in **Scheme 41** for the reductive production of Cu(I). Perhaps surprisingly, given the previously stated lack of solubility of copper acetylides in most solvents, when we used MeCN (exposed to air) to produce copper acetylides the reaction yielded a lot of diyne product **18** in addition to acetylide **17** (30% **17**, 58% **18**). The most intriguing result came when using DCM. Unlike all other solvents tested, none of the copper acetylide precipitated out of solution, allowing the highest yield of diyne **18** to be obtained (67%). This warranted further investigation as summarised in **Table 4**.[40] It is important to note that the amount of charge passed in these electrochemical tests should be included as another means of comparing the tests to one another, but we did not learn the importance of this until later in the PhD project. Therefore, the charge was not measured during these experiments and is not presented in this table.

Table 4: *Optimisation and control reactions carried out to investigate the electrochemical production of diyne **18** in a divided cell.*[a]

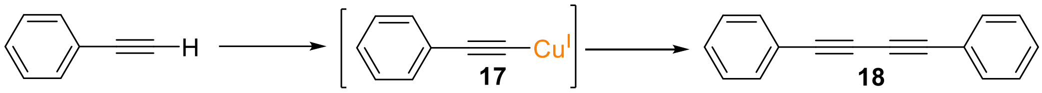

Entry	Electrodes Used[b]	Potential (vs Ag QRE)	Electrolyte Solution	Other	Isolated Yield/ %[c]
1	Cu (WE)/Pt (CE)	+2 V for 3 h then 13 h stir	0.05 M Bu_4NPF_6 / DCM	—	67
2	Cu (WE)/Pt (CE)	No potential applied, 16 h stir	0.05 M Bu_4NPF_6 / DCM	—	1
3	Al (WE)/Pt (CE)	+2 V for 3 h then 13 h stir	0.05 M Bu_4NPF_6 / DCM	—	<1
4	Cu (WE)/Pt (CE)	+2 V/-2 V for 5 s each for 3 h total, then 13 h stir	0.05 M Bu_4NPF_6 / DCM	—	25
5	Cu (WE)/Pt (CE)	+2 V for 3 h then 13 h stir	0.05 M Bu_4NPF_6 / DCM	Exclusion of O_2, solution under argon	8
6	Cu (WE)/Pt (CE)	+2 V for 6 h then 10 h stir	0.05 M Bu_4NPF_6 / DCM	—	78
7	Cu (WE)/Pt (CE)	+2 V for 3 h then 13 h stir	No Bu_4NPF_6, DCM solvent only	—	2
8	No electrodes	No potential applied, 16 h stir	0.025 M Bu_4NPF_6 / DCM	CuBr (1.0 eq) used	52
9	No electrodes	No potential applied, 16 h stir	0.025 M Bu_4NPF_6 / DCM	$CuBr_2$ (1.0 eq) used	30
10	Cu (WE)/Cu (CE)	+2 V for 3 h then 13 h stir	0.05 M Bu_4NPF_6 / DCM	Larger overall surface area electrodes[b]	75
11	Cu (WE)/Pt (CE)	+2 V for 3 h, then stop	0.05 M Bu_4NPF_6 / DCM	—	7
12	Cu (WE)/Pt (CE)	+2 V/+3 V for 10 min each for 3 h total, then stop	0.05 M Bu_4NPF_6 / DCM	—	10

*[a] In all cases DABCO (1.2 eq with respect to phenylacetylene) was used as a base. [b] Electrodes had effective surface areas of: Cu plate (5.30 cm^2), Pt wire (1.26 cm^2), Ag wire (0.79 cm^2) quasi reference electrode and Al plate (5.30 cm^2 surface area). [c] Isolated yield of diyne **18**.*

Note that in all reactions in **Table 4**, DABCO (1.2 eq) was used as the base. Different bases were also tested and are shown in **Table 5**. We found it unnecessary to run the potential for more than 3 h to produce enough copper in solution to carry out this reaction. However, a small increase in the amount of copper produced (Entries 6 and 10) did seem beneficial, giving the best yields of up to 78%. These entries pertained to using 6 h of potential, and using a larger surface area of electrodes, respectively. Entry 2 shows the control reaction where no potential was applied, giving essentially no diyne product, as expected. Different metals such as aluminium did not catalyse this reaction in a similar fashion to copper, again, as expected (Entry 3).

Entry 4 shows an interesting test to see what effect switching polarity of the potential, and thus, the possibility of both oxidation and reduction processes, would have. The yield was adversely affected, which could possibly mean that some of the copper species produced was reduced back to Cu(0), thereby slowing the reaction down. Electrodeposition of copper is not a new concept[178] but this does have quite interesting implications for the possibility of using a reducing potential, after reactions have been carried out, to reduce copper species, depositing them back onto the electrode. This would not only cut down on the issue of copper contamination of products, using electrochemical methods in a similar fashion to others,[179] but also recycle copper atoms back onto the electrode from which they were generated, ready to be used again. This technique is discussed in more detail in **Chapter 8**.

Entry 5 shows that the exclusion of oxygen from the reaction mixture greatly reduced the yield of **18**, but the fact that some product was still formed (8%) could be an indication that the anode performed the oxidation role usually carried out by molecular oxygen. It is also possible that a small amount of copper oxide present on the electrode surface could provide a source of catalytically active copper without electricity being needed. Entry 7 simply shows that electrolyte salts are vital for electrochemical reactions to proceed. Entries 8 and 9 suggest that a Cu(I) species is better to catalyse this reaction than Cu(II), likely for the formation of the copper(I) acetylide intermediate. Entry 11 shows that if the reaction time is cut short with no overnight stir, the yield drops drastically, meaning it takes time for the actual homocoupling reaction to take place, despite the copper acetylides being produced very quickly. Finally, Entry 12 shows that if the reaction time is cut short, the yield can still be increased slightly by increasing the potential, though this is somewhat moot given that it only increases up to 10%.

Table 5 shows the different bases that were screened for this reaction, with DABCO proving to be the best tested. We also noted that increasing the amount used did not improve the yield. Pyridine and DBU also worked, though given the prevalence of DBU as the base of choice in many similar reactions,[44,152,171] the low yield found here is somewhat surprising. Another interesting result is that Et_3N gave very little product at all. We reasoned that this could possibly be because the potential being used was high enough to oxidise the bases, and indeed, from CV plots carried out for DABCO and Et_3N, the oxidation peaks were well below the +2.00 V (vs Ag QRE) used in this reaction (**Figure 20**). In these examples the ferrocene peaks were not reversible, meaning that they were not used to reference the other peaks against.

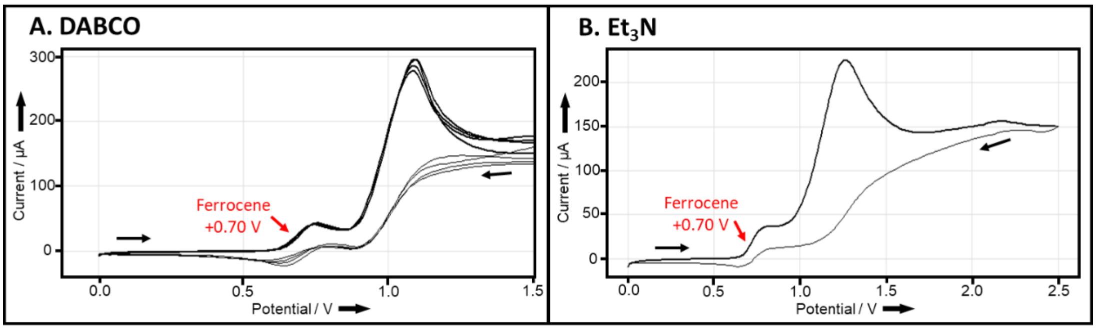

Figure 20*: A. Oxidation of DABCO (peak at: +1.1 V vs Ag QRE). B. Oxidation of Et_3N (peak at: +1.2 V vs Ag QRE). Plots recorded in 0.1 M Bu_4NPF_6 / MeCN. Axes redrawn for clarity.*

But why did DABCO (and other cyclic amine bases) work where Et_3N did not? An explanation may come from a paper by S. F. Nelsen,[180] which described the electronic structure of DABCO upon electrochemical oxidation. In this work, potentials were measured at a gold electrode in a 0.1 M sodium perchlorate / MeCN solution and referenced against a SCE. It was noted that charge could be completely delocalised around DABCO, through C-C bonds, rather than remaining centred upon the nitrogen atoms, which creates an extremely stable cationic species. This work also showed that Et_3N exhibited irreversible oxidation, whilst DABCO was almost completely reversible. However, in our CV plot (**Figure 20**), we found DABCO oxidation to be irreversible. One reason for this could be that the literature used a gold WE whilst we used a glassy carbon WE. We wondered whether the reason that Et_3N was not performing well as a base was that it was being irreversibly oxidised during our reactions.

Table 5: *The use of different bases and the effect on the isolated yield of the dimerised product.*[40]

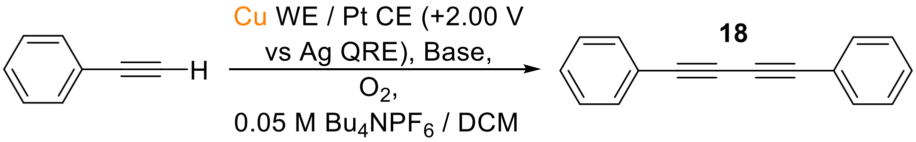

18

Entry	**Base**	**Isolated Yield/ %**
1	DABCO	67
2	None[a]	0
3	DBU	36
4	Et_3N	2
5	Pyridine	37
6	K_2CO_3	<1
7	NaOH	<1
8	DABCO[a]	67

[a] All bases were used in a 1.2 eq ratio as compared to the phenylacetylene starting material (1.0 eq) except for Entry 2, where no base was used, and Entry 8, where 2.0 eq was used.

We tested this hypothesis by performing the reaction at +0.50 V instead of +2.00 V and found that there was no significant difference in the yield of diyne produced using Et_3N as the base (3% yield obtained, compared to the 2% seen in **Table 5**), which invalidated the idea that the high potential was the issue. We also ran a reaction using +0.50 V with DABCO as the base and found that, again, there was no difference in the yield of diyne product (67% compared to the 67% seen in **Table 5**). Whilst this meant that we were still unsure as to why Et_3N proved so ineffective in our electrochemical formation of diynes, it did mean that from this point on we could use a much lower potential to carry out these reactions than previously thought, saving energy from the process. Therefore, +0.50 V was used in future experiments instead of +2.00 V.

Attempts to expand our reaction conditions to other alkynes met with partial success, producing **45** and **46** (**Figure 21**). However, the yields for these diynes were less than satisfactory, at only 46% and 36% respectively.

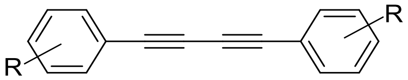

R = *p*Me Yield = **46%** **45**
= *p*F **36%** **46**

Figure 21*: Other diynes produced using 'standard conditions': alkyne (1.0 eq), DABCO (1.2 eq), 0.05 M Bu_4NPF_6 / DCM electrolyte, Cu WE, Pt CE, Ag QRE, +0.5 V vs Ag QRE for 3 h, followed by a 13 h stir exposed to O_2.*

The most peculiar thing from these tests was that **45**, which, chemically-speaking, is very similar to **18**, was only produced in 46% yield. This prompted a new wave of tests to try to improve the conditions of these reactions and increase the yields of the products, however time constraints prevented a more in-depth study on alkynes other than phenylacetylene.

It was reported in 2014 by X. Cui *et al.*[181] that benzylamine (5 mol%) could be used as a ligand for Glaser-Hay-type reactions, so we decided to test whether adding it to our standard conditions (see **Figure 21**) would have any beneficial impact on the yield of **18**. Unfortunately, the yield obtained for **18** using this approach was 62%, which was lower than our previous conditions.

We instead tried investigating the solvent used in this reaction, namely DCM. In a recent publication,[182] developing the stereoselective assembly of prodrugs, DCM was originally used as the solvent of choice for the key P-O bond-forming step in the synthesis of the phosphoramidate prodrug MK-3682 (see **Scheme 52**). The group then switched to a greener, less commonly used alternative, which appeared to function better and produce higher yields than DCM, 1,3-dioxolane. We took inspiration from this and ran our diyne reaction in 1,3-dioxolane instead of DCM, maintaining the other conditions. However, it appeared as if DCM is actually a very important component of our reaction conditions for more than just its solvating capabilities. Only 3% yield of **18** was obtained when DCM was exchanged for 1,3-dioxolane, indicating the solvent choice is critical in our reaction.

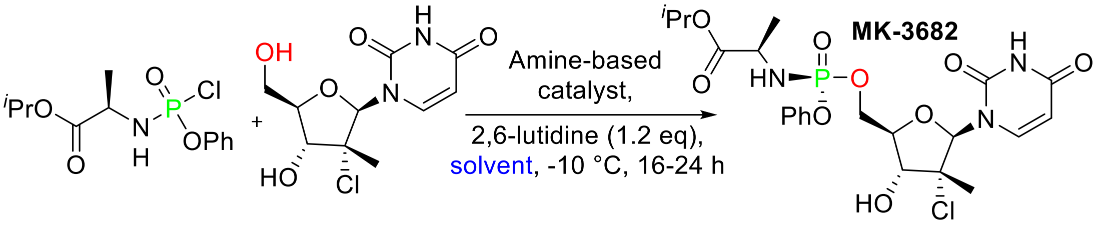

Scheme 52*: Synthesis of a phosphoramidate prodrug developed by D. A. DiRocco* et al.[182]

Given that we knew O_2 was essential for this reaction to proceed, we tried creating an artificial O_2-rich atmosphere by carefully syringing water onto potassium superoxide and collecting the O_2 gas given off in a balloon. This was then used for a test reaction to produce **18**, but no increase in yield was observed. However, this test did tell us that our reactions were not suffering from a deficiency of O_2 and that adding an additional oxidant would likely have no benefit.

Another variable that we investigated was the effect of light on the formation of the copper acetylide intermediate in the reaction. This was prompted by work carried out recently by K. C. Hwang *et al*.[93] which showed evidence to suggest that photons could help promote the oxidation of Cu(I) acetylides to Cu(II) with oxygen, by first promoting the Cu(I) to an excited state, as shown in **Scheme 53**.[93]

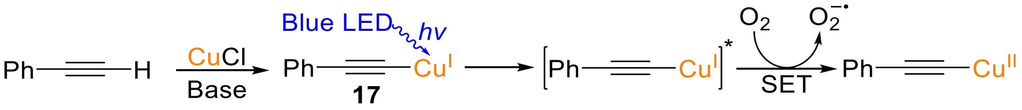

Scheme 53*: Proposed light-assisted oxidation of copper acetylides.*[93]

The oxidation of Cu(I) acetylides to Cu(II) is a key feature in most proposed mechanisms for Glaser-Hay reactions. We wondered if perhaps our reactions were suffering from a lack of light, which would slow the reactions down. However, when we attempted the reaction in complete darkness, a yield of 71% of **18** was obtained, suggesting this was not the case. Quite surprisingly, we found that when the reaction was carried out with an ‘excess’ of light (fumehood light being left on, as well as a bright lamp pointed directly at the H cell overnight) the yield actually decreased to 49% from the usual ~70%. This could mean that light of a certain wavelength, provided by the bright lamp used, promoted a side reaction, which was shut down when the reaction was left in the dark, though no other product was observed.

At this point we decided to record CV plots of the various components in the reaction to see what electrochemical analysis could reveal about the mechanism. These tests were designed to mimic the conditions used in a ‘standard’ reaction (see **Figure 21**), which meant that 0.1 M

Bu_4NPF_6 / DCM was used as the electrolyte in all cases. First we wanted to observe the production of Cu(I)/(II) from a bulk Cu(0) source, so we used a blank glassy carbon WE to record a background CV of the electrolyte solution up to +0.60 V (because our reactions were carried out at +0.50 V) (**Figure 22, A**).[40]

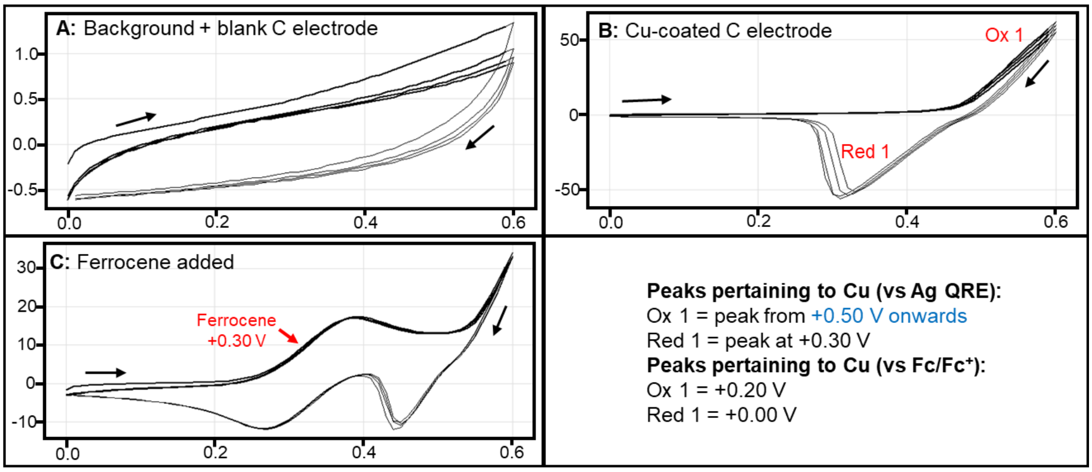

***Figure 22**: Showing the CV plot of a Cu^0-coated glassy carbon WE recorded in 0.1 M Bu_4NPF_6 / DCM with Ag QRE, Pt CE and compared to ferrocene. Y axes = Current (μA), X axes = Potential (V). Axes redrawn for clarity.*[40]

We then coated the glassy carbon rod with a fine layer of Cu(0), in the same way we did for **Figure 7**, by passing a reductive potential through a 0.5 M $CuSO_4$ / H_2O solution. This was then placed into the Bu_4NPF_6 / DCM electrolyte solution again and another CV was recorded (**Figure 22, B**). This gave an interesting graph, showing the oxidation of Cu(0) from +0.50 V (vs Ag QRE) onwards and the associated reduction at +0.30 V. This contrasts with **Figure 7** (carried out in MeCN) which showed oxidation of the copper take place as soon as an oxidative potential was applied. Regardless, **Figure 22, B** appears to visualise the generation of the catalytically active Cu used in our Glaser-Hay reactions. **Figure 22, C** shows these values referenced against ferrocene.[40]

We then investigated whether the presence of phenylacetylene or DABCO somehow altered this generation of Cu ions, starting with phenylacetylene. **Figure 23, A** and **B** were recorded in a fresh Bu_4NPF_6 / DCM solution with a blank glassy carbon WE after a small amount of phenylacetylene was added. **A** shows the graph produced at up to +1.50 V (high potential) and **B** shows the graph produced at up to +0.60 V (low/standard reaction potential). This shows that oxidation and associated reduction of phenylacetylene only takes place at higher potentials (**A**) than we use in our reactions (**B**), as there are no peaks associated with REDOX of phenylacetylene up to +0.50 V. When a Cu-coated glassy carbon WE was then used to carry out a CV plot, we obtained the graph **C**, which showed similar features to **Figure 22, B**. This suggested that phenylacetylene did not significantly affect the generation of Cu in the solution used here, or by extension, in our diyne-forming reactions.[40]

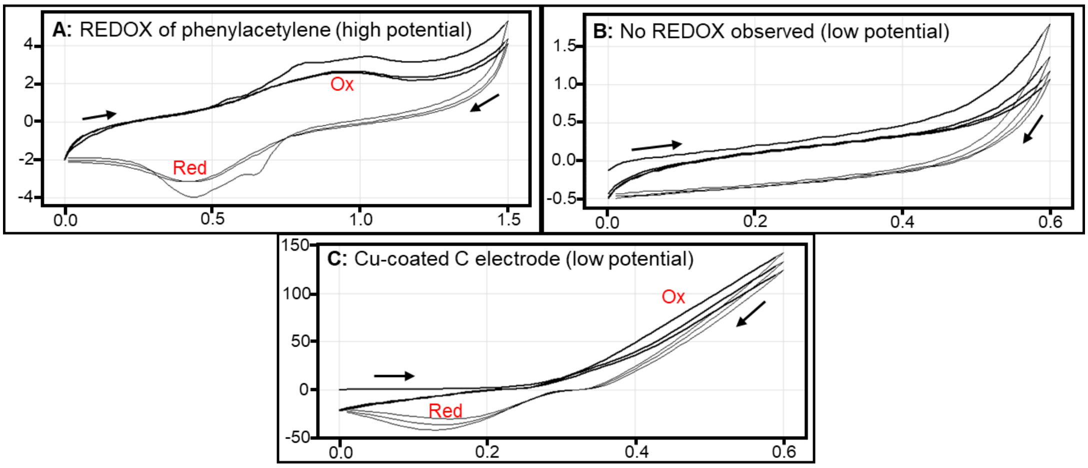

***Figure 23**: Showing the CV plot of a Cu-coated C WE with phenylacetylene recorded in 0.1 M Bu$_4$NPF$_6$ / DCM with Ag QRE and Pt CE. Y axes = Current (μA), X axes = Potential (V). Axes redrawn for clarity.*[40]

A similar process was carried out for DABCO as shown in **Figure 24**. Using a blank glassy carbon WE and a fresh electrolyte solution, we found that the oxidation of DABCO occurred at around +1.10 V, and not in the +0.50 V region that we use in our reactions (**A**). When a Cu^0-coated WE was used, however, there still appeared to be no REDOX taking place at lower potentials (**B**). This was in direct contrast to both the Cu-coated electrode on its own (**Figure 22, B**) and the Cu^0-coated electrode with phenylacetylene (**Figure 23, C**). Only when the potential was increased up to around +0.90 V did the same sort of REDOX start to take place, which means that the DABCO must inhibit the generation of copper in some way. This was initially surprising considering that DABCO overall facilitates the diyne-forming reaction.[40]

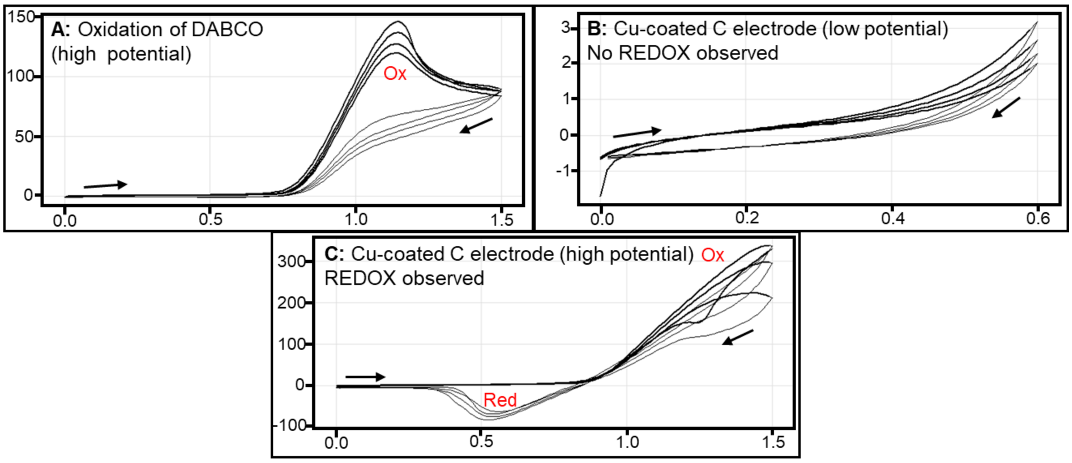

***Figure 24**: Showing the CV plot of a Cu-coated C WE with DABCO recorded in 0.1 M Bu$_4$NPF$_6$ / DCM with Ag QRE and Pt CE. Y axes = Current (μA), X axes = Potential (V). Axes redrawn for clarity.*[40]

With the CV plots not yielding particularly conclusive information about the reaction, we moved on to pinpointing exactly how much copper was being released into solution when +0.50 V (vs Ag QRE) was passed for 3 h. With a copper sheet being used as the electrode, there was of course a vast excess of available copper present in the form of Cu(0), but only a much smaller amount was being electrochemically converted into a catalytically active cationic form. To work out what this amount was, we initially attempted to monitor the amount of charge passed over the course of the 3 h, then use this value to derive how many copper atoms were being oxidised. However, this method was fraught with imprecision and there was no guarantee that the charge passed was specifically related to copper oxidation. Hence, a better method was fashioned, which involved looking at the problem from the opposite direction. Instead of trying to determine the charge passed at the end of the reaction, we measured the charge passed at the beginning, by forming a layer of a known amount of Cu(0) on a carbon electrode (in the same way that the glassy carbon WE was coated for the CV plots previously) and using **Eq. 1** (**page 1**). This allowed us to control how much copper we were putting into a reaction, and thus by comparing this to the yield of the diyne product, we could get an idea of how efficient our copper catalysis was. A couple of specific examples are shown: we found that 16.18 C of charge was passed when we plated a carbon rod with a layer of Cu(0) from a 0.5 M $CuSO_4$ / H_2O solution. Dividing this figure by the charge of an electron ($1.602x10^{-19}$ C) gives the total number of electrons passed ($1.01x10^{20}$). This must then be divided by 2 to account for the fact that 2 electrons are required for every Cu(II) to Cu(0) reduction, which equals $5.05x10^{19}$ copper atoms plated onto the carbon rod. Dividing this figure by Avogadro's constant ($6.022x10^{23}$ mol^{-1}) gives the amount of copper present in moles ($8.386x10^{-5}$ mol), which equates to approximately 4.2 mol% in a reaction where we use phenylacetylene (2 mmol) as the alkyne starting material. 4.2 mol% is a maximum value, given that in the coating process some charge is passed to water as well as the $CuSO_4$ salt. When this Cu-coated carbon rod was used as the WE for a test reaction, forming **18** from 2 mmol of phenylacetylene, we obtained a yield of 56%. Whilst this process was more time-consuming than simply using a Cu WE, it did help our mechanistic understanding of this reaction.

We then repeated this test to check the robustness of this technique with a range of different values (14.14 C charge passed in coating = a maximum of $7.329x10^{-5}$ mol Cu = 7.3 mol% as 1 mmol phenylacetylene was used) and obtained a yield for **18** of 68%.[20] We were quite encouraged by these results as it meant that not only were our conditions certainly sub-stoichiometric with respect to the copper catalyst, but also that the process was reasonably efficient.

Around the same time as this experiment was carried out, we had another encouraging result in the form of the highest yield for diyne **18** (84%) being obtained to date. This was achieved by using DABCO that had been dried overnight in a vacuum oven prior to use. This suggested that water may have been inhibiting the reactions up until now, however, when this dried

DABCO was used in a reaction to produce diyne **45**, the yield was not increased from the value obtained when using non-dried DABCO, so this idea did not hold up.[40]

It is important to mention that as well as trying to improve the conditions for the Glaser-Hay approach we had thus far been using, thought was also given to some of the other potential approaches that could yield diynes. Instead of using the Cadiot-Chodkiewicz reaction for its traditional purpose of producing asymmetrical diynes (see **Scheme 51**), we attempted to use it to produce the same symmetrical diynes we had so far been striving for. This approach is summarised in **Scheme 54**. The bromine-substituted alkyne **47** was produced from phenylacetylene using NBS and $AgNO_3$ in acetone.[183] The idea behind this was that we could improve the overall yield of the diyne product **18** by opening up the possibility of a second reaction pathway which led to the same product. To our disappointment, however, the overall conversion to **18** was only around 45% (based on ^1H NMR, as **47** had not fully reacted and the diyne could not be separated from it). A similar experiment was carried out using *p*-tolylacetylene, to produce **45**, but this yielded similarly disappointing results, as did an attempt to produce an asymmetrical diyne. This approach was therefore deemed unsuitable for our needs.

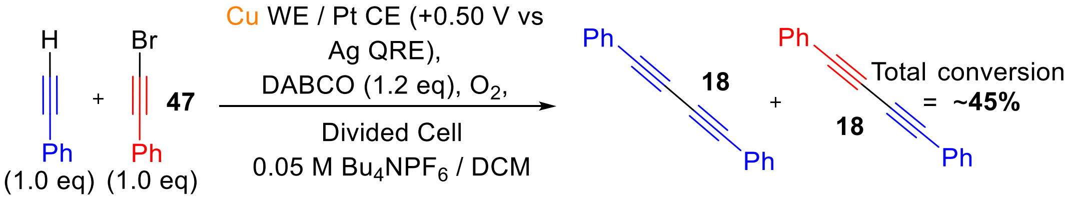

***Scheme 54**: Attempted Cadiot-Chodkiewicz approach to forming symmetrical diynes.*

A few attempts were made to produce bromo-substituted alkynes electrochemically as shown in **Scheme 55**. Initially this was achieved by simply adding recrystallised NBS to the conditions used to produce diynes, which proved only partially successful. It was found that when O_2 was present, the reaction did produce **47** as the major product, but a significant quantity of diyne **18** was also produced. Given the fact that more of the desired bromo product was formed than the diyne it was reasoned that with these conditions the formation of **47** was the favoured process and likely formed faster than the diyne product **18**. This was tested by carrying the reaction out again but working the reaction up after the 3 h of electrolysis, without any overnight stir. This produced only the bromo product **47** in 61%, but it appeared that the phenylacetylene starting material had not been consumed. Therefore, the reaction was carried out once again, but this time exposed to O_2 only for the 3 h of electrolysis. Then the reaction mixture was transferred to a sealed RBF *via* syringe and left to stir overnight under argon. To our delight this gave **47** exclusively in 78% yield, showing that the slower Glaser-Hay pathway had been shut down with the removal of oxygen. It is also important to mention that the non-electrochemical method of producing **47**, as outlined previously by using NBS and $AgNO_3$ in acetone,[183] yielded a very similar amount of the bromo product. When carrying out this procedure for use in Cadiot-Chodkiewicz reactions (**Scheme 54**) the best yield obtained for **47** was 79%, meaning that our electrochemical method was very competitive with this.

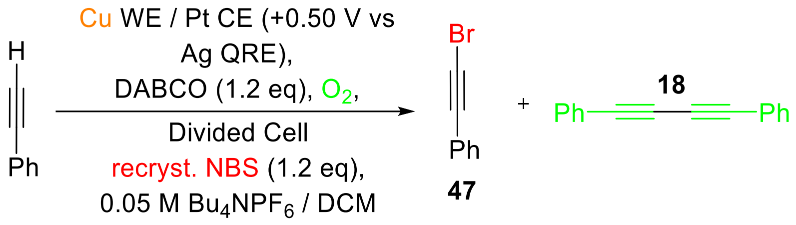

Scheme 55*: Synthesis of bromo-substituted phenylacetylene using electrochemistry.*

However, a few necessary control reactions revealed that when no Cu was present (graphite WE instead of Cu), but charge was passed to the solution, **47** was still formed in 63% yield, and when no Cu was present and no charge was passed, a similar result was observed (62% yield). This suggests that the reaction in fact proceeds regardless of whether a potential is applied, but that the presence of Cu, as we might expect, improves the conversion. Nevertheless, NBS appeared reactive enough under mild conditions to not require electrolysis to drive the reaction.

Undeterred by this unfortunate result, we decided to attempt to transfer our conditions to an ynamide-forming reaction, taking inspiration from the work of G. Evano *et al.*[87] as mentioned previously in **Scheme 24**. We attempted to suppress the formation of the diyne product by using an excess of the pyrrolidinone coupling partner in the hopes of preferentially forming the ynamide product **48** as shown in **Scheme 56**. In the original work of Evano,[87] it was noted that a TMEDA ligand was absolutely crucial to select for the ynamide product over the diyne one. We first tried the reaction in MeCN over two days (as per the literature procedure)[87] but without TMEDA, to get a baseline level of selectivity. This gave the ynamide product **48** in 10% yield and the diyne product **18** in 76%.

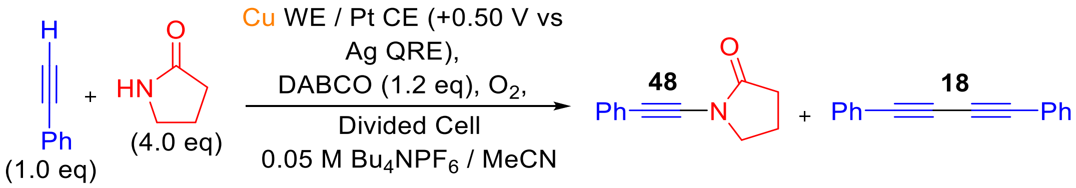

Scheme 56*: Electrochemical synthesis of an ynamide.*

Unlike the bromo-substitution reaction seen previously, we could not exclude oxygen from this reaction to shut down the Glaser-Hay reaction pathway, as oxygen was required to produce the ynamide product as well. We wondered whether slow addition of the alkyne starting material could elicit the desired selectivity in this reaction, though this was not tested.

Regardless, TMEDA (1.0 eq) was added to our conditions and the reaction was tried again. This time however, we obtained almost exclusively the diyne product. This unanticipated result prompted a series of further tests into the use of TMEDA as a ligand. It was hoped that even if TMEDA could not help produce the ynamide product **48**, it could be the answer to improving the yields of diynes. **Table 6** summarises these tests. It is important to note that the amount of charge passed in these electrochemical tests should be included as another means of comparing the tests to one another, but we did not learn the importance of this until later in the PhD project. Therefore, the charge was not measured during these experiments and is not presented in this table.

Table 6: *The use of TMEDA (1.0 eq) in diyne-forming reactions. Various control tests.*

Entry	**Potential (vs Ag QRE)**[a]	**Alkyne** (1.0 eq)	**DABCO** (1.2 eq)	**O_2**	**Electrolyte** (0.05 M Bu_4NPF_6 in DCM)	**Yield/ %**[b]
1	+0.5 V for 3 h	Phenylacetylene	Yes	Yes	Yes	96
2	No potential	Phenylacetylene	Yes	Yes	Yes	98
3	+0.5 V for 3 h	*p*-Tolylacetylene	Yes	Yes	Yes	43
4	+0.5 V for 3 h	Phenylacetlyene	No	Yes	Yes	88
5	+0.5 V for 3 h	Phenylacetylene	Yes	No[c]	Yes	18
6	No potential	Phenylacetylene	Yes	No[c]	Yes	3
7	No potential	Phenylacetylene	Yes	Yes	No	86

*[a] In all cases, the reactions were run for 16 h total. Where potential was used it was for 3 h, followed by 13 h of stirring. [b] Isolated yield of respective diynes **18** and **45**. [c] For Entry 5, the reaction was kept under argon at all times, for Entry 6, the reaction was exposed to O_2 after 3 h.*

Adding TMEDA to the existing conditions for diyne-formation yielded the diyne **18** almost quantitatively as shown in Entry 1,[20] however, a control test, where no potential was applied, gave an almost identical result (Entry 2). Upon looking through the literature we found this result is not particularly surprising. It has been documented many times that TMEDA can help produce diynes, but most relevant to the current point is the work of Y. Zhao and S.-F. Yin *et al.*,[184] which showed how copper powder could successfully be used as a catalyst source with TMEDA and chloroform. It appears that TMEDA is quite capable of forming an active Cu catalyst from Cu(0), and based on an intermediate (**49**) isolated by this same group, we believe it is most likely that TMEDA reacts with the chloroform solvent to prompt oxidative addition from any Cu(0) present, thereby oxidising the copper and leading to the true catalyst in these reactions, $CuCl_2$.[185] (See **Scheme 57**). It is entirely possible that a similar mechanism is at work here when DCM is used as the solvent, however we did not attempt to prepare a TEMPO-DCM-derived complex in this project.

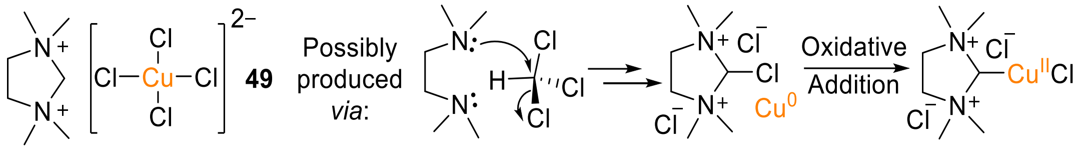

***Scheme 57**: Proposed oxidation of Cu(0) using TMEDA and $CHCl_3$.*[184]

However, **Table 4**, Entry 2 shows that a lack of applied potential when TMEDA was absent yielded a mere 1% of diyne **18**, thus, we can surmise that TMEDA must produce the copper catalyst in a different way to the electrochemical method described previously.

Entry 3 of **Table 6** showed, quite strangely, that the improved yield for diyne **18** was not observed for diyne **45**. The reason for this remains unknown to us.

Entry 4, where DABCO was excluded from the reaction, shows that TMEDA can act as a replacement base, but at a small cost to the yield of the product. It was reasoned that increasing the amount of TMEDA used would probably have compensated for the proportion of TMEDA acting as a base and brought the yield up to match Entry 1. The removal of the electrolyte salt from this reaction also had a detrimental effect on the yield as shown in Entry 7. This result has proven harder to rationalise, given that we knew potential was not required to produce the Cu needed in this reaction. By extension, this means that the electrolyte salt, used to carry charge, should likewise not have been required. It could be that the salt may have provided PF_6^- ions that acted as ligands for the copper.

Entries 5 and 6 show that oxygen is still required for carrying out this reaction with TMEDA, and in fact, Entry 6 (where oxygen was only introduced after the metal electrodes were removed from solution) seems to show that it may help TMEDA extract active copper from the Cu(0) plate. Entry 5 may appear to suggest that an applied potential could help produce copper in this reaction after all, given the comparison to Entry 6, where no potential was applied. However, this link is dubious given the difficulties associated with completely removing oxygen from the electrochemical setups. It is more likely that a small amount of oxygen managed to get into the system and initiate some reaction.

The most important discovery that came out of these tests was not even related to the TMEDA at all. In reactions where oxygen was excluded, we noticed for the first time that a white precipitate still formed, despite no copper acetylide intermediate or diyne product being produced. In other words, a reaction was still taking place even though the Glaser-Hay pathway had been completely shut down. Isolation and characterisation of this precipitate revealed that it was the DABCO salt **50**, formed by the reaction of DABCO with the DCM solvent as shown in **Scheme 58**. Furthermore, this salt has been reported as part of a dinuclear Cu(I)-based complex in the literature. B. Gustafsson *et al.*[186] isolated the complex **51** by reacting **50** with CuCl at –60 ºC. A similar structure to **51** with cadmium metal centres has also been described by L.-Z. Chen *et al*.[187]

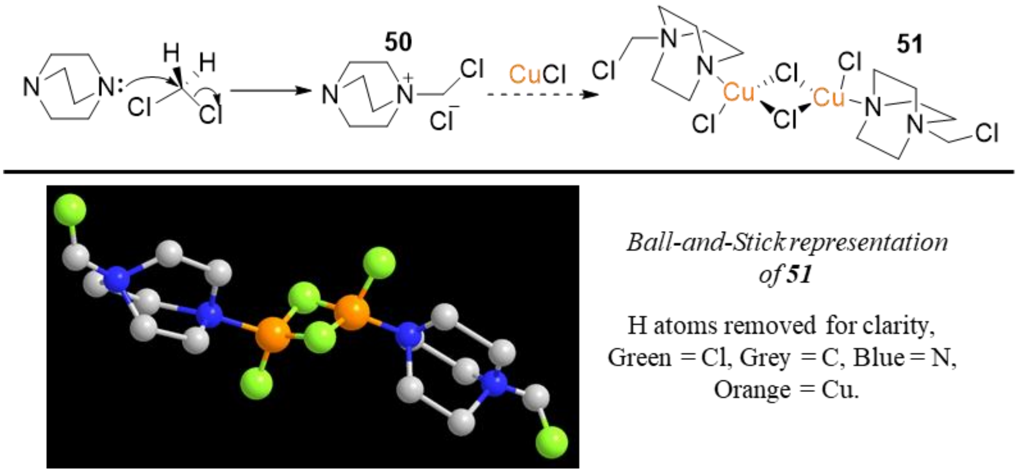

*Ball-and-Stick representation of **51***

H atoms removed for clarity,
Green = Cl, Grey = C, Blue = N,
Orange = Cu.

***Scheme 58**: Discovery of the DABCO salt **50**, formed by DABCO reacting with DCM, which can form the dinuclear complex **51**.*[40,186]

This complex is distinct from the mononuclear Cu(I) complexes with DABCO described by Sekar,[188] where DABCO molecules sit between cuprous chloride units to form linear polymers with strong intermolecular hydrogen bonds as shown in **Figure 25**.[40,188] It seems likely that the quaternization of DABCO in DCM to form **50** forces the dinuclear complex **51** to form in such conditions as the chloromethyl moiety blocks one of the coordinating/H-bonding sites of the DABCO.[40]

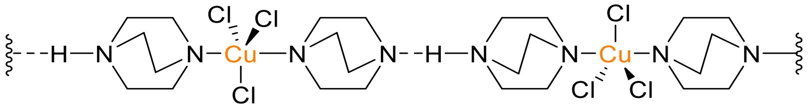

***Figure 25**: Representation of the linear polymer described by Sekar.*[40,188]

With this idea in mind, the hygroscopic DABCO salt **50** was synthesised by simply stirring DABCO in DCM under argon overnight. We then ran a CV plot of this salt in 0.1 M Bu_4NPF_6 / DCM and found an identical trace to that seen in **Figure 24, A** was obtained. This means that what we initially assumed to be the oxidation of DABCO shown in earlier CV plots, is in fact likely to be the oxidation of the DABCO salt **50**. Furthermore, this result suggests that **50** is formed very quickly and quantitatively in our reactions and that it is not oxidised at the potentials employed in our conditions (+0.50 V vs Ag QRE). It is also interesting to consider that when other bases were tested for this reaction, such as Et_3N and pyridine (**Table 5**), only poor yields of the diyne were obtained. The fact that these bases had only one lone pair/coordination site may suggest that the reduction in coordinating power caused by the quaternization of DABCO (pK_a = 8.8, 3.0) may be a key factor in the catalytic activity of the active copper species formed in this reaction.[40]

This all led to a completely new understanding of our conditions. We now believed that **51** could be the active copper complex generated in our electrochemical Glaser-Hay reactions. If this was the case it would explain why trying a different solvent such as 1,3-dioxolane had not only failed to improve the yields of diynes, but also completely attenuated the reaction. We believed the salt we had isolated, **50**, must be vitally important for forming the active Cu species used in our non-TMEDA reactions, which makes sense because the production of **50** also liberates the Cl^- ions required to produce CuCl, and thus complex **51**, *in situ*. This theory was investigated by following the original procedure for preparing a DCM solution containing **51**,[186] where we used DABCO (1.3 mmol) and Cu(I)Cl (2.4 mmol) dissolved in DCM (8 mL), then decanted a portion of this solution (3.13 mL) away from unreacted CuCl and added it to a reaction vessel containing phenylacetylene (0.5 mmol) and DABCO (0.6 mmol). We calculated that a maximum possible value of 46 mol% of **51** ended up being used in the diyne-forming reaction.[‡] After stirring overnight at RT, this resulted in a 36% yield for **18**. Whilst not a particularly high yield, the fact that **18** was produced in this control reaction tentatively lends support to the idea that **51** is the active catalyst in this reaction.[40]

We also carried out a Glaser reaction using conditions very similar to those shown in **Figure 21**, but instead of using DCM as the solvent, we used chloroform. This reaction did not produce any DABCO salt **50** or any diyne product **18**, which was an excellent result. Chloroform, being less reactive towards nucleophilic attack than DCM, was not attacked by the DABCO, which in turn completely halted the formation of any catalytic species. A second test, where TMEDA (1.0 eq) was added to these conditions (which generates catalytic copper in a different way to the DABCO salt), yielded 25% of diyne **18**. Compared to the yields seen in **Table 6**, this showed again that $CHCl_3$ was a much less effective solvent to use for this reaction. Using chloroform as the solvent therefore provided an excellent testing ground for our theory. The salt **50** was then added to the reaction mixture as shown in **Scheme 59** (red showing the yield when **50** was not included, blue, purple and green when it was). These tests show that adding **50** 'switched on' our reaction and a clear trend became apparent where adding more **50** yielded more of the diyne product. Clearly then, the DABCO salt **50** was the key to producing diynes.

[‡] This value was calculated by assuming that all DABCO used in the first step reacted with DCM in 2 h to form **50**, of which two molecules are needed to form one molecule of **51**. Assuming this complex does not decompose during transfer, this means a maximum of 2.5×10^{-4} mol of **51** was used in the diyne-forming reaction (3.13 mL transferred), equating to 46 mol% as 5.5×10^{-4} mol phenylacetylene was used.

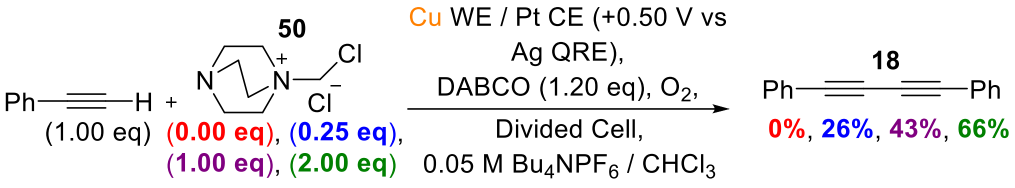

***Scheme 59**: Testing the need for DABCO salt **50** in our reactions.*

One question remained unanswered: Was the DABCO salt as a whole needed, or just the Cl^- ions? To answer this, we set up new conditions, using 0.05 M Bu_4NCl (0.25 eq Cl^-) in $CHCl_3$ as the electrolyte solution. This provided chloride ions from the start of the reaction. We knew from previous CV plots (**Figure 5**) that the chloride ions would not be oxidised by the +0.50 V used in this test. We then ran the reaction without adding any DABCO salt **50** and found that a yield of 10% was obtained for the dyine product. Furthermore, when 0.50 M Bu_4NCl / $CHCl_3$ was used (2.5 eq Cl^-), a mere 41% yield was obtained. This was quite an interesting result as it appeared to demonstrate that the chloride ions alone could help catalyse the reaction, but not as well as when **50** was used. It also suggested that some sort of CuCl species must form, but only when potential was applied to the Cu(0) plate. Indeed, when this 0.05 M Bu_4NCl / $CHCl_3$ reaction was repeated, but without any potential being applied, only 1% of **18** was isolated. Furthermore, we collected CV plots, as shown in **Figure 26**, to examine the effect of chloride ions on the oxidation of Cu^0.[40]

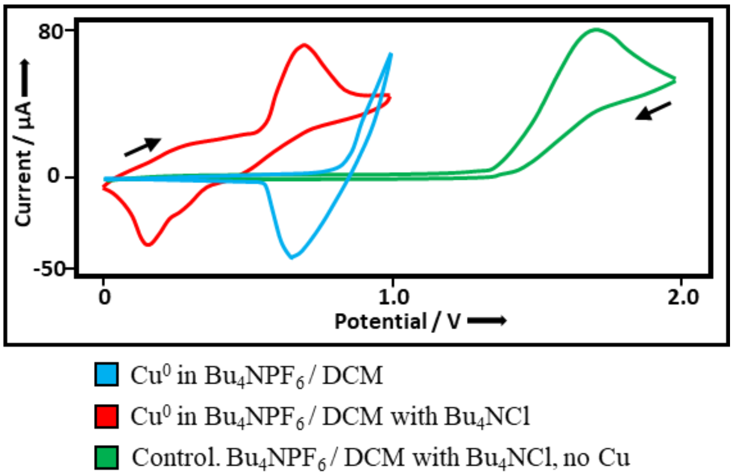

***Figure 26**: CV plots examining the effect of chloride on the release of copper ions from a Cu^0-coated glassy carbon electrode recorded in 0.1 M Bu_4NPF_6 / DCM. Axes redrawn for clarity.*[40]

To do this, a Cu^0-coated glassy carbon WE was used in, firstly, a Bu_4NPF_6 / DCM solution (blue plot). This is the same plot measured previously in **Figure 22, B**, but it is important to note that the plot is shifted up to higher potentials by around +0.30 V. We attribute this to the use of a quasi reference electrode. However, we were careful to always reference these potentials against ferrocene, so we were quite confident that these plots could be compared with others recorded previously. The blue plot shows the oxidation of Cu^0 beginning to take place at around +0.80 V vs Ag QRE, and as the ferrocene we added as reference gave peaks around +0.60 V, the Cu oxidation began at +0.20 V vs Fc/Fc^+ (in line with **Figure 22**). Next, we recorded a CV plot of Bu_4NCl as a control CV of just the chloride ions without any copper present showing that the oxidation of Cl^- to Cl_2 requires much more energy than the oxidation of copper (green plot, peak at +1.70 V vs Ag QRE, the ferrocene reference gave peaks around +0.90 V, therefore the Cl^- oxidation peaks at +0.80 V vs Fc/Fc^+, which in line with **Figure 5**), hence the plots shown in blue and red must pertain to copper oxidation only. Finally, we recorded a CV plot of Cu^0 when Bu_4NCl was present (red plot) and we were quite excited to see that the oxidation attributed to copper now seemed to be starting at a lower potential of around +0.60 V vs Ag QRE. The ferrocene we added as reference gave peaks around +0.80 V, thus the oxidation of copper in the red plot began at around -0.20 V vs Fc/Fc^+. This strongly suggests that the presence of Cl^- ions, in addition to allowing the formation of the dinuclear Cu(I) complex **51**, also cooperatively assists the release of Cu(I) from the electrode, assumedly as CuCl. This allows the reactions to be performed at lower potentials than when the chloride ions are not present. This also seems to demonstrate a pair of cooperative effects are at play when the copper is released from the electrode: the applied oxidative potential, as well as the ligating effects of the chloride ions as represented in **Figure 27**.[40]

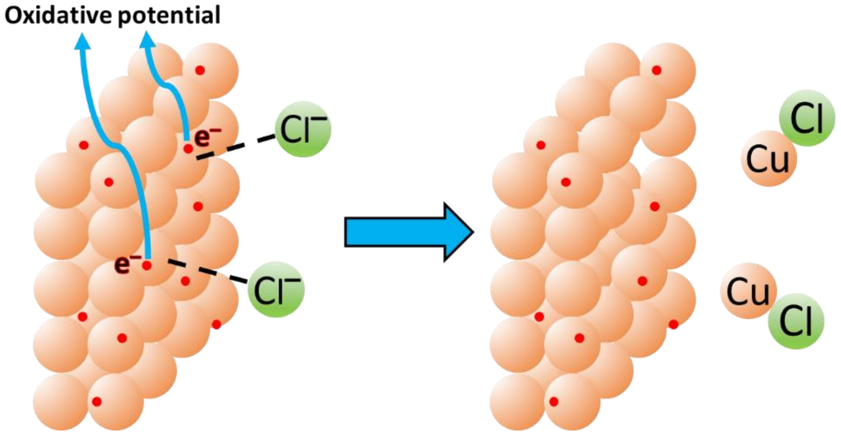

Figure 27*: Schematic representation of the cooperative effects of chloride ion ligation and an applied oxidative potential to release Cu(I) from the electrode surface.*[40]

The evidence for a Cu(I) species being generated, and not Cu(II), has been accumulated from several sources. The kinetic evidence from M. B. Nielsen *et al*.[174] (reporting a required initiation period when Cu(II) salts were used for diyne-forming reactions – likely for the concentration of Cu(I) to build up in reactions); the fact that Cu(I) acetylides, such as **17**, can readily initiate the Glaser-Hay reaction, and the fact that while in strongly coordinating solvents, such as $NH_4OH_{(aq.)}$ and H_2O, Cu(II) complexes may be favoured, other solvents, such as MeCN, stabilise Cu(I) species.[189]

Taking all the information into consideration, a reasonable mechanism for this reaction has been formulated and is shown in **Scheme 60**. This mechanism incorporates the generation of the DABCO salt **50**, which provides chloride ions to be used by Cu^{I} (generated when a +0.50 V oxidative potential is passed through a copper plate) to form the catalytic complex, **51**. Beyond this, a series of ligand replacements with alkynes seems most likely (alkyne-copper interactions in complexes are well known),[190,191] following a Bohlmann-type mechanism as shown in **Scheme 47**. The role of oxygen is accounted for by the oxidation of Cu(I) acetylides to Cu(II) acetylides. Next, in order for the diyne to form, both alkynes must end up on the same copper atom, to allow reductive elimination to occur. This would likely be the rate-determining step in the reaction. Finally, the key diyne-forming step is based on the mechanism shown in **Scheme 49**, which relies on a single-electron-transfer (essentially disproportionation) to generate Cu(I) and a Cu(III)dialkyne intermediate, which undergoes reductive elimination to form the diyne product and more of the Cu(I) catalytic species ready to be used in a new cycle.[40,185]

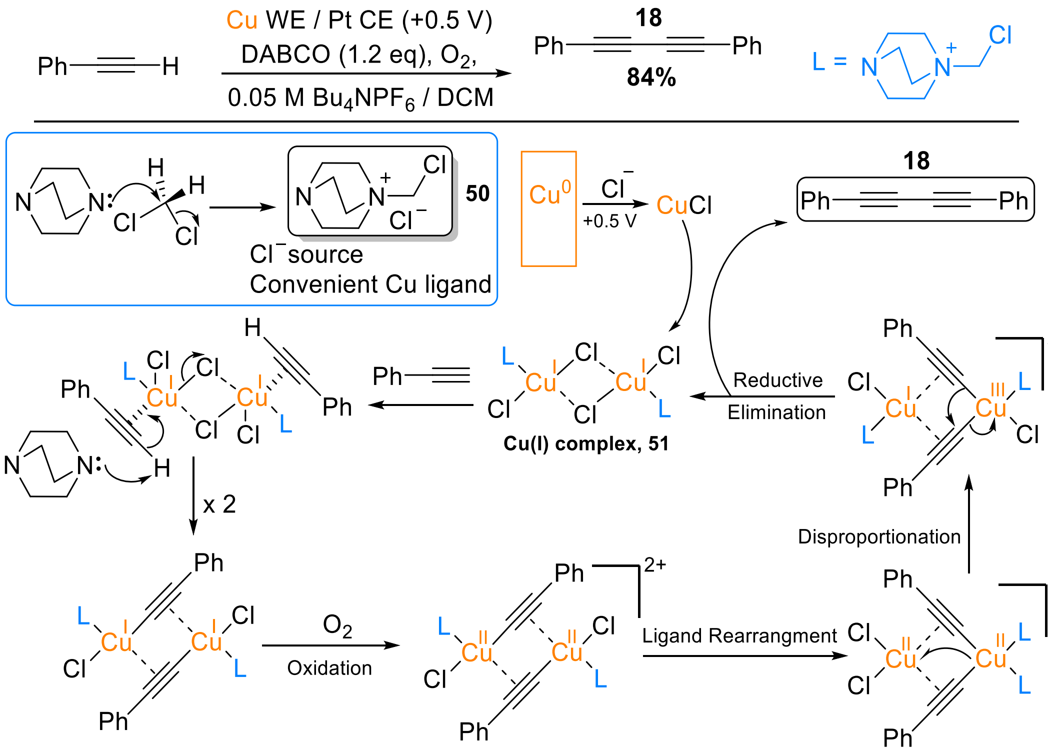

Scheme 60: *Proposed mechanism for the electrochemical dimerization of terminal alkynes.*[40,185]

Chapter 7. The Chan-Lam Reaction

The copper chemistry we had so far focused on was all copper acetylide-based. We were keen to attempt some initial investigations into biaryl coupling chemistry at the end of this PhD project to see how our methods fared in a different setting. The coupling reaction we decided to focus on was the Chan-Lam reaction, as we believed we could utilise some of the methods we had thus far developed to accomplish this transformation.

7.1 Introduction

The Chan-Lam reaction (sometimes also called Chan-Evans-Lam) is a copper-mediated cross-coupling reaction that makes use of the boronic acid functional group to form primarily C-N and C-O bonds (though examples of C-S bond formation exist) from a variety of nucleophilic species. It has a distinct advantage over the similar Ullmann-Goldberg reaction and the Pd-catalysed Buchwald-Hartwig reaction in that much lower temperatures may be used, and in the case of the Buchwald-Hartwig reaction, a large monetary saving can be made as copper is orders of magnitude cheaper than palladium.[192] The Chan-Lam reaction was first detailed in 1998 in three back-to-back papers from the groups of Dominic Chan,[193] David Evans[194] and Patrick Lam.[195] It is interesting to note that reportedly the reason Evans first became interested in this reaction is because of the importance of novel biaryl ether syntheses at this time for the total synthesis of vancomycin[192] (as highlighted previously for Nicolaou's use of the Ullmann reaction in **Scheme 17**). Some examples of the reactions shown in these initial Chan-Lam papers are given in **Scheme 61**.

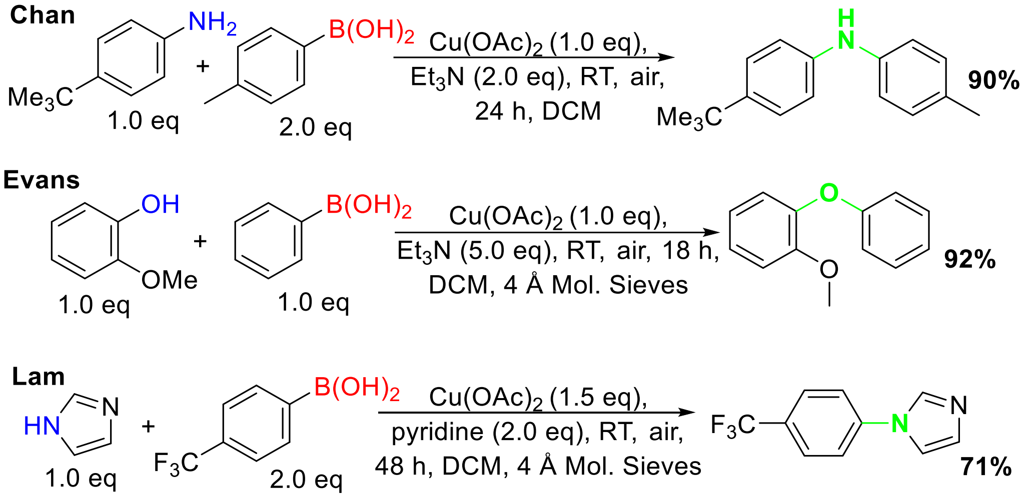

Scheme 61: *Early examples of the Chan-Lam reaction.*[193–195]

Since these early examples, the development of conditions using sub-stoichiometric quantities of copper, different catalysts such as copper halides (and even Ni catalysts),[196] as well as different solvents such as MeCN, toluene and dioxane have been developed. But certainly the most common conditions appear to still employ $Cu(OAc)_2$ as the catalyst, DCM or MeCN as the solvent and either Et_3N or pyridine as the base.[192]

Mechanistic work carried out for this reaction since its initial discovery has yielded some important understanding and whilst the overall mechanism has remained broadly similar to initial proposals, specific details are still being uncovered.[197] In terms of the etherification reaction, Evans proposed in his initial paper that the general structure for the mechanism would proceed *via* a transmetallation and reductive elimination.[194] It is still up for debate as to whether this reductive elimination would proceed from a Cu(II) species or after oxidation up to a Cu(III) species. Indeed, work carried out by Stahl on the specific example of methoxylation of arylboronic esters suggests that it is likely that reductive elimination takes place from a Cu^{III} species as this does not rely upon the disfavourable comproportionation of Cu^{II} and Cu^{0} to generate Cu^{I}. In either case, the resulting copper species is in the '+1' oxidation state and is then oxidised by O_2 to start a new catalytic cycle. A general mechanism based on these proposals is shown in **Scheme 62**.[198]

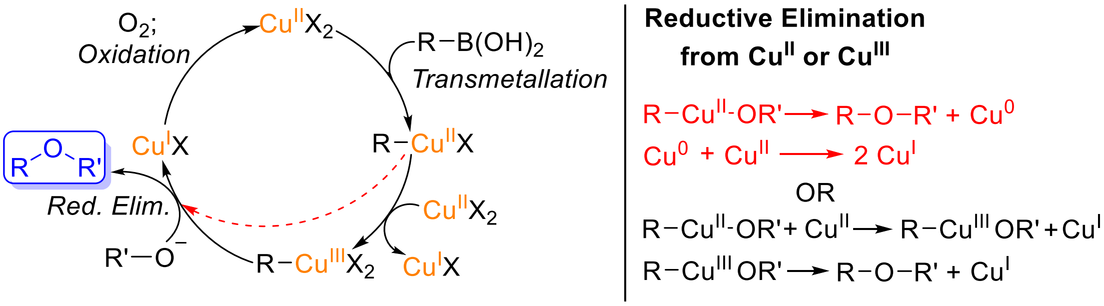

***Scheme 62**: General mechanism for the etherification Chan-Lam reaction.*[194,198]

Further work by Stahl concentrated upon the transmetallation step of the reaction between methanol and arylboronic esters and found that the disassociation of an acetate ligand, followed by the solvent (MeOH) behaving as a bridging ligand, is what facilitated the movement of the aryl group from boron to Cu^{II} as shown in **Scheme 63**.[198,199]

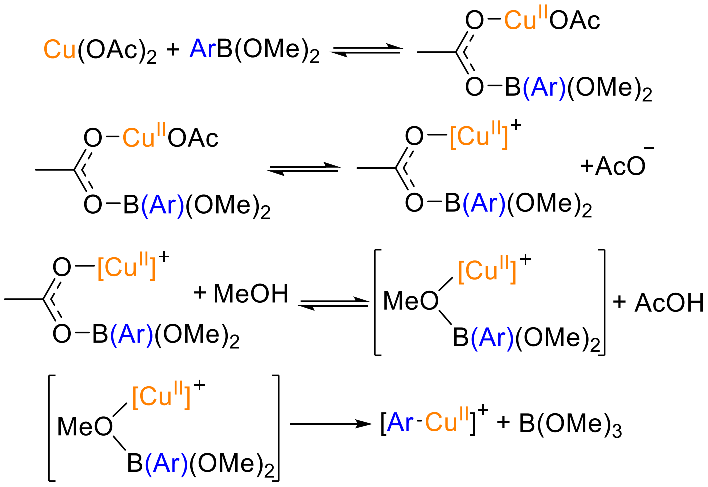

***Scheme 63**: Specific proposed transmetallation step for the methoxylation of aryl boronic esters.*[198,199]

In other words, the transmetallation step favoured a 4-membered transition state, where the methanol unit acts as a bridge, rather than a 6-membered transition state using an acetate unit as the bridge. This could perhaps be a general process across etherification Chan-Lam reactions and also perhaps amination reactions, as molecular modelling carried out recently suggests the same favoured 4-membered transition state is exhibited for aminations.[197] This molecular modelling work was carried out as part of an excellent, recent investigation of the amination variant of the Chan-Lam reaction from the Watson group. This work covered a range of mechanistic considerations and tests to derive a detailed mechanism for the Chan-Lam reaction, a simplified version of which is shown in **Scheme 64.**[197]

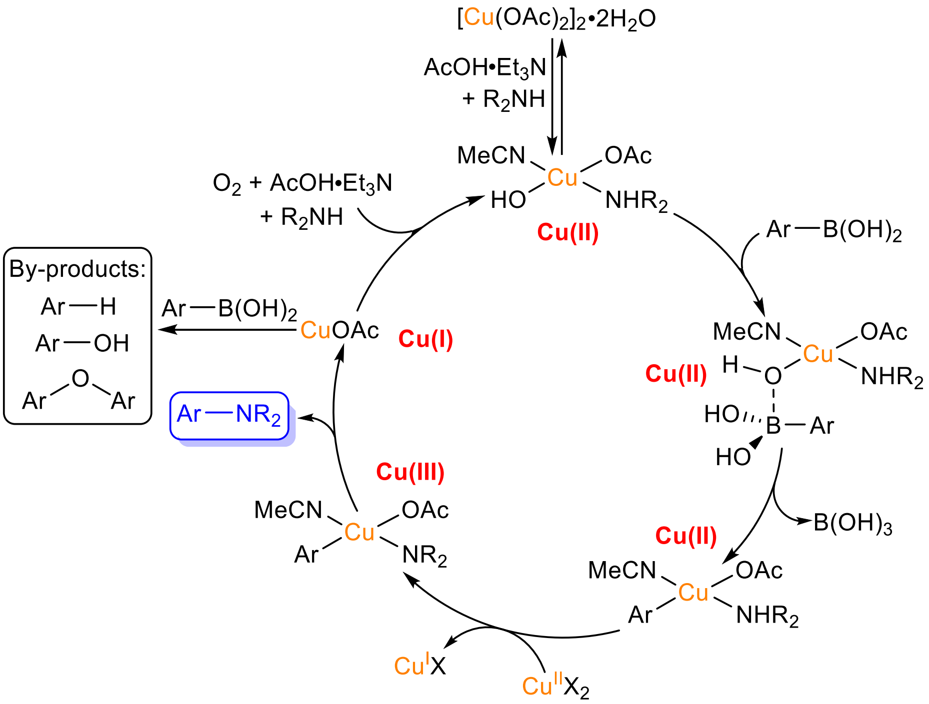

***Scheme 64**: Simplified proposed mechanism for the amination Chan-Lam reaction.*[197]

It was also mentioned in this work that the formation of various by-products often found in Chan-Lam reactions, such as: the very common deborylated coupling partner, the oxidised form of the boronic acid coupling partner (usually a phenol, given the prevalence of aryl species in Chan-Lam reactions), and the competing oxidative homo-coupled product, are likely facilitated by Cu(I) species. This means that a slow oxidation period from Cu(I) to Cu(II) can increase the yield of by-products for these reactions. The use of molecular sieves has been found to mitigate some of the by-product formation in these reactions.[194,197]

7.2 Electrochemical Chan-Lam Reaction

We began our investigation by devising the proposed system shown in **Scheme 65** (the catalytic cycle being based on literature proposals as shown in **Scheme 62** and **Scheme 64**), where the red colour highlights the oxidation of copper from the sacrificial WE (as seen in the copper acetylide reactions), followed by aerial oxidation to Cu^{II} (as seen in the diyne reactions). Copper in the '+2' oxidation state is required to initiate the Chan-Lam reaction.[§] The blue colour highlights the electrogeneration/regeneration of triethylamine (which we had used to produce copper acetylides in an undivided cell). As the Chan-Lam reaction is very

---

[§] It is important to note that when a sacrificial Cu electrode is used, the only oxidative process that appears to take place is the oxidation of Cu^0 to Cu^I, leaving O_2 as the most convenient oxidiser. However, if a Cu-coated C electrode was used, the possibility exists to release an amount of copper ions into solution to promote catalysis, then, when the copper coating is exhausted, the applied oxidative potential may begin to oxidise species in the reaction mixture, rather than the Cu^0 which is a part of the electrode itself.

often promoted by $Cu(OAc)_2$,[197] we wondered whether the nature of the anion/copper ligand shown in pink would be a key factor in our proposed reactions. This anion would very likely come from the electrolyte salt we chose and would probably play a crucial role in the transmetallation step of the mechanism. It is important to mention that whilst the Chan-Lam reaction is capable of producing various carbon-heteroatom bonds, we elected to focus on the formation of aryl ethers.

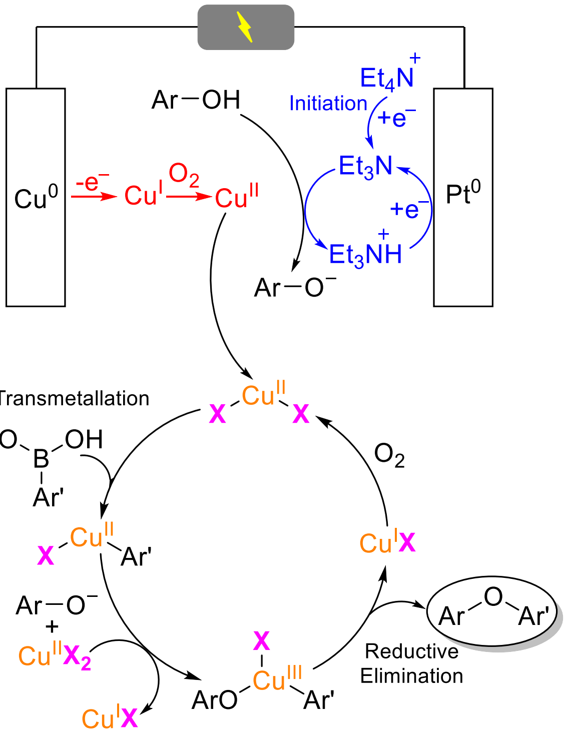

***Scheme 65**: Proposed electrochemical Chan-Lam reaction in an undivided cell.*

As DCM is often used as the solvent in this chemistry,[197] we decided to begin our experiments using a $Et_4NO_3SC_6H_4CH_3$ / DCM electrolyte solution in an undivided cell. We kept this cell exposed to air to facilitate oxidation of copper species. We also selected 2-methoxyphenol (**52**) and phenylboronic acid (**53**) to be our two coupling partners. The main reasons for this were the availability and simplicity of these compounds. When this reaction was attempted with an applied potential of +0.5 V vs Ag QRE for 16 h as shown in **Table 7**, Entry 1, we obtained a yield for **54** of 15%.

Table 7: Initial experimental attempts for an electrochemical Chan-Lam reaction.

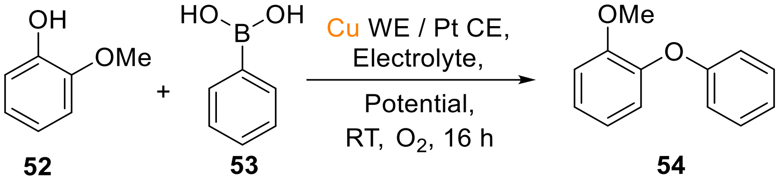

Entry	52 / eq	53 / eq	Electrolyte Solution	Potential (vs Ag QRE) and Charge Passed	Other	Yield / %[a]
1	1	1	0.1 M $Et_4NO_3SC_6H_4CH_3$ / DCM	+0.5 V for 16 h, 42.6 C	Undivided	15
2	1	1	0.1 M $Et_4NO_3SC_6H_4CH_3$ / MeCN	+0.5 V for 16 h, 160.0 C	Undivided	14
3	1	2	0.1 M $Et_4NO_3SC_6H_4CH_3$ / DCM	+0.5 V for 16 h, 100.0 C	Undivided	21
4	1	1	0.1 M $Et_4NO_3SC_6H_4CH_3$ / DCM	No applied potential	Undivided	0
5	1	1	0.05 M $Et_4NO_3SC_6H_4CH_3$ / DCM	+0.5 V for 16 h, 0.2 C	Divided, Et_3N (3 eq) added	0
6	1	1	0.1 M $Et_4NO_3SC_6H_4CH_3$ / MeCN	+0.5 V for 16 h, 43.8 C	Divided, Et_3N (3 eq) added	1
7	1	1	0.1 M $Et_4NOAc{\cdot}4H_2O$ / MeCN	+0.5 V for 16 h, 49.6 C	Undivided	6

[a] Isolated yield of ***54***.

Although this yield was low, we were pleased to obtain the coupled product on the first attempt as the systems involved in this reaction are complex and a lot of side reactions are likely to take place. One of the first things we investigated to boost the yield of this reaction was to change the solvent to MeCN. When this was attempted, an almost identical yield was obtained (Entry 2). It is important to note however, that copper seems to be oxidised from the WE much more efficiently in MeCN than DCM. This is based on the comparison of **Figure 7** with **Figure 22, B**, and the fact that 43 C charge was passed during the 16 h of applied potential in Entry 1 of **Table 7**, whilst the copper electrode appeared to completely corrode within 3 h of electrolysis in Entry 2 (160 C charge passed), causing the electrolysis to stop completely beyond this point. Clearly, therefore, there was no lack of copper in solution and so the low yields must have an alternative explanation.

A prominent issue with the Chan-Lam reaction is the proclivity of boronic acids to undergo side reactions to produce a range of undesirable products. We believed that this might be the case in our reaction, so we tried using 2 equivalents of **53** instead of 1 in Entry 3, which resulted in a slight increase in the yield. It was reasoned that this could indeed be an indication that **53** partaking in side reactions or being destroyed could be the root of the low yields observed, however no other products were obtained in any of the tests. Given the only marginal increase in yield garnered from doubling the amount of **53**, it seemed that adding vast amounts of the boronic acid would not be the best course of action. Instead more tests were carried out to see if better conditions could be developed.

Entry 4 simply shows a control reaction with no potential applied which did not yield any product. Entries 5 and 6 show that moving over to a divided cell system appeared completely ineffective in both DCM and MeCN. This could indicate that the REDOX reactions taking place at both electrodes are intrinsically connected and perhaps the proximity of the electrodes to each other in the undivided cell allows the reaction to take place, whereas in the divided cell, all the reagents being placed in the oxidative chamber was insufficient to allow the reaction to occur. We considered that it is also possible that the Et_3N added to the solution in these cases (based on the perhaps naive assumption that this is the base generated electrochemically) may not actually be the base that promotes this reaction in the undivided cell. The results of **Figure 12** lend some support to this, as we found that the initial reduction that took place to start the electrochemical tertiary amine base production in the copper acetylide reactions was in fact the reduction of the phenylacetylene starting material. We wondered if perhaps direct reduction of **52** or **53** is what initiates our Chan-Lam reaction, however CV plot analysis of these species did not show any reduction peaks for either species, in both MeCN and DCM, before reduction of the electrolyte solution (0.1 M $Et_4NO_3SC_6H_4CH_3$ used as electrolyte in all cases). For this reaction then, it appears that the initiation probably comes from direct reduction of the electrolyte to form Et_3N, Furthermore, the employment of Et_3N as a base in Chan-Lam reactions is common throughout the literature, which means that there is no obvious reason why the transfer over to a divided cell and adding, instead of generating, Et_3N would cause a major disruption to the reaction.

The nature of the anionic species (pink ‘X’ in **Scheme 65**) was something that we attempted to alter in an effort to improve the yield of this reaction. In Entries 1-6 of **Table 7**, the species ‘X’ was presumed to be $^{-}O_3SC_6H_4CH_3$, however, as copper acetate is very commonly used in the Chan-Lam reaction, we wondered if switching this species to an acetate anion could be beneficial. To that end, the electrolyte $Et_4NOAc\cdot 4H_2O$ was used, as in Entry 7, and this only yielded 6% of **54**. As shown in **Scheme 63** and **Scheme 64**, transmetallation in this reaction appears to proceed favourably *via* a 4-membered transition state, rather than a 6-membered one. This does not, however, mean that a 6-membered transition state is impossible, and perhaps some of the low yields obtained here could be attributed to our reactions being forced to proceed *via* disfavourable 6-membered transition states as shown in **Scheme 66**.

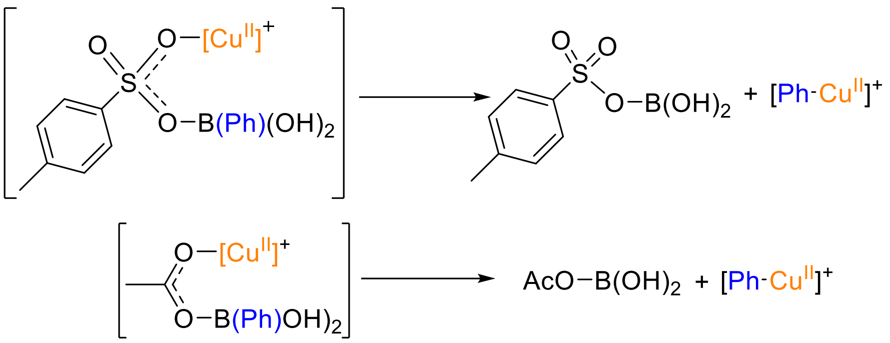

Scheme 66: Showing possible disfavoured 6-membered transition states for transmetallation in our Chan-Lam reactions.

Another potential issue, as mentioned previously, is that protodeborylation of boronic acids is a very common problem in Chan-Lam reactions (and indeed generally when using boronic acids).[197] In the case of **53** this would form benzene. It is possible that the presence of a large amount of water in solution could have encouraged this by-product formation. Furthermore, it has been reported that even in otherwise anhydrous conditions, water may be generated from phenylboronic acid itself through triphenylboroxine (**55**) formation (though this is generally observed at elevated temperatures).[194] There is also precedent for the oxidation of arylboronic acids to their respective phenols, which is a process facilitated by H_2O and which can lead to competing homocoupling in Chan-Lam reactions.[197] These side reactions are summarised in **Scheme 67**. All of this means that an increase in the yield could be obtained when acetate anions are used in this reaction, but the presence of a large amount of water most likely masked any beneficial effect through the destruction of the boronic acid coupling partner.

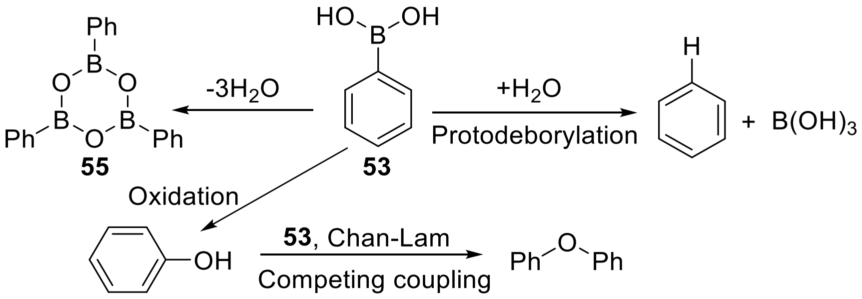

Scheme 67: Some potential fates of the boronic acid coupling partner.[194,197]

In the case of Entry 7, where water of crystallisation from the electrolyte is added into the reaction mixture, this would likely strongly promote protodeborylation. It would therefore seem prudent for future attempts of this reaction to be carried out using an acetate source not containing water of crystallisation, and indeed for all Chan-Lam reactions to be carried out in the presence of molecular sieves (as is often the case in the literature).

Unfortunately, when these initial exploratory experiments were carried out, more promising results in other areas and a lack of remaining time in the project prevented a more in-depth investigation of this reaction. However, with the benefit of hindsight, it seems that there are several ways in which this reaction could be developed and improved. The most important thing would be to try these reactions again with molecular sieves included to mitigate the destruction of the boronic acid caused by water. Somewhat related to this is to use two equivalents of boronic acid as standard procedure to further mitigate the loss of yield of the desired product caused by side reactions. Finally, the use of elevated temperatures when carrying out this reaction may give some boost to the yield and should be investigated, at least when MeCN is used as the solvent. The reason this was not tested already was due to the non-standardised equipment we used to carry out the experiments being unsuitable for heating (**Figure 2, B**). In essence, a reflux condenser could not be connected up to the reaction vessel we were using, nor were we comfortable heating a reaction vessel that was not intended for such a purpose. Indeed, this problem extends into the wider electro-organic field wherein it is common for research groups to develop their own equipment to carry out reactions in the absence of widely used, standardised apparatus.

Chapter 8. Recovering Metal Catalysts

8.1 Recovering Copper

Finally, we were very intrigued by the possibility of utilising the various techniques we had developed in this project to potentially recover the metal ion catalysts electrochemically after a reaction was complete. Such a concept is ambitious but would represent a major advantage of carrying synthetic reactions out electrochemically by offering an easy way of reusing the catalyst and cleaning up the reaction mixture, both of which are major considerations in ‘green’ sustainable chemistry. The benefits of such an approach would be especially great when undertaking large scale reactions and when the catalyst used is a precious metal. Currently, such a process is used to remove metal ions from industrial wastewater to mitigate water pollution,[200] so this process is certainly viable, at least when using aqueous media. We began investigating this idea using materials and reactions that were familiar to us, namely using copper in the Glaser-Hay reaction. The method we decided to attempt first was to use a Cu-coated C electrode to perform a Glaser-Hay reaction, then, after the reaction had been completed, switch the polarity of the working electrode to reduce copper ions that were in solution back onto our WE. This approach is conceptualised in **Figure 28**.[20]

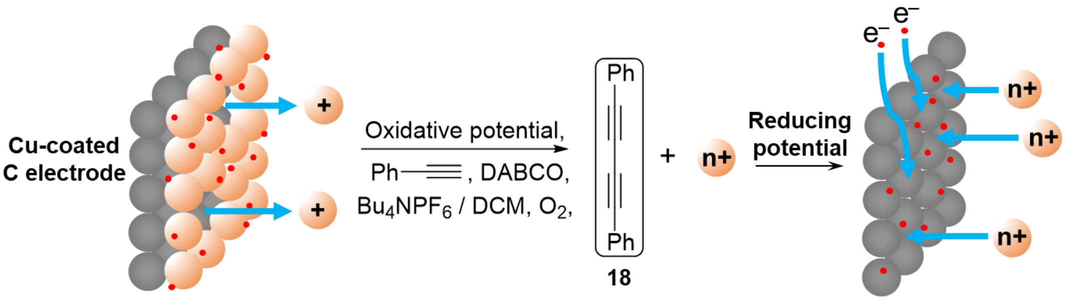

***Figure 28**: Concept of releasing Cu ions through oxidation of a Cu-coated C electrode to carry out a Glaser-Hay reaction, then recovering the Cu through reduction.*[20]

We began by using a Cu^0-coated C WE (8 mol% Cu^0 based on -15.45 C passed during coating), Pt CE, Ag QRE, phenylacetylene (1 mmol), DABCO (1.2 eq) and 0.05 M Bu_4NPF_6 / DCM electrolyte. Our first attempts at recovering the metal directly from the reaction mixture proved troublesome as whilst the diyne product was formed, we found it impossible to recover the copper ions by simply applying a reducing potential. We attributed this to the copper not actually existing as copper ions in the reaction mixture, but as the unreacted copper acetylide intermediate **17**. This species, being very sparingly soluble in DCM, essentially acted as a trap for the copper, preventing it from being recovered. This is shown in **Figure 29, A**. We therefore decided to add HCl to the solution with vigorous stirring to break down the copper acetylide intermediate producing the phenylacetylene starting material and releasing the copper.** This of course had the effect that the copper species (most likely $CuCl_2$) migrated up into the aqueous phase of our now two-phase mixture (**Figure 29, B**). This allowed us to separate the organic phase which could be worked-up and purified to yield the diyne product, but the aqueous phase containing the copper remained. We realised that with the 1 M HCl (10 mL) used, the excess acid would probably corrode the Ag QRE and any copper that we did manage to reduce onto our graphite WE, so we wanted to neutralise the HCl that was in solution. This would have the added benefit of affording us more of a potential window in which to reduce only the copper ions, rather than the H^+ in solution or water itself, as shown by the Pourbaix diagram in **Figure 29, C**. It is important to note that when we neutralised our solution with NaOH it appeared that adding too much caused the copper to precipitate out of solution as presumably $Cu(OH)_2$, which caused a similar problem to when the copper acetylide precipitate was present as the copper was now unavailable for reduction (**Figure 29, D**). A compromise of just below pH 7 seemed optimal.

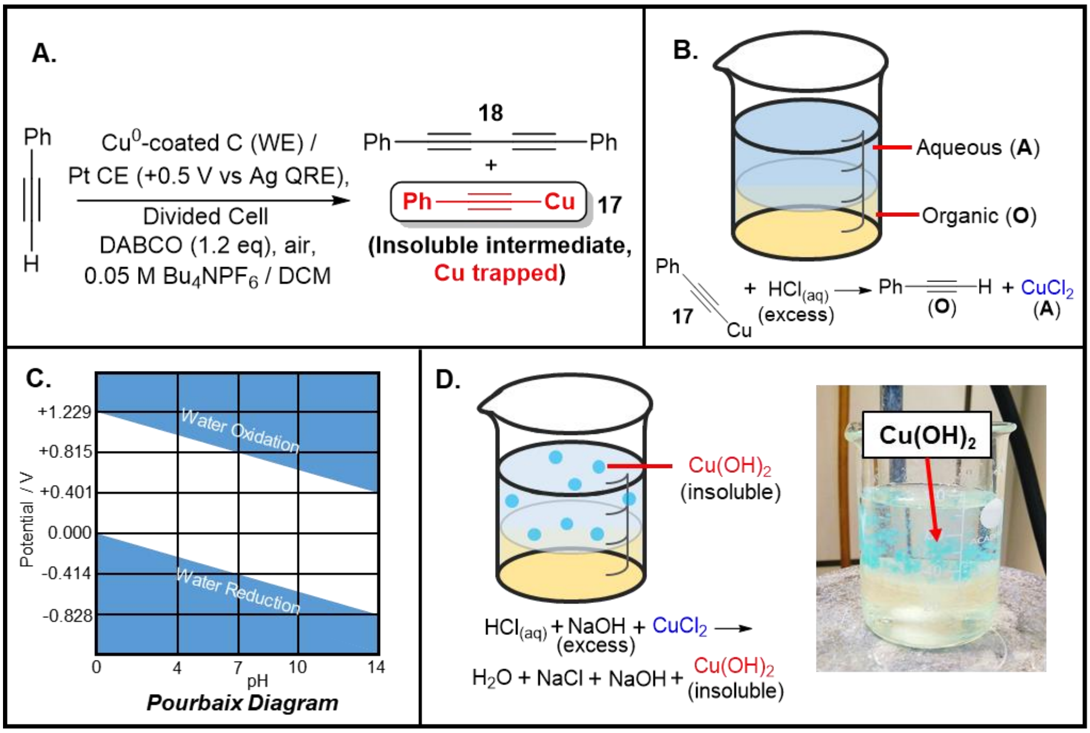

Figure 29: *Showing some of the problems associated with recovering Cu from our reaction mixture.*

We achieved initial success using this method, being able to recover some of the copper we had initially plated onto the carbon rod, along with a yield for the diyne product of up to 68% when 7 mol% Cu was used (based on -14.14 C charge passed in coating and phenylacetylene 1 mmol being used). However, we had no accurate way of determining the exact amount of

---

** In a simple test we found that the copper acetylide **17** was broken down by HCl in a sample vial in a few hours, whilst H_2SO_4 seemed incapable of breaking down **17** even after being left for a couple of days.

copper recovered. We realised that using the charge passed when reducing the aqueous copper-containing solution was flawed as despite almost completely neutralising the acid we had in solution, our estimates of the percentage of copper being recovered must be an overestimate and that the electrolysis of water must still be significantly contributing to this overall charge figure. This is corroborated by the fact that gas evolution (very likely H_2) was observed at the surface of the WE during the reduction.

Without an accurate way to measure the amount of copper we were recovering at this time, we next decided to improve the coupling reaction itself and hopefully make our method more sustainable. We realised that adding TMEDA as a ligand could improve the efficiency of our Glaser-Hay reaction as demonstrated by the excellent yields in **Table 6**. As stated previously, TMEDA facilitates oxidation of the Cu making the use of an oxidative potential for release redundant, however, we opted to include the ligand in these reactions as it led to a smoother reaction in which none of the copper acetylide intermediate precipitated out of solution (thereby maximising the amount of copper accessible for recovery) and meaning we only needed to add a fraction of the amount of $HCl_{(aq.)}$ (and H_2O) before recovering as we did previously (3 drops vs 10 mL of HCl). It was found that we still needed to add this small amount of acid however, because it appeared as if the amine additives, TMEDA and DABCO, held the copper in the organic phase, making it resistant to reduction at the electrode surface when we tried to directly recover the copper from the reaction mixture. Interestingly, adding just H_2O to the reaction mixture and vigorously stirring it allowed the copper to migrate up into the aqueous phase with no acid being required. This is potentially quite useful if this approach were extended to other reactions where the desired products are sensitive to acid. However, the copper could not then be directly recovered from this aqueous layer until the HCl (3 drops) had been added. The movement of copper ions from the organic to aqueous phase after water was added is clearly observable in **Figure 30** (**A** and **B**).[20]

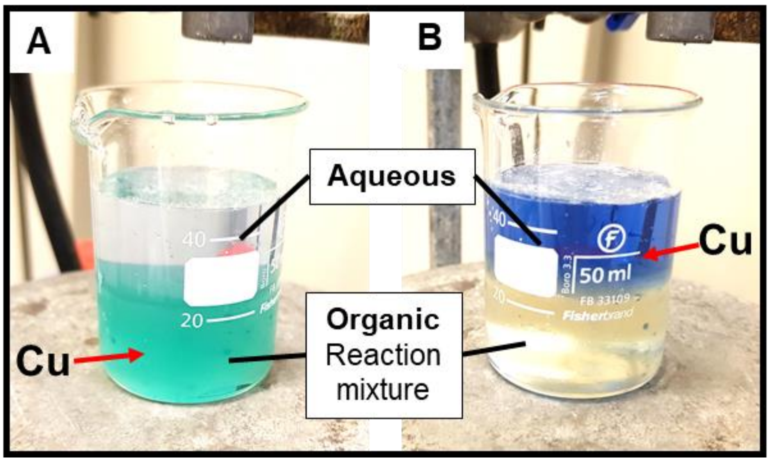

Figure 30*: Location of copper species in: A. the organic phase just after H_2O was added and B. the aqueous phase after 30 min vigorous stirring.*[20]

The TMEDA-coordinated copper is likely converted to $CuCl_2$ upon acidification which is much more easily reduced and recovered. Pleasingly, application of a reducing potential to the aqueous solution then allowed us to re-coat the electrode with copper. The details for this experiment are shown in **Scheme 68** where 6 mol% Cu was used (from the fact that 1 mmol phenylacetylene was used and an initial charge was passed of -11.99 C, see **Figure 31, A**).[20]

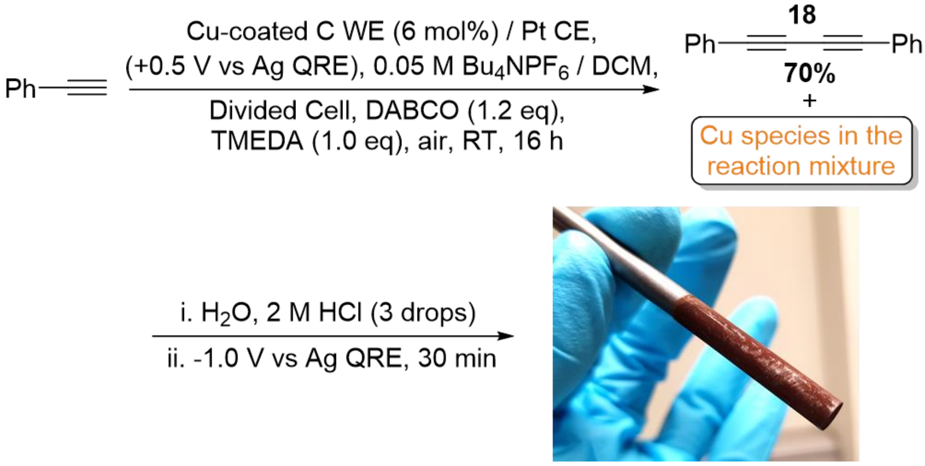

***Scheme 68**: Recovery of Cu onto a graphite WE after a Glaser-Hay reaction using TMEDA as a ligand.*[20]

We then undertook experiments to accurately determine the amount of copper redeposited on the electrode. As mentioned previously, using the charge passed when recovering copper from the $HCl_{(aq.)}$ solution proved unreliable as a significant component of the charge must be attributed to the electrolysis of the acidic solution itself. Therefore, we transferred the newly re-coated electrode to a fresh solution of acetonitrile with 0.1 M Bu_4NPF_6 as background electrolyte to oxidise the copper coating into solution as $Cu(MeCN)_4PF_6$ while monitoring the charge passed. We know from previous experiments that the copper is released reliably and efficiently in the '+1' oxidation state in MeCN (See **Chapter 4**) which allows us to accurately use the charge passed in this oxidation to determine how much copper we had managed to recover. It also allows us to ignore any electrolysis of the acidic aqueous solution that may be taking place during the recovery phase. As the metallic copper coating is exhausted, the current falls to zero and the charge approaches a maximum as can be seen from the plots of current (**B**) and charge (**C**) vs. time in **Figure 31**.[20]

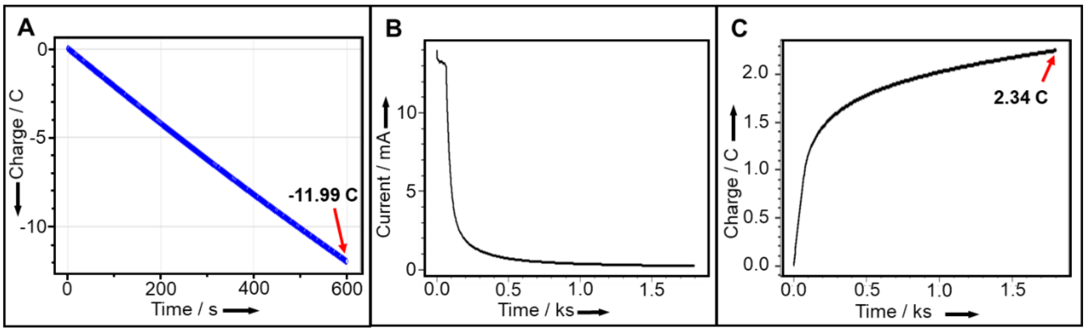

Figure 31*: A. charge graph of initial coating of graphite rod. B. Current graph and C. charge graph when releasing recovered copper coating into MeCN. Axes redrawn for clarity.*[20]

When the current approaches zero (i.e. when all of the copper metal had been stripped from the graphite surface) a charge of 2.34 C had passed. This corresponds to 2.43×10^{-5} mol Cu and a corresponding recovery efficiency of 39%, as the graphite rod was initially coated with 6.21×10^{-5} mol of copper. We were very pleased with this as it meant that we could finally assign an accurate value to the amount of copper we were recovering and felt that 39% was a reasonably good result considering the experimental difficulties of recovering metal catalysts by traditional methods. But we did not stop there.[20]

We believed we could improve this methodology by tweaking a couple of aspects of our current conditions. Firstly, we wanted to test whether this recovery could be achieved using much less TMEDA ligand and secondly, we wanted to see if using a different acid would improve the recovery efficiency. To this end we carried out a new test using the same conditions as in **Scheme 68** except that: TMEDA (20 mol%), a graphite CE instead of Pt (for a larger surface area of the CE) and a Cu loading of 8 mol% (from -15.46 C passed during coating and 1 mmol phenylacetylene used) were used. We then ran this test and treated the reaction mixture with $HCl_{(aq.)}$ as before to separate out the copper. The organic phase was purified to yield 71% of **18** which validated the idea that 20 mol% TMEDA was adequate for this reaction. But most importantly, when the aqueous phase was neutralised with NaOH, then re-acidified with conc. H_2SO_4 (1-2 drops) and subjected to a reducing potential of -0.5 V (vs Ag QRE) for 2 h we obtained a noticeably more complete coating of recovered Cu on the graphite surface than in previous attempts. Indeed, when this Cu-coated C electrode was then oxidised into a 0.05 M Bu_4NPF_6 / MeCN solution, the charge passed (4.915 C) showed that 64% of the original Cu coating had been recovered, which is a significant increase from previous tests. Furthermore, we decided to utilise this second release of the Cu coating to show that the electrodes can effectively be re-used so we added an excess of phenylacetylene and DABCO to this MeCN solution to allow a simple copper acetylide reaction to take place. From the copper that we calculated was released from our recovered Cu-coated C electrode, we isolated 5.6 mg of **17**, showing that 67% was incorporated into the copper acetylide product. These tests are summarised in **Scheme 69** and **Figure 32**.

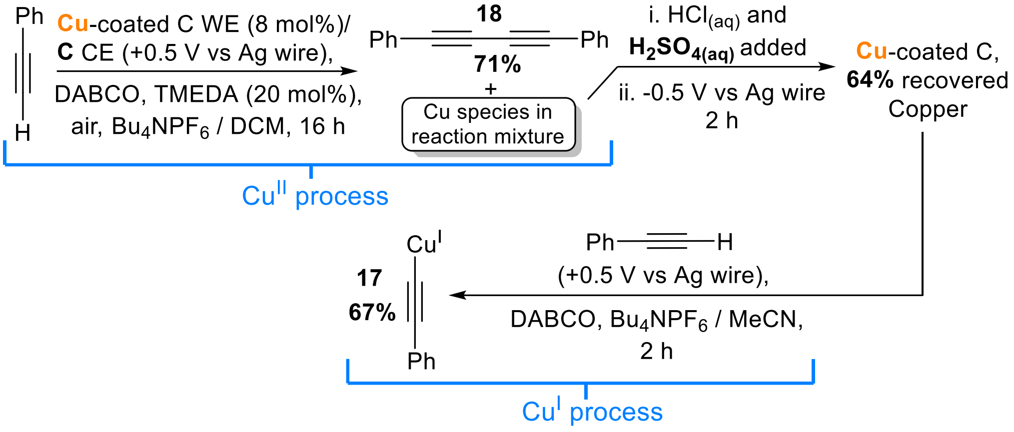

***Scheme 69**: Multistage reactions showing the release, recovery and release of a copper coating to promote both Cu^I and Cu^{II} reactions.*

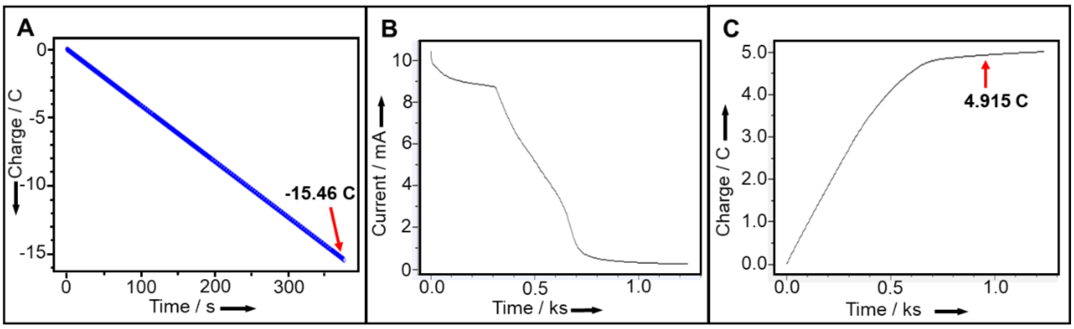

***Figure 32**: A. charge graph of initial coating of graphite rod. B. Current graph and C. charge graph when releasing recovered copper coating into MeCN. Axes redrawn for clarity.*

We wondered if the reason adding the H_2SO_4 to the recovery step proved so successful was because the SO_4^{2-} anion was perhaps less strongly coordinating than Cl^-, and so did not hold the copper in solution as effectively. The competition for coordination to Cu between the Cl^- and SO_4^{2-} ions may, therefore, have allowed more copper to be recovered than when Cl^- was the only anion present. However, when we carried out an almost identical test to that shown in **Scheme 69** but using just conc. $H_2SO_{4(aq.)}$ (3 drops) / H_2O (20 mL) in the recovery stage, we achieved a lower recovery percentage of 48% (-15.98 C initial coating, 3.855 C release into MeCN). This test also gave 76% for **18** and 70% for **17**. With this result in mind it appears as if the combination of HCl and H_2SO_4 is necessary to obtain the best recovery of copper, or perhaps the recovery success is tied to the precise concentration of acid used (as slightly differing concentrations of acid would have been used across the various tests). More tests would need to be carried out to investigate this relationship further.

Overall, we were very pleased with these results as they demonstrated that a significant percentage of the original copper coating could be recovered, and even used again immediately to promote another reaction. Not only this but we managed to show that the oxidation state of the copper could be effectively controlled with the conditions employed to facilitate a Cu^{II} process (Glaser-Hay coupling) in the first reaction, then a Cu^{I} process (copper acetylide synthesis) in the second reaction. This high level of control over the oxidation state of the Cu (Cu^0-Cu^{II}-Cu^0-Cu^I) shows a great deal of potential for carrying out electrochemically promoted catalytic reactions in the future with copper, and even with other metals. The financial benefits of being able to recover a relatively cheap base metal catalyst like copper in this way are limited, but if this methodology were extended to expensive noble metals such as Pd, the benefits would be substantial. The ability to recover all (or even a significant portion) of a catalyst into an immediately reusable form after a reaction is complete, essentially at the click of a button, is a highly attractive proposition in terms of sustainability. As such, we believe the results shown here represent a major advancement in the methodology of electro-organic reactions and with some work in the future could make a large impact in this area.

8.2 The Bubble Paradox

A closer look at the Cu-coated C electrodes after the copper had been recovered from solution revealed an interesting phenomenon. Small holes in the Cu coating were observed (**Figure 33**) which were not seen in the initial coatings from $CuSO_{4(aq.)}$ solutions and which we deduced must have arisen from bubbles of H_2 gas being generated from the reduction of protons in the slightly acidic recovery solution. This creates a certain paradox as we know the acid is required to get the copper into a 'recoverable' form (likely $CuCl_2$) as attempts at reduction of the copper directly from organic solutions or from aqueous solutions with strongly coordinating ligands (such as aqueous ammoniacal solutions – $[Cu(NH_3)_4(H_2O)_2]^{2+}$) failed. However, it also appears that the presence of this acid allows significant competing H^+ reduction to take place that creates bubbles on the surface of the electrode hindering the copper recovery. If the Cu-coated C electrodes are left in these acidic solutions the copper coating also begins to be dissolved by the acid. Clearly then, our acid-based method is imperfect and will require future refinement.

***Figure 33**: Image of the recovered Cu coating with noticeable holes probably created by H_2 gas evolution.*

Inspired by this line of thinking, a theory with regards to the ligands surrounding the copper ions and what effect this has on the ease with which the copper may be reduced during recovery was formed. It seems likely that when a reducing potential is passed through the graphite rod in solutions, Coulombic repulsion would push anionic ligands away, allowing the copper cations to be ‘freed’ from anionic ligands much more readily than from neutral ligands. This would explain why copper was recoverable from $CuSO_{4(aq.)}$ and $CuCl_{2(aq.)}$ solutions but was not from aqueous ammoniacal solutions.

8.3 Other Metal Coatings

Some initial work has been conducted on the coating of graphite rods with metals other than copper in the hopes that this will open up large new areas of electro-catalytic research. Given that we managed to employ Cu-coated C electrodes to carry out various Cu-catalysed reactions and even recover the Cu after the reaction was completed, it is our belief that this could be a viable approach when extended to other metals. We therefore investigated the coating of Ag, Pd and Zn onto graphite rods.

Silver proved straightforward to coat, in a similar way to copper, where we simply applied a reducing potential (-1.0 V vs Ag QRE) to a 0.1 M aqueous $AgNO_3$ solution (undivided cell, graphite WE, Pt CE, Ag wire QRE). This allowed the coating to form very easily (**Figure 34, A**).

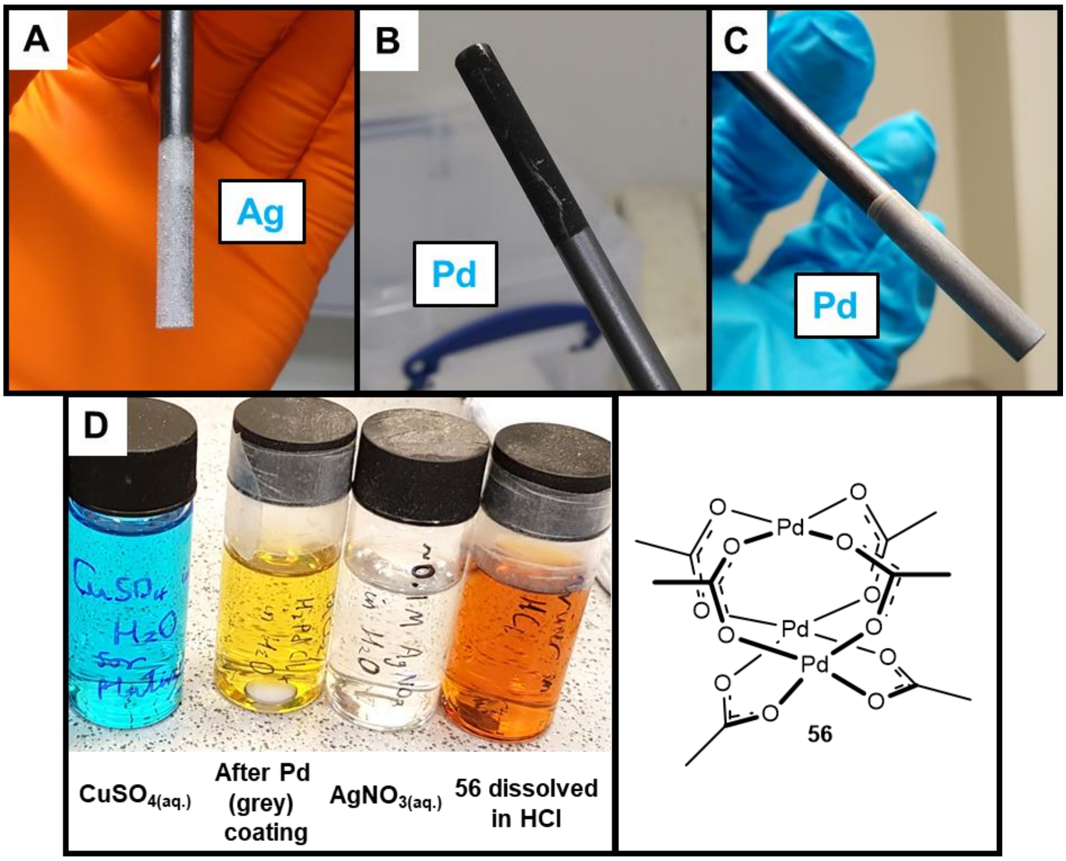

***Figure 34**: Showing: A. Silver, B. Palladium, C. Palladium coatings, D. Coating solutions and Pd(OAc)$_2$ trimer, **56**.*

By contrast, the method used for palladium proved much more difficult and convoluted, probably due to the use of less than optimal reagents. We did not want to buy any new, expensive Pd salts and so were forced to use what was to hand in the lab, namely, a Pd(OAc)$_2$ trimer reagent, **56**. We dissolved this in water to create a brown 0.01 M solution and tried to directly reduce the Pd^{II} as a coating of Pd^0 onto our graphite electrode but had no success. We therefore added HCl$_{(aq.)}$ (creating a ~0.5 M solution with respect to HCl and ~0.007 M solution with respect to Pd acetate) and left this to stir overnight to hopefully break up the palladium acetate and make it easier to recover. The resulting dark orange solution was then subjected to -1.0 V (vs Ag QRE), which turned the solution more red in colour and produced a black coating of Pd on the surface of the graphite rod (**Figure 34, B**). We then placed this electrode in 0.1 M Bu$_4$NCl / MeCN in a divided cell and applied a reasonably strongly oxidising potential of +1.5 V (vs Ag QRE) to it to release all of the coating into solution (lower potentials proved ineffective). The resulting dark orange solution, which we very tentatively propose could have been solubilised PdCl$_2$(MeCN)$_2$, was then reduced with -0.5 V vs Ag QRE to re-coat the graphite rod with a light grey coating of Pd this time (**Figure 34, C**). After this final reduction the solution was now a pale yellow colour. Interestingly, when this light grey Pd-coated C electrode was left exposed to air overnight, the palladium appeared to darken in colour, suggesting perhaps oxidation to a more stable Pd^{II} oxide. The various solutions used for the coating of graphite electrodes are shown in **Figure 34, D**.

Based on the techniques described in this section and on the work described in this thesis using Cu-coated C electrodes, our group has recently had success with Zn-coated electrodes. This work, carried out by Diyuan Li,[201] involved the plating of zinc by applying a potential of -1.2 V (vs Ag QRE) to a $ZnCl_{2(aq.)}$ solution containing K_2CO_3. This addition of base proved essential as the zinc would not coat effectively otherwise. These Zn-coated C electrodes were then employed in iodocyclisation reactions where an oxidative potential was applied in a divided cell containing NaI. This had the effect of first releasing the Zn into solution as Zn^{II} and then also producing I_2 in a dual oxidative process. See **Scheme 70**.[201]

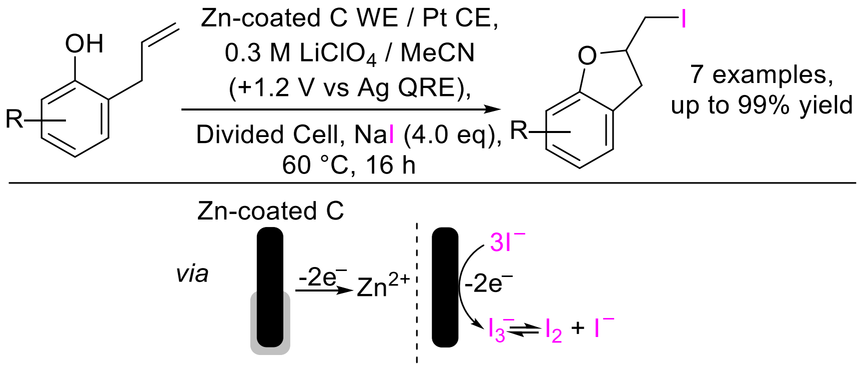

***Scheme 70**: The use of Zn-coated C electrodes for iodocyclisation reactions.*[201]

Chapter 9. Conclusions and Future Work

Some major progress has been made in several Cu-based reactions using electrochemistry. The development of two electrochemical protocols (undivided cell and divided cell) for producing copper acetylides has a lot of potential as these are valuable synthetic building blocks used in a multitude of organic reactions. The key advantage of these syntheses is that they are highly sustainable, generating no halide waste at all and, in the case of the undivided cell reaction, obviate the requirement of an added base as this is first generated from quaternary ammonium electrolyte salts and then regenerated electrochemically, making it catalytic in nature. The next logical step for these electrochemical syntheses would be to integrate them into the organic transformations where copper acetylides are intermediates to create new, sustainable reactions. Indeed, we demonstrated some initial success with this approach for the CuAAC reaction. Owing to the widespread use of this reaction in pharmaceutical chemistry, a reliable electrochemical synthetic route would be very useful to develop and research further. However, the yields obtained in our work currently fall short of traditional methods and so require improvement before the electrochemical method can compete.

We had success with the Glaser-Hay reaction, helping to shed new light on the mechanism of this 150-year old homocoupling. The use of electrochemical techniques such as CV plot analysis proved vital to our understating and revealed that the chloride ions that were generated when DABCO reacted with DCM appeared to play a part in the oxidation of the sacrificial Cu electrode, lowering the potential required. Furthermore, the identification of a dinuclear Cu complex, derived from DABCO, DCM and the electrogenerated Cu, as the probable active catalyst in this reaction helped to build up a picture of the likely processes taking place and allowed us to propose a mechanism for our electrochemical Glaser-Hay reactions.

Investigating copper coupling reactions that were not based on copper acetylide chemistry proved informative, if not particularly high yielding. The Chan-Lam reaction was theoretically the most difficult reaction we attempted in this project due to the host of different processes we were trying to get to work in concert to yield the final product. Releasing the Cu from the electrode and oxidising it up to Cu^{II}; relying upon the catalytic base generation from the electrolyte salt, and prompting the transmetallation with the boronic acid coupling partner may have been too much for our current conditions to handle effectively. However, the fact that we managed to get this reaction to work and produce some of the desired product is a good result from such a difficult task. In the future, if this reaction were revisited it seems clear that using 2 equivalents of the boronic acid and using molecular sieves could both help to improve the yield by mitigating some destruction of the boronic acid.

Finally, the use of Cu-coated C electrodes proved to be very useful throughout this project. We found that they could be used to determine the oxidation state of the Cu we were releasing, that they allowed us to effectively control the catalytic loading of Cu we used in our reactions and, perhaps most significantly of all, they gave us the opportunity to recover the metal catalyst after reactions were complete. This may be a significant advancement in the methodology of electro-organic reactions, not just when using Cu, but potentially with other metals as well. To date the highest recovery percentage of Cu is 64%. When thinking about the significance of this figure, there is both an environmental and a financial benefit. By essentially merely switching the polarity of the applied potential we have shown that almost two thirds of the metal catalyst can be recovered from solution in an immediately reusable form (as demonstrated in this work). This means less metal waste is created and that less catalyst is lost. We have also managed to demonstrate that other metals, such as Ag, Pd and Zn can be coated onto cheap graphite rods, thus opening up the possibility of investigating vast new areas of electrochemically promoted catalysis chemistry (with some initial success already being shown with Zn in iodocyclisation reactions)[201] and also opening up the possibility of recovering these metals electrochemically. Financially, the ability to do this with an expensive, versatile metal like Pd would be very attractive indeed, even with relatively low recovery percentages.

In theory, this methodology could be extended to many metals other than copper for a vast number of catalytic reactions (**Figure 35**). Of course, the work presented in this thesis has only taken the first steps towards this possibility. A lot of work to improve the recovery percentages further and extend the approach to other reactions and metals is needed, but this thesis does at least represent good initial results towards such a general approach.

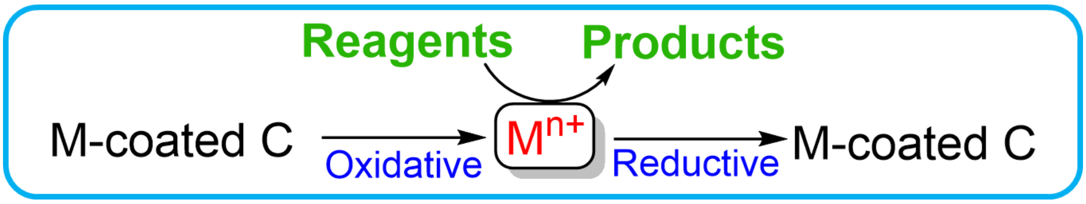

***Figure 35**: General approach to electrochemically promoted catalysis using metal-coated graphite electrodes.*

Additionally, future work could be focused on utilising the electrochemical copper acetylide syntheses to see whether our electrochemical approach can be used in similar ways as photocatalysis has been. Work carried out by M. Rueping *et al*.[202] (**Scheme 71**) shows how C-

H bond functionalisation has been achieved using light-promoted ruthenium catalysts (blue). We believe that anodic oxidation could be used to produce the same intermediates in these types of reactions, thus yielding the same products, without the need for expensive photoredox catalysts.

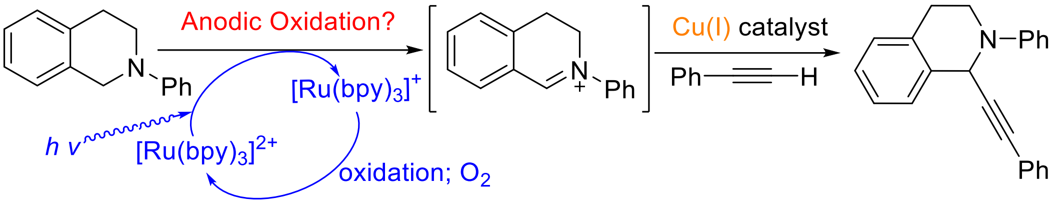

***Scheme 71**: Possible C-H functionalisation inspired by photocatalysis.*[202]

Furthermore, the characterisation of the metal coatings we were forming and using in this project could be carried out to reveal important information about the oxidation state and thickness of the coatings. Such factors probably determine how these electrodes perform in reactions. Measuring the exact surface area of the electrodes and investigating how best to scale them up would also be important. It is likely that other materials would prove much more effective as the core electrode material to plate the metals on in terms of surface area and so finding out what these materials are would allow reactions to be carried out on much larger scales.

Finally, it often occurred to us throughout this project that carrying out reactions with palladium could be a fruitful area of research and so, leading on from the work in this thesis, a promising reaction to investigate would be the Sonogashira reaction as it proceeds *via* copper acetylide intermediates. This may provide a foothold into Pd-catalysed chemistry. Another potential idea that may be worth investigating is the application of oxidative potentials to efficiently facilitate Pd^{II} to Pd^{IV} transitions, as transient Pd^{IV} intermediates have often been proposed in the mechanisms of C-H bond functionalisations, alkene borylations and difunctionalisations.[203,204] Early examples of this approach exist,[205] but further exploration could yield even more valuable results.

Chapter 10. Experimental

10.1 General Experimental

Solvents and reagents were purchased from suppliers and used without any further purification unless otherwise stated. Normal phase silica gel (Merck KGaA) and sand (VWR) were used for column chromatography. Reactions were monitored by TLC unless otherwise stated. TLC plates pre-coated with silica gel 60 F_{254} on aluminium (Merck KGaA) were used, detection by UV (254 nm) and chemical stain (potassium permanganate). Mass spectra were measured on Thermo Finnigan MAT900 XE and Waters LCT Premier XE machines operating in EI, CI and ESI modes. ^{1}H NMR spectra were recorded at either 300, 400, 500, 600 or 700 MHz, ^{13}C NMR spectra were recorded at either 75, 100, 125, 150 or 176 MHz and ^{19}F NMR spectra were recorded at 282 MHz on Bruker Avance spectrometers at ambient temperature. All chemical shifts were referenced to the residual proton impurity of the deuterated solvent. In ^{1}H NMR the multiplicity of the signal is indicated as s (singlet), d (doublet), t (triplet), q (quartet), quin (quintet), dt (doublet of triplets) or m (multiplet), defined as all multipeak signals where overlap or complex coupling of signals makes definitive descriptions of peaks difficult. The ^{13}C NMR is assigned as C (quaternary), CH, CH_2 and CH_3 as determined by DEPT 135. Coupling constants are defined as J and quoted in Hz to one decimal place. Infrared spectra were obtained on a Bruker Alpha FTIR Spectrometer operating in ATR mode. Melting points were measured with a Gallenkamp apparatus and are uncorrected. Decomposition points were recorded on this same apparatus but should not be taken as definitive characterisation values due to their inherently large margins of error. *In vacuo* is used to describe solvent removal by Büchi rotary evaporation between 17-40 °C. For NMR experiments, $CDCl_3$ denotes deuterated (d_1) chloroform and $(CD_3)_2SO$ denotes deuterated (d_6) DMSO. Electrochemical reactions were carried out using an Ivium Technologies Vertex model potentiostat operating in chronoamperometry mode. CV plots were carried out using this same potentiostat with a glassy carbon working electrode, a Pt wire counter electrode and a Ag wire quasi reference electrode. Where a Cu-coated graphite electrode was used, it was prepared by placing a graphite rod working electrode (4.12 cm^2 area) into an undivided cell containing a 0.5 M $CuSO_{4(aq.)}$ solution. A Ag wire quasi reference electrode (0.79 cm^2 area) and a Pt wire counter electrode (1.26 cm^2 area) were added and all electrodes were then connected up to a potentiostat. The potential was set to -0.50 V for 600 s and the charge passed was recorded and used to determine how much copper had been plated onto the graphite surface with the use of **Eq. 1**.

10.2 Details of Electrochemical Methods

The general experimental setup we used for electrochemical reactions was designed to be as simple and accessible as possible. In doing so we hoped to minimise the disparity and lack of reproducibility of results inherent in electro-organic synthesis due to there being a lack of standardised experimental setups. A divided 'H' cell was often used as our reaction vessel (dimensions shown in **Figure 36, A**). Each chamber had a size B19 ground-glass neck and a total volume of 20 mL. A semi-porous sintered glass divider sat between each chamber. All reactions were however carried out using 10 mL of electrolyte solution in each chamber as this was sufficient to sit above the line of the sintered glass divider and thus allow sufficient ion transfer. Copper 'plate' or 'sheet' electrodes were made by cutting strips from a roll of copper sheet metal (around 0.5 mm thickness) to create plates with dimensions of 10 mm x 40 mm. When used, these were placed into solution to a depth of 25 mm, meaning the area of electrode exposed to solution was approximately 530 mm^2. A silver wire, which was 1 mm thick, was used as a quasi reference electrode and was likewise placed into solution to a depth of 25 mm giving an effective area of 79 mm^2. Both the copper plate and the silver wire were placed into the same chamber to minimise the potential drop arising from resistance and kept 10 mm apart. A platinum wire of 1 mm thickness was used as the counter electrode and placed in the other chamber of the H cell, this time at a depth of 40 mm giving an effective area of 126 mm^2. Where graphite electrodes were used for the working electrode and/or counter electrode, rods of 5 mm diameter were used at a depth of 25 mm giving an effective area of 412 mm^2.[20,39,40]

Where an undivided cell was required, we used a 10 mL sample vial as our reaction vessel (dimensions shown in **Figure 36, B**) as a size B19 Suba-Seal fit perfectly in the neck to create a seal. A balloon could be fitted into the centre of the Suba-Seal for degassing and maintaining a specific gaseous environment during electrolysis. Three metal wire electrodes were also inserted into the Suba-Seal in a triangular pattern, to a depth of 20 mm into the 10 mL electrolyte solutions used in the reactions. The electrodes were held at 7-10 mm distance between any two electrodes over the course of reactions. As the three electrodes used were the same diameter (1 mm), and all held at the same depth into the solution, they all had the same effective surface area of 64 mm^2. All reactions were run using an Ivium Technologies Vertex model potentiostat operating in chronoamperometry mode. This model allowed for real-time charge over time and current over time graphs to be generated which we found exceedingly useful for this work, especially for measuring charge passed over the course of reactions.[20,39,40]

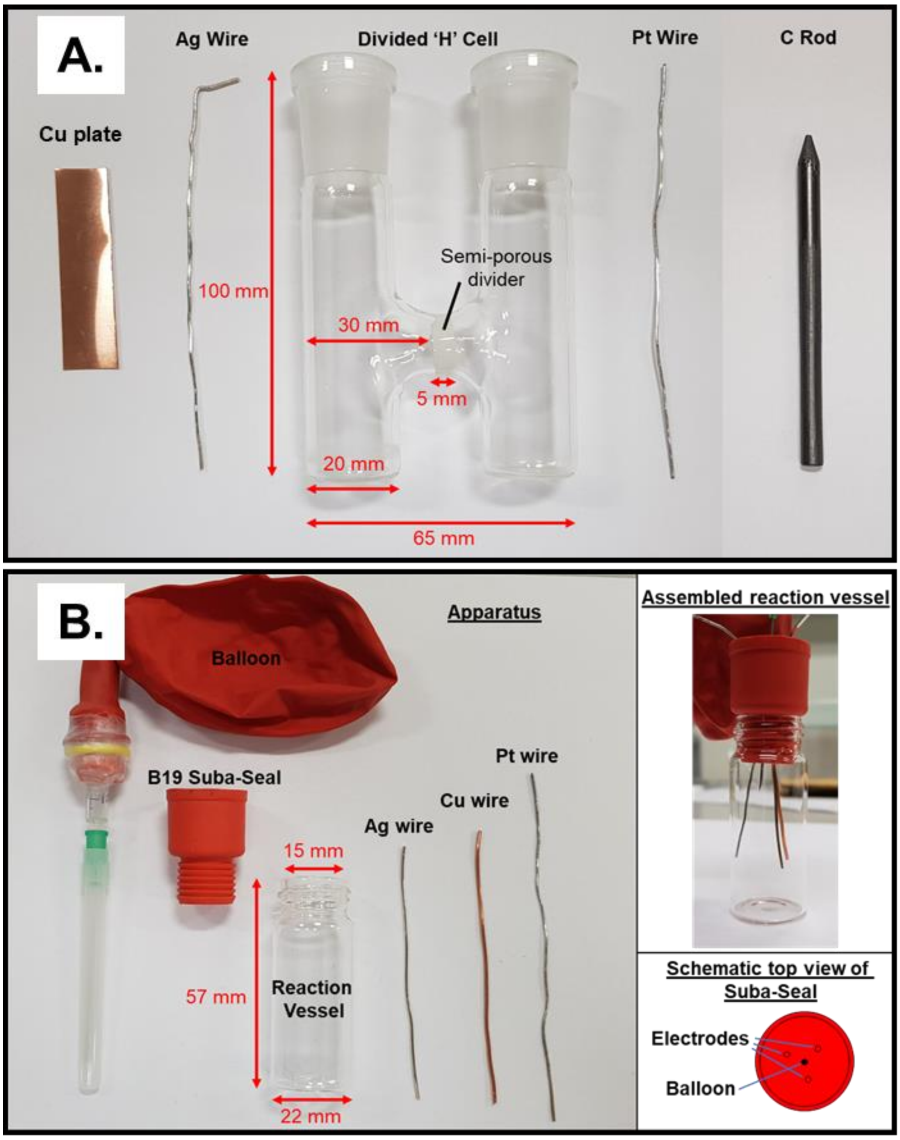

Figure 36: *A. Example of a divided 'H' cell and B. example of an undivided cell used in this project. (Same as **Figure 2**).*[20,39,40]

10.3 Experimental Procedures

Electrochemical dibromination reaction

1,2-Dibromo-1,2-diphenylethane, 5

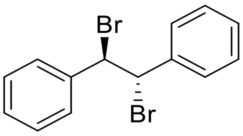

Bu_4NBr (6.45 g, 20.0 mmol, 10.0 eq) was dissolved in MeCN (20 mL) to make up a 1 M solution. A divided (H) cell was charged with this solution (10 mL each side) followed by *trans*-stilbene (0.18 g, 1.0 mmol, 1.0 eq) in one chamber only. The solution was stirred at RT for 5 min to allow all solids to dissolve. A platinum wire (0.95 cm^2 area) and a silver wire (0.95 cm^2 area) were then placed into the chamber of the H cell with the stilbene substrate, and a carbon rod (4.91 cm^2 area) was placed into the other chamber. These electrodes were then connected up to a potentiostat (Pt = WE, Ag = QRE, C = CE) and the potential was set to run at +1.00 V for 16 h, whilst stirring at RT. The precipitate formed was then filtered out of the dark brown solution and washed with MeCN to give the product as a white solid (0.23 g, 68%); m.p. 241-243 °C (lit.,[206] 240-242 °C); R_f 0.45 (10% EtOAc/pet. ether.); IR ν_{max} (neat) 2962, 1496, 1452, 1135, 762, 689, 596, 551 cm^{-1}; ^{1}H NMR (600 MHz, $CDCl_3$) δ_H 7.51-7.53 (4H, m, Ar*H*), 7.41-7.44 (4H, m, Ar*H*), 7.36-7.39 (2H, m, Ar*H*), 5.49 (2H, s, C*H*Br) ppm; ^{13}C NMR (150 MHz, $CDCl_3$) δ_C 140.1 (*C*), 129.1 (*C*H), 128.9 (*C*H), 128.0 (*C*H), 56.2 (*C*H) ppm; LRMS (CI) m/z 360 ([M(^{81}Br^{81}Br)+NH_4]$^+$, 12%), 358 ([M(^{81}Br^{79}Br)+NH_4]$^+$, 24%), 356 ([M(^{79}Br^{79}Br)+NH_4]$^+$, 12%), 305 (17%), 278 (97%), 276 (96%), 196 (48%), 180 (100%); HRMS (CI) calc'd for $C_{14}H_{16}NBr_2$ [M(^{79}Br^{79}Br)+NH_4]$^+$ 355.9644, found 355.9645. Data in agreement with literature.[207]

Electrochemical methoxybromination reaction

(1-Bromo-2-methoxyethane-1,2-diyl)dibenzene, 16

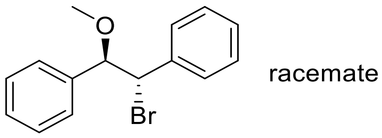

NaBr (2.06 g, 20.0 mmol, 5.0 eq) was dissolved in MeOH (20 mL) to make up a 1 M solution. A divided (H) cell was charged with this solution (10 mL each side) followed by *trans*-stilbene (0.36 g, 2.0 mmol, 1.0 eq) in one chamber only. A platinum wire (0.95 cm^2 area) and a silver wire (0.95 cm^2 area) were then placed into the chamber of the H cell with the stilbene substrate, and a carbon rod (4.91 cm^2 area) was placed into the other chamber. These electrodes were connected up to a potentiostat (Pt = WE, Ag = QRE, C = CE) and the potential was set to run at +1.30 V for 16 h whilst stirring at RT. The precipitate formed was then filtered out of the pale yellow solution and washed with MeOH to give a white solid (0.26 g, in an approximate ratio 1:3 of **5** and **16** respectively (conversion = 9% **5** and 33% **16**) by ^{1}H NMR). Partial isolation of **16** was achieved by column chromatography on silica gel (5% EtOAc/pet. ether.) to give a white solid (0.08 g, 14%); m.p. 114-116 °C (lit.,[208] 115-118 °C); R_f 0.34 (5% EtOAc/pet. ether.); IR ν_{max} (neat) 2930, 2884, 1493, 1453, 1161, 1091, 1072, 692, 581 cm^{-1}; ^{1}H NMR (400 MHz, $CDCl_3$) δ_H 7.37-7.39 (2H, m, Ar*H*), 7.25-7.35 (8H, m, Ar*H*), 5.07 (1H, d, *J* = 6.9, C*H*Br), 4.68 (1H, d, *J* = 6.9, C*H*OMe), 3.22 (3H, s, OC*H*$_3$) ppm; ^{13}C NMR (75 MHz, $CDCl_3$) δ_C 138.9 (*C*), 138.5 (*C*), 129.0 (*C*H), 128.6 (*C*H), 128.5 (*C*H), 128.3 (*C*H), 128.3 (*C*H), 128.1 (*C*H), 87.2 (*C*H), 57.8 (*C*H$_3$), 57.2 (*C*H) ppm; LRMS (ESI) m/z 261 ([M(^{81}Br)-

OMe]$^+$, 11%), 259 ([M(^{79}Br)-OMe]$^+$, 11%), 211 ([M-Br]$^+$, 13%), 197 (100%), 180 (92%). [M+H]$^+$ not observed. Data in agreement with literature.[208]

Divided cell method for preparing (phenylethynyl)copper, 17 from an aqueous ammoniacal solution[20]

(Phenylethynyl)copper, 17

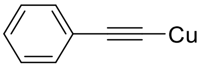

$LiClO_4$ (0.16 g, 1.5 mmol, 0.8 eq) was dissolved in ~30% $NH_4OH_{(aq.)}$ solution (19 mL) and EtOH (11 mL) to make up a 0.05 M solution. A divided (H) cell was charged with this solution (15 mL each side). A copper sheet (6.00 cm^2 area) and a silver wire (0.95 cm^2 area) were then placed into one chamber, and a platinum wire (0.95 cm^2 area) was placed into the other chamber. These electrodes were connected up to a potentiostat (Cu = WE, Ag = QRE, Pt = CE) and the potential was set to run at +2.00 V for 30 min whilst stirring at RT. Phenylacetylene (0.22 mL, 2.0 mmol, 1.0 eq) was then added to the blue solution in the chamber containing the copper electrode, immediately causing a yellow solid precipitate to form. The potentiostat was then set to +2.00 V for a further 16 h whilst stirring at RT. The yellow precipitate was filtered out of solution and washed with ~30% $NH_4OH_{(aq.)}$ solution (30 mL), H_2O (30 mL), EtOH (30 mL) and Et_2O (30 mL) to yield the product as a bright yellow solid (0.07 g, 21%); m.p. 228-230 °C (lit.,[209] 226-229 °C); IR ν_{max} (neat) 3046, 1929, 1481, 1440, 745, 682, 521, 511 cm^{-1}. Data in agreement with literature.[20,39,95,209,210] Note that due to the insolubility of copper acetylides, NMR was not an effective form of characterisation for these compounds.

General Method A. Divided cell method for preparing copper acetylides from an MeCN-based solution[20]

Bu_4NPF_6 (0.77 g, 2.0 mmol, 4.0 eq) was dissolved in reagent grade MeCN (20 mL) to make up a 0.1 M solution. A divided (H) cell was charged with this solution (10 mL each side). A copper plate (5.30 cm^2 area) and a silver wire (0.79 cm^2 area) were then placed into one chamber, and a platinum wire (1.26 cm^2 area) was placed into the other chamber. These electrodes were connected up to a potentiostat (Cu = WE, Ag = QRE, Pt = CE) and the potential was set to run at +0.50 V for 4 h whilst stirring at RT and exposed to air. The potential was then stopped and the pale green solution from the chamber containing the Cu electrode was transferred to a flame-dried RBF and degassed with argon for 5 min. DABCO (0.11 g, 1.0 mmol, 2.0 eq) and the terminal alkyne (0.5 mmol, 1.0 eq) were then added, immediately causing a yellow precipitate to form. The solution was then degassed for a further 5 min before being left to stir for 1 h at RT under argon. The yellow precipitate was then collected by Büchner filtration and washed with MeCN (30 mL), then H_2O (30 mL), then acetone (30 mL) before being dried in a vacuum oven to yield the copper acetylide product.

General Method A. **(Phenylethynyl)copper, 17**, phenylacetylene (0.06 mL, 0.55 mmol) used, giving a bright yellow solid (83 mg, 92%).[20]

((3-Methoxyphenyl)ethynyl)copper, 21

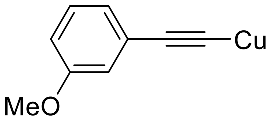

General Method A. 3-Ethynylanisole (0.06 mL, 0.47 mmol) used to yield a bright yellow solid (82 mg, 89%); m.p. 186-188 °C (dec.); IR ν_{max} (neat) 3064, 2937, 2830, 1951, 1934, 1588, 1482, 1460, 1414, 1315, 1261, 1189, 1147, 1036, 994, 915, 842, 787, 774, 684 cm^{-1}.[20]

(*p*-Tolylethynyl)copper, 22

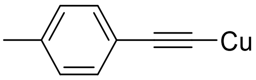

General Method A. *p*-Tolylacetylene (0.06 mL, 0.47 mmol) used to yield a bright yellow solid (76 mg, 91%); m.p. 235-237 °C (dec.) (lit.,[211] 236 °C); IR ν_{max} (neat) 3017, 2915, 1931, 1887, 1500, 805, 515 cm^{-1}. Data in agreement with literature.[20,95,211]

(Thiophen-3-ylethynyl)copper, 23

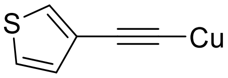

General Method A. 3-Ethynylthiophene (0.05 mL, 0.51 mmol) used to yield a bright yellow solid (56 mg, 64%); m.p. 193-195 °C (dec.); IR ν_{max} (neat) 3102, 2926, 2869, 1936, 763, 621 cm^{-1}.[20]

(3-Ethoxy-3-oxoprop-1-yn-1-yl)copper, 24

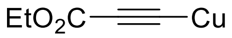

General Method A. Ethyl propiolate (0.05 mL, 0.49 mmol) used to yield a bright yellow solid (70 mg, 88%); m.p. 182-184 °C (dec.); IR ν_{max} (neat) 2983, 2876, 1954, 1914, 1694, 1453, 1194, 1021, 791, 743 cm^{-1}.[20]

(4-Phenylbut-1-yn-1-yl)copper, 25

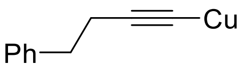

General Method A. 4-Phenyl-1-butyne (0.07 mL, 0.50 mmol) used to yield a bright yellow solid (62 mg, 64%); m.p. 174-176 °C (dec.); IR ν_{max} (neat) 3055, 2929, 1941, 1605, 1496, 1451, 1436, 764, 688, 461 cm^{-1}.[20]

(Cyclohex-1-en-1-ylethynyl)copper, 26

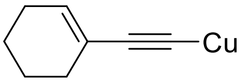

General Method A. 1-Ethynylcyclohexene (0.06 mL, 0.51 mmol) used to yield a dark yellow solid (63 mg, 73%); m.p. 163-165 °C (dec.); IR ν_{max} (neat) 2926, 2855, 1433, 833, 793, 556 cm^{-1}.[20]

((Trimethylsilyl)ethynyl)copper, 27

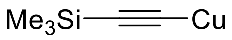

General Method A. Trimethylsilylacetylene (0.07 mL, 0.51 mmol) used to yield an orange-red solid (60 mg, 73%), stored at -20 ºC to mitigate decomposition; m.p. 142-144 °C (dec.); IR ν_{max} (neat) 2955, 2895, 2189, 2139, 1878, 1245, 839, 757, 668 cm^{-1}. Data in agreement with literature.[20,212]

General Method B. Undivided cell method for preparing copper acetylides from an MeCN-based solution[39]

$Et_4N(O_3SC_6H_4CH_3)$ (0.03 g, 0.10 mmol, 1.0 eq) was weighed out into a reaction vessel and sealed as shown in **Figure 36, B** with Cu wire (WE), Ag wire (QRE) and Pt wire (CE) electrodes pushed through the Suba-Seal. Anhydrous MeCN (10 mL) was then added to make up a 0.01 M solution. The terminal alkyne (0.20 mmol, 2.0 eq) was then added *via* syringe and the solution was degassed with argon for 5 min. The electrodes were then connected up to a potentiostat and the potential was set to run at +0.50 V for 4 h whilst stirring at RT under argon, immediately causing a yellow precipitate to form. The potential was then stopped and the yellow precipitate was collected by Büchner filtration and washed with reagent grade MeCN (20 mL), then H_2O (20 mL), then acetone (20 mL) before being dried in a vacuum oven for 30 min to yield the dry copper acetylide product.

General Method B. **(Phenylethynyl)copper, 17**, phenylacetylene (32 mg, 0.32 mmol) used, giving a bright yellow solid (50 mg, 97%).[39]

General Method B. **(*p*-Tolylethynyl)copper, 22**, *p*-tolylacetylene (25 mg, 0.21 mmol) used, giving a yellow solid (37 mg, 96%).[39]

General Method B. **(3-Ethoxy-3-oxoprop-1-yn-1-yl)copper, 24**, ethyl propiolate (32 mg, 0.32 mmol) used, giving a bright yellow solid (26 mg, 51%).[39]

General Method B. **(4-Phenylbut-1-yn-1-yl)copper, 25**, 4-phenyl-1-butyne (27 mg, 0.20 mmol) used, giving a yellow solid (25 mg, 63%).[39]

General Method B. **(Cyclohex-1-en-1-ylethynyl)copper, 26**, 1-ethynylcyclohexene (21 mg, 0.20 mmol) used giving an orange solid (29 mg, 86%).[39]

((4-(Trifluoromethyl)phenyl)ethynyl)copper, 30

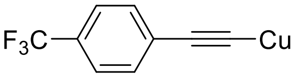

General Method B. 4-Ethynyl-α,α,α-trifluorophenylacetylene (31 mg, 0.18 mmol) used to yield a yellow solid (40 mg, 95%); m.p. 186-188 °C (dec.); IR ν_{max} (neat) 2920, 1916, 1607, 1402, 1315, 1160, 1113, 1101, 1063, 1014, 835, 592, 513, 442 cm^{-1}.[39]

((2-(Trifluoromethyl)phenyl)ethynyl)copper, 31

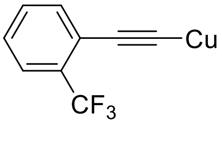

General Method B. 2-(Trifluoromethyl)-phenylacetylene (32 mg, 0.19 mmol) used to yield a bright yellow solid (43 mg, 99%); m.p. 243-245 °C (dec.); IR ν_{max} (neat) 3065, 1930, 1600, 1570, 1484, 1445, 1313, 1157, 1120, 1107, 1052, 1031, 756, 744, 650, 530 cm^{-1}.[39]

((4-Methoxyphenyl)ethynyl)copper, 32

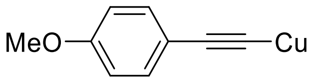

General Method B. 4-Ethynylanisole (25 mg, 0.19 mmol) used to yield a bright yellow solid (36 mg, >99%); m.p. 247-249 °C (dec.) (lit.,[211] 260 °C); IR ν_{max} (neat) 3031, 2836, 1600, 1499, 1247, 1168, 1029, 818, 533, 449 cm^{-1}. Data in agreement with literature.[39,210,211]

((Triisopropylsilyl)ethynyl)copper, 33

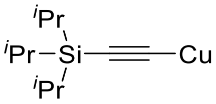

General Method B. Triisopropylsilyl acetylene (37 mg, 0.20 mmol) used to yield a dark yellow solid (11 mg, 21%); m.p. 161-165 °C (dec.); IR ν_{max} (neat) 3315, 2945, 2867, 1460, 1372, 883, 835, 613, 451 cm^{-1}.[39]

(3,3-Dimethylbut-1-yn-1-yl)copper, 34

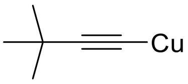

General Method B. 3,3-Dimethyl-1-butyne (16 mg, 0.19 mmol) used to yield a yellow solid (13 mg, 47%); m.p. 147-150 °C (dec.) (lit.,[213] 80-150 °C); IR ν_{max} (neat) 3322, 2965, 2923, 2896, 2864, 2183, 1471, 1453, 1360, 1239, 455 cm^{-1}. Data in agreement with literature.[39,213]

Traditional method for preparing (phenylethynyl)copper, 17[39,88]

To a flask backfilled with argon, a mixture of $NH_4OH_{(aq.)}$ (30% solution, 50 mL), EtOH (30 mL) and CuI (3.80 g, 20 mmol, 2.0 eq) was added to create a deep blue solution. Phenylacetylene (1.02 g, 10 mmol, 1.0 eq) was then added dropwise whilst stirring to immediately cause a bright yellow preciptate to form. The solution was then left to stir at RT under argon for 16 h, before the precipitate was collected by Büchner filtration and washed successively with $NH_4OH_{(aq.)}$ (10% solution, 100 mL), then H_2O (50 mL), then EtOH (30 mL) and finally Et_2O (100 mL). The bright yellow solid was then dried in a vacuum oven for 2 h to yield the dry product **17** as a bright yellow solid (1.64 g, 99%).

Traditional method for preparing 1-benzyl-4-phenyl-1*H*-1,2,3-triazole, 39 from (phenylethynyl)copper, 17, used as a 'Click test'[39,91]

A flask was charged with (phenylethynyl)copper, **17** (1.0 eq), followed by BnN_3 (1.5 eq) dissolved in reagent grade cyclohexane (3 mL). The solution was stirred at RT as glacial acetic acid (1.0 eq) was added dropwise, causing an immediate colour change from yellow to pale green. The flask was then sealed with a Suba-Seal and degassed for 3 min, before being left to stir at RT under argon for 16 h. The solution was then diluted with EtOAc (15 mL) and filtered into a separating funnel, before being washed with 1 M $HCl_{(aq.)}$ (10 mL), then 1 M $K_2CO_{3(aq.)}$ (10 mL), then H_2O (15 mL). The organic layer was then dried over Na_2SO_4, filtered and concentrated *in vacuo*. The crude off-white solid was then purified by column chromatography (25% EtOAc/pet. ether.) to give the pure product 1-benzyl-4-phenyl-1*H*-1,2,3-triazole, **39** as a white crystalline solid.

General Method C. CuAAC reactions using Cu-coated C electrodes

A graphite rod working electrode (4.12 cm^2 area) was first coated with a layer Cu by placing it into an undivided cell containing a 0.5 M $CuSO_{4(aq.)}$ solution. A Ag wire quasi reference electrode (0.79 cm^2 area) and a Pt wire counter electrode (1.26 cm^2 area) were added and all electrodes were then connected up to a potentiostat. The potential was set to -0.50 V for the length of time required for the calculated charge to be passed (for example, if a 10 mol% Cu coating was desired and 0.2 mmol phenylacetylene was to be used then 2×10^{-5} mol Cu was needed. Using **Eq. 1** 2×10^{-5} mol x 2 x 1.602×10^{-19} C x 6.022×10^{23} mol^{-1} = 3.86 C needs to be passed). These electrodes were then carefully cleaned with water and acetone and placed into a divided (H) cell (Cu-coated graphite and Ag wire in one chamber, Pt wire in the other chamber) which had been charged with a 0.01 M solution of $Et_4NOAc{\cdot}4H_2O$ (0.05 g, 0.2 mmol, 1.0 eq) dissolved in reagent grade MeCN (20 mL) (10 mL each side of H cell). The electrodes were connected up to a potentiostat (Cu-coated graphite = WE, Ag = QRE, Pt = CE). The solution was briefly degassed with argon then the potential was set to run at +0.50 V until all of the Cu had been released. The electrodes were then removed, and the solution was transferred to an RBF and degassed with argon again. Et_3N (0.04 mL, 0.3 mmol, 1.5 eq), BnN_3 (0.04 mL, 0.3 mmol, 1.5 eq) and phenylacetylene (0.02 mL, 0.2 mmol, 1.0 eq) were then added *via* syringe, the solution was degassed one final time, then the solution was left to stir at RT under argon for 16 h. The solution was then concentrated *in vacuo*, before being dissolved in EtOAc (15 mL) and filtered into a separating funnel. The organic layer was then washed with 1 M $HCl_{(aq.)}$ (10 mL), then 1 M $K_2CO_{3(aq.)}$ (10 mL) and dried over Na_2SO_4 before being filtered and concentrated *in vacuo*. The crude off-white solid was then purified by column chromatography to yield the pure products.

General Method D. Undivided cell method for CuAAC reaction[39]

$Et_4NOAc\cdot4H_2O$ (0.10 mmol, 0.5 eq) was weighed out into a reaction vessel and sealed as shown in **Figure 36, B** with Cu wire (WE), Ag wire (QRE) and Pt wire (CE) electrodes pushed through the Suba-Seal. Anhydrous MeCN (10 mL) was then added to make up a 0.01 M solution. The terminal alkyne (0.20 mmol, 1.0 eq) and BnN_3 (0.30 mmol, 1.5 eq) were then added *via* syringe and the solution was degassed with argon for 5 min. The electrodes were then connected up to a potentiostat and the potential was set to run at +0.50 V for 3 h whilst stirring at RT under argon. The potential was then stopped and the solution was left to stir for a further 13 h at RT, under argon. The solution was then concentrated *in vacuo,* before being dissolved in EtOAc (15 mL) and filtered into a separating funnel. The organic layer was then washed with 1 M $HCl_{(aq.)}$ (10 mL), then 1 M $K_2CO_{3(aq.)}$ (10 mL) and dried over Na_2SO_4 before being filtered and concentrated *in vacuo*. The crude off-white solid was then purified by column chromatography to yield the pure product.

1-Benzyl-4-phenyl-1*H*-1,2,3-triazole, 39

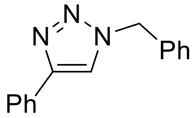

Highest yield from the General Method D. when phenylacetylene (22 mg, 0.22 mmol) was used to yield a white solid (41 mg, 79%). (General Method C. also used); m.p. 127-128 °C (lit.,[91] 130-131 °C); R_f 0.20 (25% EtOAc/pet. ether.); IR ν_{max} (neat) 3142, 2976, 2924, 2853, 1450, 1223, 1045, 767, 727, 694 cm^{-1}; ^1H NMR (600 MHz, $CDCl_3$) δ_H 7.79-7.81 (2H, m, Ar*H*), 7.65 (1H, s, N-C*H*), 7.35-7.41 (5H, m, Ar*H*), 7.30-7.33 (3H, m, Ar*H*), 5.58 (2H, s, N-C*H₂*) ppm; ^{13}C NMR (100 MHz, $CDCl_3$) δ_C 148.3 (*C*), 134.8 (*C*), 130.6 (*C*), 129.2 (*C*H), 128.9 (*C*H), 128.2 (*C*H), 128.1 (*C*H), 125.8 (*C*H), 119.5 (*C*H), 54.4 (*C*H_2) ppm; LRMS (ESI) m/z 236 ($[M+H]^+$, 100%). Data in agreement with literature.[39,91,214]

1-Benzyl-4-phenyl-5-(phenylethynyl)-1*H*-1,2,3-triazole, 40

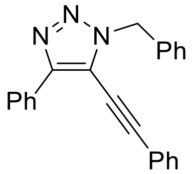

General Method C. was used (not obtained in General Method D. where exclusively 1-benzyl-4-phenyl-1*H*-1,2,3-triazole, **39** was produced). The highest yield was obtained when the 30 mol% electrode was used with phenylacetylene (20 mg, 0.2 mmol) to give a colourless oil (15 mg, 46%); R_f 0.32 (25% EtOAc/pet. ether.); IR ν_{max} (neat) 3063, 3032, 2926, 2853, 2220, 1606, 1497, 1481, 1454, 1442, 1357, 774, 756, 736, 719, 690 cm^{-1}; ^{1}H NMR (400 MHz, CDCl$_3$) δ_H 8.17-8.20 (2H, m, Ar*H*), 7.49-7.52 (2H, m, Ar*H*), 7.33-7.48 (11H, m, Ar*H*), 5.68 (2H, s, C*H*$_2$) ppm; ^{13}C NMR (100 MHz, CDCl$_3$) δ_C 148.2 (*C*), 134.8 (*C*), 131.6 (*C*H), 130.4 (*C*), 129.8 (*C*H), 129.0 (*C*H), 128.8 (x2)(*C*H x2), 128.7 (*C*H), 128.6 (*C*H), 128.2 (*C*H), 126.3 (*C*H), 121.5 (*C*), 117.3 (*C*), 102.4 (*C*), 75.7 (*C*), 53.1 (*C*H$_2$) ppm; LRMS (ESI) m/z 336 ([M+H]$^+$, 100%). Data in agreement with literature.[215]

1-Benzyl-4-(4-methoxyphenyl-1*H*-1,2,3-triazole, 41

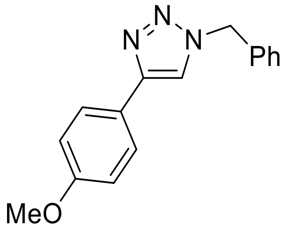

General Method D. 4-Ethynylanisole (27 mg, 0.2 mmol) used to yield a white solid (6 mg, 11%); m.p. 137-138 °C (lit.,[216] 140-142 °C); R$_f$ 0.14 (25% EtOAc/pet. ether.); IR ν_{max} (neat) 3126, 2924, 2852, 1499, 1247, 1026, 830, 818, 708 cm^{-1}; ^{1}H NMR (300 MHz, CDCl$_3$) δ_H 7.69-7.74 (2H, m, Ar*H*), 7.57 (1H, s, N-C*H*), 7.35-7.42 (3H, m, Ar*H*), 7.29-7.34 (2H, m, Ar*H*), 6.90-6.95 (2H, m, Ar*H*), 5.56 (2H, s, N-C*H*$_2$), 3.82 (3H, s, O-C*H*$_3$) ppm; ^{13}C NMR (75 MHz, CDCl$_3$) δ_C 159.7 (*C*), 148.3 (*C*), 134.9 (*C*), 129.3 (*C*H), 128.9 (*C*H), 128.2 (*C*H), 127.1 (*C*H), 123.4 (*C*), 118.8 (*C*H), 114.4 (*C*H), 55.5 (*C*H$_3$), 54.3 (*C*H$_2$) ppm; LRMS (ESI) m/z 266 ([M+H]$^+$, 100%). Data in agreement with literature.[216,217]

1-Benzyl-4-(4-(trifluoromethyl)phenyl)-1*H*-1,2,3-triazole, 42

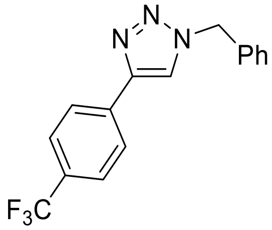

General Method D. 4-Ethynyl-α,α,α-trifluorophenylacetylene (33 mg, 0.19 mmol) used to yield a white solid (38 mg, 65%); m.p. 133-135 °C (lit.,[218] 133-134 °C); R$_f$ 0.48 (40% EtOAc/pet. ether.); IR ν_{max} (neat) 3107, 1620, 1327, 1121, 834, 718, 698 cm^{-1}; ^{1}H NMR (400 MHz, CDCl$_3$) δ_H 7.90-7.92 (2H, d, *J* = 8.1, Ar*H*), 7.75 (1H, s, N-C*H*), 7.63-7.65 (2H, d, *J* = 8.1, Ar*H*), 7.37-7.43 (3H, m, Ar*H*), 7.30-7.34 (2H, m, Ar*H*), 5.59 (2H, s, N-C*H*$_2$) ppm; ^{13}C NMR (100 MHz, CDCl$_3$) δ_C 146.9 (*C*), 134.5 (*C*), 134.1 (*C*) (doublet, $J_{F\text{-}C}$ = 1.3), 130.0 (*C*) (doublet, $J_{F\text{-}C}$ = 32.6), 129.3 (*C*H), 129.0 (*C*H), 128.2 (*C*H), 125.9 (*C*H), 125.8 (*C*H), 124.2 (*C*) (doublet, $J_{F\text{-}C}$ = 272.1), 120.3 (*C*H), 54.4 (*C*H$_2$) ppm; ^{19}F NMR (282 MHz, CDCl$_3$) δ_F -

62.6 (CF_3) ppm; LRMS (ESI) m/z 304 ([M+H]$^+$, 100%), 214 (62%), 181 (62%), 165 (45%), 149 (28%). Data in agreement with literature.[218]

1-Benzyl-4-(*p*-tolyl)-1*H*-1,2,3-triazole, 43

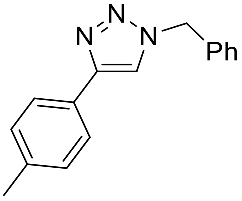

General Method D. *p*-Tolylacetylene (23 mg, 0.19 mmol) used to yield a white solid (17 mg, 35%) as well as 1-Benzyl-4-(*p*-tolyl)-5-(*p*-tolylethynyl)-1*H*-1,2,3-triazole, **44**; m.p. 146-147 °C (lit.,[216] 142-143 °C); R$_f$ 0.20 (25% EtOAc/pet. ether.); IR ν_{max} (neat) 3095, 3019, 2921, 1495, 1455, 1221, 1047, 792, 720, 513 cm^{-1}; ^{1}H NMR (300 MHz, CDCl$_3$) δ_H 7.66-7.70 (2H, m, Ar*H*), 7.62 (1H, s, N-C*H*), 7.29-7.42 (5H, m, Ar*H*), 7.19-7.22 (2H, d, *J* = 8.0, Ar*H*), 5.56 (2H, s, N-CH_2), 2.36 (3H, s, CH_3) ppm; ^{13}C NMR (100 MHz, CDCl$_3$) δ_C 148.4 (*C*), 138.1 (*C*), 134.8 (*C*), 129.6 (*C*H), 129.2 (*C*H), 128.8 (*C*H), 128.1 (*C*H), 127.8 (*C*), 125.7 (*C*H), 119.2 (*C*H), 54.3 (*C*H$_2$), 21.3 (*C*H$_3$) ppm; LRMS (ESI) m/z 250 ([M+H]$^+$, 100%). Data in agreement with literature.[216,217]

1-Benzyl-4-(*p*-tolyl)-5-(*p*-tolylethynyl)-1*H*-1,2,3-triazole, 44

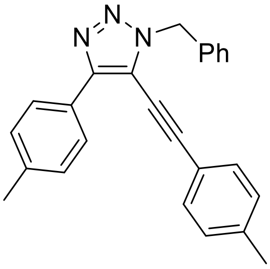

General Method D. *p*-Tolylacetylene (23 mg, 0.19 mmol) used to yield a colourless oil (16 mg, 45%) as well as 1-Benzyl-4-(*p*-tolyl)-1*H*-1,2,3-triazole, **43**; R$_f$ 0.37 (25% EtOAc/pet. ether.); IR ν_{max} (neat) 3030, 2921, 2856, 2219, 1665, 1496, 1001, 817, 730, 697, 527 cm^{-1}; ^{1}H NMR (300 MHz, CDCl$_3$) δ_H 8.05-8.09 (2H, m, Ar*H*), 7.31-7.42 (7H, m, Ar*H*), 7.20-7.27 (4H, m, Ar*H*), 5.66 (2H, s, N-CH_2), 2.41 (3H, s, CH_3), 2.39 (3H, s, CH_3) ppm; ^{13}C NMR (100 MHz, CDCl$_3$) δ_C 148.2 (*C*), 140.1 (*C*), 138.5 (*C*), 134.9 (*C*), 131.5 (*C*H), 129.5 (*C*H), 129.4 (*C*H), 128.9 (*C*H), 128.5 (*C*H), 128.2 (*C*H), 127.6 (*C*), 126.2 (*C*H), 118.6 (*C*), 117.2 (*C*), 102.6 (*C*), 75.2 (*C*), 53.0 (*C*H$_2$), 21.7 (*C*H$_3$), 21.4 (*C*H$_3$) ppm; LRMS (ESI) m/z 364 ([M+H]$^+$, 100%). Data in agreement with literature.[219]

General Method E. Electrochemical Glaser-Hay reaction[40]

Bu_4NPF_6 (0.39 g, 1.0 mmol, 0.5 eq) was dissolved in DCM (20 mL) to make up a 0.05 M solution. A divided (H) cell was charged with this solution (10 mL each side). A copper sheet (6.00 cm^2 area) and a silver wire (0.95 cm^2 area) were then placed into one chamber, and a platinum wire (0.95 cm^2 area) was placed into the other chamber. These electrodes were connected up to a potentiostat (Cu = WE, Ag = QRE, Pt = CE) and the potential was set to run at +0.50 V for 30 min whilst stirring at RT and exposed to air. The terminal alkyne (2.0 mmol, 1.0 eq) was then added to the chamber containing the copper sheet, followed by DABCO (0.27 g, 2.4 mmol, 1.2 eq) which had been dried in a vacuum oven overnight. The potentiostat was set to run at +0.50 V for a further 2.5 h whilst stirring at RT, then the solution was left to stir for a further 13 h. The solution was then filtered into a separating funnel and extracted once with brine (30 mL), before the aqueous layer was diluted with DCM (30 mL). The organic layer was extracted and combined with the other organic layer, then washed once with H_2O (30 mL), dried over $MgSO_4$ and concentrated *in vacuo*. The resulting yellow solid was dissolved in 20% EtOAc/pet. ether. and passed through a plug of silica gel before being concentrated *in vacuo* to give the product.

1,4-Diphenylbuta-1,3-diyne, 18

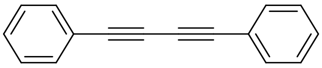

General Method E. Phenylacetylene used (0.22 mL, 2.0 mmol) to yield a white crystalline solid (0.17 g, 84%); m.p. 86-88 °C (lit.,[220] 86-88 °C); R_f 0.54 (20% EtOAc/pet. ether.); IR ν_{max} (neat) 3047, 2143, 1483, 1438, 914, 751, 682, 523 cm^{-1}; ^1H NMR (600 MHz, $CDCl_3$) δ_H 7.53-7.55 (4H, m, Ar*H*), 7.33-7.40 (6H, m, Ar*H*) ppm; ^{13}C NMR (150 MHz, $CDCl_3$) δ_C 132.6 (*C*H), 129.3 (*C*H), 128.6 (*C*H), 121.9 (*C*), 81.7 (*C*), 74.0 (*C*) ppm; LRMS (ESI) m/z 203 ($[M+H]^+$, 6%), 201 (48%), 199 (100%). Data in agreement with literature.[20,40,220]

1,4-Di-*p*-tolylbuta-1,3-diyne, 45

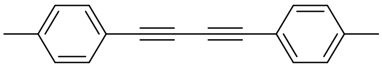

General Method E. *p*-Tolylacetylene (0.25 mL, 2.0 mmol) was used to yield the product as a white solid (0.11 g, 46%); m.p. 175-177 °C (lit.,[221] 177-178 °C); R_f 0.54 (20% EtOAc/pet. ether.); IR ν_{max} (neat) 3027, 2916, 2133, 1501, 805, 520 cm^{-1}; ^1H NMR (400 MHz, $CDCl_3$) δ_H 7.41-7.44 (4H, dt, *J* = 8.0, 1.6, Ar*H*), 7.15 (4H, d, *J* = 7.8, Ar*H*), 2.37 (6H, s, C*H*$_3$) ppm; ^{13}C NMR (75 MHz, $CDCl_3$) δ_C 139.6 (*C*), 132.5 (*C*H), 129.4 (*C*H), 118.9 (*C*), 81.7 (*C*), 73.6 (*C*), 21.8 (*C*H_3) ppm; LRMS (EI) m/z 230 (M^+, 100%), 229 (21%), 215 (16%); HRMS (EI) calc'd for $C_{18}H_{14}$ M^+ 230.1090, found 230.1727. Data in agreement with literature.[220]

1,4-Bis-(4-fluorophenyl)buta-1,3-diyne, 46

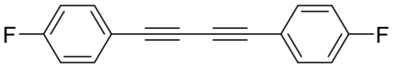

General Method E. 4-Fluorophenylacetylene (0.16 mL, 1.4 mmol) was used to yield the product as a cream-coloured solid (0.06 g, 36%); m.p. 189-190 ºC (lit.,[222] 189-190 °C); R_f 0.60 (20% EtOAc/pet. ether.); IR ν_{max} (neat) 3071, 2143, 1887, 1593, 1500, 1216, 1157, 826, 524 cm^{-1}; ^{1}H NMR (600 MHz, $CDCl_3$) δ_H 7.50-7.53 (4H, m, Ar*H*), 7.03-7.06 (4H, m, Ar*H*) ppm; ^{13}C NMR (150 MHz, $CDCl_3$) δ_C 163.1 (*C*) (doublet, $J_{F\text{-}C}$ = 251.8), 134.7 (*C*H) (doublet, $J_{F\text{-}C}$ = 8.3), 117.9 (*C*) (doublet, $J_{F\text{-}C}$ = 3.5), 116.0 (*C*H) (doublet, $J_{F\text{-}C}$ = 22.0), 80.5 (*C*), 73.6 (*C*) ppm; ^{19}F NMR (282 MHz, $CDCl_3$) δ_F -108.5 ppm; LRMS (CI) m/z 256 ($[M+NH_4]^+$, 5%), 238 (100%), 204 (63%), 203 (81%), 186 (55%), 185 (53%). Data in agreement with literature.[223]

Procedure used to produce (bromoethynyl)benzene, 47

(Bromoethynyl)benzene, 47

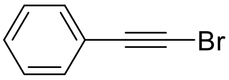

Bu_4NPF_6 (0.39 g, 1.0 mmol, 0.5 eq) was dissolved in DCM (20 mL) to make up a 0.05 M solution. A divided (H) cell was charged with this solution (10 mL each side). A copper sheet (6.00 cm^2 area) and a silver wire (0.95 cm^2 area) were then placed into one chamber, and a platinum wire (0.95 cm^2 area) was placed into the other chamber. These electrodes were connected up to a potentiostat (Cu = WE, Ag = QRE, Pt = CE) and the potential was set to run at +0.50 V for 30 min whilst stirring at RT and exposed to air. Phenylacetylene (0.22 mL, 2.0 mmol, 1.0 eq) was then added to the chamber containing the copper sheet, followed by DABCO (0.27 g, 2.4 mmol, 1.2 eq) and freshly recrystallised NBS (0.43 g, 2.4 mmol, 1.2 eq). The potentiostat was set to run at +0.50 V for a further 2.5 h whilst stirring at RT, then the solution was transferred to an RBF and left to stir under argon for a further 13 h. The solution was then filtered into a separating funnel and extracted once with saturated $Na_2S_2O_3$ solution (30 mL), before the aqueous layer was diluted with DCM (30 mL). The organic layer was extracted and combined with the other organic layer, then washed once with H_2O (30 mL), dried over $MgSO_4$ and concentrated *in vacuo*. The resulting yellow solid was dissolved in 20% EtOAc/pet. ether. and passed through a plug of silica gel before being concentrated *in vacuo* to give the product as a yellow oil (0.28 g, 78%); R_f 0.54 (20% EtOAc/pet. ether.); IR ν_{max} (neat) 3061, 2201, 1485, 1442, 906, 752, 731, 688 cm^{-1}; ^{1}H NMR (300 MHz, $CDCl_3$) δ_H 7.51-

7.53 (2H, m, Ar*H*), 7.35-7.41 (3H, m, Ar*H*) ppm; ^{13}C NMR (75 MHz, $CDCl_3$) δ_C 132.2 (*C*H), 128.9 (*C*H), 128.6 (*C*H), 122.9 (*C*), 80.3 (*C*), 50.1 (*C*) ppm; LRMS (EI) m/z 182 (M(^{81}Br)$^+$, 96%), 180 (M(^{79}Br)$^+$, 98%), 101 (100%), 75 (54%). Data in agreement with literature.[224]

Procedure used to produce 1-(phenylethynyl)pyrrolidin-2-one, 48

1-(Phenylethynyl)pyrrolidin-2-one, 48

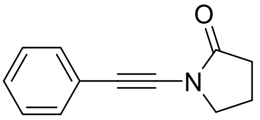

Bu_4NPF_6 (0.39 g, 1.0 mmol, 0.5 eq) was dissolved in MeCN (20 mL) to make up a 0.05 M solution. A divided (H) cell was charged with this solution (10 mL each side). A copper sheet (6.00 cm^2 area) and a silver wire (0.95 cm^2 area) were then placed into one chamber, and a platinum wire (0.95 cm^2 area) was placed into the other chamber. These electrodes were connected up to a potentiostat (Cu = WE, Ag = QRE, Pt = CE) and the potential was set to run at +0.50 V for 30 min whilst stirring at RT and exposed to air. Phenylacetylene (0.22 mL, 2.0 mmol, 1.0 eq) was then added to the chamber containing the copper sheet, followed by DABCO (0.27 g, 2.4 mmol, 1.2 eq) and 2-pyrrolidinone (0.61 mL, 8.0 mmol, 4.0 eq). Immediately a bright yellow precipitate formed. The potentiostat was set to run at +0.50 V for a further 2.5 h whilst stirring at RT, then the solution was left to stir for a further 40 h. The resulting dark blue solution was concentrated *in vacuo* and purified by column chromatography (20-50% EtOAc/pet. ether) to give the undesired diyne product, **18**, as a white solid (0.15 g, 76%) and the desired ynamide product as a yellow oil (0.04 g, 10%); R_f 0.30 (50% EtOAc/pet. ether.); IR ν_{max} (neat) 2980, 2895, 2245, 1716, 1684, 1393, 1217, 1195, 755, 691 cm^{-1}; ^{1}H NMR (600 MHz, $CDCl_3$) δ_H 7.43-7.45 (2H, m, Ar*H*), 7.27-7.31 (3H, m, Ar*H*), 3.78 (2H, t, *J* = 7.2, C*H*$_2$N), 2.48 (2H, t, *J* = 8.0, C*H*$_2$CO), 2.17 (2H, app. quin, *J* = 7.7, CH_2C*H*$_2$$CH_2$) ppm; ^{13}C NMR (150 MHz, $CDCl_3$) δ_C 176.0 (*C*), 131.6 (*C*), 128.4 (*C*H), 128.1 (*C*H), 122.7 (*C*H), 80.5 (*C*), 72.7 (*C*), 50.3 (*C*H$_2$), 29.8 (*C*H$_2$), 19.0 (*C*H$_2$) ppm; LRMS (CI) m/z 203 ([M+NH_4]$^+$, 100%), 186 ([M+H]$^+$, 93%). Data in agreement with literature.[95]

Preparation of DABCO-DCM-derived salt, 50[40]

1-(Chloromethyl)-1,4-diazabicyclo[2.2.2]octan-1-ium chloride, 50

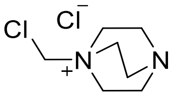

A flame-dried flask, that had been back-filled with argon, was charged with DCM (25 mL), followed by DABCO (0.29 g, 2.58 mmol, 1.0 eq). The solution was left to stir under argon at RT for 16 h. The solution was then carefully concentrated *in vacuo* and immediately stored under argon at -20 °C to prevent decomposition of the resulting hygroscopic white salt (0.47 g, 92%); m.p. 146-148 °C (dec.) (lit.,[225] 148 °C dec.); IR ν_{max} (neat) 3413, 3372, 3004, 2968, 1637, 1460, 1362, 1092, 1051, 840, 619, 534 cm^{-1}; ^{1}H NMR (300 MHz, $(CD_3)_2SO$) δ_H 5.39 (2H, s, C*H*$_2$Cl), 3.41 (6H, t, *J* = 7.5, (C*H*$_2$)$_3$N), 3.08 (6H, t, *J* = 7.5, (C*H*$_2$)$_3$N$^+$) ppm; ^{13}C NMR (176 MHz, $(CD_3)_2SO$) δ_C 67.5 (*C*H$_2$), 50.6 (*C*H$_2$), 44.4 (*C*H$_2$) ppm. Data supported by literature.[40,225,226]

Standard conditions for Chan-Lam reaction

1-Methoxy-2-phenoxybenzene, 54

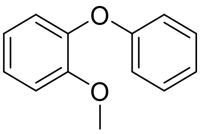

$Et_4N(O_3SC_6H_4CH_3)$ (0.30 g, 1.0 mmol, 2.0 eq) was weighed out into a reaction vessel and sealed as shown in **Figure 36, B** with Cu wire (WE), Ag wire (QRE) and Pt wire (CE) electrodes pushed through the Suba-Seal. DCM (10 mL) was then added to make up a 0.1 M solution (alternatively MeCN could be used). The phenylboronic acid (0.06 g, 0.5 mmol, 1.0 eq) was then added and the solution was stirred to dissolve all solids. 2-Methoxyphenol (0.06 mL, 0.5 mmol, 1.0 eq) was then added, followed by the reaction vessel being sealed and kept under an atmosphere of air (balloon). The potential was set to run at +0.50 V for 16 h whilst stirring at RT. The resulting solution was then concentrated *in vacuo* and purified by column chromatography (10-50% EtOAc/pet. ether) to give the product as a white solid (16 mg, 15%); m.p. 76-77 °C (lit.,[227] 76 °C); R_f 0.71 (50% EtOAc/pet. ether.); IR ν_{max} (neat) 3064, 3023, 2980, 2953, 2923, 2846, 1597, 1581, 1489, 1221, 748 cm^{-1}; ^{1}H NMR (400 MHz, $CDCl_3$) δ_H 7.27-7.32 (2H, m, Ar*H*), 7.11-7.15 (1H, m, Ar*H*), 6.90-7.06 (6H, m, Ar*H*), 3.84 (3H, s, C*H*$_3$) ppm; ^{13}C NMR (100 MHz, $CDCl_3$) δ_C 158.0 (*C*), 151.6 (*C*), 145.2 (*C*), 129.6 (*C*H), 124.8

(*C*H), 122.5 (*C*H), 121.2 (*C*H), 121.1 (*C*H), 117.3 (*C*H), 112.9 (*C*H), 56.1 (*C*H_3) ppm; LRMS (ESI) m/z 201 ($[M+H]^+$, 56%), 149 (29%), 130 (11%). Data in agreement with literature.[227]

Copper recovery/multistage synthesis procedures

Initial conditions[20]

A graphite rod working electrode (4.12 cm^2 area) was first coated with a layer Cu by placing it into an undivided cell containing a 0.5 M $CuSO_{4(aq.)}$ solution. A Ag wire quasi reference electrode (0.79 cm^2 area) and a Pt wire counter electrode (1.26 cm^2 area) were added and all electrodes were then connected up to a potentiostat. The potential was set to -0.50 V for 600 s (11.99 C passed, 62.14 µmol, 3.95 mg Cu deposited). These electrodes were then carefully cleaned with water and acetone and placed into a divided (H) cell (Cu-coated graphite and Ag wire in one chamber, Pt wire in the other chamber) which had been charged with a 0.05 M solution of Bu_4NPF_6 (0.39 g, 1.0 mmol, 1.0 eq) dissolved in reagent grade DCM (20 mL) (10 mL each side of H cell). TMEDA (0.15 mL, 1.0 mmol, 1.0 eq) was then added to the chamber containing the Cu and the electrodes were connected up to a potentiostat (Cu-coated graphite = WE, Ag = QRE, Pt = CE). The potential was set to run at +0.50 V for 30 min whilst stirring at RT and exposed to air. At the end of this time all Cu had been released from the graphite electrode and the solution was pale blue. Phenylacetylene (0.11 mL, 1.0 mmol, 1.0 eq) was then added to the chamber containing the graphite and silver electrodes, followed by DABCO (0.14 g, 1.2 mmol, 1.2 eq). The potentiostat was set to run at +0.50 V for a further 2.5 h whilst stirring at RT, then the solution was left to stir for a further 13 h whilst exposed to air. H_2O (20 mL) was then added to the solution and stirred vigorously for 1 h, causing the Cu species to migrate into the aqueous phase. The two layers were separated into the aqueous layer and the organic layer:

The dark blue aqueous layer was treated with 2 M $HCl_{(aq.)}$ (3 drops) and then placed into one chamber of an H cell, along with NaCl (0.20 g, 3.42 mmol). The other chamber was filled with a slightly acidic (2 M $HCl_{(aq.)}$ (3 drops)) brine solution (NaCl (0.20 g, 3.42 mmol) dissolved in H_2O (20 mL)) and the H cell was charged with a graphite rod working electrode, a Ag wire quasi reference electrode and a Pt wire counter electrode (graphite and silver in copper solution chamber, platinum in brine-only chamber). The electrodes were then connected up to a potentiostat and the potential was set to run at -1.00 V for 30 min, causing Cu metal to once more be plated onto the surface of the graphite rod. To accurately determine how much copper had been recovered, this Cu-coated graphite rod was used as a working electrode when placed into an H cell charged with a 0.1 M (Bu_4NPF_6 (0.77 g, 2.0 mmol) dissolved in reagent grade MeCN (20 mL)) solution (10 mL each side). A silver wire quasi reference electrode was added to the same chamber as the Cu-coated graphite electrode and a platinum wire counter electrode was placed into the other chamber, before all electrodes were connected up to a potentiostat and the potential was set to run at +0.50 V for 1800 s at RT and exposed to air (2.34 C passed, 24.26 µmol, 1.54 mg Cu recovered, 39%).

The organic layer was washed once with H_2O (30 mL), dried over $MgSO_4$ and concentrated *in vacuo*. The resulting yellow solid was dissolved in 20% EtOAc/pet. ether. and passed through a plug of silica gel before being concentrated *in vacuo* to give the product **18** as a white crystalline solid (71 mg, 70%).

Improved conditions

A graphite rod working electrode (4.12 cm^2 area) was first coated with a layer Cu by placing it into an undivided cell containing a 0.5 M $CuSO_{4(aq.)}$ solution. A Ag wire quasi reference electrode (0.79 cm^2 area) and a graphite rod counter electrode (4.12 cm^2 area) were added and all electrodes were then connected up to a potentiostat. The potential was set to -0.50 V to form a coating (15.46 C passed, 80.13 µmol, 5.09 mg Cu deposited). These electrodes were then carefully cleaned with water and acetone and placed into a divided (H) cell (Cu-coated graphite and Ag wire in one chamber, graphite in the other chamber) which had been charged with a 0.05 M solution of Bu_4NPF_6 (0.39 g, 1.0 mmol, 1.0 eq) dissolved in reagent grade DCM (20 mL) (10 mL each side of H cell). Phenylacetylene (0.11 mL, 1.0 mmol, 1.0 eq) was then added to the chamber containing the graphite and silver electrodes, followed by DABCO (0.14 g, 1.2 mmol, 1.2 eq). The electrodes were connected up to a potentiostat (Cu-coated graphite = WE, Ag = QRE, C = CE). The potential was set to run at +0.50 V for 2 h whilst stirring at RT and exposed to air. At the end of this time all Cu had mostly been released from the working electrode and the solution was orange. TMEDA (0.03 mL, 0.2 mmol, 0.2 eq) was then added to the chamber containing the Cu and the potentiostat was set to run at +0.50 V for a further 1 h whilst stirring at RT, then the solution was left to stir for a further 13 h whilst exposed to air. H_2O (20 mL) was then added to the solution and stirred vigorously for 30 min, causing the Cu species to migrate into the aqueous phase. The two layers were separated into the aqueous layer and the organic layer:

The organic layer was washed once with 2 M $HCl_{(aq.)}$ (10 mL) to collect the last of the copper (which was then added to the other aqueous layer), then dried over $MgSO_4$ and concentrated *in vacuo*. The resulting yellow solid was dissolved in 20% EtOAc/pet. ether. and passed through a plug of silica gel before being concentrated *in vacuo* to give the product **18** as a white crystalline solid (72 mg, 71%).

The combined aqueous layers were treated with NaOH to neutralise the HCl and then re-acidified with conc. H_2SO_4 (1-2 drops). This solution was then placed into one chamber of an H cell, along with NaCl (0.20 g, 3.42 mmol). The other chamber was filled with a slightly acidic (2 M $HCl_{(aq.)}$ (3 drops)) brine solution (NaCl (0.20 g, 3.42 mmol) dissolved in H_2O (30 mL)) and the H cell was charged with a graphite rod working electrode, a Ag wire quasi reference electrode and a graphite rod counter electrode (graphite and silver in copper solution chamber, other graphite in brine-only chamber). The electrodes were then connected up to a potentiostat and the potential was set to run at -0.5 V for 2 h, causing Cu metal to once more be plated onto the surface of the graphite rod. To accurately determine how much copper had been recovered, this Cu-coated graphite rod was used as a working electrode when placed into an H cell charged with a 0.05 M (Bu_4NPF_6 (0.39 g, 1.0 mmol) dissolved in reagent grade MeCN (20 mL)) solution (10 mL each side). A silver wire quasi reference electrode was added to the same chamber as the Cu-coated graphite electrode and a graphite rod counter electrode was placed into the other chamber, before all electrodes were connected up to a potentiostat and the potential was set to run at +0.50 V for around 1200 s at RT and exposed to air (4.915 C passed, 50.95 µmol, 3.24 mg Cu recovered, 64%). This solution was then transferred to an RBF and degassed thoroughly with argon, a large excess of DABCO (0.06 g, 0.5 mmol) and phenylacetylene (0.06 mL, 0.5 mmol) were added and the solution was degassed again before being left to stir at RT under argon for 2 h. Immediately a bright yellow precipitate formed. This precipitate was then collected by Büchner filtration and washed with reagent grade MeCN (20 mL), then H_2O (20 mL), then acetone (20 mL) before being dried in a vacuum oven for 30 min to yield the dry copper acetylide **17** (5.6 mg, 67%).

Chapter 11. References

1 M. Yan, Y. Kawamata and P. S. Baran, *Chem. Rev.*, 2017, **117**, 13230–13319.

2 J. Simonet and J.-F. Pilard, in *Organic Electrochemistry*, eds. H. Lund and O. Hammerich, Marcel Dekker, New York, 4th edn., 2001, ch. 29, pp. 1163–1225.

3 K. Surowiec and T. Fuchigami, *J. Org. Chem.*, 1992, **57**, 5781–5783.

4 K. Uneyama, H. Asai, Y. Dan-oh and H. Matta, *Electrochim. Acta*, 1997, **42**, 2005–2007.

5 S. Torii, K. Uneyama and M. Ono, *Tetrahedron Lett.*, 1980, **21**, 2741–2744.

6 T. Siu, C. J. Picard and A. K. Yudin, *J. Org. Chem.*, 2005, **70**, 932–937.

7 A. Guirado, A. Zapata, J. L. Gomez, L. Trabalon and J. Galvez, *Tetrahedron*, 1999, **55**, 9631–9640.

8 M. Hayyan, M. A. Hashim and I. M. AlNashef, *Chem. Rev.*, 2016, **116**, 3029–3085.

9 L.-J. Li, Y.-Y. Jiang, C. M. Lam, C.-C. Zeng, L.-M. Hu and R. D. Little, *J. Org. Chem.*, 2015, **80**, 11021–11030.

10 F. Kakiuchi, T. Kochi, H. Mutsutani, N. Kobayashi, S. Urano, M. Sato, S. Nishiyama and T. Tanabe, *J. Am. Chem. Soc.*, 2009, **131**, 11310–11311.

11 J.-I. Yoshida, R. Hayashi and A. Shimizu, in *Green Oxidation in Organic Synthesis*, eds. N. Jiao and S. S. Stahl, John Wiley & Sons Ltd, Hoboken, 2019, ch. 15, pp. 409–437.

12 T. Sunaga, M. Atobe, S. Inagi and T. Fuchigami, *Chem. Commun.*, 2009, 956–958.

13 T. Morofuji, A. Shimizu and J.-I. Yoshida, *J. Am. Chem. Soc.*, 2013, **135**, 5000–5003.

14 F. Lebreux, F. Buzzo and I. E. Marko, *Synlett*, 2008, **18**, 2815–2820.

15 L. D. Pachon, C. J. Elsevier and G. Rothenberg, *Adv. Synth. Catal.*, 2006, **348**, 1705–1710.

16 Z.-W. Hou, Z.-Y. Mao, H.-B. Zhao, Y. Y. Melcamu, X. Lu, J. Song and H.-C. Xu, *Angew. Chem. Int. Ed.*, 2016, **55**, 9168–9172.

17 H. Takakura and S. Yamamura, *Tetrahedron Lett.*, 1999, **40**, 299–302.

18 A. Wiebe, T. Gieshoff, S. Mohle, E. Rodrigo, M. Zirbes and S. R. Waldvogel, *Angew. Chem. Int. Ed.*, 2018, **57**, 5594–5619.

19 A. Volta, *Philos. Trans. R. Soc.*, 1800, **90**, 403–431.

20 P. W. Seavill, K. B. Holt and J. D. Wilden, *Green Chem.*, 2018, **20**, 5474–5478.

21 M. Faraday, *Philos. Trans. R. Soc.*, 1834, **124**, 77–122.

22 H. Kolbe, *J. Prakt. Chem.*, 1847, **41**, 138.

23 M. Paidar, V. Fateev and K. Bouzek, *Electrochim. Acta*, 2016, **209**, 737–756.

24 A. Hickling, *Trans. Faraday Soc.*, 1942, **38**, 27–33.

25 J. E. B. Randles, *Trans. Faraday Soc.*, 1948, **44**, 327–338.

26 M. Yan, Y. Kawamata and P. S. Baran, *Angew. Chem. Int. Ed.*, 2018, **57**, 4149–4155.

27 P. E. Iversen and H. Lund, *Tetrahedron Lett.*, 1969, **40**, 3523–3524.

28 T. Shono, H. Hamaguchi and Y. Matsumura, *J. Am. Chem. Soc.*, 1975, **97**, 4264–4268.

29 E. Steckhan, *Angew. Chem. Int. Ed. Engl.*, 1986, **25**, 683–701.

30 R. D. Little, D. P. Fox, L. Van Hijfte, R. Dannecker, G. Sowell, R. L. Wolin, L. Moens and M. M. Baizer, *J. Org. Chem.*, 1988, **53**, 2287–2294.

31 K. D. Moeller, *Tetrahedron*, 2000, **56**, 9527–9554.

32 J.-I. Yoshida, T. Murata and S. Isoe, *Tetrahedron Lett.*, 1986, **27**, 3373–3376.

33 B. R. Rosen, E. W. Werner, A. G. O’Brien and P. S. Baran, *J. Am. Chem. Soc.*, 2014, **136**, 5571–5574.

34 B. Elsler, D. Schollmeyer, K. M. Dyballa, R. Franke and S. R. Waldvogel, *Angew. Chem. Int. Ed.*, 2014, **53**, 5210–5213.

35 R. Francke and R. D. Little, *ChemElectroChem*, 2019, **6**, 4373–4382.

36 Y. Okada, Y. Yamaguchi, A. Ozaki and K. Chiba, *Chem. Sci.*, 2016, **7**, 6387–6393.

37 T. Broese, A. F. Roesel, A. Prudlik and R. Francke, *Org. Lett.*, 2018, **20**, 7483–7487.

38 G. Mabon, G. Le Guillanton and J. Simonet, *J. Electroanal. Chem.*, 1981, **130**, 387–390.

39 P. W. Seavill, K. B. Holt and J. D. Wilden, *RSC Adv.*, 2019, **9**, 29300–29304.

40 P. W. Seavill, K. B. Holt and J. D. Wilden, *Faraday Discuss.*, 2019, **220**, 269–281.

41 P. T. Kissinger, in *Laboratory Techniques in Electroanalytical Chemistry*, eds. P. T. Kissinger and W. R. Heineman, Marcel Dekker, New York, 2nd edn re., 1996, ch. 1, pp. 1–9.

42 G. Hilt, *ChemElectroChem*, 2020, **7**, 395–405.

43 S. Torii, K. Uneyama, T. Nakai and T. Yasuda, *Tetrahedron Lett.*, 1981, **22**, 2291–2294.

44 K. Mitsudo, T. Shiraga, J.-I. Mizukawa, S. Suga and H. Tanaka, *Chem. Commun.*, 2010, **46**, 9256–9258.

45 H. Maeda and H. Ohmori, *Acc. Chem. Rev.*, 1999, **32**, 72–80.

46 A. G. O’Brien, A. Maruyama, Y. Inokuma, M. Fujita, P. S. Baran and D. G. Blackmond, *Angew. Chem. Int. Ed.*, 2014, **53**, 11868–11871.

47 E. J. Horn, B. R. Rosen and P. S. Baran, *ACS Cent. Sci.*, 2016, **2**, 302–308.

48 A. Sagadevan, A. Ragupathi and K. C. Hwang, *Angew. Chem. Int. Ed.*, 2015, **54**, 13896–13901.

49 E. Barrado, R. A. S. Couto, M. B. Quinaz, J. L. F. C. Lima and Y. Castrillejo, *J. Electroanal. Chem.*, 2014, **720–721**, 139–146.

50 N. G. Tsierkezos and U. Ritter, *J. Appl. Electrochem.*, 2010, **40**, 409–417.

51 J. Hoffman and J. Voß, *Chem. Ber.*, 1992, **125**, 1415–1419.

52 E. Leonel, E. Dolhem, M. Devaud, J. P. Paugam and J. Y. Nedelec, *Electrochim. Acta*, 1997, **42**, 2125–2132.

53 B. C. Willet, W. M. Moore, A. Salajegheh and D. G. Peters, *J. Am. Chem. Soc.*, 1979, **101**, 1162–1167.

54 D. G. Peters, in *Organic Electrochemistry*, eds. H. Lund and O. Hammerich, Marcel Dekker, New York, 4th edn., 2001, ch. 8, pp. 341–377.

55 D. Lexa, J. M. Saveant and J. P. Soufflet, *J. Electroanal. Chem.*, 1979, **100**, 159–172.

56 M. Durandetti, J.-Y. Nedelec and J. Perichon, *J. Org. Chem.*, 1996, **61**, 1748–1755.

57 S. Torii, K. Uneyama, M. Ono, H. Tazawa and S. Matsunami, *Tetrahedron Lett.*, 1979, **48**, 4661–4662.

58 S. Torii, K. Uneyama, H. Tanaka, T. Yamanaka, T. Yasuda, M. Ono and Y. Kohmoto, *J. Org. Chem.*, 1981, **46**, 3312–3315.

59 S. Torii, N. Sayo and H. Tanaka, *Tetrahedron Lett.*, 1979, **46**, 4471–4474.

60 A. I. Popov and D. H. Geske, *J. Am. Chem. Soc.*, 1958, **80**, 5346–5349.

61 T. Iwasita and M. C. Giordano, *Electrochim. Acta*, 1969, **14**, 1045–1059.

62 M. Brand and S. Rozen, *J. Fluor. Chem.*, 1982, **20**, 419–424.

63 J.-E. Dubois and J. R. Chretien, *J. Am. Chem. Soc.*, 1978, **100**, 3506–3513.

64 J. R. Chretien, J.-D. Coudert and M.-F. Ruasse, *J. Org. Chem.*, 1993, **58**, 1917–1921.

65 L. Sun, K. Sahloul and M. Mellah, *ACS Catal.*, 2013, **3**, 2568–2573.

66 L. K. H. K. Alwis, M. R. Mucalo, B. Ingham and P. Kappen, *J. Electrochem. Soc.*, 2015, **162**, H434–H448.

67 J. S. Banait and P. K. Pahil, *Synth. React. Inorg. Met.-Org. Chem.*, 1986, **16**, 1217–1224.

68 J. S. Banait and P. K. Pahil, *Synth. React. Inorg. Met.-Org. Chem.*, 1988, **18**, 309–315.

69 S. L. Buchwald, in *Copper-Mediated Cross-Coupling Reactions*, eds. G. Evano and N. Blanchard, John Wiley & Sons, Inc., Hoboken, 1st edn., 2014, pp. xvii–xviii.

70 R. Trammell, K. Rajabimoghadam and I. Garcia-Bosch, *Chem. Rev.*, 2019, **119**, 2954–3031.

71 A. Hossain, A. Bhattacharyya and O. Reiser, *Science*, 2019, **364**, eaav9713.

72 G. Evano and N. Blanchard, in *Copper-Mediated Cross-Coupling Reactions*, eds. G. Evano and N. Blanchard, John Wiley & Sons, Inc., Hoboken, 1st edn., 2014, pp. xix–xxxv.

73 F. Ullmann and J. Bielecki, *Ber. Dtsch. Chem. Ges.*, 1901, **34**, 2174–2185.

74 F. Ullmann, *Ber. Dtsch. Chem. Ges.*, 1903, **36**, 2382–2384.

75 I. Goldberg, *Ber. Dtsch. Chem. Ges.*, 1906, **39**, 1691–1692.

76 K. C. Nicolaou and C. N. C. Boddy, *J. Am. Chem. Soc.*, 2002, **124**, 10451–10455.

77 A. Tlili and M. Taillefer, in *Copper-Mediated Cross-Coupling Reactions*, eds. G. Evano and N. Blanchard, John Wiley & Sons, Inc., Hoboken, 1st edn., 2014, ch. 2,

pp. 41–92.

78 Y. Feng, X. Zhao, J. Wang, F. Zheng and H. Wu, *Chin. J. Chem.*, 2009, **27**, 2423–2425.

79 C. Alayrac and A.-C. Gaumont, in *Copper-Mediated Cross-Coupling Reactions*, eds. G. Evano and N. Blanchard, John Wiley & Sons, Inc., Hoboken, 1st edn., 2014, ch. 3, pp. 93–112.

80 A. Osuka, N. Ohmasa, Y. Yoshida and H. Suzuki, *Synthesis (Stuttg).*, 1983, 69–71.

81 A. Casitas and X. Ribas, in *Copper-Mediated Cross-Coupling Reactions*, eds. G. Evano and N. Blanchard, John Wiley & Sons, Inc., Hoboken, 1st edn., 2014, ch. 6, pp. 239–252.

82 A. Klapars and S. L. Buchwald, *J. Am. Chem. Soc.*, 2002, **124**, 14844–14845.

83 T. Schareina and M. Beller, in *Copper-Mediated Cross-Coupling Reactions*, eds. G. Evano and N. Blanchard, John Wiley & Sons, Inc., Hoboken, 1st edn., 2014, ch. 9, pp. 313–334.

84 J. Zanon, A. Klapars and S. L. Buchwald, *J. Am. Chem. Soc.*, 2003, **125**, 2890–2891.

85 G. Evano, N. Blanchard and M. Toumi, *Chem. Rev.*, 2008, **108**, 3054–3131.

86 D. Yang and H. Fu, in *Copper-Mediated Cross-Coupling Reactions*, eds. G. Evano and N. Blanchard, John Wiley & Sons, Inc., Hoboken, 1st edn., 2014, ch. 15, pp. 533–588.

87 G. Evano, K. Jouvin, C. Theunissen, C. Guissart, A. Laouiti, C. Tresse, J. Heimburger, Y. Bouhoute, R. Veillard, M. Lecomte, A. Nitelet, S. Schweizer, N. Blanchard, C. Alayrac and A.-C. Gaumont, *Chem. Commun.*, 2014, **50**, 10008–10018.

88 K. Jouvin, J. Heimburger and G. Evano, *Chem. Sci.*, 2012, **3**, 756–760.

89 R. D. Stephens and C. E. Castro, *J. Org. Chem.*, 1963, **28**, 3313–3315.

90 D. H. Ryu and E. J. Corey, *J. Am. Chem. Soc.*, 2003, **125**, 6388–6390.

91 C. Shao, G. Cheng, D. Su, J. Xu, X. Wang and Y. Hu, *Adv. Synth. Catal.*, 2010, **352**, 1587–1592.

92 B. Wang, J. Zhang, X. Wang, N. Liu, W. Chen and Y. Hu, *J. Org. Chem.*, 2013, **78**, 10519–10523.

93 A. Sagadevan, V. P. Charpe, A. Ragupathi and K. C. Hwang, *J. Am. Chem. Soc.*, 2017, **139**, 2896–2899.

94 D. K. Das, V. K. K. Pampana and K. C. Hwang, *Chem. Sci.*, 2018, **9**, 7318–7326.

95 C. Theunissen, M. Lecomte, K. Jouvin, A. Laouiti, C. Guissart, J. Heimburger, E. Loire and G. Evano, *Synthesis (Stuttg).*, 2014, **46**, 1157–1166.

96 F. P. Byrne, S. Jin, G. Paggiola, T. H. M. Petchey, J. H. Clark, T. J. Farmer, A. J. Hunt, C. R. McElroy and J. Sherwood, *Sustain. Chem. Process.*, 2016, **4**.

97 E. C. Corker, U. V. Mentzel, J. Mielby, A. Riisager and R. Fehrmann, *Green Chem.*, 2013, **15**, 928–933.

98 B. Li and H. Ge, *Sci. Adv.*, 2019, **5**, eaaw2774.

99 G. M. Martins, B. Shirinfar, T. Hardwick, A. Murtaza and N. Ahmed, *Catal. Sci.*

Technol., 2019, **9**, 5868–5881.

100 Z.-W. Hou, Z.-Y. Mao, J. Song and H.-C. Xu, *ACS Catal.*, 2017, **7**, 5810–5813.

101 Z.-W. Hou, Z.-Y. Mao, Y. Y. Melcamu, X. Lu and H.-C. Xu, *Angew. Chem. Int. Ed.*, 2018, **57**, 1636–1639.

102 F. Xu, Y.-J. Li, C. Huang and H.-C. Xu, *ACS Catal.*, 2018, **8**, 3820–3824.

103 C. E. Dahm and D. G. Peters, *J. Electroanal. Chem.*, 1996, 91–96.

104 J. E. Dubois, A. Monvernay and P. C. Lacaze, *Electrochim. Acta*, 1970, **15**, 315–323.

105 S. D. Ross, M. Finkelstein and R. C. Petersen, *J. Am. Chem. Soc.*, 1960, **82**, 1582–1585.

106 J. S. Mayell and A. J. Bard, *J. Am. Chem. Soc.*, 1963, **85**, 421–425.

107 B. D. McCarthy, D. J. Martin, E. S. Rountree, A. C. Ullman and J. L. Dempsey, *Inorg. Chem.*, 2014, **53**, 8350–8361.

108 P. T. Anastas and J. C. Warner, in *Green Chemistry: Theory and Practice*, Oxford University Press, New York, 1998, ch. 4, pp. 29–55.

109 M. P. S. Mousavi, S. Kashefolgheta, A. Stein and P. Buhlmann, *J. Electrochem. Soc.*, 2016, **163**, H74–H80.

110 J. Gal, J. C. Folest, M. Troupel, M. O. Moingeon and J. Chaussard, *New J. Chem.*, 1995, **19**, 401–407.

111 H. Lund, in *Organic Electrochemistry*, eds. H. Lund and O. Hammerich, Marcel Dekker, New York, 4th edn., 2001, ch. 5, pp. 223–292.

112 P.-G. Echeverria, D. Delbrayelle, A. Letort, F. Nomertin, M. Perez and L. Petit, *Aldrichimica Acta*, 2018, **51**, 3–19.

113 M. Feroci, M. Orsini, L. Palombi, L. Rossi and A. Inesi, *Electrochim. Acta*, 2005, **50**, 2029–2036.

114 M. Feroci, M. Orsini, L. Rossi, G. Sotgiu and A. Inesi, *Electrochim. Acta*, 2006, **51**, 5540–5547.

115 J. Ashenhurst, The Hofmann Elimination, *Master Organic Chemistry*, [online] available at: https://www.masterorganicchemistry.com/2017/10/18/the-hofmann-elimination/, [accessed 7 November 2019].

116 C. D. Hein, X.-M. Liu and D. Wang, *Pharm. Res.*, 2008, **25**, 2216–2230.

117 R. Huisgen, G. Szeimies and L. Mobius, *Chem. Ber*, 1967, **100**, 2494–2507.

118 F. Amblard, J. H. Cho and R. F. Schinazi, *Chem. Rev.*, 2009, **109**, 4207–4220.

119 C. W. Tornoe, C. Christensen and M. Meldal, *J. Org. Chem.*, 2002, **67**, 3057–3064.

120 V. V. Rostovtsev, L. G. Green, V. V. Fokin and K. B. Sharpless, *Angew. Chem. Int. Ed.*, 2002, **41**, 2596–2599.

121 H. C. Kolb, M. G. Finn and K. B. Sharpless, *Angew. Chem. Int. Ed.*, 2001, **40**, 2004–2021.

122 H. C. Kolb and K. B. Sharpless, *Drug Discov. Today*, 2003, **8**, 1128–1137.

123 R. Berg and B. F. Straub, *Beilstein J. Org. Chem.*, 2013, **9**, 2715–2750.

124 B. T. Worrell, J. A. Malik and V. V. Fokin, *Science*, 2013, **340**, 457–460.

125 W. G. Lewis, F. G. Magallon, V. V. Fokin and M. G. Finn, *J. Am. Chem. Soc.*, 2004, **126**, 9152–9153.

126 L. Jin, D. R. Tolentino, M. Melaimi and G. Bertrand, *Sci. Adv.*, 2015, **1**, e1500304.

127 M. Meldal and C. W. Tornoe, *Chem. Rev.*, 2008, **108**, 2952–3015.

128 W. J. Tipping, M. Lee, V. G. Brunton, G. C. Lloyd-Jones and A. N. Hulme, *Faraday Discuss.*, 2019, **220**, 71–85.

129 S. Diez-Gonzalez, *Catal. Sci. Technol.*, 2011, **1**, 166–178.

130 D. Bonnet, B. Ilien, J.-L. Galzi, S. Riche, C. Antheaune and M. Hibert, *Bioconjugate Chem.*, 2006, **17**, 1618–1623.

131 M. B. Davies, *Polyhedron*, 1992, **11**, 285–321.

132 L. Li, X. Fan, Y. Zhang, A. Zhu and G. Zhang, *Tetrahedron*, 2013, **69**, 9939–9946.

133 Y. Angell and K. Burgess, *Angew. Chem. Int. Ed.*, 2007, **46**, 3649–3651.

134 V. Malnuit, M. Duca, A. Manout, K. Bougrin and R. Benhida, *Synlett*, 2009, **13**, 2123–2128.

135 D. N. Barsoum, C. J. Brassard, J. H. A. Deeb, N. Okashah, K. Sreenath, J. T. Simmons and L. Zhu, *Synthesis (Stuttg).*, 2013, **45**, 2372–2386.

136 L. Li, G. Zhang, A. Zhu and L. Zhang, *J. Org. Chem.*, 2008, **73**, 3630–3633.

137 B. H. M. Kuijpers, G. C. T. Dijkmans, S. Groothuys, P. J. L. M. Quaedflieg, R. H. Blaauw, F. L. van Delft and F. P. J. T. Rutjes, *Synlett*, 2005, **20**, 3059–3062.

138 J. E. Hein, J. C. Tripp, L. B. Krasnova, K. B. Sharpless and V. V. Fokin, *Angew. Chem. Int. Ed.*, 2009, **48**, 8018–8021.

139 Y. Zhou, T. Lecourt and L. Micouin, *Angew. Chem. Int. Ed.*, 2010, **49**, 2607–2610.

140 C. J. Pickens, S. N. Johnson, M. M. Pressnall, M. A. Leon and C. J. Berkland, *Bioconjugate Chem.*, 2018, **29**, 686–701.

141 B. T. Worrell, J. E. Hein and V. V. Fokin, *Angew. Chem. Int. Ed.*, 2012, **51**, 11791–11794.

142 R. De Simone, M. G. Chini, I. Bruno, R. Riccio, D. Mueller, O. Werz and G. Bifulco, *J. Med. Chem.*, 2011, **54**, 1565–1575.

143 J. C. Morris, J. Chiche, C. Grellier, M. Lopez, L. F. Bornaghi, A. Maresca, C. T. Supuran, J. Pouyssegur and S.-A. Poulsen, *J. Med. Chem.*, 2011, **54**, 6905–6918.

144 J. M. Schulman, A. A. Friedman, J. Panteleev and M. Lautens, *Chem. Commun.*, 2012, **48**, 55–57.

145 J.-L. Chaubard, C. Krishnamurthy, W. Yi, D. F. Smith and L. C. Hsieh-Wilson, *J. Am. Chem. Soc.*, 2012, **134**, 4489–4492.

146 Y. Kamamoto, Y. Nitta, K. Kubo, T. Mizuta and S. Kume, *Chem. Commun.*, 2016, **52**, 10486–10489.

147 N. K. Devaraj, P. H. Dinolfo, C. E. D. Chidsey and J. P. Collman, *J. Am. Chem. Soc.*, 2006, **128**, 1794–1795.

148 I. Choi, Y.-K. Kim, D.-H. Min, S. Lee and W.-S. Yeo, *J. Am. Chem. Soc.*, 2011, **133**, 16718–16721.

149 I. U. Khand, G. R. Knox, P. L. Pauson, W. E. Watts and M. I. Foreman, *J. Chem. Soc. Perkin Trans. 1*, 1973, 977–981.

150 P. Magnus and L. M. Principe, *Tetrahedron Lett.*, 1985, **26**, 4851–4854.

151 C. Glaser, *Ber. Dtsch. Chem. Ges.*, 1869, **2**, 422–424.

152 R. Hua, in *Copper-Mediated Cross-Coupling Reactions*, eds. G. Evano and N. Blanchard, John Wiley & Sons, Inc., Hoboken, 1st edn., 2014, ch. 12, pp. 455–483.

153 A. S. Hay, *J. Org. Chem.*, 1962, **27**, 3320–3321.

154 X. Meng, C. Li, B. Han, T. Wang and B. Chen, *Tetrahedron*, 2010, **66**, 4029–4031.

155 J. D. Crowley, S. M. Goldup, N. D. Gowans, D. A. Leigh, V. E. Ronaldson and A. M. Z. Slawin, *J. Am. Chem. Soc.*, 2010, **132**, 6243–6248.

156 T. Hayes, *A Novel Enediyne Synthesis from Alkynyl Sulfonamides via Non-Classical Carbenoids*, PhD Thesis: University College London, 2018.

157 S.-N. Chen, W.-Y. Wu and F.-Y. Tsai, *Green Chem.*, 2009, **11**, 269–274.

158 A. Lei, M. Srivastava and X. Zhang, *J. Org. Chem.*, 2002, **67**, 1969–1971.

159 V. Lavallo, G. D. Frey, B. Donnadieu, M. Soleilhavoup and G. Bertrand, *Angew. Chem. Int. Ed.*, 2008, **47**, 5224–5228.

160 L. Wang, X. Yu, X. Feng and M. Bao, *Org. Lett.*, 2012, **14**, 2418–2421.

161 S. Kramer, J. L. H. Madsen, M. Rottlander and T. Skrydstrup, *Org. Lett.*, 2010, **12**, 2758–2761.

162 A. L. K. S. Shun and R. R. Tykwinski, *Angew. Chem. Int. Ed.*, 2006, **45**, 1034–1057.

163 D. Lechner, M. Stavri, M. Oluwatuyi, R. Pereda-Miranda and S. Gibbons, *Phytochemistry*, 2004, **65**, 331–335.

164 H. Yun, T.-C. Chou, H. Dong, Y. Tian, Y.-M. Li and S. J. Danishefsky, *J. Org. Chem.*, 2005, **70**, 10375–10380.

165 A. Takahashi, T. Endo and S. Nozoe, *Chem. Pharm. Bull.*, 1992, **40**, 3181–3184.

166 T. Ohta, K. Uwai, R. Kikuchi, S. Nozoe, Y. Oshima, K. Sasaki and F. Yoshizaki, *Tetrahedron*, 1999, **55**, 12087–12098.

167 M. L. Lerch, M. K. Harper and D. J. Faulkner, *J. Nat. Prod.*, 2003, **66**, 667–670.

168 J. Liu, J. W. Y. Lam and B. Z. Tang, *Chem. Rev.*, 2009, **109**, 5799–5867.

169 J. A. Marsden and M. M. Haley, *J. Org. Chem.*, 2005, **70**, 10213–10226.

170 D. Xiang, X. Wang, C. Jia, T. Lee and X. Guo, *Chem. Rev.*, 2016, **116**, 4318–4440.

171 M. Nasr-Esfahani, I. Mohammadpoor-Baltork, A. R. Khosropour, M. Moghadam, V. Mirkhani, S. Tangestaninejad, V. Agabekov and H. A. Rudbari, *RSC Adv.*, 2014, **4**, 14291–14296.

172 F. Bohlmann, H. Schonowsky, E. Inhoffen and G. Grau, *Chem. Ber.*, 1964, **97**, 794–800.

173 L. D. Fedenok and M. S. Shvartsberg, *Tetrahedron Lett.*, 2011, **52**, 3776–3778.

174 M. H. Vilhelmsen, J. Jensen, C. G. Tortzen and M. B. Nielsen, *Eur. J. Org. Chem.*, 2013, 701–711.

175 L. Fomina, B. Vazquez, E. Tkatchouk and S. Fomine, *Tetrahedron*, 2002, **58**, 6741–6747.

176 G. Eglinton and A. R. Galbraith, *Chem. Ind.*, 1956, 737–738.

177 W. Chodkiewicz and P. Cadiot, *C. R. Hebd. Seances Acad. Sci.*, 1955, **241**, 1055–1057.

178 J. W. Dini and D. D. Snyder, in *Modern Electroplating*, eds. M. Schlesinger and M. Paunovic, John Wiley & Sons, Inc., 5th edn., 2010, ch. 2, pp. 33–78.

179 N. Jasinski, A. Lauer, P. J. M. Stals, S. Behrens, S. Essig, A. Walther, A. S. Goldmann and C. Barner-Kowollik, *ACS Macro Lett.*, 2015, **4**, 298–301.

180 S. F. Nelsen and P. J. Hintz, *J. Am. Chem. Soc.*, 1972, **94**, 7114–7117.

181 G. Cheng, H. Zhang and X. Cui, *RSC Adv.*, 2014, **4**, 1849–1852.

182 D. A. DiRocco, Y. Ji, E. C. Sherer, A. Klapars, M. Reibarkh, J. Dropinski, R. Mathew, P. Maligres, A. M. Hyde, J. Limanto, A. Brunskill, R. T. Ruck, L.-C. Campeau and I. W. Davies, *Science*, 2017, **356**, 426–430.

183 Y.-X. Xue, Y.-Y. Zhu, L.-M. Gao, X.-Y. He, N. Liu, W.-Y. Zhang, J. Yin, Y. Ding, H. Zhou and Z.-Q. Wu, *J. Am. Chem. Soc.*, 2014, **136**, 4706–4713.

184 L. Su, J. Dong, L. Long, M. Sun, R. Qiu, Y. Zhou and S.-F. Yin, *J. Am. Chem. Soc.*, 2016, **138**, 12348–12351.

185 Y. Aoki, M. Bauer, T. Braun, J. A. Cadge, G. E. Clarke, D. J. Durand, O. Eisenstein, S. Gallarati, M. Greaves, J. Harvey, A. Haynes, U. Hintermair, A. N. Hulme, Y. Ishii, M. Jakoobi, V. R. Jensen, P. Kennepohl, S. Kuwata, A. Lei, G. Lloyd-Jones, J. Love, J. Lynam, S. Macgregor, R. H. Morris, D. Nelson, A. Odom, R. Perutz, M. Reiher, J. Renny, J. Roithova, L. Schafer, S. Scott, P. W. Seavill, J. Slattery, T. Takao, J. Walton, J. D. Wilden, C.-Y. Wong and T. Young, *Faraday Discuss.*, 2019, **220**, 282–316.

186 B. Gustafsson, M. Hakansson and S. Jagner, *Inorganica Chim. Acta*, 2005, **358**, 1309–1312.

187 L.-Z. Chen, D.-D. Huang, Q.-J. Pan and L. Zhang, *J. Mol. Struct.*, 2014, **1078**, 68–73.

188 S. Mannam, S. K. Alamsetti and G. Sekar, *Adv. Synth. Catal.*, 2007, **349**, 2253–2258.

189 C. E. Housecroft and A. G. Sharpe, in *Inorganic Chemistry*, eds. C. E. Housecroft and A. G. Sharpe, Pearson Education Limited, Harlow, 4th edn., 2012, ch. 21, pp. 716–777.

190 B. M. Mykhalichko, O. N. Temkin and M. G. Mys’kiv, *Russ. Chem. Rev.*, 2000, **69**, 957–984.

191 H. Lang, K. Kohler and S. Blau, *Coord. Chem. Rev.*, 1995, **143**, 113–168.

192 J. X. Qiao and P. Y. S. Lam, *Synthesis (Stuttg).*, 2011, **6**, 829–856.

193 D. M. T. Chan, K. L. Monaco, R.-P. Wang and M. P. Winters, *Tetrahedron Lett.*, 1998, **39**, 2933–2936.

194 D. A. Evans, J. L. Katz and T. R. West, *Tetrahedron Lett.*, 1998, **39**, 2937–2940.

195 P. Y. S. Lam, C. G. Clark, S. Saubern, J. Adams, M. P. Winters, D. M. T. Chan and A. Combs, *Tetrahedron Lett.*, 1998, **39**, 2941–2944.

196 D. S. Raghuvanshi, A. K. Gupta and K. N. Singh, *Org. Lett.*, 2012, **14**, 4326–4329.

197 J. C. Vantourout, H. N. Miras, A. Isidro-Llobet, S. Sproules and A. J. B. Watson, *J. Am. Chem. Soc.*, 2017, **139**, 4769–4779.

198 A. E. King, T. C. Brunold and S. S. Stahl, *J. Am. Chem. Soc.*, 2009, **131**, 5044–5045.

199 A. E. King, B. L. Ryland, T. C. Brunold and S. S. Stahl, *Organometallics*, 2012, **31**, 7948–7957.

200 T.-K. Tran, K.-F. Chiu, C.-Y. Lin and H.-J. Leu, *Int. J. Hydrog. Energy*, 2017, **42**, 27741–27748.

201 D. Li, P. W. Seavill and J. D. Wilden, *ChemElectroChem*, 2019, **6**, 5829–5835.

202 M. Rueping, R. M. Koenigs, K. Poscharny, D. C. Fabry, D. Leonori and C. Vila, *Chem. Eur. J.*, 2012, **18**, 5170–5174.

203 M. V. Twigg, *Platin. Met. Rev.*, 2012, **56**, 104–109.

204 J. Racowski and M. Sanford, in *Higher Oxidation State Organopalladium and Platinum Chemistry*, ed. A. J. Canty, Springer, Berlin, 2011, ch. 3, pp. 61–84.

205 Q.-L. Yang, C.-Z. Li, L.-W. Zhang, Y.-Y. Li, X. Tong, X.-Y. Wu and T.-S. Mei, *Organometallics*, 2019, **38**, 1208–1212.

206 D. C. Braddock, D. Roy, D. Lenoir, E. Moore, H. S. Rzepa, J. I.-C. Wu and P. von R. Schleyer, *Chem. Commun.*, 2012, **48**, 8943–8945.

207 M. Karki and J. Magolan, *J. Org. Chem.*, 2015, **80**, 3701–3707.

208 S. Bar, *Can. J. Chem.*, 2010, **88**, 605–612.

209 J. Comes-Barcelo, R. S. Foster, B. Fiser, E. Gomez-Bengoa and J. P. A. Harrity, *Chem. Eur. J.*, 2015, **21**, 3257–3263.

210 D. Gallego, A. Bruck, E. Irran, F. Meier, M. Kaupp, M. Driess and J. F. Hartwig, *J. Am. Chem. Soc.*, 2013, **135**, 15617–15626.

211 Y. Okamoto and S. K. Kundu, *J. Phys. Chem.*, 1973, **77**, 2677–2680.

212 M. W. Logue and G. L. Moore, *J. Org. Chem.*, 1975, **40**, 131–132.

213 H. O. House and M. J. Umen, *J. Org. Chem.*, 1973, **38**, 3893–3901.

214 J. M. Perez, R. Cano and D. J. Ramon, *RSC Adv.*, 2014, **4**, 23943–23951.

215 M. Yamada, D. Matsuura, M. Hasegawa, Y. Murata, N. Kakusawa, M. Matsumura and S. Yasuike, *J. Organomet. Chem.*, 2018, **871**, 79–85.

216 V. R. Velpuri and K. Muralidharan, *J. Organomet. Chem.*, 2019, **884**, 59–65.

217 Y. Masuyama, K. Yoshikawa, N. Suzuki, K. Hara and A. Fukuoka, *Tetrahedron Lett.*, 2011, **52**, 6916–6918.

218 H. Hiroki, K. Ogata and S.-I. Fukuzawa, *Synlett*, 2013, **24**, 843–846.

219 F. Alonso, Y. Moglie, G. Radivoy and M. Yus, *Synlett*, 2012, **23**, 2179–2182.

220 M. L. N. Rao, P. Dasgupta, B. S. Ramakrishna and V. N. Murty, *Tetrahedron Lett.*, 2014, **55**, 3529–3533.

221 S. Banerjee and N. T. Patil, *Chem. Commun.*, 2017, **53**, 7937–7940.

222 J. Xue, M.-T. Luo, Y.-L. Wen, M. Ye, L.-X. Liu and Z.-W. Chen, *Synthesis (Stuttg).*, 2014, **46**, 3191–3198.

223 J. R. Suarez, D. Collado-Sanz, D. J. Cardenas and J. L. Chiara, *J. Org. Chem.*, 2015, **80**, 1098–1106.

224 Y.-S. Feng, Z.-Q. Xu, L. Mao, F.-F. Zhang and H.-J. Xu, *Org. Lett.*, 2013, **15**, 1472–1475.

225 R. E. Banks, M. K. Besheesh, S. N. Mohialdin-Khaffaf and I. Sharif, *J. Fluor. Chem.*, 1997, **81**, 157–161.

226 J. C. Sarie, C. Thiehoff, R. J. Mudd, C. G. Daniliuc, G. Kehr and R. Gilmour, *J. Org. Chem.*, 2017, **82**, 11792–11798.

227 S. Jammi, S. Sakthivel, L. Rout, T. Mukherjee, S. Mandal, R. Mitra, P. Saha and T. Punniyamurthy, *J. Org. Chem.*, 2009, **74**, 1971–1976.

228 B. C. Boren, S. Narayan, L. K. Rasmussen, L. Zhang, H. Zhao, Z. Lin, G. Jia and V. V. Fokin, *J. Am. Chem. Soc.*, 2008, **130**, 8923–8930.

Appendix: Associated Publications

Green Chemistry

COMMUNICATION

View Article Online
View Journal | View Issue

Cite this: *Green Chem.*, 2018, **20**, 5474

Received 17th October 2018,
Accepted 13th November 2018

DOI: 10.1039/c8gc03262a

rsc.li/greenchem

Electrochemical preparation and applications of copper(I) acetylides: a demonstration of how electrochemistry can be used to facilitate sustainability in homogeneous catalysis†

Peter W. Seavill, Katherine B. Holt and Jonathan D. Wilden *

Copper(I) acetylides are important intermediates for many syntheses and have been prepared here electrochemically in an energy efficient manner. These were subsequently employed in simple organic C–C bond forming reactions. We also demonstrate that application of Faraday's laws allows the charge to be calculated so that only the required amount of metal is used. In addition, the application of copper-coated graphite electrodes allows the maximum atom efficiency for this process and even offers a recovery strategy to extract the metal following completion of the reaction.

Introduction

Recent years have seen a renaissance in organocopper chemistry as our understanding of the mechanistic pathways of the catalytic systems involved has grown. The elegant work of Evano[1a,b] and Hwang[1c–e] has done much to popularise the chemistry of copper(I) acetylides as versatile reagents for a wealth of synthetic operations. The observation that the reagents can behave 'classically' by reacting with electrophiles to form C–C bonds as well as displaying 'Umpolung' behaviour to react with nucleophiles makes them attractive building blocks for the construction of complex molecular frameworks.[1a] Furthermore, they can be utilised cooperatively in a variety of noble metal-catalysed processes (most notably the palladium-catalysed Sonogashira reaction) to produce an even greater diversity of products.[2] As shelf-stable yellow solids these species can be prepared in bulk and stored almost indefinitely. We here demonstrate that the preparation and utility of these species can be improved in terms of energy efficiency and waste management by the application of electrochemistry and by considering the practical issues that classical methods present.

There are two main methods for the preparation of copper acetylides: (i) reaction of two equivalents of CuI with the parent acetylene in an alcohol solvent with aqueous ammonia or (ii) reaction of CuI with the parent alkyne in the presence of K_2CO_3 (Scheme 1). In terms of their 'green' credentials[3] the solvent system of method (i) is reasonably good, however the method requires two equivalents of cuprous halide to combat the known propensity of Cu^I salts to undergo disproportionation in aqueous solvent mixtures and thus produces both excess copper and iodide waste that must be disposed of appropriately.

Method (ii) requires the use of dimethylformamide:[4] a dipolar aprotic solvent which has been identified as a major problem for industrial scale synthesis.[5] Where dipolar aprotic solvents are required, acetonitrile is much preferred, particularly with new 'green' processes being identified for its preparation from benign feedstocks.[6] Drawbacks aside, both methods allow easy access to the copper acetylide as they can simply be collected *via* filtration.

Our group has long been interested in the chemistry of acetylenes[7–9] and has also developed a more recent interest in electro-organic synthesis and its application to 'green' and sustainable synthesis.[10,11] As such, we wanted to explore the reactivity of acetylenes under electrochemical conditions and were attracted to the prospect of preparing the functionalised acetylides using a sacrificial copper anode where Cu^I ions could be released selectively by control of the applied potential. A schematic representation of our approach is outlined in Scheme 2.

Some years ago, Mitsudo demonstrated that silver(I) acetylides could be prepared *via* a constant current protocol and successfully demonstrated their applicability in palladium catalysed coupling reactions.[12] We were keen to know if the cheaper and potentially more versatile copper reagents would

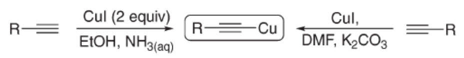

Scheme 1 Classical methods of copper acetylide synthesis.

Department of Chemistry, University College London, 20 Gordon Street, London, WC1H 0AJ, UK. E-mail: j.wilden@ucl.ac.uk

† Electronic supplementary information (ESI) available: Full experimental detail, control experiments and characterisation data. See DOI: 10.1039/c8gc03262a

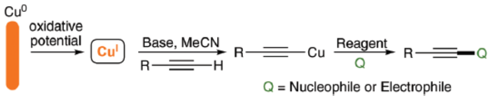

Scheme 2 Proposed electrochemical generation of Cu acetylides.

behave similarly, as such an approach would offer various advantages to the preparation of these species and their subsequent reactions. Firstly, with electrochemical techniques it is (theoretically at least) possible to calculate and measure the charge required to generate the desired amount of Cu^I. Therefore, only the energy required for the formation of the copper acetylide is consumed. Secondly, bulk copper metal is cheap and readily available in pure forms due to its almost ubiquitous applications in electrical wiring systems. Finally, the process is atom efficient as there is no iodide present in the starting copper species; for comparison only around 33% of a sample of CuI is copper, not to mention the issues surrounding the disposal of iodide waste.

Results and discussion

We therefore began by examining whether this approach would deliver copper acetylides in yields competitive with those known in the literature. We elected to use a divided cell ('H-cell') with a copper working-electrode, a Pt wire counter-electrode and a silver wire quasi reference-electrode. Initial cyclic voltammetry (CV) experiments (Fig. 1) indicated that copper ions (we hypothesised Cu^I ions in the form of stabilised Cu(MeCN)$_4$PF$_6$ complexes) could be released at oxidising potentials in acetonitrile so we were confident that including the alkyne and a suitable base in the mixture would yield the corresponding copper(I) acetylides.

Pleasingly, application of an oxidative potential (constant potential, +0.5 V *vs.* Ag wire) to the copper electrode in a solution of the terminal alkyne in a 0.1 M Bu$_4$NPF$_6$/MeCN background electrolyte and the organic base 1,4-diazabicyclo[2.2.2]octane (DABCO) yielded the copper acetylides in excellent yields, when O$_2$ was excluded, allowing isolation simply by filtration. Presumably, the current flow is maintained by the well-known electrochemically-mediated Hofmann elimination of the Bu$_4$NPF$_6$ electrolytic salt occurring in the cathodic chamber.[13] Control and optimisation reactions are summarised in the ESI (Table S1†) and include a demonstration that commercial Cu(MeCN)$_4$PF$_6$ complex also successfully liberates **1** supporting our hypothesis regarding the identity of the active copper species released from the electrode. The yields and reaction times compare favourably with the classical methods outlined in the literature (Scheme 3).[1a,b] As a synthetic preparation of these species, this method is extremely efficient, however we wanted to develop a more sustainable and general method of generating and using these species without having to use a bulk metal plate as the electrode, which would be less viable if a similar approach were to be extended to other, potentially precious, metals. In addition, we wanted to develop a method where the amount of metal and charge passed could be more accurately measured to determine the efficiency of the process.

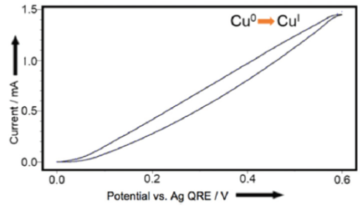

Fig. 1 CV plot, using Cu^0-coated glassy carbon working-electrode, Pt wire counter-electrode, Ag wire quasi reference-electrode in 0.1 M Bu$_4$NPF$_6$/MeCN. Axes redrawn for clarity.

We were attracted by the prospect of electroplating a thin layer of metal onto the surface of an inert electrode. In doing so we hoped to be able to: (i) measure the exact amount of metal deposited and used in reactions and (ii) use the metal catalytically to perform carbon–carbon bond forming reactions. We envisaged that the surface of a graphite rod could be coated with metal by electroplating from an aqueous solution of the metal salt. The metal ions could then be released by the application of an oxidative potential as required. This approach is outlined in Fig. 2.

As expected, a simple graphite rod was easily plated with a fine layer of copper metal by application of a reducing potential (−0.5 V *vs.* Ag wire) to a 0.5 M solution of CuSO$_{4(aq.)}$. In an example where this potential was applied for 600 s, a total charge of 11.99 C was passed, and copper was clearly visible on the graphite surface (Fig. 3). By applying Faraday's laws (eqn (1)), this corresponds to a maximum of 6.21 × 10^{-5} moles of copper metal deposited (or 3.95 mg). To place this in context, the mass of cuprous iodide containing the same amount of copper would be 11.83 mg.

We found that this method proved effective at confirming our suspicion that Cu^I was released into solution rather than

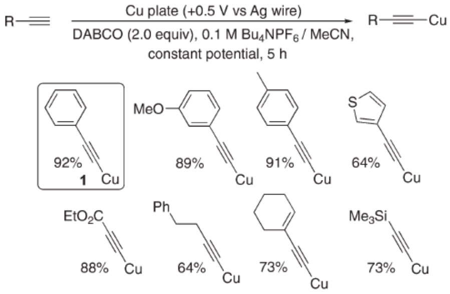

Scheme 3 Electrochemical preparation of copper acetylides.

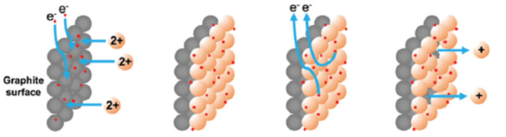

Fig. 2 Selective coating and release of copper ions for organic catalysis.

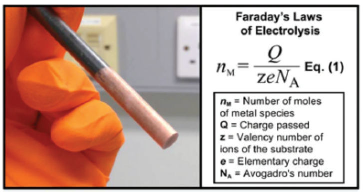

Fig. 3 Graphite rod electrode coated with metallic copper and Faraday's Laws of Electrolysis represented in eqn (1).

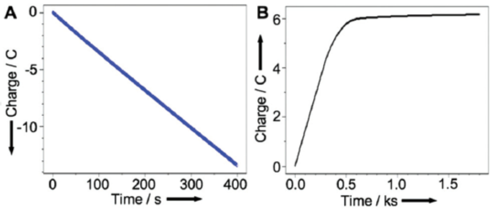

Fig. 4 Charge passed as a function of time when: (A) coating the graphite rod from a $CuSO_{4(aq.)}$ solution and (B) for the release of Cu^I. Axes redrawn for clarity.

Cu^{II}. A simple experiment was devised in which a graphite rod was coated with Cu^0 from $CuSO_{4(aq.)}$ (13.40 C passed during coating, equating to a maximum of 6.94×10^{-5} moles of Cu^0) and used to produce copper acetylide **1** from phenylacetylene (0.5 mmol) with the conditions seen in Scheme 3 (Pt wire counter electrode), with the exception that all of the Cu present on the graphite rod was released within 30 min and in this experiment the alkyne was the reagent that was in excess rather than the Cu. Our maximum theoretical yield for this experiment was 11.43 mg of **1** if all available oxidised Cu reacted. We isolated 8.10 mg (4.92×10^{-5} moles) of **1**, which pertains to an excellent 71% efficiency of Cu atom integration into the product. Furthermore, the charge passed during the release of Cu ions was measured to be 6.17 C. Substituting this figure back into eqn (1) along with the number of moles of isolated **1** gives a good approximation of the oxidation state of the copper released into solution, z, as being 1.30 (1) or in other words, Cu^I rather than Cu^{II}. When employing a graphite counter electrode of the same dimensions as the working electrode, a value of z of 1.12 was obtained and an efficiency of 77% was recorded (more details are available in the ESI†). This indicates our method is robust even when asymmetric electrodes are employed.

Graphs showing charge passed as a function of time for the Cu coating (A) and release (B) in this experiment are shown in Fig. 4. These plots demonstrate that the charge employed to coat the electrode *via* reduction of Cu^{II} (A) is approximately twice that required to release it (B), consistent with the release of Cu^I into the solution.

In addition to preparing copper acetylides for isolation we wished to examine the possibility of using the metal-coated rod to generate copper acetylides *in situ* which would then undergo a catalytic reaction requiring only a sub-stoichiometric amount of copper. It also occurred to us that if an oxidising potential of +0.5 V could release Cu^I into the solution, then it should also be possible to recover at least some of the copper at the end of the reaction by the application of a reducing potential as a method of 'cleaning up' the reaction mixture. In order to test this 'inverting potential' approach, we chose to examine the simple Glaser–Hay[14] oxidative dimerization of phenylacetylene to see if the copper-coated graphite could serve as a catalytic Cu^I source for this C–C bond forming reaction. We hoped that the graphite electrode would then serve as a vehicle for the removal of the copper from the solution at the end of the reaction by switching to a reducing potential (−1.0 V). For this reaction we found that dichloromethane proved to be a more effective solvent than MeCN in that the intermediary copper acetylide did not precipitate out of solution upon formation as it did in MeCN, providing better yields of the diyne product when exposed to aerial O_2. Work is ongoing to find more sustainable conditions for this reaction. We found that when 1 mmol phenylacetylene was used with a Cu-coated graphite electrode (14.14 C passed when coating, equating to a maximum of 7.33×10^{-5} moles of Cu^0) we had a maximum catalytic loading of 7.33 mol%. Pleasingly, when we applied an oxidative potential of +0.5 V to the coated graphite electrode in this coupling reaction, the corresponding diyne, **2**, was isolated in a good yield of 68%, in spite of a small portion of the copper acetylide intermediate precipitating out of solution (Scheme 4). We also found that while the yield of the reaction could be improved by adding a tetramethylethylenediamine (TMEDA) ligand, interestingly, the TMEDA proved capable of oxidising the electroplated Cu, without requiring an applied potential. The ligand-free conditions are shown in Scheme 4.

Emboldened by this result, we attempted the ambitious concept of recovering the copper after the reaction had been completed by switching the polarity of the potential of the working electrode. Such an approach would represent a major

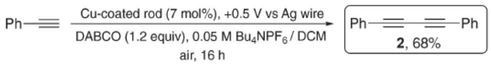

Scheme 4 Electrochemically-controlled ligand-free Glaser–Hay coupling.

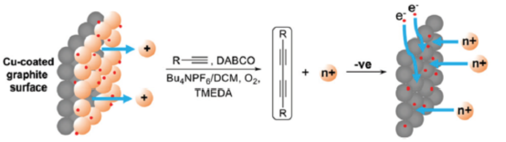

Fig. 5 Conceptualized approach to Glaser–Hay coupling from a Cu-coated electrode and recovery of the metal catalyst by switching to a reducing potential.

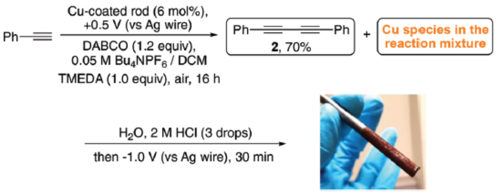

Scheme 5 Glaser–Hay coupling and recovery of copper post reaction.

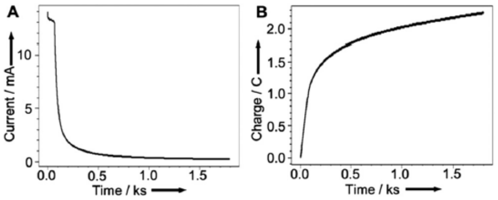

Fig. 7 (A) Current and (B) Charge passed as a function of time for Cu recovery efficiency determination. Axes redrawn for clarity.

advantage in terms of reusing the catalyst and cleaning up the reaction mixture which are major considerations in sustainable chemistry, especially when undertaking large scale reactions where the catalyst is often a precious metal. The approach is conceptualised in Fig. 5.

Our first attempts at recovering the metal post reaction proved troublesome, since the amine additives (*e.g.* TMEDA, amine bases, *etc.*) commonly added in such reactions to enhance their efficiency coordinate the copper and hold it in the organic solvent making it resistant to reduction at the electrode surface. As stated previously, TMEDA facilitates oxidation of the coated Cu making the use of an oxidative potential for release redundant, however, we opted to include the ligand in these reactions as it lead to a smoother reaction in which none of the copper acetylide intermediate precipitated out of solution (thereby maximising the amount of copper accessible for recovery) and allowed the use of a slightly lower catalyst loading (6 mol%) than that seen in ligand-free attempts (Scheme 4). Acidification allowed the copper to be liberated from the TMEDA, however also reduced the reductive potential window for recovering the copper. As such, we acidified the reaction medium with a minimum amount of 2 M HCl and water to drive all the available copper into the aqueous phase. The movement of copper ions from the organic to aqueous phase is clearly observable as displayed in Fig. 6.

Essentially, the TMEDA-coordinated copper is converted to $CuCl_2$ which is much more easily reduced and recovered. Pleasingly, application of a reducing potential to the solution then allowed us to re-coat the electrode with copper, again clearly visible as shown in Scheme 5.

We then undertook experiments to accurately determine the amount of copper redeposited on the electrode. Using the charge passed when recovering copper from the $HCl_{(aq.)}$ solution proved unreliable as a large component of the charge must be attributed to the electrolysis of the aqueous solution itself. Therefore, we transferred the electrode to a fresh solution of acetonitrile with 0.1 M Bu_4NPF_6 as background electrolyte to release the copper into solution as $Cu(MeCN)_4PF_6$ while monitoring the current and charge passed. As the metallic copper is exhausted, the current falls to zero and the charge approaches a maximum as can be seen from the plots of current (A) and charge (B) *vs.* time in Fig. 7.

At the point where the current approaches zero (*i.e.* when all of the copper metal had been stripped from the graphite surface) a charge of 2.34 C had passed. This corresponds to 24.26 μmol (1.54 mg of copper) and a corresponding recovery efficiency of 39%, as the graphite rod was initially coated with 3.95 mg of copper. In light of the difficulty of recovering metal catalysts from reaction media this is a remarkably good initial proof of concept. This preliminary study is highly promising, and we are confident that future refinements of the technology will only see the efficiency improve.

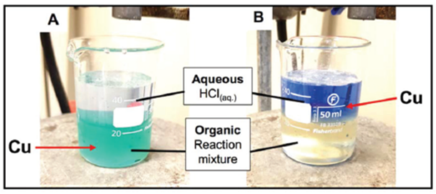

Fig. 6 Location of copper species in: (A) organic phase (just after HCl (aq.) added) and (B) aqueous phase (after 30 min vigorous stirring).

Conclusions

In conclusion, we have demonstrated how the combination of simple electrochemical techniques can be employed to improve the efficiency and sustainability of a copper-mediated organic reaction. The novel application of a metal-coated carbon electrode has also enabled us to perform simple calculations to consider the energy and atom efficiency of the process. We have also demonstrated that the technique could, with further refinements, offer opportunities to recover transition metals from reaction media. This offers an attractive and industrially-relevant approach for the future of transition metal-mediated organic synthesis, in particular where the metals involved are toxic and/or expensive.

Conflicts of interest

The authors declare no conflict of interest.

Acknowledgements

The authors gratefully acknowledge financial support from the Engineering and Physical Sciences Research Council (grant no. EP/M02220X/1), University College London and UCL Business. The contributions of the UCL Mass Spectrometry service (Dr K. Karu) and NMR Service (Dr A. Aliev) are also gratefully acknowledged.

Notes and references

1 (*a*) G. Evano, K. Jouvin, C. Theunissen, C. Guissart, C. Tresse, J. Heimburger, Y. Bouhoute, R. Veillard, M. Lecomte, A. Nitelet, S. Schweizer, N. Blanchard, C. Alayrac and A.-C. Gaumont, *Chem. Commun.*, 2014, **50**, 10008; (*b*) K. Jouvin, J. Heimburger and G. Evano, *Chem. Sci.*, 2012, **3**, 756; (*c*) A. Sagadevan, A. Ragupathi and K. C. Hwang, *Angew. Chem., Int. Ed.*, 2015, **54**, 13896; (*d*) A. Sagadevan, V. P. Charpe, A. Ragupathi and K. C. Hwang, *J. Am. Chem. Soc.*, 2017, **139**, 2896; (*e*) D. K. Das, V. K. K. Pampana and K. C. Hwang, *Chem. Sci.*, 2018, **9**, 7318–7326.

2 S. Díez-González, *Adv. Organomet. Chem.*, 2016, **66**, 93.

3 P. T. Anastas and J. C. Warner, *Green Chemistry: Theory and Practice*, Oxford University Press, New York, 1998, p. 30.

4 N. A. Bumagin, A. B. Ponomarev, A. N. Ryabtsev and I. P. Beletskaya, *Bull. Acad. Sci. USSR, Div. Chem. Sci.*, 1988, **37**, 507.

5 F. P. Byrne, S. Jin, G. Paggiola, T. H. M. Petchy, J. C. Clark, T. J. Farmer, A. J. Hunt, C. R. McElroy and J. Sherwood, *Sustainable Chem. Processes*, 2016, **4**, 7.

6 E. C. Corker, U. V. Mentzel, J. Mielby, A. Riisager and R. Fehrmann, *Green Chem.*, 2013, **15**, 928.

7 V. J. Gray, J. Cuthbertson and J. D. Wilden, *J. Org. Chem.*, 2014, **79**, 5869.

8 J. D. Wilden and V. J. Gray, *Org. Biomol. Chem.*, 2016, **14**, 9695.

9 R. M. Chowdhury and J. D. Wilden, *Org. Biomol. Chem.*, 2015, **13**, 5859.

10 E. J. Horn, B. R. Rosen and P. S. Baran, *ACS Cent. Sci.*, 2016, **2**, 302.

11 B. A. Frontana-Uribe, R. D. Little, J. G. Ibanez, A. Palma and R. Vasquez-Medrano, *Green Chem.*, 2010, **12**, 2099.

12 K. Mitsudo, T. Shiraga, J.-I. Mizukawa, S. Suga and H. Tanaka, *Chem. Commun.*, 2010, **46**, 9256.

13 C. E. Dahm and D. G. Peters, *J. Electroanal. Chem.*, 1996, **402**, 91.

14 (*a*) C. Glaser, *Ber. Dtsch. Chem. Ges.*, 1869, **2**, 422; (*b*) A. S. Hay, *J. Org. Chem.*, 1960, **25**, 1275; (*c*) A. S. Hay, *J. Org. Chem.*, 1962, **27**, 3320.

Faraday Discussions

Cite this: *Faraday Discuss.*, 2019, **220**, 269

PAPER

View Article Online
View Journal | View Issue

Investigations into the mechanism of copper-mediated Glaser–Hay couplings using electrochemical techniques†

Peter W. Seavill, Katherine B. Holt and Jonathan D. Wilden *

Received 10th April 2019, Accepted 31st May 2019

DOI: 10.1039/c9fd00031c

The mechanism of the copper mediated C–C bond forming reaction known as Glaser–Hay coupling (alkyne dimerization) has been investigated using electrochemical techniques. Applying an oxidative potential to a copper or copper-coated graphite electrode in the presence of the organic base DABCO results in the dimerization of phenylacetylene in good yield. Further mechanistic investigation has shown that this reaction medium results in the assembly of a dinuclear Cu(I) complex which, although previously reported, has never been shown to have catalytic properties for C–C bond formation. The complex is reminiscent of that proposed in the Bohlmann model for the Glaser–Hay reaction and as such lends weight to this proposed mechanism above the alternative proposed mononuclear catalytic cycle.

Introduction

The creation of carbon–carbon bonds and the subsequent construction of more complex organic frameworks is the cornerstone of organic chemistry. Over numerous years, metal (particularly transition-metal)-catalyzed processes have been among the most valuable and investigated methods of carbon–carbon bond formation.[1] One of the earliest and most useful examples that has been employed numerous times in synthesis is the oxidative homocoupling of alkynes, known as the Glaser reaction, originally reported in 1869.[2] This reaction and the related Hay coupling[3] have become essential tools in the synthetic chemist's toolbox for the preparation of diynes; compounds with numerous applications such as in the preparation of heterocycles and natural products,[4] π-conjugated polymers[5] and for use in the field of molecular electronics,[6] but with few other methods of preparation.

At the most fundamental level, Glaser–Hay coupling involves exposure of an acetylene to a copper(I) salt in the presence of a base in air. The reaction leads to a diyne with concomitant reduction of molecular oxygen (Scheme 1).

Department of Chemistry, University College London, 20 Gordon St, London, WC1H 0AJ, UK. E-mail: j.wilden@ucl.ac.uk

† Electronic supplementary information (ESI) available. See DOI: 10.1039/c9fd00031c

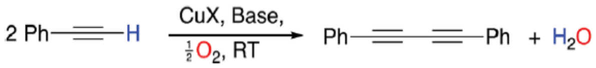

Scheme 1 General Glaser–Hay Reaction.

The advantages of such a system are numerous; the conditions are mild, yields are often excellent and the use of air as an oxidant is a welcome alternative to the hazardous and toxic reagents often employed as oxidants in chemical synthesis.

Despite the reaction, and its variations (*e.g.* the Eglinton coupling)[7] and the Cadiot–Chodkiewicz reaction,[8] having been known and used for many years, the underlying mechanistic pathway has been the subject of intense debate with two main proposals emerging as the most likely. The Bohlmann proposal[9] involves a dinuclear copper intermediate where the two copper atoms move cooperatively between the Cu(I) and Cu(II) oxidation states to activate the alkyne and oxygen (Scheme 2).

Alternatively, the mechanism recently championed by Nielsen and Vilhelmsen[10] involves a Cu(III) intermediate as outlined in Scheme 3.

Due to recent interest in the development of novel electrochemical techniques as applied to reactions of synthetic value, we were curious to investigate how electrochemistry could be used to facilitate the preparation of organocopper species and to explore whether any specific advantages could be identified. Originally, we envisaged that the Glaser–Hay coupled product could be obtained by the application of an oxidizing potential to a sacrificial copper electrode or a copper-coated graphite electrode where Cu(I) could be released selectively by the control of the applied potential. We were particularly attracted to the use of a metal-coated electrode as the desired amount of metal (copper in this case) could be deposited and more expensive metals could potentially be studied without the requirement for expensive bulk metal electrodes. The approach is outlined in Scheme 4.

We hoped that such an approach would offer various advantages to the preparation of these species in terms of the efficiency and sustainability, as well as offer a new electrochemical point of view on the investigation of the reaction mechanism.

Results and discussion

We have demonstrated previously that copper(I) ions could be released as stabilized $Cu(MeCN)_4PF_6$ complexes by the application of an oxidizing potential to a sacrificial copper electrode or copper-coated graphite electrode.[11] The principle of adopting a metal-coated (electroplated) graphite electrode is attractive for a number of reasons: (i) it is possible to measure the exact amount of metal

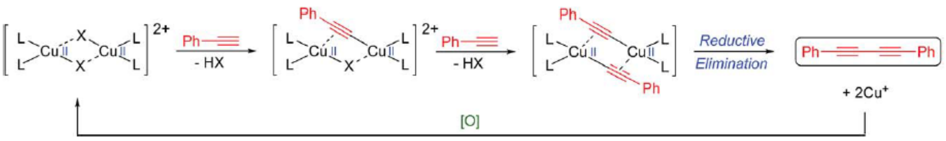

Scheme 2 Bohlmann-proposed mechanism.[9]

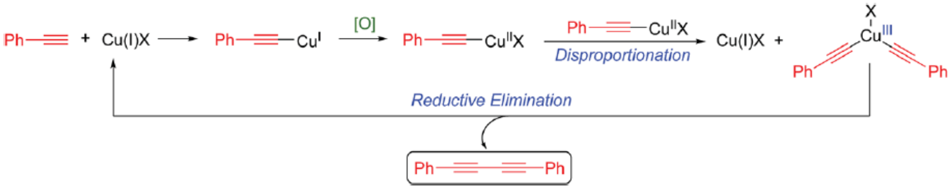

Scheme 3 Nielsen and Vilhelmsen-proposed mechanism.[10]

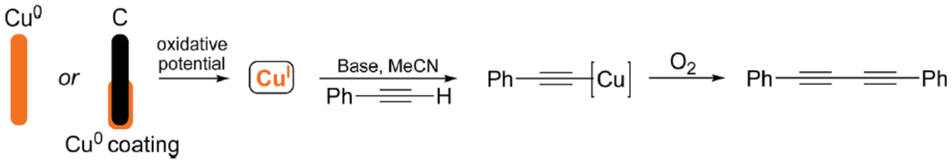

Scheme 4 Proposed electrochemical Glaser–Hay reaction.

deposited and used in reactions and (ii) the potential exists to employ the metal catalytically to perform carbon–carbon bond forming reactions. We envisaged that the surface of a graphite rod could be coated with metal by electroplating from an aqueous solution of the metal salt. The metal ions could then be released by the application of an oxidative potential as required. This approach is outlined in Fig. 1.

As expected, a simple graphite rod was easily plated with a fine layer of copper metal by the application of a reducing potential (−0.5 V *vs.* Ag wire Quasi-Reference Electrode (QRE)) to a 0.5 M aqueous solution of $CuSO_4$. In an example where this potential was applied for 600 s, a total charge of 11.99 C was passed and copper was clearly visible on the graphite surface (Fig. 2). By applying Faraday's laws (eqn (1)), this corresponds to a maximum of 6.21×10^{-5} moles of copper metal deposited (or 3.95 mg).[11]

Accordingly, cyclic voltammetry using a copper-coated glassy carbon working electrode (WE) (Pt wire counter electrode (CE), Ag wire QRE in 0.1 M Bu_4NPF_6/MeCN) shows a smooth increase in current as the potential is increased, which corresponds to the increasing rate of Cu(I) release, as shown in Fig. 3.

As such, we were confident that the inclusion of a base and a terminal alkyne in a divided cell would therefore lead to the dimerized product. Disappointingly, however, when we attempted the reaction outlined in Scheme 4 with a sacrificial Cu(0) electrode, we only obtained yields of 58% for the dimerized product, along with 30% for the copper acetylide intermediate (which precipitated out of

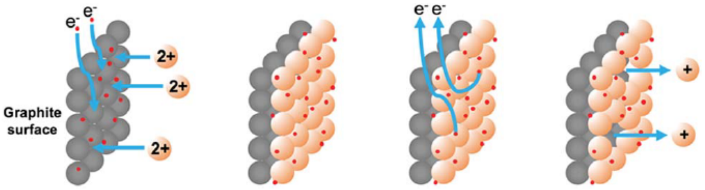

Fig. 1 Selective coating and release of copper ions for organic catalysis.[11]

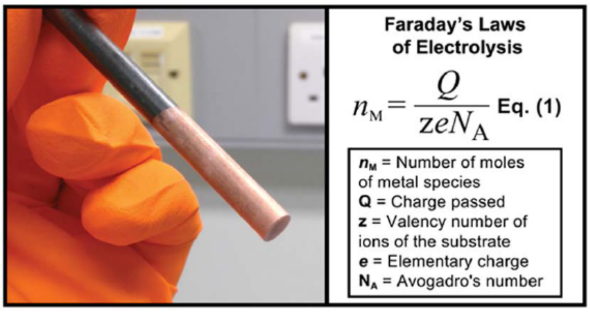

Fig. 2 Graphite rod electrode coated with metallic copper and Faraday's laws of electrolysis represented in eqn (1).[11]

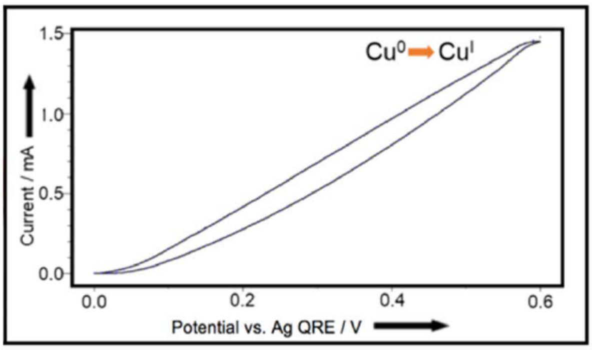

Fig. 3 CV plot, using Cu(0)-coated glassy carbon working-electrode, Pt wire counter-electrode, and Ag wire quasi reference-electrode in 0.1 M Bu_4NPF_6/MeCN.[11]

solution). Such species are known to be polymeric in nature[12] and their extreme insolubility in acetonitrile was clearly impairing their reactivity in this case. Accordingly, we chose to examine the reaction in dichloromethane, a solvent in which such species are known to have higher solubility and therefore reactivity.[12] Pleasingly, this relatively minor change led to the dimerized product in much improved yield (Scheme 5). The control experiments where the individual reactive components (copper, DABCO, O_2) were omitted from the reaction led to a dramatic retardation of the reaction.

With this encouraging result in hand, we then proceeded to examine the reaction more closely with a view to further optimizing the conditions. At this point we decided to record the CV plots of the various components in the reaction to see what electrochemical analysis could reveal about the reaction mechanism. These tests were designed to mimic the conditions used in a 'standard' reaction (see Scheme 5), which meant that 0.1 M Bu_4NPF_6/DCM was used as the electrolyte in all cases. First we wanted to observe the production of Cu(I)/(II) from a bulk

Scheme 5 Successful electrochemical Glaser–Hay reaction in DCM.

Cu(0) source, so we used a blank glassy carbon WE to record a background CV plot of the electrolyte solution up to +0.60 V (because our reactions are carried out at +0.50 V) (Fig. 4A).

We then coated the glassy carbon rod with a fine layer of Cu(0) by passing a reducing potential through a 0.5 M $CuSO_4/H_2O$ solution (reducing the Cu(II) to Cu(0) and forming a metallic coating). This was then placed into the Bu_4NPF_6/DCM electrolyte solution again and another CV plot was recorded (Fig. 4B). This shows the oxidation of Cu(0) from +0.50 V onwards and the associated reduction, with a peak at +0.30 V. This appears to visualise the liberation of Cu(I) from the electrode.

We then investigated whether the presence of phenylacetylene or DABCO somehow altered this generation of Cu ions, starting with phenylacetylene. Fig. 5A and B were recorded in a fresh Bu_4NPF_6/DCM solution with a blank glassy carbon WE after a small amount of phenylacetylene was added. A shows the CV plot produced at up to +1.50 V (high voltage) and B shows the graph produced at up to +0.60 V (low/standard reaction voltage). An indistinct, broad oxidation peak is observed at *ca.* +0.9 V, with a broad reduction peak at 0.45 V; additional oxidation currents can be seen above +1.2 V. In the more limited potential range (B) although currents are a little higher than in the background scans (Fig. 4A) there

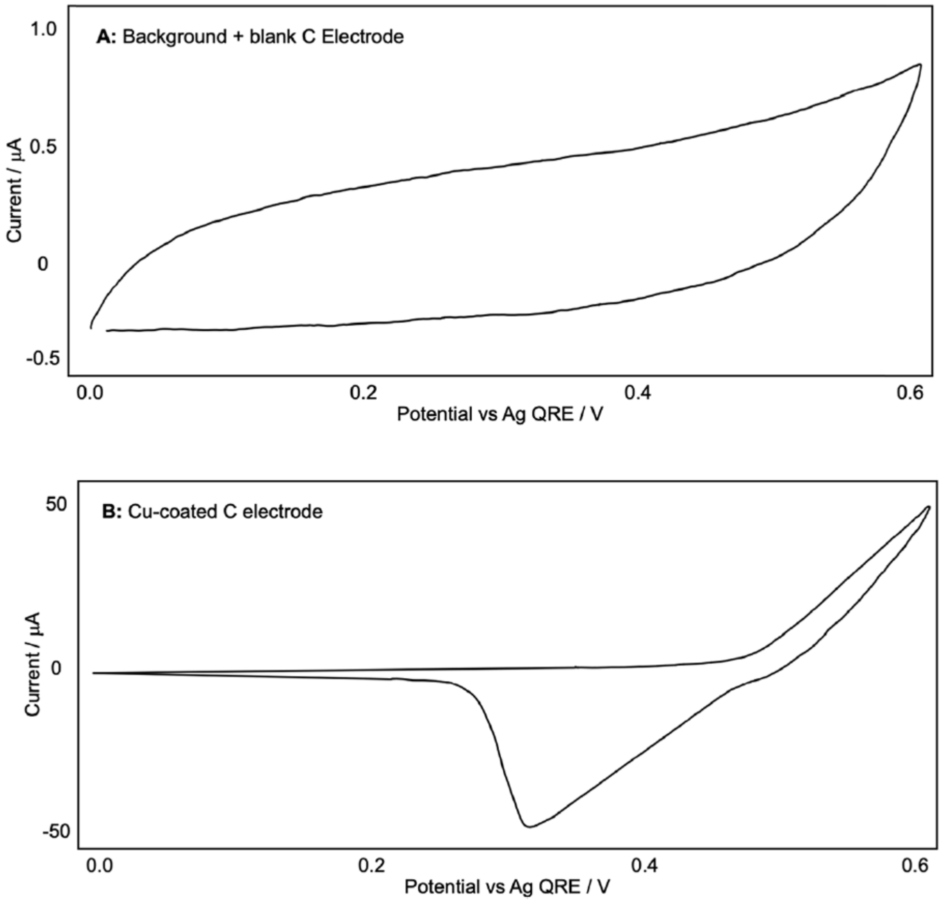

Fig. 4 (A and B): representative CV plots of a Cu-coated C electrode recorded in 0.1 M Bu_4NPF_6/DCM with a Ag QRE and a Pt CE.

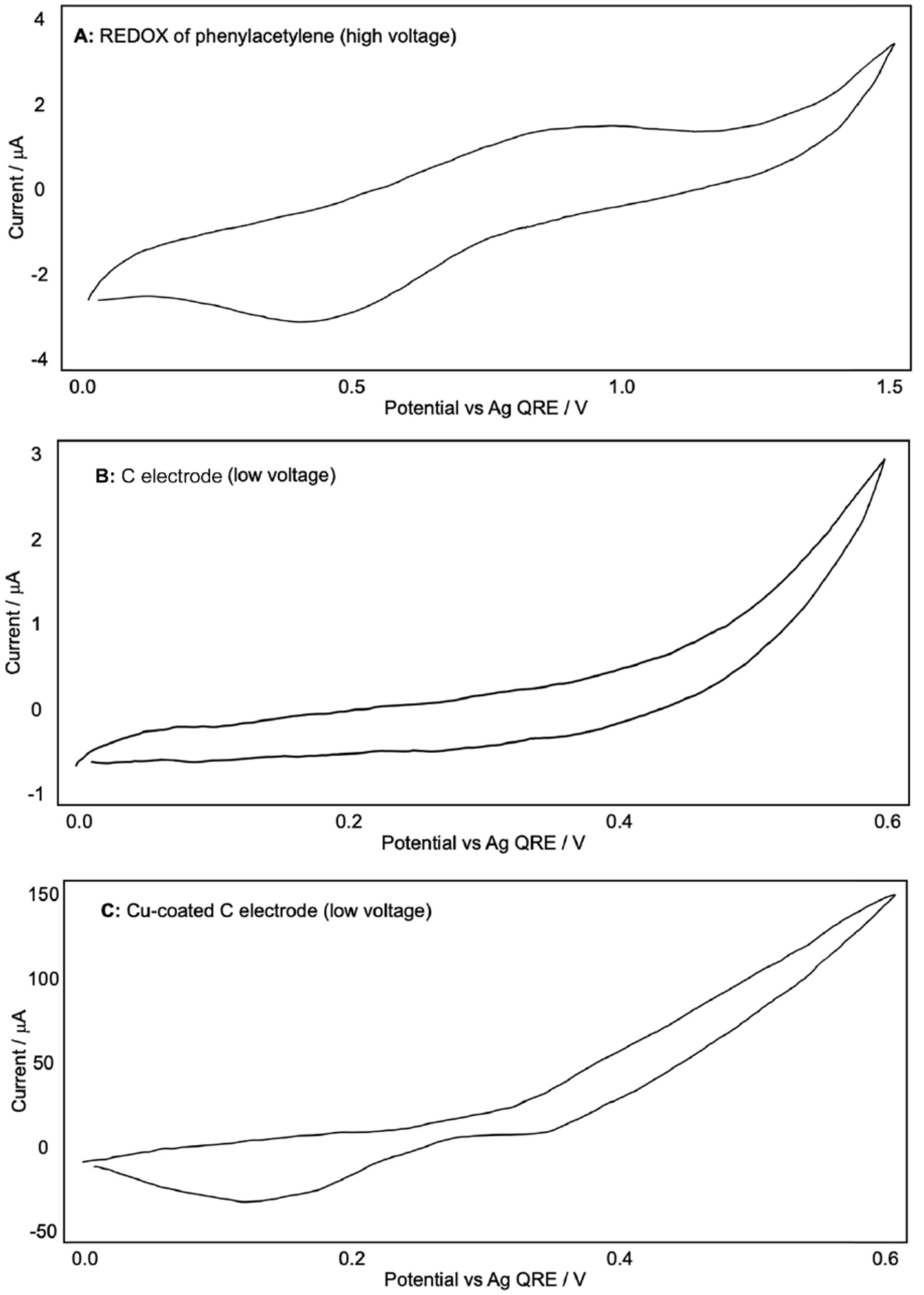

Fig. 5 (A–C): representative CV plots of phenylacetylene recorded in 0.1 M Bu_4NPF_6/DCM with a Ag QRE and a Pt CE.

is little evidence of phenylacetylene undergoing any significant oxidation up to +0.5 V, which is the potential used in our reactions. When a Cu-coated glassy carbon WE was then used to measure the CV, we obtained plot C, which shows the same potential of Cu oxidation onset and reduction peak as Fig. 4B. This suggested that phenylacetylene did not significantly affect the generation of Cu in the solution used here, or by extension in our diyne-forming reactions.

A similar process was carried out for DABCO, as shown in Fig. 6. Using a blank glassy carbon WE and a fresh electrolyte solution, we found that the oxidation of DABCO occurred at a surprisingly high potential of around +1.10 V, and not in the +0.50 V region that is employed in our reactions (A). Other sources[13] have noted the ease with which DABCO is oxidised due to the unusual stabilisation of the resulting radical cation.

When a Cu-coated WE was used, no redox currents were observed in the potential range 0 to 0.6 V in the presence of DABCO (Fig. 6B), in direct contrast to

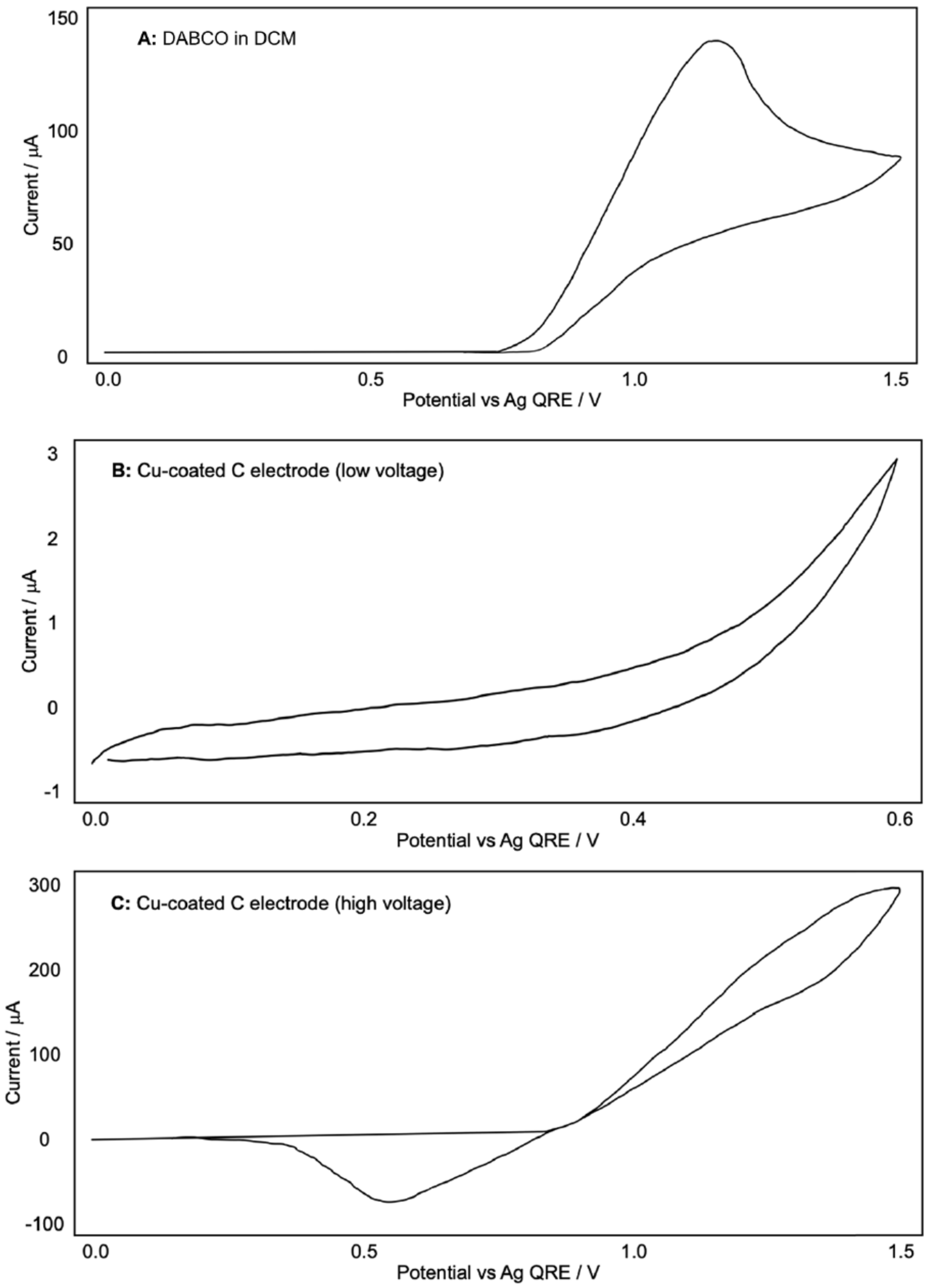

Fig. 6 (A–C) Representative CV plots of DABCO recorded in 0.1 M Bu_4NPF_6/DCM with a Ag QRE and a Pt CE.

the CV plots obtained for both the Cu-coated electrode on its own (Fig. 4B) and the Cu-coated electrode with phenylacetylene (Fig. 5C). Extending the potential range enabled us to see that the onset of Cu oxidation under these conditions was +0.9 V, compared to +0.5 V observed in the absence of DABCO. The results seem to suggest that DABCO alone inhibits the dissolution of Cu and hence the formation of the reactive Cu catalyst. This is surprising given the need for DABCO in the diyne forming reactions.

Having gained some insight into the electrochemical behavior of the reactive components we then turned our attention to the effect of the solvent on our reaction. Making the seemingly trivial change of solvent from dichloromethane to chloroform resulted in an almost complete loss of reactivity with virtually no diyne being produced. This was somewhat surprising given the similarities between these two chlorinated solvents, often used interchangeably. After consulting the literature and noting that occasionally catalytic species are generated by reaction with the solvent, particularly Zhou and Yin's observation[14] that chloroform reacts with TMEDA in the presence of Cu(I), we wondered if a similar situation was occurring in this case. Accordingly, we noted that Jagner[15] had discovered that DABCO, CuCl and dichloromethane readily react to generate the dinuclear Cu(I) complex shown in Scheme 6. This complex ('Jagner's complex') has not to our knowledge been tested for catalytic activity in the formation of C–C bonds.

It is also distinct from the mononuclear complexes of copper(I) and DABCO described by Sekar[16] where the DABCO, Cu(I) and Cl ions form linear polymeric structures with strong intermolecular hydrogen bonds (Fig. 7).

As such, it seems likely that the quaternization of DABCO by the chloromethyl moiety prevents the mononuclear polymer from forming by 'blocking' one of the coordinating and H-bonding sites on the DABCO molecule thereby favouring the discrete dinuclear complex. This also explains our observations in Fig. 6A where the oxidation of what we originally assumed to be DABCO occurred at a higher potential than would have been expected. Accordingly, when we performed cyclic voltammetry on the DABCO chloromethyl chloride salt prepared independently, a trace identical to that in Fig. 6A was observed. This indicates that the quaternized DABCO salt is formed very quickly (and quantitatively) in the reaction mixture and consequently is not subsequently oxidized at the potentials employed in the reaction. Interestingly, when we attempted to perform the reaction using mononuclear bases, such as NEt_3, pyridine, *etc.* (ESI, Table S1†), only very poor conversions to the diyne were observed. This suggests that a reduction in coordinating power induced by the quaternization (DABCO pK_a = 8.8, 3.0) may also be an important factor in the switch from linear mononuclear polymeric structures to discrete dinuclear copper complexes with catalytic activity.

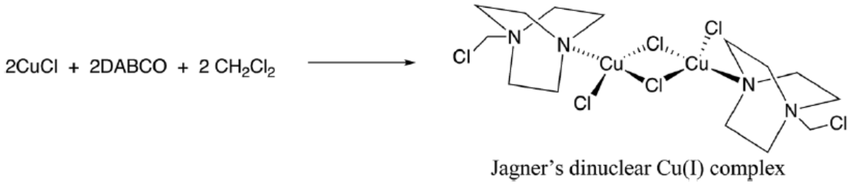

Scheme 6 Formation of Jagner's complex.[15]

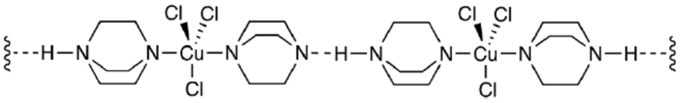

Fig. 7 Representation of the linear, polymeric DABCO–Cu complex described by Sekar.[16]

Although the source of Cu(I) in our reactions is from the electrochemical oxidation of Cu(0), we realized that the reaction of DABCO with DCM also liberates the chloride ions necessary for the formation of CuCl *in situ* and thus Jagner's complex, which we now suspected was the active catalytic species in our system. In order to confirm that this was the active species in our reaction, we used Jagner's original procedure to independently prepare a solution of the complex. Decanting the solution away from any unreacted CuCl and then adding phenylacetylene resulted in 36% of the diyne being isolated (details in the ESI†). This suggests that Jagner's complex is indeed the active species in our reaction. Although the yield was lower than that outlined in Scheme 5, we have attributed this to the fact that preparing the catalyst independently involves transfer losses and inefficiencies that are absent when the catalyst is prepared *in situ via* the electrode. Furthermore, we performed a number of experiments to establish the necessity of both DABCO and the chloride ions in the solution. The DABCO methylene chloride salt was prepared independently and added to a chloroform reaction medium (where we had previously observed a lack of reactivity) according to Scheme 7A–D.

Scheme 7A indicates that DABCO alone is not sufficient to promote the reaction. Full activity as observed in our original findings is only observed when all of the Cu(I), chloride ions and DABCO salt are present. Consistent with our hypothesis is that low concentrations of the added DABCO salt promoted the Glaser–Hay coupling (Scheme 7B) but less efficiently than when the concentration was increased (Scheme 7C). We also wanted to check that it was not the

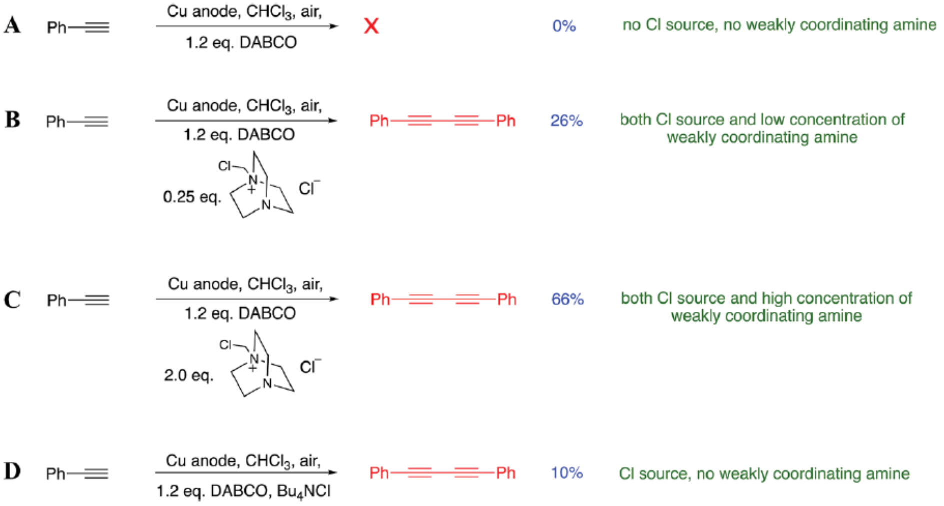

Scheme 7 (A–D): investigation into the importance of various reaction components. In (A–C) 0.05 M $Bu_4NPF_6/CHCl_3$ was used as electrolyte, whilst in D 0.05 M $Bu_4NCl/CHCl_3$ was used.

presence of chloride ions (rather than a monoquaternized DABCO derivative) that was promoting the reaction. Accordingly, the addition of tetrabutylammonium chloride (0.25 eq.) to the reaction mixture (Scheme 7D) in the presence of DABCO gave only a very poor conversion to the diyne, further suggesting that the DABCO salt is specifically responsible for the assembly of the active catalytic species.

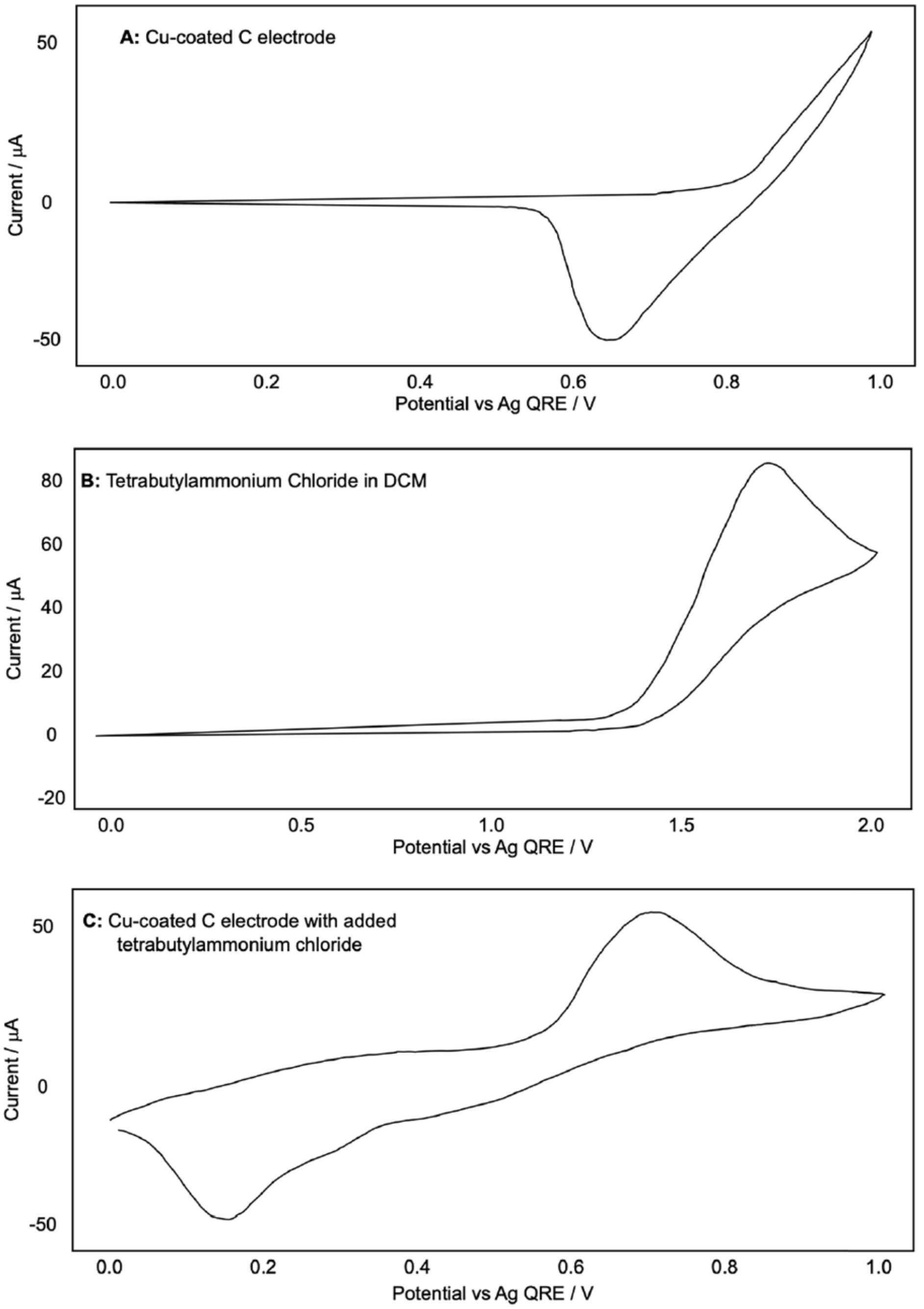

Fig. 8 (A–C): representative CV plots examining the effect of chloride on the release of copper from a Cu-coated glassy carbon electrode recorded in 0.1 M Bu_4NPF_6/DCM with a Ag QRE and a Pt CE.

We were also intrigued by the observation that the Glaser–Hay reaction could be efficiently promoted by potentials that, when compared to the original CV plots for the copper-coated electrode, were at the limits or even below the potential required for Cu(I) generation. We therefore chose to examine this phenomenon more closely. Having established the necessity for the DABCO chloromethyl salt in the reaction we also wondered if the presence of chloride ions were not only required for assembly of the catalytic complex but are also cooperatively assisting Cu(I) dissociation from the electrode surface and allowing the oxidation of Cu(0) to occur at lower potentials than the original CV plots (in the absence of chloride) would suggest. Fig. 8 shows the CV plots of (A) a Cu(0)-coated glassy carbon electrode in DCM (as described previously), (B) a blank WE with a solution of tetrabutylammonium chloride in DCM and (C) a mixture of the two.

The redox values appear shifted to slightly higher values than in Fig. 4B. We attributed this observation to our use of a quasi-reference electrode. To ensure that our measurements were comparable with previous experiments, we proceeded to reference our CV plots against the ferrocene redox couple. After performing this referencing experiment, we were confident in the comparability of

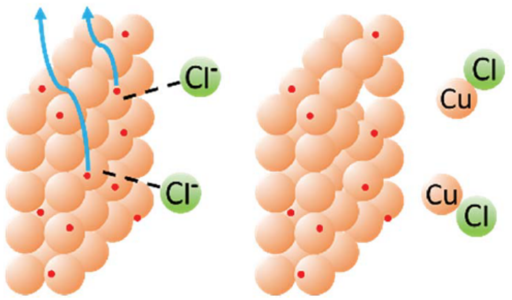

Fig. 9 Schematic representation of the cooperative effects between chloride and copper in the release of Cu(I) from the electrode surface.

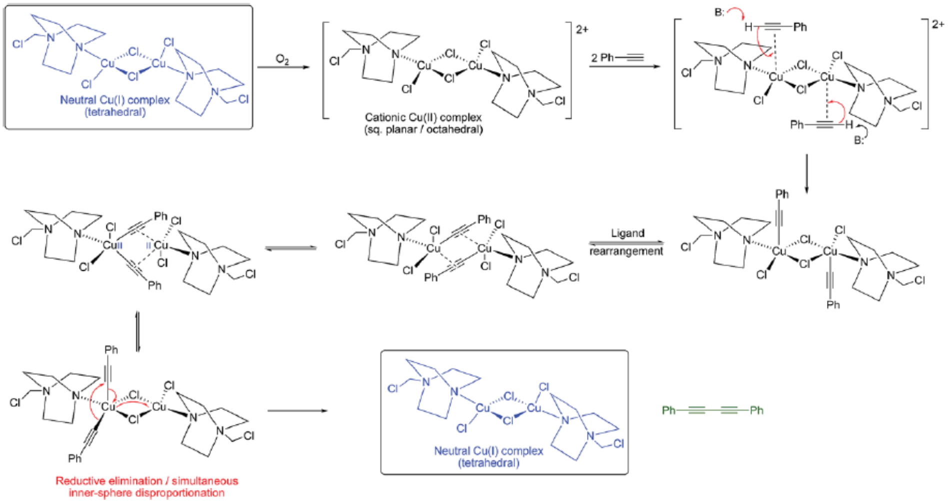

Scheme 8 Proposed mechanistic pathway for a Glaser–Hay reaction promoted by Jagner's complex.

the two plots with the caveat that the values were shifted up by around +0.30 V in Fig. 8A.

Fig. 8A shows clearly that the oxidation of copper from the electrode begins only at around +0.83 V and Fig. 8B shows that the oxidation of chloride to Cl_2, as expected, does not occur until much higher potentials have been reached (beginning at +1.40 V and reaching a peak at +1.75 V). When chloride ions are present with a Cu-coated electrode, however, a well-defined oxidation peak is observed at +0.72 V, attributed to the oxidation of Cu(0) to Cu(I). Furthermore, this oxidation actually begins at around +0.58 V. Since oxidation is beginning at potentials lower than either individual component of the mixture, this strongly suggests that the presence of chloride, in addition to allowing the formation of a dinuclear copper complex, also cooperatively assists the release of Cu(I) from the electrode (presumably as CuCl). This allows the reactions to be performed at lower potentials than expected based on the redox behavior of any individual component of the reaction mixture (Fig. 9).

Given that Jagner's complex is almost certainly the copper complex generated in our system, we realized that the identification of such a dinuclear copper complex lends support, at least in this case, to the Bohlmann proposal for the oxidative dimerization of alkynes. Such a dinuclear complex would not necessarily require a Cu(III) intermediate as in the Vilhelmsen model since redox-cooperative interactions between the two copper centres could occur (although we cannot rule out a Cu(III) intermediate at this stage). A possible pathway is outlined in Scheme 8.

Conclusion

In conclusion, we have described an electrochemical approach to Glaser–Hay coupling and have exploited the electrochemical technique to give valuable insight into the reaction mechanism. The identification of Jagner's complex as a catalytic entity for Glaser–Hay coupling is the first time that this complex has been implicated in this C–C bond forming process. The results suggest that, in this case, the Bohlmann proposal for the Glaser–Hay reaction is likely. We have demonstrated how the complex might be formed and shown that the cooperativity between the chloride and the copper electrode allows facile dissociation of Cu(I) from the electrode surface at lower potentials than would be expected based on the redox behavior of either of those species. More generally, these results demonstrate that electrochemistry can be a useful tool for the investigation of organic reaction mechanisms and in synthetic chemistry.

Conflicts of interest

There are no conflicts to declare.

Acknowledgements

The authors thank UCL for a studentship to PWS.

References

1 (*a*) R. Bates, *Organic Synthesis Using Transition Metals*, Wiley-Blackwell, Sheffield, UK, 2000; (*b*) J. F. Hartwig, *Organotransition Metal Chemistry: From Bonding to Catalysis*, University Science Books, US, Sausalito, 2009.

2 (*a*) C. Glaser, *Ber. Dtsch. Chem. Ges.*, 1869, **2**, 422; (*b*) C. Glaser, *Justus Liebigs Ann. Chem.*, 1870, **154**, 137.

3 (*a*) A. Hay, *J. Org. Chem.*, 1960, **25**, 1275–1276; (*b*) A. Hay, *J. Org. Chem.*, 1962, **27**, 3320–3321.

4 R. R. Tykwinski and A. L. K. Shi Shun, *Angew. Chem., Int. Ed.*, 2006, **45**, 1034–1057.

5 J. Liu, J. W. Y. Lam and B. Z. Tang, *Chem. Rev.*, 2009, **109**, 5799–5867.

6 J. A. Marsden and M. M. Haley, *J. Org. Chem.*, 2005, **70**, 10213–10216.

7 G. Eglinton and A. R. Galbraith, *J. Chem. Soc.*, 1959, 889–896.

8 W. Chodkiewicz, P. Cadiot and C. R. Hebd, *Seances Acad. Sci.*, 1955, **241**, 1055–1057.

9 F. Bohlmann, H. Schönowsky, E. Inhoffen and G. Grau, *Chem. Ber.*, 1964, **97**, 794–800.

10 M. H. Vilhelmsen, J. Jensen, C. G. Tortzen and M. B. Nielsen, *Eur. J. Org. Chem.*, 2013, 701–711.

11 P. W. Seavill, K. B. Holt and J. D. Wilden, *Green Chem.*, 2018, **20**, 5474–5478.

12 K. Jouvin, J. Heimburger and G. Evano, *Chem. Sci.*, 2012, **3**, 756–760.

13 (*a*) S. F. Nelsen and P. J. Hintz, *J. Am. Chem. Soc.*, 1972, **94**, 7114–7117; (*b*) R. Hoffmann, A. Imamura and W. J. Hehre, *J. Am. Chem. Soc.*, 1968, **90**, 1499–1509.

14 L. Su, J. Dong, L. Liu, M. Sun, R. Qiu, Y. Zhou and S.-F. Yin, *J. Am. Chem. Soc.*, 2016, **138**, 12348–12351.

15 B. Gustafsson, M. Håkansson and S. Jagner, *Inorg. Chim. Acta*, 2005, **358**, 1309–1312.

16 S. Mannam, S. K. Alamsetti and G. Sekar, *Adv. Synth. Catal.*, 2007, **349**, 2253–2258.

RSC Advances

PAPER

View Article Online
View Journal | View Issue

Check for updates

Cite this: *RSC Adv.*, 2019, **9**, 29300

Electrochemical synthesis of copper(I) acetylides *via* simultaneous copper ion and catalytic base electrogeneration for use in click chemistry†

Peter W. Seavill,* Katherine B. Holt and Jonathan D. Wilden*

Received 27th August 2019
Accepted 11th September 2019

DOI: 10.1039/c9ra06782e

rsc.li/rsc-advances

We report an efficient and sustainable electrochemical synthesis of copper(I) acetylides using simultaneous copper oxidation and Hofmann elimination of quaternary ammonium salts. The electrochemically-generated base was also regenerated electrochemically, making it catalytic. A 'Click test' (CuAAC reaction) was performed to assess product purity and an electrochemically-promoted, one-pot CuAAC reaction was performed, which serves as a promising initial demonstration of this approach in a pharmaceutically-relevant reaction.

Introduction

Copper has great potential utility in electro-organic chemistry due to its readily accessible redox states. The application of mild electrical potentials to exert control over oxidation states of copper catalysts introduced to solutions has previously been exploited to select for either Glaser–Hay (Cu^{II} pathway) or CuAAC (Cu^{I} pathway) reactions.[1] However, the use of elemental copper as an electrode material to produce Cu^{I} ions *in situ* for reactions has only recently been published by our group.[2] This work represented an electrochemical synthesis and isolation of copper(I) acetylides, which are valuable intermediates in many synthetic processes, such as Huisgen-type/Click,[3] Castro–Stephens,[4] halogenation,[3] Sonogashira,[5] ynamide-formation[6] and phosphorus-substitution reactions,[6] as well as for the formation of a variety of products *via* photochemical protocols.[7] Traditionally prepared by reacting a terminal alkyne with a copper halide in aqueous ammonia with EtOH or in DMF with K_2CO_3,[8] we found that in a divided cell, applying a positive potential whilst using a Cu^0 working-electrode, having DABCO present as a base and using Bu_4NPF_6/MeCN as an electrolyte solution, we could efficiently produce Cu^{I} ions that were used to form the desired copper(I) acetylides in excellent yields. An electrochemical synthesis has advantages over traditional methods in terms of sustainability, particularly in removing halide waste from the process entirely.[2] In this current work, we aimed to develop this process further. We hypothesised that we could carry out this reaction in an undivided cell by incorporating the reduction reaction of the tetrabutylammonium (TBA) electrolyte salt used in our previous conditions to produce Bu_3N *in situ* and obviate the requirement for any added base, such as DABCO, in our protocol. Furthermore, we hoped to demonstrate and make use of a catalytic base cycle by electrochemically reducing protonated base species, releasing only H_2 gas as a clean by-product,[9] improving the efficiency of this method further still (Fig. 1).

It is well-understood in the literature that the generation of various carbon, oxygen and nitrogen-centred anions and radical anions *via* cathodic reduction of appropriate probases can be used to promote reactions in a basic fashion.[10] Many of these reductions are carried out in the presence of quaternary ammonium salts (QAS), in particular, tetraethylammonium (TEA) and TBA salts, which are commonly used in electrochemical cells as background electrolytes. Importantly, in the absence of common probases, QAS can themselves be reduced by single-electron-transfer/Hofmann-type elimination processes to generate tertiary amine bases (Scheme 1).[11]

By comparison to most probases, QAS are more resistant to electrochemical reduction; the effects of chain length,

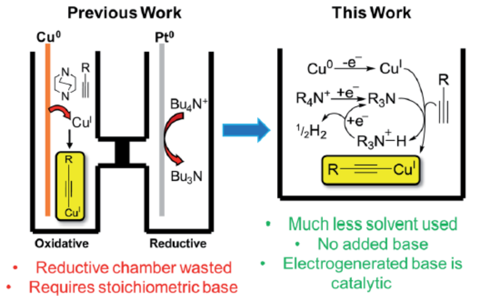

Fig. 1 Previous electrochemical copper(I) acetylide synthesis and proposed improvements.[2]

Department of Chemistry, University College London, 20 Gordon Street, London, WC1H 0AJ, UK. E-mail: pseavill@gmail.com; j.wilden@ucl.ac.uk

† Electronic supplementary information (ESI) available: Full experimental detail and characterisation data. See DOI: 10.1039/c9ra06782e

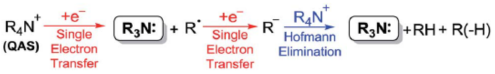

Scheme 1 Quaternary ammonium salt (QAS) reduction.[11]

branching and steric hindrance having very little effect on both their stability towards reduction and the electronic environment around their cationic nitrogen centres.[12] Such features are generally desirable for their use as 'inert' electrolytes. However, there are benefits to employing such salts as both the background electrolytes and as probases in electrochemical systems, namely, the increased sustainability incurred from omitting any additional base or probase reagents. The advantages to using an electrochemical approach to generate bases *in situ* over non-electrochemical methods are that many QAS are less hazardous than their tertiary amine counterparts, through careful selection of anions used, making the associated risks of the starting materials preferable. There is also the potential to use bases catalytically by electro-regeneration of the base species.[9] Such factors embody several of the key principles of green chemistry,[13] yet whilst examples of electro-reduction of QAS exist,[14] to the best of our knowledge, none have been utilised specifically for the *in situ* production of tertiary amine bases.

Results and discussion

We began by using similar reagents to our previous method,[2] therefore Bu_4NPF_6/MeCN was used as the electrolyte solution, causing Cu^I to be produced from the Cu^0 working electrode (WE) and (so we initially believed) Bu_3N to be formed directly at the Pt counter electrode (CE). Over the course of 2 h of applied potential (+0.50 V *vs.* Ag wire quasi-reference electrode (QRE)), a modest yield of 54% for **1a** was achieved (Table 1). The reaction vessel was kept under argon to prevent any diyne **2** forming *via* the Cu^{II}-promoted Glaser–Hay reaction.[15] To demonstrate the proposed catalytic nature of the base, 0.1 mmol electrolyte was used with respect to 0.3 mmol phenylacetylene, hence, if all QAS was converted into tertiary amine bases **3** or **4**, a maximum theoretical yield for **1a** of 33% is predicted. Yields greater than this demonstrate the base must be electrochemically regenerated after initial deprotonation of a molecule of alkyne (Fig. 1).

We propose that the active Cu species in this reaction is $Cu(MeCN)_4X$ (where X = PF_6^- or $CH_3C_6H_4SO_3^-$) based on our previous work and supported again by control reactions carried out in this work. Entry 3 shows that without an applied potential, the reaction proceeded when this Cu species was added along with an amount of **3** that mirrored the total available QAS used in entry 1 (*i.e.* 0.33 eq. with respect to the alkyne), although the reaction was much less efficient. Furthermore, it was found that when a stoichiometric/slight excess of **3** was used the yield increased dramatically. This further indicates that when a potential is applied, the base is regenerated, making this process catalytic in nature.

The absence of any appropriate QAS probase ($LiClO_4$ used as substitute) completely shut the reaction down even when a potential was applied (**1a** was not produced over the 2 h electrolysis) as shown in entry 5. However, when Bu_4NPF_6 was added to this same solution and a potential (+0.5 V *vs.* Ag QRE) was applied again, within 15 min a bright yellow precipitate of **1a** was produced. Whilst we initially interpreted this to be evidence of direct electrochemical reduction of a QAS as in Scheme 1, we decided to run cyclic voltammetry (CV) plots of the various components of this reaction mixture to obtain evidence for this hypothesis (CV plots shown in the ESI and Fig. S2–S4†). Fig. S2† appears to show that at around −3.0 V (*vs.* Ag QRE) the

Table 1 Optimisation and control reactions[a]

Entry	Electrolyte/solvent used	Voltage (*vs.* Ag QRE) and total charge passed	Additive(s)	Yield[b]/%
1	Bu_4NPF_6/MeCN	+0.50 V for 2 h, 19.2C passed	—	54
2	Bu_4NPF_6/MeCN	No potential applied (20 h)	—	0
3	MeCN	No potential applied (2 h)	$Cu(MeCN)_4PF_6$ (1.1 eq.), Bu_3N (0.33 eq.)	3
4	MeCN	No potential applied (2 h)	$Cu(MeCN)_4PF_6$ (1.1 eq.), Bu_3N (1.1 eq.)	38
5	$LiClO_4$/MeCN	+0.50 V for 2 h, 14.8C passed	—	0
6	$LiClO_4$/MeCN	+0.50 V for 2 h, 5.0C passed	Bu_3N (0.33 eq.)	9
7	$Et_4N(CH_3C_6H_4SO_3)$/MeCN	+0.50 V for 2 h, 19.0C passed	—	66
8	$Et_4N(CH_3C_6H_4SO_3)$/MeCN	No potential applied (2 h)	—	<1
9	MeCN	No potential applied (2 h)	$Cu(MeCN)_4PF_6$ (1.1 eq.), Et_3N (0.50 eq.)	44
10	MeCN	No potential applied (2 h)	$Cu(MeCN)_4PF_6$ (1.1 eq.), Et_3N (1.1 eq.)	51
11	**$Et_4N(CH_3C_6H_4SO_3)$/MeCN**	**+0.50 V for 4 h, 45.7C passed**	—	**97**

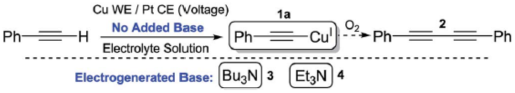

[a] In all cases 0.3 mmol phenylacetylene and 0.1 mmol electrolyte salt in 10 mL reagent grade MeCN (0.01 M) were used. All reactions carried out under argon with a Cu wire WE, a Pt wire CE and a Ag wire QRE each with an effective surface area of 64 mm^2. [b] Isolated yield of copper acetylide **1a**.

background electrolyte solution begins to be reduced. It has been reported that under a reducing potential MeCN itself can form a strong base, $[NCCH_2]^-$,[16] which has been shown to be capable of initiating β-lactam synthesis through substrate deprotonation.[16b–d] However, this direct reduction of MeCN appears to only take place in the absence of other proton donors,[16a] suggesting that the reduction peak shown in these CV plots likely relates to QAS reduction. This distinction is rendered somewhat moot by the fact that at the lower potential of −2.2 V, phenylacetylene starts to be reduced to $[PhCC]^-$ (Fig. S3†), showing that under the conditions used here, this is the most likely first reductive process to take place. Deprotonation of QAS *via* Hofmann elimination would then produce a stable tertiary amine base, thereby initiating the copper acetylide-producing reaction. The subsequent electrochemical reduction of any protonated tertiary amine bases would then almost certainly take over as the dominant reductive process for the rest of the reaction. It is not immediately apparent as to why the production of the phenylacetylide anion does not directly lead to the formation of **1a**. One explanation could be that this reactive anion (formed in low concentration at the beginning of the electrolysis) is quenched too quickly to react directly with the similarly low concentration of Cu^I ions produced. The stable bases **3** and **4**, produced by way of Hofmann elimination, would not suffer from this problem. Scheme 2 shows this proposed reaction initiation.

Entries 5 and 6 also proved important for other reasons. Given that these reactions were carried out in the presence of reagent grade (rather than anhydrous) MeCN, it was postulated that a build-up of hydroxide ions was possible. This could facilitate the reaction by providing another base for the deprotonation step of the reaction and increase the rate at which **3** or **4** were regenerated by deprotonating any protonated **3** or **4**. Entries 5 and 6 seem to suggest that these processes were not in effect.

To improve the yield and atom efficiency of the reaction, we tested an alternative electrolyte salt, $Et_4N(O_3SC_6H_4CH_3)$, aiming to produce the less sterically-hindered base **4**. Work carried out by Dahm and Peters[11a] makes it clear that during the formation of **3** from TBA^+, a sterically-demanding gauche interaction must exist in order to obtain the necessary antiperiplanar geometry required in Hofmann elimination processes. However, this same interaction is much smaller when using TEA^+, promoting the generation of **4** much more readily than **3**. Confirming this hypothesis, the move over to this TEA salt increased the yield significantly, the catalytic nature of the base was maintained and as this salt was more atom-efficient we continued its use. We also found that for optimal yields of **1a** the potential should be applied for 4 h, giving us our optimised conditions as shown in entry 11 of Table 1, highlighted in yellow. Applying these conditions to a range of substrates proved successful, as shown in Scheme 3, with yields comparing well with classical literature methods and a variety of substituents and functional groups being tolerated. However, we found that when trimethylsilyl acetylene was used, the product appeared to decompose *in situ*, presumably due to exposure to the reducing counter electrode. This contrasts our previous method.[2] A bulkier silane, **1i**, was produced, albeit in low yield.

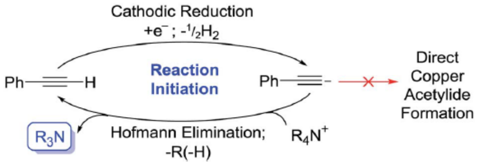

Scheme 2 Proposed reaction initiation.

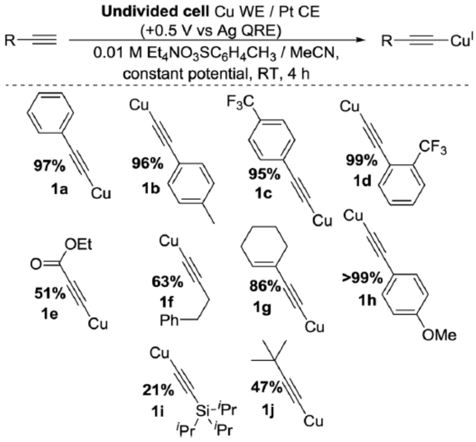

Scheme 3 General conditions and scope of reaction.

Initially we found that some substrates gave impure products when reagent grade MeCN was employed, likely due to overoxidation of the copper. To remedy this, we switched to anhydrous MeCN and obtained superior results.

A schematic mechanism for this reaction is given in Fig. 2, highlighting the various single-electron-transfer redox reactions taking place at electrode surfaces (red arrows).

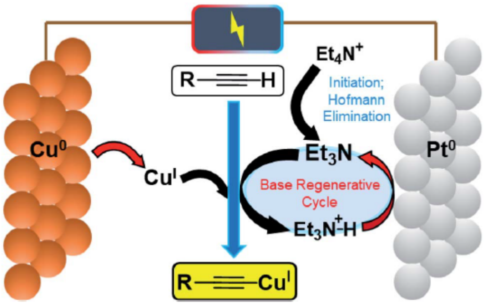

Fig. 2 Schematic mechanism of electrochemical Cu^I and base generation/catalytic regeneration.

The generally high yields, absence of any detectable diyne by-products and lack of degradation of the materials post reaction suggested that our products were indeed pure, but to rigorously test our copper acetylides and the validity of our method, we performed a simple Huisgen-type reaction (the most famous of the 'Click' reactions)[17] to form a 1,2,3-triazole product *via* Cu-promoted azide–alkyne coupling (CuAAC) which proceeds through a copper(I) acetylide intermediate. This reaction is a good exemplar because it is so widely-used, especially in pharmaceutical chemistry where many drug molecules, biomaterials and polymers are routinely produced using this chemistry.[18] It is also a reaction known to be efficient and relies upon a Cu^{I}-based catalytic cycle, meaning that if our copper acetylides were in a mixed oxidation state, this would be highlighted clearly. We therefore adapted conditions from Shao *et al.*,[19] deliberately selecting a method without a reducing agent such as sodium ascorbate to remove the possibility of Cu^{II} being converted into Cu^{I} mid-reaction (Fig. 3).

To our delight, we found that the yields and spectral data for **5** produced using **1a** from both the traditional method (synthesised using CuI in NH_3–H_2O–EtOH[8]) and our new electrochemical method matched very well, reaffirming that our new method for producing copper acetylides is robust. We also noted that when **1a** of questionable oxidation state, *i.e.* a possible mixture of Cu^{I} and Cu^{II} acetylides as in picture B of Fig. 3 was used, a significantly lower yield of 48% was obtained for **5**. Emboldened by these results, we attempted to integrate our electrochemical copper(I) acetylide formation with the Click reaction to produce a sustainable, one-pot electrochemical process, as shown in Scheme 4. Previously, groups have carried out electro-assisted CuAAC-type reactions on electrode surfaces coated with either alkyne or azide functional groups, where Cu(II) salts added to solution are electrochemically reduced to Cu(I), initiating the Click reaction.[20] Another approach involving the generation of the alkyne moiety on the surface of electrodes through the reduction of $Co_2(CO)_6$ has also been demonstrated,[21] but to our knowledge this is the first example of both an electro-oxidised Cu(0) to Cu(I) approach and of such a reaction on preparative-scale. We obtained yields of 49% for **5** with $Et_4NO_3SC_6H_4CH_3$ and 79% with $Et_4NOAc\cdot 4H_2O$ (control reactions with no potential applied yielded 2% and 0% respectively).

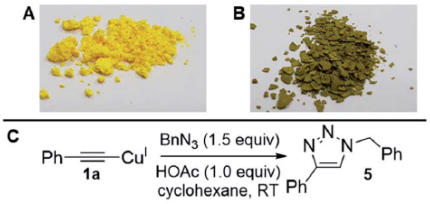

- **75%** using pure **1a** produced by traditional method
- **72%** using pure **1a** produced by this electrochemical method
- **48%** using **1a** of questionable oxidation state

Fig. 3 (A) Picture of 1a that matches literature physical descriptions. (B) Picture of 1a that is of questionable oxidation state. (C) 'Click test' of copper acetylides to assess product purity.[19]

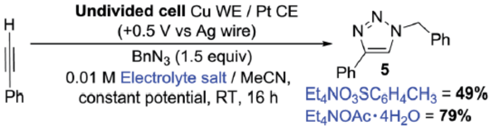

Scheme 4 One-pot electrochemical CuAAC reaction.

These results suggest that the presence of acetate anions permits the generation of a potent copper acetate catalyst, indeed, control reactions using Cu(I)OAc and Et_3N produced **5**, but in lower yields than the electrochemical method. Furthermore, trace amounts of diyne **2** were also produced (presumably from Cu(II) contamination of the Cu(I)OAc catalyst) which was not observed in any of the electrochemical tests where Cu(I) is generated *in situ*.

Conclusions

In summary, we have successfully improved the efficiency and sustainability of copper(I) acetylide synthesis using electrochemistry in an undivided cell. This decreased the amount of solvent required, the base was generated from the background electrolyte and regenerated electrochemically to make it catalytic and halogen waste was completely eliminated from the process. We rigorously assessed the fidelity of our products through a 'Click test' (CuAAC reaction) and we successfully integrated the two reactions into a sustainable, one-pot electrochemical process, which serves as a promising initial demonstration of this approach in a pharmaceutically-relevant reaction.

Conflicts of interest

There are no conflicts to declare.

Acknowledgements

We thank UCL for financial support *via* a studentship awarded to PWS and Dr D. MacMillan (UCL) for MS support.

Notes and references

1 Y. Kamamoto, Y. Nitta, K. Kubo, T. Mizuta and S. Kume, *Chem. Commun.*, 2016, **52**, 10486–10489.
2 P. W. Seavill, K. B. Holt and J. D. Wilden, *Green Chem.*, 2018, **20**, 5474–5478.
3 B. Wang, J. Zhang, X. Wang, N. Liu, W. Chen and Y. Hu, *J. Org. Chem.*, 2013, **78**, 10519–10523.
4 R. D. Stephens and C. E. Castro, *J. Org. Chem.*, 1963, **28**, 3313–3315.
5 D. H. Ryu and E. J. Corey, *J. Am. Chem. Soc.*, 2003, **125**, 6388–6390.
6 G. Evano, K. Jouvin, C. Theunissen, C. Guissart, A. Laouiti, C. Tresse, J. Heimburger, Y. Bouhoute, R. Veillard, M. Lecomte, A. Nitelet, S. Schweizer, N. Blanchard,

C. Alayrac and A.-C. Gaumont, *Chem. Commun.*, 2014, **50**, 10008–10018.

7 (*a*) A. Sagadevan, A. Ragupathi and K. C. Hwang, *Angew. Chem., Int. Ed.*, 2015, **54**, 13896–13901; (*b*) A. Sagadevan, V. P. Charpe, A. Ragupathi and K. C. Hwang, *J. Am. Chem. Soc.*, 2017, **139**, 2896–2899; (*c*) D. K. Das, V. K. K. Pampana and K. C. Hwang, *Chem. Sci.*, 2018, **9**, 7318–7326.

8 K. Jouvin, J. Heimburger and G. Evano, *Chem. Sci.*, 2012, **3**, 756–760.

9 B. D. McCarthy, D. J. Martin, E. S. Rountree, A. C. Ullman and J. L. Dempsey, *Inorg. Chem.*, 2014, **53**, 8350–8361.

10 J. H. P. Utley and M. F. Nielsen, in *Organic Electrochemistry*, ed. H. Lund and O. Hammerich, Marcel Dekker, Inc., New York, 4th edn, 2001, ch. 30, pp. 1227–1257.

11 (*a*) C. E. Dahm and D. G. Peters, *J. Electroanal. Chem.*, 1996, 91–96; (*b*) J. E. Dubois, A. Monvernay and P. C. Lacaze, *Electrochim. Acta*, 1970, **15**, 315–323; (*c*) S. D. Ross, M. Finkelstein and R. C. Petersen, *J. Am. Chem. Soc.*, 1960, **82**, 1582–1585; (*d*) J. S. Mayell and A. J. Bard, *J. Am. Chem. Soc.*, 1963, **85**, 421–425.

12 M. P. S. Mousavi, S. Kashefolgheta, A. Stein and P. Buhlmann, *J. Electrochem. Soc.*, 2016, **163**, H74–H80.

13 P. T. Anastas and J. C. Warner, *Green Chemistry: Theory and Practice*, Oxford University Press, New York, 1998, pp. 29–55.

14 J. Gal, J. C. Folest, M. Troupel, M. O. Moingeon and J. Chaussard, *New J. Chem.*, 1995, **19**, 401–407.

15 (*a*) C. Glaser, *Ber. Dtsch. Chem. Ges.*, 1869, **2**, 422–424; (*b*) A. S. Hay, *J. Org. Chem.*, 1960, **25**, 1275–1276; (*c*) A. S. Hay, *J. Org. Chem.*, 1962, **27**, 3320–3321.

16 (*a*) H. Lund, in *Organic Electrochemistry*, ed. H. Lund and O. Hammerich, Marcel Dekker, Inc., New York, 4th edn, 2001, ch. 5, pp. 223–292; (*b*) P.-G. Echeverria, D. Delbrayelle, A. Letort, F. Nomertin, M. Perez and L. Petit, *Aldrichimica Acta*, 2018, **51**, 3–19; (*c*) M. Feroci, M. Orsini, L. Palombi, L. Rossi and A. Inesi, *Electrochim. Acta*, 2005, **50**, 2029–2036; (*d*) M. Feroci, M. Orsini, L. Rossi, G. Sotgiu and A. Inesi, *Electrochim. Acta*, 2006, **51**, 5540–5547.

17 C. D. Hein, X.-M. Liu and D. Wang, *Pharm. Res.*, 2008, **25**, 2216–2230.

18 (*a*) F. Amblard, J. H. Cho and R. F. Schinazi, *Chem. Rev.*, 2009, **109**, 4207–4220; (*b*) M. Meldal and C. W. TornØe, *Chem. Rev.*, 2008, **108**, 2952–3015; (*c*) C. J. Pickens, S. N. Johnson, M. M. Pressnall, M. A. Leon and C. J. Berkland, *Bioconjugate Chem.*, 2018, **29**, 686–701.

19 C. Shao, G. Cheng, D. Su, J. Xu, X. Wang and Y. Hu, *Adv. Synth. Catal.*, 2010, **352**, 1587–1592.

20 N. K. Devaraj, P. H. Dinolfo, C. E. D. Chidsey and J. P. Collman, *J. Am. Chem. Soc.*, 2006, **128**, 1794–1795.

21 I. Choi, Y.-K. Kim, D.-H. Min, S. Lee and W.-S. Yeo, *J. Am. Chem. Soc.*, 2011, **133**, 16718–16721.